UNIVERSIDADE ESTADUAL DE CAMPINAS

INSTITUTO DE BIOLOGIA

BIANCA FAZIO RIUS

MODELING FUNCTIONAL DIVERSITY AND RESILIENCE OF THE AMAZON FOREST TO CLIMATE CHANGE BEYOND CARBON STOCKS

MODELAGEM DA DIVERSIDADE FUNCIONAL E RESILIÊNCIA DA FLORESTA AMAZÔNICA ÀS MUDANÇAS CLIMÁTICAS ALÉM DOS ESTOQUES DE CARBONO

CAMPINAS

2024

BIANCA FAZIO RIUS

MODELING FUNCTIONAL DIVERSITY AND RESILIENCE OF THE AMAZON FOREST TO CLIMATE CHANGE BEYOND CARBON STOCKS

MODELAGEM DA DIVERSIDADE FUNCIONAL E RESILIÊNCIA DA FLORESTA AMAZÔNICA ÀS MUDANÇAS CLIMÁTICAS ALÉM DOS ESTOQUES DE CARBONO

Thesis presented to the Institute of Biology of the University of Campinas in partial fulfillment of the requirements for the degree of Doctor in Ecology

Tese apresentada ao Instituto de Biologia da Universidade Estadual de Campinas como parte dos requisitos exigidos para a obtenção do Título de Doutora em Ecologia

Orientador: DAVID MONTENENGRO LAPOLA

ESTE ARQUIVO DIGITAL CORRESPONDE À VERSÃO FINAL DA TESE DEFENDIDA PELA ALUNA BIANCA FAZIO RIUS E ORIENTADA PELO DAVID MONTENEGRO LAPOLA.

CAMPINAS

2024

Ficha catalográfica
Universidade Estadual de Campinas (UNICAMP)
Biblioteca do Instituto de Biologia
Gilberto Martins Vicentin - CRB 8/8620

Rius, Bianca Fazio, 1991-
R52m Modeling functional diversity and resilience of the Amazon forest to climate change beyond carbon stocks / Bianca Fazio Rius. – Campinas, SP : [s.n.], 2024.

Orientador: David Montenegro Lapola.
Tese (doutorado) – Universidade Estadual de Campinas (UNICAMP), Instituto de Biologia.

1. Resiliência (Ecologia). 2. Mudanças climáticas. 3. Florestas - Amazônia. 4. Vegetação e clima - Modelos matemáticos. 5. Diversidade funcional. I. Lapola, David Montenegro, 1982-. II. Universidade Estadual de Campinas (UNICAMP). Instituto de Biologia. III. Título.

Informações Complementares

Título em outro idioma: Modelagem da diversidade funcional e resiliência da floresta amazônica às mudanças climáticas além dos estoques de carbono
Palavras-chave em inglês:
Resilience (Ecology)
Climatic changes
Forests and forestry - Amazon River Region
Vegetation and climate - Mathematical models
Functional diversity
Área de concentração: Ecologia
Titulação: Doutora em Ecologia
Banca examinadora:
David Montenegro Lapola [Orientador]
Tomas Ferreira Domingues
Simone Aparecida Vieira
Celso von Randow
Carolina Casagrande Blanco
Data de defesa: 19-07-2024
Programa de Pós-Graduação: Ecologia

Identificação e informações acadêmicas do(a) aluno(a)
- ORCID do autor: https://orcid.org/0000-0002-7623-9152
- Currículo Lattes do autor: https://lattes.cnpq.br/1595987248608949

Campinas, 19 de julho de 2024.

COMISSÃO EXAMINADORA

Prof.(a). Dr.(a). David Montenegro Lapola

Prof.(a). Dr.(a). Tomas Ferreira Domingues

Prof.(a). Dr.(a). Celso von Randow

Prof.(a). Dr.(a). Simone Aparecida Vieira

Prof.(a). Dr.(a). Carolina Casagrande Blanco

Os membros da Comissão Examinadora acima assinaram a Ata de defesa, que se encontra no processo de vida acadêmica do aluno.

A Ata da defesa com as respectivas assinaturas dos membros encontra-se no SIGA/Sistema de Fluxo de Dissertação/Tese e na Secretaria do Programa de Pós Graduação em Ecologica da Unidade Instituto de Biologia.

Para Jorge, Vera e Bruno

AGRADECIMENTOS

O presente trabalho foi realizado com apoio da Coordenação de Aperfeiçoamento de Pessoal de Nível Superior - Brasil (CAPES) - Código de Financiamento 001- Nº de bolsa concedida: 88887.177275/2018-00. Este trabalho também contou com o financiamento da Fundação de Amparo à Pesquisa do Estado de São Paulo (FAPESP) através do processo de número de 2019/04223-0.

Escrever esta seção é, sem dúvida, a tarefa mais desafiadora de toda a minha tese. É impossível agradecer a todos que seguraram a minha mão durante a jornada de desenvolvimento deste trabalho. Sei que não poderei mencionar cada pessoa individualmente, mas cada uma delas ocupa um lugar especial em meu coração e contribuiu para a construção do que me tornei. Chegar até aqui não foi fácil, mas durante este doutorado, aprendi a acreditar em mim mesma e a confiar no processo, por mais clichê que possa parecer. Sem o apoio e a orientação dessas pessoas, nada disso teria sido possível, e certamente eu teria desistido deste desafio.

Não poderia começar meus agradecimentos de outra forma senão expressando minha profunda gratidão ao meu pai e à minha mãe. Desde sempre, eles lutaram para que eu pudesse seguir meus próprios caminhos e enfrentar minhas próprias batalhas. Hoje, posso afirmar que alcançaram esse objetivo com maestria, e graças a eles me tornei uma mulher forte, determinada e realizadora. Muitas vezes, só consegui prosseguir com este trabalho ao lembrar das palavras do meu pai: "é preciso matar UM leão por dia". Foi enfrentando esses pequenos desafios diários que consegui finalizar este trabalho, sendo uma prova árdua de resiliência, com o perdão do trocadilho com o título desta tese. Encontrei forças para buscar essa resiliência porque me espelho em vocês todos os dias, honrando o que sempre me disseram ser a única herança que poderiam oferecer a mim e ao meu irmão e que ninguém poderia nos tirar: o conhecimento. Agradeço por terem criado a mim e ao meu irmão, Bruno, com tanto amor e dedicação. Obrigada, Bruno, por fazer parte da minha vida e por sempre me apoiar e vibrar com as minhas vitórias. Obrigada, pai e mãe por terem formado essa família tão linda, sem esquecer das nossas pequenas Maya, Mel e Tina que nos despertam tanto amor e alegria. Serei eternamente grata por todo o apoio de vocês.

Obrigada a todos os meus tios, tias, primos e avós por me ensinarem o valor que reside nos nossos laços tão fortes e por tanto carinho dedicado. Um obrigada especial à minha vó Neyde, que me deixa muita saudade mas também muitos ensinamentos e orgulho pela mulher que foi e pela família que criou junto do meu avô Décio.

Não tenho palavras para agradecer a pessoa que topou compartilhar a vida comigo. Caio, hoje meu marido, foi com certeza uma das pessoas que segurou a minha mão mais forte ao longo do meu doutorado. Eu jamais teria conseguido sem você. Obrigada por me dar forças nos momentos mais difíceis, por me ouvir e me acolher, pela sua compreensão e por acreditar tão profundamente em mim. Mas, acima de tudo, obrigada pelos momentos bons, pelas risadas, pelo amor e principalmente pela nossa parceria. Obrigada por estar comigo em cada uma das minhas conquistas e por fazer delas as suas também e aceitando que elas nos levem até mesmo para o outro lado do mundo. Obrigada por acreditar em mim e em nós. Obrigada por trazer de presente junto com você uma nova família pra mim: Newton, Rô e Luna. Obrigada também por trazer pra minha vida a nossa Pitucha que faz dos nossos dias mais felizes, alegres e amorosos.

Agradeço ao meu querido orientador, David, por tantos anos de parceria. Obrigado por acreditar em mim mesmo quando eu não pude. Agradeço por abrir tantas portas importantes para mim e por tornar a ciência uma jornada leve e divertida. Minha admiração por você me inspira a continuar nesta luta. Acima de tudo obrigada por me permitir alçar meus próprios vôos.

Agradeço imensamente à minha coorientadora, Marina Hirota, pela incrível oportunidade que me proporcionou de desenvolver parte do meu trabalho em colaboração. Agradeço por ter me dado essa oportunidade em um momento tão delicado da minha vida. Além disso, agradeço por me permitir morar em um lugar tão maravilhoso por um tempo. Não poderia deixar de agradecer também por mostrar uma abordagem tão única e inspiradora para a educação e para a prática da ciência. E, por fim, agradeço por me proporcionar a chance de fazer parte de um laboratório com pessoas tão incríveis quanto o IpEs.

Obrigada aos meus queridos amigos do LabTerra por estarem ao meu lado durante tanto tempo, por todas as nossas trocas científicas que têm me feito crescer como cientista a cada discussão de trabalho. Agradeço imensamente pela força que vocês me deram, especialmente nesta fase final. Que o trabalho de todos nós continue contribuindo cada vez mais para a ciência brasileira. O LabTerra também me deu o grandíssimo prazer de conhecer pessoas incríveis que se tornaram amigos para toda a vida.

Aos CAETÊr's do LabTerra, agradeço por persistirem nesse trabalho desafiador e muitas vezes pouco reconhecido de desenvolver um modelo, mesmo sem serem especialistas em programação. Mesmo diante de tantos desafios, vocês não se intimidam com a complexidade que decidiram enfrentar. Agradeço pelos trabalhos desenvolvidos, pelas publicações que já fizemos juntos e pelas muitas que ainda virão. Mais ainda, agradeço pela amizade que construímos. Um agradecimento especial ao João, que dedicou tanto tempo para solidificar e construir as bases para a versão dinâmica do CAETÊ. E um agradecimento muito especial também à Bárbara, por ter me acompanhado e auxiliado no desenvolvimento do modelo para este trabalho, pelas inúmeras horas de dedicação para construirmos o módulo de alometria e alocação, e por todos os nossos momentos de amizade e trocas.

Agradeço a todos (não ousarei citar nomes por medo de esquecer de pessoas tão importantes pra mim) os amigos maravilhosos que Barão Geraldo me apresentou, com os quais compartilhei uma casa, muitas vezes por alguns anos, ao longo do meu doutorado. Nossas amizades serão para sempre, sem dúvida. Obrigada também a todos os meus amigos mais antigos de Rio Claro, que foram peças fundamentais para que eu chegasse até aqui. E obrigada aos tantos amigos maravilhosos de Jundiaí, que estão ao meu lado desde sempre.

Por último, expresso minha gratidão a todas as mulheres cientistas que abriram caminhos para que eu pudesse realizar meu sonho de fazer da ciência um propósito de vida. Espero sinceramente que meu trabalho também possa inspirar e facilitar a jornada de outras.

RESUMO

A floresta Amazônica tem mostrado sinais preocupantes de perda de resiliência nas últimas décadas. Dada a sua função crítica na preservação da biodiversidade, no sequestro de carbono, na regulação do clima e na oferta de inúmeros serviços ecossistêmicos em escala global, compreender a resiliência da floresta amazônica em meio às condições climáticas em mudança é de extrema importância. No entanto, significativas incertezas persistem nessa área de estudo. Esta tese explora os impactos da redução da precipitação no funcionamento do ecossistema amazônico e na diversidade funcional das plantas usando um modelo de vegetação baseado em traços, o CAETÊ. No primeiro capítulo, apresentamos, pela primeira vez, o modelo, investigamos como a diversidade de traços das plantas afeta o armazenamento de carbono da vegetação e a produtividade primária líquida (NPP) sob cenários atuais e de baixa precipitação. Dois enfoques de modelagem são comparados: um enfoque de tipo funcional de planta (PFT) com três PFTs e um enfoque baseado em traços representando 3000 estratégias de vida de plantas (PLSs). Nossos resultados revelam que a inclusão da variabilidade de traços melhora a precisão do modelo na representação da NPP e do armazenamento de carbono da vegetação. Sob precipitação reduzida, ambos os enfoques simulam uma perda significativa de armazenamento de C (~60%), mas o enfoque baseado em traços mostra uma resposta mais sutil com o surgimento de combinações de traços raros e uma maior relação raiz-parte aérea. Esses resultados destacam a importância de considerar a diversidade funcional das plantas na avaliação da sensibilidade da Amazônia às mudanças climáticas. O segundo capítulo foca na resiliência das florestas amazônicas sob aumento da frequência e intensidade de secas. Simulamos uma redução de 30% na precipitação aplicada em duas frequências: a cada oito anos (frequência de oito anos) e a cada dois anos (frequência de 2 anos), usando 6000 PLSs definidos por traços como densidade da madeira, área foliar específica (SLA) e sensibilidade da condutância estomática à assimilação de CO_2 (g1). Nossos resultados indicam que secas frequentes levam ao colapso do ecossistema (para a frequência de 2 anos) e a uma resiliência diminuída (frequência de 8 anos), resultando em mudanças notáveis na configuração do ecossistema e na composição funcional. Vários indicadores ecossistêmicos como NPP, evapotranspiração, eficiência no uso da água (WUE) e a diversidade de PLSs sobreviventes exibem sensibilidades diversas à seca. Esta pesquisa enfatiza o papel crítico de múltiplos indicadores ecossistêmicos, além dos estoques de carbono, na avaliação da resiliência e sugere que as florestas tropicais podem ser mais suscetíveis aos impactos climáticos do que anteriormente assumido. Juntos, esses capítulos oferecem uma

visão abrangente sobre a diversidade funcional e a resiliência da floresta Amazônica, destacando a necessidade de estratégias de conservação holísticas para enfrentar os desafios impostos pelas mudanças climáticas.

ABSTRACT

The Amazon forest has exhibited concerning signs of diminishing resilience in recent decades. Given its critical role in preserving biodiversity, sequestering carbon, regulating the climate, and offering a myriad of ecosystem services on a global scale, comprehending the resilience of the Amazon rainforest amidst shifting climatic conditions is of utmost importance. Nonetheless, significant uncertainties persist in this area of study. This thesis explores the impacts of reduced precipitation on the Amazon's ecosystem functioning and plant functional diversity using a trait-based vegetation model, CAETÊ. In the first chapter, we present, for the first time the model, investigate how plant trait diversity affects vegetation carbon storage and net primary productivity (NPP) under current and low precipitation scenarios. Two modeling approaches are compared: a plant functional type (PFT) approach with three PFTs and a trait-based approach representing 3000 plant life strategies (PLSs). Our findings reveal that including trait variability improves the model's accuracy in representing NPP and vegetation carbon storage. Under reduced precipitation, both approaches simulate significant C storage loss (~60%), but the trait-based approach shows a more nuanced response with the emergence of rare trait combinations and a higher root-to-shoot ratio. These results underscore the importance of accounting for plant functional diversity in evaluating the Amazon's sensitivity to climate change. The second chapter focuses on the resilience of Amazon forests under increased drought frequency and intensity. We simulate a 30% reduction in precipitation applied at two frequencies: every eight years (8-year frequency) and alternately every other year (2-year frequency), using 6000 PLSs defined by traits such as wood density, specific leaf area (SLA), and stomatal conductance sensitivity to CO_2 assimilation (g1). Our results indicate that frequent droughts lead to ecosystem collapse (for the 2-year frequency) and diminished resilience (8-year frequency), resulting in notable shifts in ecosystem configuration and functional composition. Various ecosystem indicators such as NPP, evapotranspiration, water use efficiency (WUE), and the diversity of surviving PLSs exhibit diverse sensitivities to drought. This research emphasizes the critical role of multiple ecosystem indicators, beyond carbon stocks, in evaluating resilience and suggests that tropical forests may be more susceptible to climate impacts than previously assumed. Together, these chapters offer a comprehensive insight into the functional diversity and resilience of the Amazon forest, highlighting the necessity for holistic conservation strategies to address the challenges posed by climate change

Summary

GENERAL INTRODUCTION

Global climate change refers to significant and lasting changes in the Earth's climate and weather patterns, primarily driven by human activities. While natural processes have historically influenced the climate, the current trend is overwhelmingly attributed to anthropogenic factors, such as the burning of fossil fuels and deforestation (IPCC, 2021). These activities release large amounts of greenhouse gases like carbon dioxide (CO_2) into the atmosphere, enhancing the natural greenhouse effect and leading to a rise in global temperatures (Hare & Meinshausen, 2015). This phenomenon, known as global warming, is a critical aspect of climate change, contributing to various environmental impacts such as more frequent and severe drought events (IPCC, 2007), and, ultimately, disruptions to ecosystems (Jones et al., 2009; Seddon et al., 2016).

Changes in precipitation patterns are a critical component of global climate change, significantly altering the distribution, intensity, and frequency of rainfall across the globe (Marengo et al., 2009). Regions that previously experienced consistent rainfall may now face irregular and extreme weather, including prolonged droughts and sudden, heavy downpours. These alterations in precipitation patterns play a pivotal role in natural ecosystems, directly impacting ecological processes, biodiversity, and overall ecosystem dynamics (Bellard et al., 2012; Oliveira et al., 2014). For instance, precipitation patterns determine water availability, influencing fundamental aspects such as the composition of plant communities (Allen et al., 2010), the ecosystem's capacity to sequester and store carbon (Breshears et al., 2009; Doughty et al., 2015) and, ultimately, ecosystem resilience by affecting the ability of ecosystems to withstand and recover from disturbances (Staal et al., 2018; Wu et al., 2022). (Kannenberg et al., 2020; Müller & Bahn, 2022; Van Passel et al., 2024).

Ecological resilience, as articulated by Holling (1973), refers to a system's capacity to endure disturbances without compromising its function, structure, and inherent identity. This concept underscores the ecosystem's remarkable ability to assimilate environmental pressures while continuing to deliver the essential goods and services characteristic of its original state. Forest resilience is commonly evaluated by assessing the capacity of ecosystems to sequester and retain carbon (e.g., Boulton et al., 2022; Huntingford et al., 2013; Sakschewski et al., 2016). While carbon storage is a crucial indicator of ecosystem health and functionality (Poorter et al., 2016; Yang et al., 2024), it is essential to analyze other ecosystem processes and properties to gain a comprehensive understanding of ecosystem vulnerability (Dakos et al., 2019; Hu et al., 2022). For instance, even in a disturbance such as drought event, the carbon stock of an ecosystem may remain resilient, but changes in evapotranspiration could occur (de Bello et al., 2021; Mori et al., 2013). Evapotranspiration plays a vital role in terrestrial ecosystems, particularly in tropical regions like the Amazon forest, as it significantly influences precipitation patterns (Aragăo, 2012; Staal et al., 2018). Therefore, to enhance our understanding of ecosystem resilience, it is imperative to move beyond solely focusing on carbon stocks and consider a broader range of ecosystem functions and dynamics.

Understanding the resilience of natural ecosystems is crucial in our dynamic and ever-changing world (Hirota et al., 2011). These ecosystems play a vital role in regulating global processes, including climate dynamics, biodiversity conservation, and the provision of essential ecosystem services. Additionally, they serve as critical buffers, helping to mitigate the impacts of climate change. For instance, tropical forests like the Amazon are central in sequestering carbon in both vegetation and soil (Doughty et al., 2015; Malhi et al., 2011; Malhi & Phillips, 2004). If their resilience weakens and their capacity to store carbon diminishes, it could trigger a significant feedback loop that exacerbates climate change by releasing stored carbon into the atmosphere

(Phillips et al., 2009; Poulter et al., 2010; Rowland et al., 2015). Concurrently, research indicates that tropical forests are exhibiting indications of diminishing resilience (Flores et al., 2024; Rocha et al., 2022), with factors such as deforestation and climate change identified as primary drivers of this decline (Boulton et al., 2022b). Among climate-related changes, reduced precipitation emerges as a crucial factor impacting these ecosystems (Flores et al., 2024; Scheiter et al., 2024). For example, reduced precipitation can increase mortality rates (Doughty et al., 2015), reduce productivity (Van der Molen et al., 2011), and compromise the growth capacity of trees (Cavin et al., 2013), reducing its ability to sequester and store carbon (Müller & Bahn, 2022). Water scarcity can also alter the species/functional composition within the Amazon forest as certain species or plant life strategies may be more resilient to drought conditions than others (Aguirre-Gutiérrez et al., 2019; Enquist & Enquist, 2011; Esquivel-Muelbert et al., 2018). Nevertheless, significant uncertainties remain regarding the resilience of the Amazon forest to these changes, underscoring the imperative for additional research to evaluate the resilience of this ecosystem and other tropical forests.

One of the widely used tools to comprehend the resilience of natural ecosystems and their responses to climate change is vegetation models, such as Dynamic Global Vegetation Models (DGVMs; Albrich et al., 2020; Fisher et al., 2010). While these models have been extensively employed, they often yield varying results depending on the specific model used (Huntingford et al., 2013; Rammig et al., 2010). A significant source of uncertainty lies in how the majority of vegetation models simplify the representation of plant diversity (Fyllas et al., 2014; Scheiter et al., 2013; van Bodegom et al., 2014). Typically, the diversity of plants is condensed into a few and fixed Plant Functional Types (PFTs), that represent broad groupings of plant species that share similar characteristics (e.g. growth form) and roles (e.g. photosynthetic pathway) in ecosystem function (Van Bodegom et al., 2012; Wullschleger et al., 2014). However, this approach faces significant challenges when applied to highly diverse ecosystems such as the Amazon forest. In many cases, the Amazon forest is represented by only a handful of PFTs, typically two or three, which limits the representation of the vast range of plant life strategies found in nature. Relying on a restricted set of PFTs may lead to an underestimation of the forest's capacity to respond and adapt to climate changes.

In recent years, a new generation of vegetation models known as trait-based models has emerged, representing a significant advancement in the field (Sakschewski et al., 2015; Verheijen et al., 2013). Unlike traditional discrete PFTs, these trait-based models incorporate a multitude of plant types, representing vegetation based on how plants with different functional trait combinations (i.e., co-variation of traits) perform in a given environment. Functional traits are specific characteristics of an organism that directly influence its performance, fitness, and interactions within its environment. Functional traits can include physiological, morphological, phenological, or life history attributes that determine how an organism responds to environmental conditions, interacts with other species, and contributes to ecosystem processes (Díaz et al., 2013; Violle et al., 2007). By encompassing a diverse array of strategies that plants can employ in varying environmental conditions, these models capture a broader spectrum of plant behaviors and provide a more nuanced representation of plant diversity. This approach allows for a more detailed exploration of how different plant traits interact and influence ecosystem processes, leading to a more comprehensive understanding of vegetation dynamics and responses to environmental changes (Pavlick et al., 2013; Wullschleger et al., 2014).

Trait-based models offer a valuable platform for exploring a broader spectrum of inquiries, delving into the significance of functional diversity and its multifaceted dimensions, a depth of analysis previously unattainable with traditional PFT approaches. Integrating representations of functional diversity into vegetation models is pivotal for advancing our comprehension of how climate change impacts the resilience of forest ecosystems, particularly those classified as "hyperdiverse." Functional diversity plays a pivotal role in shaping forest resilience by influencing the ecosystem's ability to respond to environmental stressors and disturbances (Cadotte et al., 2011). As a critical element of biodiversity, functional diversity encompasses the diverse traits and roles that different plant species contribute to the ecosystem (Carmona et al., 2016). For instance, a rich array of plant traits can enhance response diversity, empowering the ecosystem to adjust to dynamic conditions and uphold essential functions (Elmqvist et al., 2003; Mori et al., 2013). At the same time, functional diversity encompasses various aspects called “facets”, such as richness, evenness, and divergence, each exerting a distinct influence on ecosystem functioning and vulnerability (Carmona et al., 2016). However, the precise mechanisms of these interactions are still in need of further elucidation and despite ongoing research efforts, conflicting findings persist, underscoring the existing uncertainties surrounding this complex subject matter.

Even with the increasing development and application of trait-based vegetation models, only a limited number have been specifically utilized to investigate the impact of functional diversity on forest resilience (but see Sakschewski et al., 2016 and Schmitt et al., 2019). Then, trait-based models are still to be fully leveraged to their maximum potential. In that sense, we developed the CAETÊ model (fully described in Chapter I). The CAETÊ (Carbon and Ecosystem functional-Trait Evaluation) model is a trait-based vegetation model designed to represent the diversity of plant strategies and functional traits observed in nature. As a trait-based model, CAETÊ emphasizes the variability of plant functional traits by simulating various plant life strategies (PLSs) through the random assignment of functional trait values. Each PLS is represented by a unique combination of values for each functional trait, allowing for the simulation of diverse plant strategies using the same eco-physiological parameterizations and climatic forcings.

GENERAL OBJECTIVES

In this study, our aim was to investigate the effects of reduced precipitation on the functioning and resilience of the Amazon forest, with a focus on the various facets of functional diversity. Utilizing the CAETÊ model, our research was structured into two distinct chapters.

Chapter I delves into a comprehensive description of the model, comparing a traditional approach using a limited number of PFTs with a trait-based version of the model. This comparison aimed to assess whether the enhanced representation of functional diversity could improve the model's accuracy in depicting biomass distribution across the Amazon basin. Subsequently, we implemented a uniform 50% reduction in precipitation to analyze its impacts on net primary productivity and carbon stock under both the PFT and trait-based frameworks. This analysis provided valuable insights into the influence of functional diversity on the Amazon forest's susceptibility to reduced precipitation scenarios. Additionally, we examined the effects of reduced precipitation on various aspects of functional diversity through both single and multi-trait evaluations.

In Chapter II, we outline the novel enhancements made to the model to further refine its capabilities. We then explored the implications of increased frequency and intensity of drought events by simulating a 30% reduction in precipitation at two different frequencies in the central Amazon region: every two years and every eight years. Through this experimentation, we assessed the resilience of the Amazon forest by evaluating its ability to sustain and recover in terms of ecosystem functioning. This assessment extended beyond the conventional focus on carbon stock to encompass a broader range of ecosystem functions and properties, including net primary productivity (NPP), evapotranspiration, water use efficiency (WUE), and functional richness.

CHAPTER I - Higher functional diversity improves modeling of Amazon forest carbon storage

Published in: Ecological Modeling

Year: 2023

Higher functional diversity improves modeling of Amazon forest carbon storage

Authors: Bianca Fazio Rius[a,b,*], João Paulo Darela Filho[a,c], Katrin Fleischer[d,e,], Florian Hofhansl[f], Carolina Casagrande Blanco[a], Anja Rammig[e], Tomas Domingues[g], David Montenegro Lapola [a]

Institutional affiliations:
[a]University of Campinas (Unicamp), Center for Meteorological and Climatic Research Applied to Agriculture, Earth System Science Laboratory, Campinas - SP, Brazil

[b]University of Campinas (Unicamp), Biology Institute, Campinas - SP, Brazil

[c]São Paulo State University (Unesp), Institute of Biosciences, Rio Claro - SP, Brazil

[d]Max-Planck-Institute for Biogeochemistry, Department Biogeochemical Signals, Jena, Germany

[e]Technical University of Munich (TUM), School of Life Sciences, Freising, Germany

[f]International Institute for Applied Systems Analysis (IIASA), Biodiversity and Natural Resources Program, Laxenburg, Austria

[g]Universidade de São Paulo (USP), Faculdade de Filosofia, Ciências e Letras de Ribeirão Preto, Departamento de Biologia, Ribeirão Preto - SP, Brazil

[*]Corresponding author:
Bianca Fazio Rius
Earth System Science Lab, Center for Meteorological and Climatic Research Applied to Agriculture, University of Campinas (Unicamp), Campinas, 1308-886 - SP, Brazil
email: b211466@dac.unicamp.br

Coauthors' email address:

João Paulo Darela Filho - joao.darela@tum.de
Katrin Fleischer - kfleischer@bgc-jena.mpg.de
Florian Hofhansl - hofhansl@iiasa.ac.at
Carolina Casagrande Blanco - cblanco@unicamp.br
Anja Rammig - anja.rammig@tum.de
Tomas Domingues - tomas@ffclrp.usp.br

David Montenegro Lapola – dmlapola@unicamp.br

Highlights

We present a novel trait-based vegetation model to represent the diversity of plant life strategies

Plant life strategies are created in a hypervolume through trait value combinations

Including plant trait variability improves representation of plant carbon storage and NPP

Diversity allows communities' functional reorganization under environmental change

Low precipitation leads to increase in roots investment at the expense of leaves and wood

Abstract

The impacts of reduced precipitation on plant functional diversity and how its components (richness, evenness, divergence and composition) modulate the Amazon carbon balance remain elusive. We present a novel trait-based approach, the CArbon and Ecosystem functional-Trait Evaluation (CAETÊ) model to investigate the role of plant trait diversity in representing vegetation carbon (C) storage and net primary productivity (NPP) in current climatic conditions. We assess impacts of plant functional diversity on vegetation C storage under low precipitation in the Amazon basin, by employing two approaches (low and high plant trait diversity, respectively): (i) a plant functional type (PFT) approach comprising three PFTs, and (ii) a trait-based approach representing 3000 plant life strategies (PLSs). The PFTs/PLSs are defined by combinations of six traits: C allocation and residence time in leaves, wood, and fine roots. We found that including trait variability improved the model's performance in representing NPP and vegetation C storage in the Amazon. When considering the whole basin, simulated reductions in precipitation caused vegetation C storage loss by ~60% for both model approaches, while the PFT approach simulated a more widespread C loss and abrupt changes in neighboring grid cells. We found that owing to high trait variability in the trait-based approach, the plant community was able to functionally reorganize itself via changes in the relative abundance of different plant life strategies, which therefore resulted in the emergence of previously rare trait combinations in the model simulation. The trait-based approach yielded strategies that invest more heavily in fine roots to deal with limited water availability, which allowed the occupation of grid cells where none of the PFTs were able to establish. The prioritization of root investment at the expense of other tissues in response to drought has been observed in other studies. However, the higher investment in roots also had consequences: it resulted, for the trait-based approach, in a higher root:shoot ratio (a mean increase of 74.74%) leading to a lower vegetation C storage in some grid cells. Our findings highlight that accounting for plant functional diversity is crucial when evaluating the sensitivity of the Amazon forest to climate change, and therefore allow for a more mechanistic understanding of the role of biodiversity for tropical forest ecosystem functioning.

Keywords: trait-based model, climate change, carbon allocation, functional trait space, functional reorganization, trait variability

1. Introduction

Climate model projections based on future socioeconomic scenarios indicate that the Amazon forest will experience more frequent and more extreme moisture stress in the 21st century (Lee et al., 2021). Moisture stress can induce biodiversity shifts, including changes in functional diversity (Aguirre-Gutiérrez et al., 2019; Esquivel-Muelbert et al., 2018) and associated effects on vegetation carbon (hereafter C) storage (da Costa et al., 2010; Hubau et al., 2020). However, how these climatic changes will affect different components of functional diversity – composition, richness, evenness and divergence (Carmona et al., 2016; Mason et al., 2005), and the role functional diversity plays in determining vegetation C storage remains poorly understood (Esquivel-Muelbert et al., 2017; 2018; Poorter et al., 2015; Sakschewski et al., 2016).

Due to differences in life-history strategies among plants (Adler et al., 2014; Reich et al., 2003), functional diversity plays a vital role in determining ecosystem functioning and its responses to environmental changes (Díaz & Cabido, 2001; Song et al., 2014; Cadotte, 2017). Ultimately, functional traits delineate plant communities' responses and effects to biotic and abiotic conditions and also shape ecosystem processes and functions such as vegetation C storage (Lavorel & Garnier, 2002; Funk et al., 2017; Violle et al., 2007). It is widely accepted that more taxonomically and functionally diverse communities are less impacted by environmental changes (Cadotte et al., 2011; Mori et al., 2013; Sakschewski et al., 2016; Schmitt et al., 2019). The “insurance hypothesis”, for example, postulates that a higher diversity (richness) of plant functional strategies provides higher variability of plant functional responses under new environmental conditions (Mori et al., 2013; Yachi & Loreau, 1999), thus maintaining ecosystem functioning by providing a buffer effect against environmental fluctuations (Fauset et al., 2015; Lohbeck et al., 2016; Yachi & Loreau, 1999). Such a buffering effect is expected through the process of functional density compensation which enables the functional composition of a community to reorganize and adjust to new environmental conditions, thus enabling types of plants that previously exerted a less relevant functional role (low density) to increase their dominance and vice versa (Mori et al., 2013; Smith et al., 2022).

Accordingly, it has been suggested that environmental fluctuations lead to changes in the abundance of plant strategies that compose the communities and, consequently, changes on how the available functional trait space is occupied, then redefining plant functional diversity components (Boersma et al., 2016; Carmona et al., 2019; de Bello et al., 2021; Enquist et al., 2017). However, there is no consensus under which condition whether environmental changes select traits and lead to homogenization (decrease in functional diversity) or allow multiple functional traits to persist generating diversification (increase in functional diversity; Smith et al., 2022). For example, reduced precipitation was found to exert a strong environmental filter by selecting a subset of functional trait combinations that are more suitable to cope with moisture stress (Mouillot et al., 2013a). In such a scenario, according to the optimal partitioning theory (Cannell & Dewar, 1994; Metcalfe et al., 2010; Thornley, 1972), a common strategy would be to invest more C to fine root production to acquire limiting belowground resources, such as soil water and nutrients required for aboveground plant productivity. Such a selection for more conservative resource-use would restrict the range of functional trait values and thus reduce the functional trait space occupied by the community (lower functional richness; Cornwell et al., 2006; Funk et al., 2017; Kleidon et al., 2009). On the other hand, it has been found that disturbances, especially intermediate disturbances, can trigger an increase in the occupation of the functional trait space (higher functional richness; Herben et al., 2018). In line with the intermediate disturbance hypothesis (Bongers et al., 2009), which predicts that local species diversity is maximized at an intermediate level of disturbance, it has been suggested that also functional diversity should increase via the functional reorganization of the community allowing new ecological strategies to be more abundant in the communities (Smith et al., 2022). Vegetation models have been widely used to explore the fate of the Amazon forest carbon balance under future potential climatic conditions (Cox et al., 2004; Galbraith et al., 2010; Huntingford et al., 2013; Lapola et al., 2009; Longo et al., 2018; Rammig et al., 2010). Some of these models project a dramatic loss in Amazon forest C stocks due to reduced precipitation (Cox et al., 2000, 2004; Lapola et al., 2009; Oyama and Nobre, 2003). Most model simulations have not reproduced these patterns afterward but there is ongoing discussion on the likelihood of such projections (Levine et al., 2016; Malhi et al., 2009; Malhi et al 2018; Lapola et al. 2018). Other models simulate an abrupt replacement of the dominant humid tree cover found in large parts of Amazon forests with more arid-affiliated vegetation under reduced precipitation

(Hutyra et al., 2005; Salazar et al., 2007). One of the underlying reasons that models are challenged by simulating unprecedent climatic conditions, is their underrepresentation of plant diversity (Pavlick et al., 2013; Scheiter et al., 2013). Commonly, models represent plant functions based on a very small and discrete set of PFTs (plant functional types) and plant functional traits parameters are previously (*a priori)* defined (Prentice et al., 2007). Consequently, the diversity of plant life strategies, *i.e.*, the combination of traits, found in these model ecosystems is oversimplified and the emergence of alternative trait combinations in response to a changing environmental scenario is strongly limited or is not even captured due to the small number of PFTs that compose the communities (Fyllas et al., 2014; Mori et al., 2013; Sakschewski et al., 2016). As a result, fixed a priori defined parameters commonly lead to an overestimation of the impacts of environmental changes due to abrupt changes in plant performance and establishment success (Berzaghi et al., 2020; Pavlick et al., 2013; Sakschewski et al., 2016; Verheijen et al., 2015) and important mechanisms involved in ecosystem resilience, such as the functional reorganization of the plant community (Enquist & Enquist, 2011; Fauset et al., 2012, 2015; Wieczynski et al., 2019), are not represented in such model approaches.

The development of the models with a higher representation of trait variability, so-called trait-based vegetation models (*e.g.*, Fyllas et al., 2014; Joshi et al., 2020, 2022; Pavlick et al., 2013; Sakschewski et al., 2015; Scheiter et al., 2013; Schmitt et al., 2019) is an attempt to overcome these limitations of underrepresenting functional diversity with PFTs. Such a modeling approach allows replacing the small number of PFTs with a more realistic representation of functional diversity, and thus increasing the representation of possible functional traits combinations by several orders of magnitude (Pavlick et al., 2013; Reu et al., 2014; Webb et al., 2010; Wullschleger et al., 2014). This provides the opportunity to explore multiple aspects of plant ecology and community composition in combination with biogeochemical fluxes and pools (Berzaghi et al., 2020; Sakschewski et al., 2016; Zakharova et al., 2019). For example, trait-based vegetation models are able to explore the role of different components of plant functional diversity on ecosystem functioning, the processes that determine community assembly and structure, and how these interact with environmental changes (Fisher et al., 2018; Mason et al., 2005; Mouillot et al., 2013b; Song et al., 2014).

An increasing number of trait-based models has been applied to understand the impacts of climate change on ecosystem functioning and the role of functional diversity on these impacts. Nonetheless, most of the functional ecological aspects highlighted in the scientific literature remain underexplored (but see: Hofhansl et al., 2021). Few studies applying trait-based vegetation models have explored how environmental changes affect plant functional diversity *per se*, and when they do, the focus is specially on functional richness (Pappas et al., 2015; Sakschewski et al., 2016; Scheiter et al., 2013). None of them investigated how these changes affect the underlying components of functional diversity (*i.e.*, functional richness, evenness and divergence) and how these different components affect ecosystem functioning. Hence, despite the proposed mechanistic linkage between functional diversity and ecosystem functioning (Mason et al., 2005; Mouillot et al., 2013b), the ability of trait-based models to conjointly capture plant functional diversity and ecosystem functional responses to environmental changes has yet to be tested.

Building on these previous efforts, we here present a new trait-based vegetation model, the CArbon and Ecosystem functional-Trait Evaluation (CAETÊ) model. To assess the effect of including trait variability in vegetation models, we compare two approaches of CAETÊ: a standard PFT approach that represents vegetation through three PFTs (*i.e.,* low functional diversity) and a trait-based approach (hereafter called as PLS approach) that represents a higher level of functional diversity by using 3000 combinations of trait values that seeks to express the variability of plant life strategies (PLSs) found in nature. Six traits are used to characterize the PFTs and the PLSs: C allocation and C residence time in three plant structural compartments (leaves, wood and fine roots). We compared the performance of the two modeling approaches in representing vegetation C storage and NPP for the Amazon basin region to evaluate whether plant trait diversity improves the representation of biogeochemical cycling. We also applied a scenario of reduced precipitation in the study area and by comparing model results generated from either the low-diversity (*i.e.*, PFT) versus the high-diversity (*i.e.*, PLS) parameterization, we assess whether the degree of plant functional diversity affects the response of ecosystem to moisture deficits using vegetation C stocks as an indicative. Additional analyses are made with PLS approach to evaluate the impacts of lower water availability on simulated functional composition and functional diversity components (richness, evenness and divergence) and its association with the impacts on C storage.

2. Material and Methods

2.1.The CAETÊ model: an overview

We present an overview of the CAETÊ model and how the two used levels of diversity parametrization are defined. In this study, and for both approaches, we employed a non-transient version of the CAETÊ model, which calculates equilibrium solutions based on long-term mean monthly climate variables. The difference between the PFT and the PLS approach is only the degree of trait variability represented, the model process formulations and principles are the same for both. Each plant functional type (for PFT approach) or plant life strategy (for PLS approach) represents an average individual like in LPJ model (Sitch et al. 2003). The next section presents the procedures of model setup for this study, and the Supplementary Material SM.1 provides a more detailed description of the CAETÊ model.

For the PLS approach, the underlying premise for creating the PLSs is that the range of values of a functional trait observed in nature can be regarded as one axis of a multidimensional hypervolume formed by the combination of *n* chosen functional traits (Fig. 1; Blonder, 2017;

Villéger et al., 2008). In that sense, each point inside of this hypervolume is a unique combination of values for each of the functional traits representing a PLS. The values of traits that compose them are sampled from the complete range of values used as reference (see SM.1.1.1.). The volume occupied by the sampled traits can be seen as a potential functional space with tens of thousands of combinations. Like other trait-based models (*e.g.*, Pavlick et al., 2013; Reu et al., 2011), CAETÊ assumes that sampling an appropriate number of PLSs from the potential functional space (see sensitivity test in SM.2.), combined with an environmental filtering mechanism, allows the model to produce reasonable biogeochemical and functional diversity patterns. On the other hand, in its PFT approach, the model's user previously defines the number of PFTs and their traits values are based on previous vegetation models.

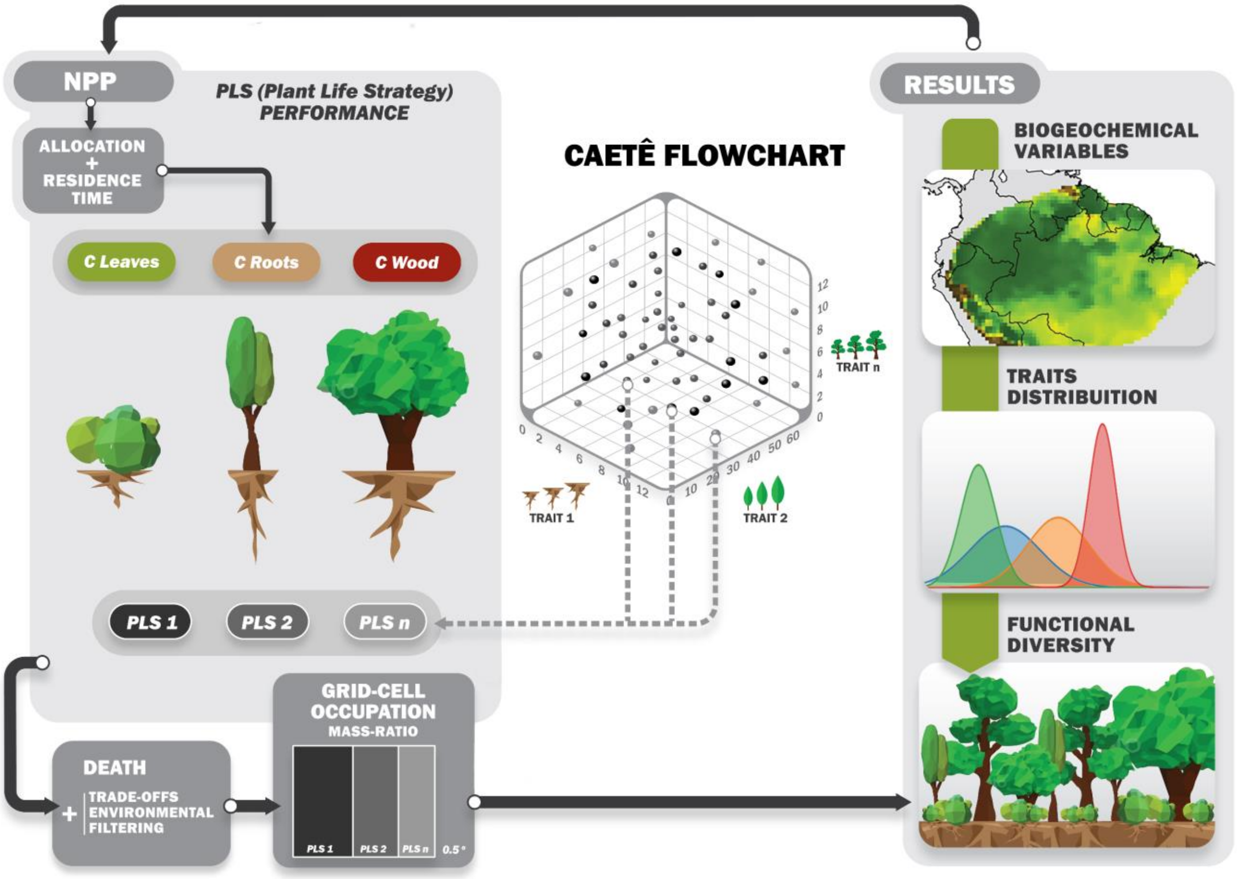

Figure 1. Schematic diagram of the CAETÊ functional trait-based model approach. From the initial plant functional trait ranges (the axis of the hypervolume), values are uniformly sampled and combined to create hundreds of thousands of what we define as plant life strategy (PLS). The set of all created PLSs composes a hypervolume that represents the potential functional trait space in which each point inside the volume is a unique combination of functional trait values. From the potential functional trait space, 3000 PLSs are randomly sampled. Environmental filtering, the trade-offs between functional traits and the physiological processes determine the performance of a PLS (abundance), if it survives (positive carbon balance) or dies and is excluded from the grid cell. Then, the grid cell is filled as a mosaic of PLSs, in which each of them occupies an amount of space proportional to its abundance, calculated from the PLS' relative contribution to the total carbon storage in that grid cell. From the PLSs occupation, the ecophysiological variables are updated and return to the model for iteration. This modeling framework allows us to assess the model results not only regarding biogeochemical variables but also in terms of trait distribution and, therefore, the different components of functional diversity. NPP: net primary productivity; C Leaves: amount of carbon allocated to leaves; C Roots: amount of carbon allocated to fine roots; C wood: amount of

The physiological processes and the interaction of each PLS/PFT with the environment are determined by several functional traits, for example the maximum rate of Rubisco carboxylation (Eq. SM.16) and nitrogen to carbon ratio on plant tissues (Eq. SM.25). However, in this study six functional traits are used to distinguish each PLS or PFT. Since the analyses presented here are focused on the assessment of vegetation C storage, three traits represent the C allocation percentage of the NPP distributed to different plant tissues/compartments (leaves, fine roots and wood), and the other three traits represented C residence time in the respective plant tissues. The combination of allocation and residence time for each tissue define its C stock and, then, the total plant C stock.

The functional trait values assigned to each PLS/PFT determine its ecophysiological behavior and its responses and effects to the environment. For example, each PLS/PFT, as a distinct combination of functional traits, constitutes a differential way of storing C and capturing water and light. Thus, the functional traits of a PLS or a PFT ultimately determine its performance and survivorship. During each iteration, in a daily time step, the distinct performances of PLSs/PFTs determines the ecosystem scale processes and properties (Eq. 6) such as GPP (growth primary productivity), evapotranspiration and C storage, which together with environmental conditions will determine the composition of PLSs and PFTs in each grid cell for the next iteration. The performance is determined as the relative abundance (Eq. 1) of a PLS/PFT in a specific grid cell.

From now on, the symbol i refers to an average individual of a PLS or PFT, y to a grid cell and z to a plant compartment. The values for the allocation (α) and residence time (τ) traits can be found on Table SM.1 for the PLS approach and on Table SM.2 for the PFT approach. The relative abundance ($A_{r_{i,y}}$) of a PLS/PFT is the fraction of the grid cell that it occupies based on the relative contribution of this strategy to the total carbon stock in this grid cell (C_{T_y}) considering the number of living PLS/PFT (S):

$$A_{r_{i,y}} = \frac{C_{i,y}}{C_{T_y}} \tag{1}$$

$$C_{T_y} = \sum_{i=1}^{S} C_{i,y} \tag{2}$$

where $C_{i,y}$ is the carbon stock of a PLS/PFT (Eq. 3). This procedure has support on the biomass-ratio hypothesis (Grime, 1998) which predicts that immediate effects of a species are proportional to its relative contribution to the total C storage of the community.

The $C_{i,y}$ is the sum of carbon stored ($C_{z_{i,y}}$) in each of the three plant compartments:

$$C_{i,y} = \sum_{z=1}^{3} C_{z_{i,y}} \tag{3}$$

and the $C_{z_{i,y}}$ in a certain time step t is determined by the percentage of $NPP_{i,y}$ allocated to each plant C compartment (α_{z_i}) and the carbon residence time (τ_{z_i}) in these compartments:

$$\frac{dC_{z_{i,y}}}{d_t} = \alpha_{z_i} NPP_{i,y} - \frac{C_{z_{i,y}}}{\tau_{z_i}} \tag{4}$$

$NPP_{i,y}$ is the carbon available for allocation derived from gross primary productivity ($GPP_{i,y}$; Eq. SM.3) discounting the costs of autotrophic respiration ($R_{a_{i,y}}$; Eq. SM.23):

$$NPP_{i,y} = GPP_{i,y} - R_{a_{i,y}} \tag{5}$$

From the relative abundances, it is possible to aggregate the biogeochemical variables from the PLS/PFT scale to the grid cell scale. That is, the flux or state of a variable in a grid cell is given by the sum of the values of this variable for each existing PLS/PFT (S) weighted by their relative abundance. For example, the net primary productivity in a grid cell scale (NPP_{grid_y}) is:

$$NPP_{grid_y} = \sum_{i=1}^{S} \left(NPP_{i,y} A_{r_{i,y}} \right) \tag{6}$$

Accordingly, the composition of PLSs/PFTs and their respective traits in a grid cell determine ecosystem scale processes and properties.

Each functional trait (F) is represented in a grid cell scale (F_{grid_y}) by a unique value, which is the sum of this trait value ($F_{i,y}$) calculated for each PLS/PFT alive in the grid cell, weighted by their relative abundances ($A_{r_{i,y}}$):

$$F_{grid_y} = \sum_{i=1}^{S} A_{r_{i,y}} F_{i,y} \tag{7}$$

This community weighted mean value can be understood as the dominant trait value in a community (Díaz et al., 2007).

Differential survival and performance between PLSs/PFTs are also possible because each functional trait is related to at least one trade-off (Pavlick et al., 2013; Reu et al., 2014). Trade-offs are here defined as relationships of costs and benefits that impact the ecophysiological processes of a PLS or functional type. They ultimately determine the PLS/PFT's performances and whether they will be able to deal with a specific environmental condition (Pavlick et al., 2013; Reu et al., 2011). Importantly, the trade-offs also prevent the model from enabling the survivorship of the so-called "Darwinian demons" (Law, 1979), in other words, optimal but rather unrealistic strategies that maximize all the functions that contribute to plant fitness and survival (Pavlick et al., 2013; Scheiter et al., 2013). For example, to respect mass conservation (Scheiter et al., 2013), any C investment (*i.e.*, allocation and residence time traits combination) in one tissue will always be at the expense of other: investing C in leaves can increase photosynthesis rate by increasing solar radiation absorption (Eq. SM.21 and SM.22), however, such investment is at the expense of investing in fine roots, which is responsible for water uptake, also a limiting resource for photosynthesis (Eq. SM.35). Beyond that, an intrinsic trade-off emerges from the allocation traits: per principle, their combination for each plant tissue must add up to 1 and the traits combination that do not respect this rule is excluded before model starts running (see SM.1.1.1). Carbon allocation strategies also lead to indirect competitive ability for light, what may also exclude life strategies (see SM.1.6.). The ecophysiological processes linked to each functional trait, its trade-offs, and associated formulations are summarized in Table SM.3.

2.2. Simulation setup

For both CAETÊ approaches, we employed mean monthly climate variables and atmospheric CO_2 concentration from 1980 to 2010 for the Amazon basin (Fig. SM.1) at a spatial resolution of 0.5º x 0.5º (see SM.1.2. for input data). For the modeling experiment, the precipitation was reduced in 50% for the same 1980-2010 monthly climatology used in the control. This reduction was homogeneous: it was applied for the whole period of the study and for all the grid cells equally. We are aware that the frequency and intensity of droughts are not homogeneous over time or along environmental gradients across the basin. Furthermore, this precipitation reduction is quite severe, despite having occurred in isolated events in the past (Marengo, 2008) and it is also within some projections (Cox et al., 2000; 2004; Betts et al., 2004). This massive decrease in water availability is also justifiable for modelling purposes as extreme scenarios can be used to test the sensibility of ecological processes and properties simulated. Then, for this study, we did not intend to make reliable predictions of drought for the region. Instead, we used this 50% precipitation reduction scenario as a proof of concept and as a mean to test our hypotheses once the effects of extreme drought events to ecosystem processes and biodiversity it is still not entirely clear (Allen et al., 2010).

For the PFT approach we defined 3 tropical PFTs, and their traits values were chosen based on those used by other vegetation models (Table SM.2). For the PLS approach we used 3000 PLSs, and this number was defined based on a sensitivity test (see Supplementary Material SM.2). The ranges of values of each functional trait considered in this approach were based on empirical/experimental literature and are presented in Table SM.1

In both approaches, all grid cells are initialized with the same set of PLSs or PFTs, under conditions that are analogous to bare soil. However, in each grid cell the PLSs/PFTs will perform differently such that some strategies will survive, each of them occupying a different portion of the cell, while others will be excluded from the spatial grain in the simulation and cannot be reestablished. Importantly, for this study, there is no repopulation of the PFTs or

PLSs excluded. Rather, the model is run until equilibrium with 3000 PLSs/3 PFTs and regular climate condition and, after, it is run again with the same 3000 PLSs/3 PFTs but with reduced precipitation. that is why it is possible that PLSs/PFTs can be excluded with regular climatic conditions but increase/decrease their abundance with reduced precipitation.

Before the model execution a model initialization phase is performed: (i) to determine the initial C content in plant compartments and it is run until the attaining the stability attained for the total C stock (*i.e*., the sum of C in all plant compartments) in all the grid cells (see details in SM.1.1.2); and (ii) to check the viability of each newly created PLS (see SM.1.1.1). After the initialization phase, the model runs by continuously repeating the input data series (under regular climate or under reduced precipitation) until the stability of simulated results was attained.

2.3. CAETÊ performance evaluation

The performance of the two modeling approaches in representing the spatial distribution of vegetation C storage and NPP in the Amazon region was compared with reference data. For C storage we used data from Baccini et al. (2012) and Saatchi et al. (2011); and for NPP the data came from MODIS NPP Project (MOD17A3; Running & Zhao, 2021). These comparisons were made under current climatic conditions (1980 – 2010). We considered that 47.5% of living dry biomass from reference data is comprised of C (Thomas & Martin, 2012). Following the reference data, only the aboveground component was considered. For the model performance evaluation, we estimated the absolute difference between maps from CAETÊ simulations and maps from reference data and a scatterplot analysis was performed to identify the trends in the model approaches simulations.

2.4. Assessing functional diversity and composition

In this study we focused on large-scale analyses of functional diversity and its components across the Amazon basin. It means that trait distributions used to evaluate functional diversity corresponds to the distribution of the set of dominant trait values obtained for each grid cell, as explained in section 2.1 (Eq. 4). As mentioned in the introduction, using only a small number of PFTs to represent variability precludes access to functional diversity analyses. Hence, functional diversity analyses are here limited only to the PLS approach.

Functional diversity and functional composition of communities were analyzed both considering each functional trait independently (single-trait analyses) and the combinations of traits (multi-trait analyses). The single-trait and multi-trait analyses allow a broader understanding of how the community occupies the functional trait space and how it is functionally organized by computing its composition (occurrence and abundance of trait values), the relative dominance between trait values and the functional diversity components.

In the single-trait analyses, distribution curves were generated by using the functional traits' occurrence following the study by Carmona et al. (2016), emphasizing that each trait value is derived from a grid cell. In this method, the full range of trait values is considered as the total functional trait space, and the occurrence and abundance of the trait values express the occupancy of this space calculated through probability density distributions, *i.e.*, the trait probability density distributions. From these distributions, we assessed the three functional diversity components as defined by Carmona et al. (2016): (i) functional richness: the amount of functional space occupied by the community, *i.e.* the total range of trait values for a specific functional trait considering all organisms (PLSs in our case); (ii) functional evenness: the regularity of the density distribution of the PLSs' trait values in the functional trait space; and (iii) functional divergence: the degree to which the abundance of trait values of PLSs are distributed toward the extremes of their functional trait space.

For the multi-trait analyses, we used the hypervolume metric proposed by Blonder et al. (2014), which combines the distribution of *n* trait values to create a multidimensional functional space and calculates functional diversity component metrics. Within such a hypervolume, the functional richness can be interpreted as the amount of volume that is occupied by the community relative to the potentially available functional space, based on the frequency of trait values that compose this community. The distribution of trait values around the centroid, that is, the variation around the mean value, can be used to evaluate the functional composition of the system (Barros et al., 2016). Following the recommendation by Barros et al. (2016), we performed a principal component analysis (PCA) with a centered and scaled method before creating the hypervolumes (for more detail, see SM.3). Using the factor scores on the chosen principal components, we were able to fulfill the statistical assumptions for constructing the hypervolumes.

Despite the focus of our analyses being on the basin scale, we made some additional functional diversity analyses on a finer scale using three spatial windows of 10x10 grid cells each along a northwest to southeast axis (Fig. SM.2). Looking into finer scales enables the evaluation whether the results obtained from the whole amazon basin scale analyses are not only a product of the natural environmental heterogeneity, once the basin is well known to present a large-scale variation in climatic and edaphic properties (Ter Steege et al., 2006; Quesada et al., 2012; Sombroek, 2000).

2.5 Assessing effects of decreased precipitation

In the experiment of 50% reduction in precipitation, we compared the degree of change in C stock between the two modeling approaches used in this study to evaluate if trait variability influences C storage under environmental change.

Further, from the results simulated by the PLS approach we also evaluated the role of the different components of functional diversity in this change. For this, we assessed whether the plant communities were functionally reorganized in the scenario of reduced precipitation by computing the dissimilarity index (degree of overlap) between the trait probability density distributions from the regular climate scenario and those from the reduced precipitation scenario

(Carmona et al. 2016). This index varies from 0 (completely functionally similar; overlapping density curves) to 1 (completely functionally different; no overlap). To estimate the changes in hypervolumes due to precipitation reduction we computed their overlap degree through the Jaccard similarity index, which ranges from 0 (completely different; no overlap) to 1 (completely similar, overlapping hypervolumes). In addition, we assessed whether a centroid displacement occurred with the applied precipitation reduction. The displacement indicates how much the mean values of the communities were dislocated from their previous location within the hypervolume. To test the degree of communities' functional reorganization we analyzed the changes in trait abundance throughout the functional space generated by the trait probability density distributions. From this analysis we were able to observe, for example, the exclusion of trait values and/or the increase in the occurrence of trait values that were rare under regular climatic conditions. To understand the impacts of precipitation reduction on functional diversity facets (richness, evenness, and divergence) for the single-trait analysis, we computed the percentage change in their values between regular and reduced precipitation climatic conditions. For the multi-trait analysis, we compared the hypervolume sizes before and after the reduced precipitation application once change in volume sizes represents a shift in the community functional richness. We also performed these analyses for the finer scale: we estimated the change in trait distributions with reduced precipitation using the same method described before (for single and multi-traits), but, in this scale, with focus on the functional reorganization of the community and on functional richness.

3. Results

3.1. CAETÊ model performance evaluation

Within the studied region, the PFT approach simulates 127.9 Pg C stored in aboveground C and the PLS approach simulates 86.0 Pg C, while Baccini et al (2012) estimates 80.2 Pg C of total aboveground C stock and Saatchi et al. (2011) estimates 71.7 Pg C. In terms of spatial patterns in vegetation C storage, both modeling approaches show over- or underestimation in the values simulated. The overestimation is especially concentrated in naturally drier areas, for example in North-Western Amazonia. We also observed an overestimation along the basin edges, which are known as regions of transition to drier areas, fire-prone vegetations and subject to the intensive land use (Haghtalab et al., 2020; Morton et al., 2013; Nobre et al., 2016). However, the CAETÊ in its PFT approach tends to show the overestimation in a much higher degree and in more locations throughout the basin, with emphasis on the central region and basin edges when compared to the PLS (Fig. 2). On the other hand, the PLS approach tends to underestimate mean C values in some regions, for example, in the east and southwest parts of the basin. The PLS approach presented more areas with no differences between simulated and reference values, (white cells in Figures 2b and 2e) and a higher number of points closer to the 1:1 line in the scatter plot (Fig. 2c and f) thereby matching the values used as reference reasonably well.

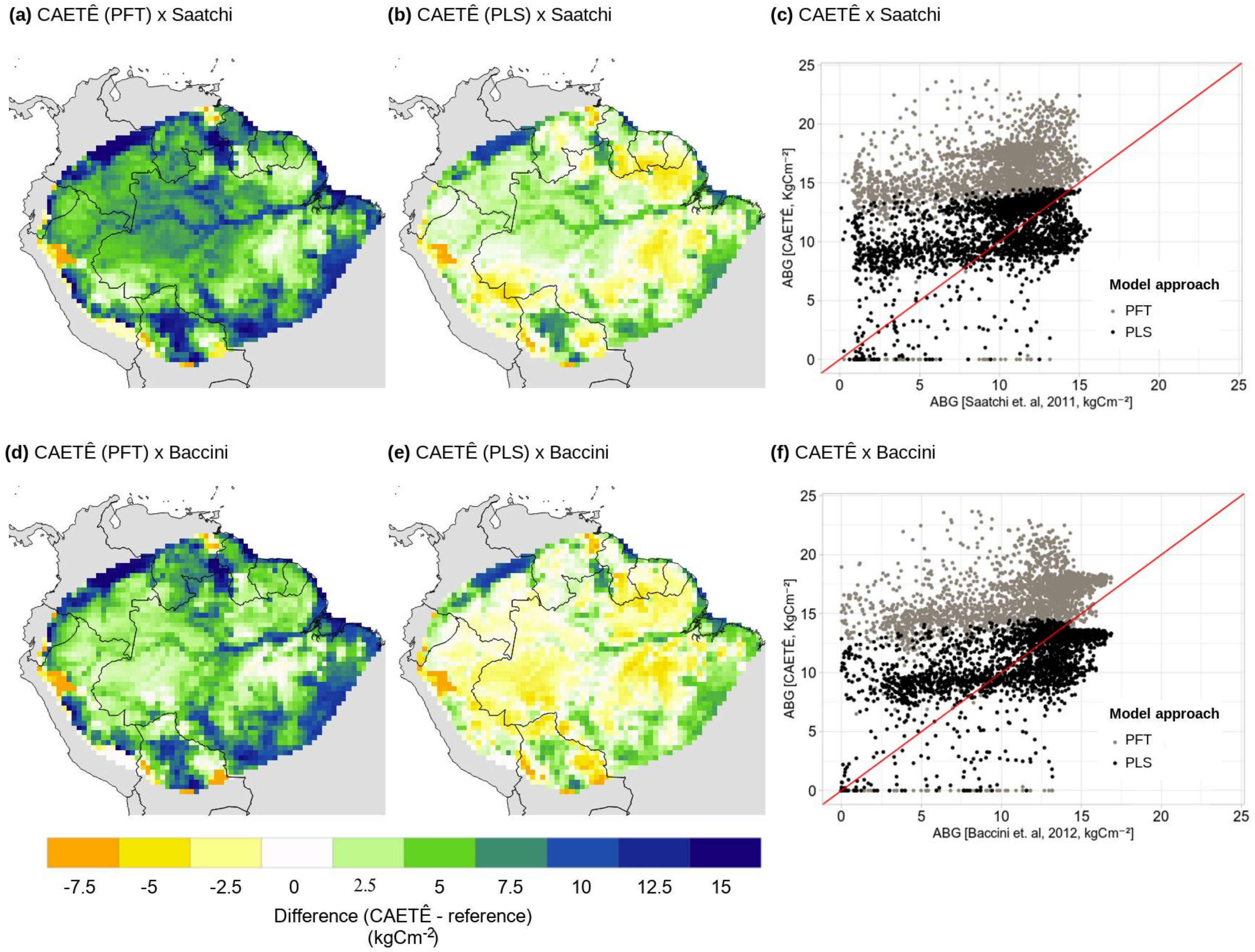

Figure 2. Evaluation of CAETÊ performance in representing aboveground carbon storage for both modeling approaches, PFT and trait-based approach, when compared to two reference maps: Baccini et al. (2012) and Saatchi et al. (2011). The plots (a), (b), (d) and (e) show the spatial absolute difference between values simulated by CAETÊ and those simulated by references. The plots (c) and (f) show the linear regression between CAETÊ and reference maps for all the simulated grid cells. The 1:1 line is represented in red. AGB: aboveground carbon storage. The carbon projected by CAETÊ can be found in the Supplementary Material (Fig. SM.8). PFT: PFT approach. PLS: trait-based approach.

The CAETÊ model simulated a total annual NPP of 122.3 Pg C yr^{-1} (PFT approach) and 76.0 Pg C yr^{-1} (PLS approach) for the Amazon basin. MODIS-based estimation is 74.6 Pg C yr^{-1} (Running & Zhao, 2021). By comparing the NPP simulated by CAETÊ with remote sensing NPP estimations (MODIS; Running & Zhao, 2021), the PLS approach revealed a reasonably good ability to capture broad spatial patterns of remotely sensed NPP estimations (MODIS; Running & Zhao, 2021; Fig. SM.3b and SM.3c), despite an underestimation in the Andean region and a small overestimation in the northwest/central basin region. In contrast, using a small number of PFTs resulted in a widespread and prominent overestimation for this variable (Fig. SM.3b and SM3c), except for the underestimation in the Andean region.

3.2. Carbon stocks under reduced precipitation

The 50% reduction in precipitation caused a widespread decrease in C stocks throughout the basin in both model approaches (Fig. 3a and b). When considering the whole basin, total C loss was equal to 73.48 Pg C and 49.43 Pg C for the PFT and PLS approach respectively, representing a similar percentage decrease compared to regular climatic conditions: -57.75% for PFT and -57.48% for PLS approach. However, the spatial pattern of change was significantly distinct. The PLS approach was able to maintain C stocks in several grid cells where none of the PFTs survived in the PFT approach. This difference is more evident in central Amazon and naturally drier areas, such as in the transition between the Amazon forest and the Cerrado savannah in the southeast. Furthermore, the C losses simulated by the PLS approach presents a smoother gradient between a grid cell value and its neighboring cells and across different basin regions, unlike in the PFT approach, which shows more abrupt differences between grid cells. Surprisingly, in grid cells where both modeling approaches maintained at least a minimum C stock, the PFT approach presented higher values when compared to those from the PLS one (Fig. 3a and b).

Specific plant compartments also showed distinct patterns of changes when comparing the employed modeling approaches (Fig. 3c and d for fine roots, Fig. SM.4 for leaves and wood). None of the compartments showed an increase in C stock with precipitation reduction, except for the fine roots compartment in the simulation with the PLS approach (blue areas in Fig. 3d), such an increase is more apparent in the transition between the Amazon and Cerrado and in the northeast part of the basin. The increased investment in fine roots resulted in a rise in the root:shoot ratio for the PLS approach, with an average increase of 74.7%, in contrast to an average decrease of 7.7% for the PFT approach.

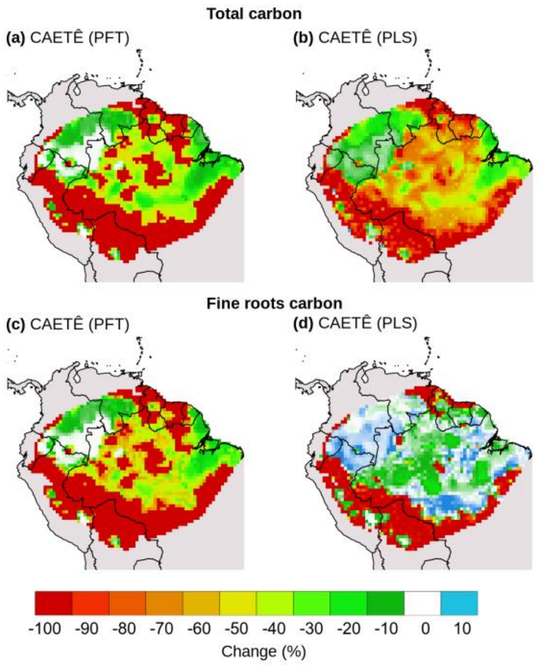

Figure 3. Percentage change in total carbon stock (a and b) and in fine roots carbon stock (c and d) after reduced precipitation application (-50%) for the two employed modeling approaches: PFT and trait-based approach. The change of carbon storage in the compartment of leaves and wood can be found in the Supplementary Material (Fig. SM.4). PFT: PFT approach. PLS: trait-based approach.

3.3. Effects of reduced precipitation on functional composition

After applying the precipitation reduction, we found high dissimilarity index values (close to 1; Table 1) owing to changes in the trait probability density distributions for the six plant functional traits (Fig. 4). These dissimilarities degrees indicate that the communities significantly changed in terms of their structure and composition under moisture stress. For example, trait composition shifted away from hyperdominance (decrease in the peaks of the curves) of a previously restricted range of values toward a density increase in other trait values that were previously rare (very low density) or absent (Fig. 4). Additionally, the traits in the hypervolumes presented a pronounced modification in the way they occupy the functional space

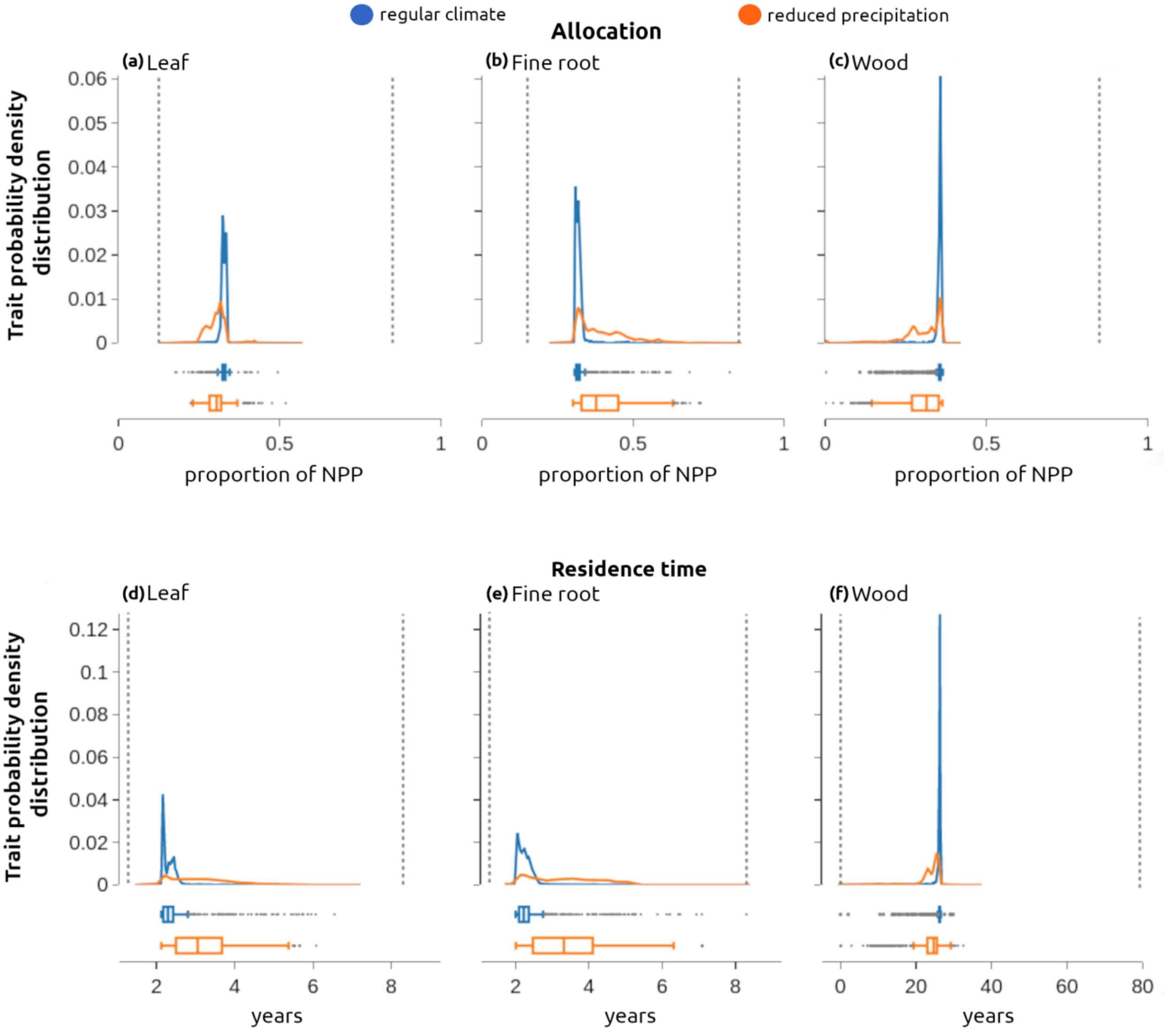

Figure 4. Density distributions of functional traits using the trait probability density method (Carmona et al., 2016) for the trait-based approach. The curves correspond to the probability density distribution of trait values across the Amazon basin. Each boxplot represents the median value and variance for each trait in each climatic condition. The boxes extend from the first to the third quartiles, and the whiskers extend from the minimum and maximum data. The outliers are shown in grey dots. The orange curves/boxplots represent the results with the applied low precipitation scenario, and the blue curves/boxplots represent the results concerning the regular climate conditions. The plots from (a) to (c) show the results concerning the allocation traits, and the plots from (d) to (f) display the results for the residence time traits. NPP: net primary productivity. The dissimilarities between the distributions before and after the reduced precipitation are presented in Table 1. Note that the scales of the y and x axes are different for allocation and residence time traits. The graphs are presented in this way to improve readability. The gray dotted lines represent the initial possible range of values for each trait (showed in Table SM.1). The plot (c) only shows one dotted line since the grass strategies present no allocation to wood tissues, hence the line in the point 0 overlap the y axes.

(Fig. 5): the overlap degree between the hypervolumes of the two climatic scenarios yielded a value of 0.038 when considering the whole Amazon. Finally, the centroid showed a displacement after imposing the climatic alteration, indicating a change in the communities' mean values and compositions (Fig. 5).

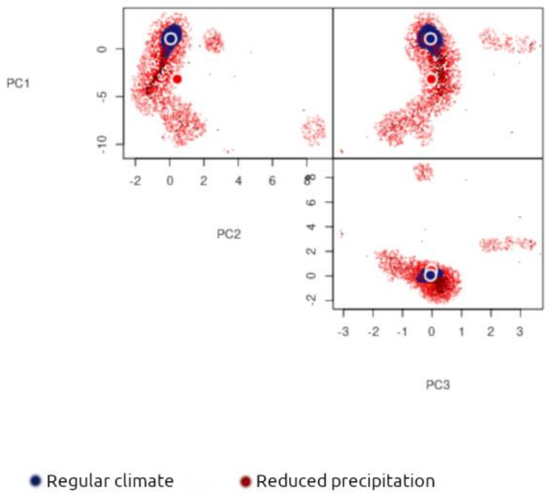

Figure 5. Hypervolumes created with the six functional traits together through the method of Blonder et al. (2018). The volumes here represented refer to the trait-based modeling approach simulations. The hypervolumes were created after the data were submitted to a PCA (see Fig. SM.10.). The blue points indicate the data in a regular climate scenario, and the red points indicate the scenario of -50% of precipitation in the study area. The darker the color of the point, the higher the density of the value within the functional space. The bigger circles represent the centroid (i.e., the mean values) of data distribution.

Beyond that, with lower water availability, the distribution of the single-traits along the functional space showed a higher diversity of values that presented an increase in density, that is, a higher probability of occurrence, which resulted in a much more diffuse distribution within the functional space (Fig. 4). The same pattern of distribution along functional space observed for single traits arose when considering all traits combined through the hypervolumes: an increase in the functional space occupation by the traits (Fig. 5). The increase in density was observed in traits with higher carbon allocation values to fine roots, lower carbon allocation to leaves and to wood (Fig. 4a, b and c). Also, higher values for carbon residence time in leaves and fine roots but a decrease in wood (Fig. 4d, e and f).

Regarding the analyses in the finer scale, our results show the same pattern that was found when considering the large scale (the whole Amazon basin): an increase in the occupation of the functional space for all the six functional traits in their probability distributions (Fig. SM.5 and SM.6) and an increase in the volume occupied when considering the six traits together (Fig.

SM.7). The high dissimilarity indices between trait probability density distributions with regular climate and decreased precipitation (Table SM.4), together with the small overlap between hypervolume, indicate that as well as found in the Amazon basin scale, the communities in the three 10x10 grid region underwent a functional restructuration.

Table 1. Dissimilarities of trait probability density distributions (Fig. 4) with the applied reduction in precipitation (-50%) for the PLS approach. The closer the value is to 1, the more dissimilar the curves are to each other.

Functional trait	Distribution dissimilarity
leaf allocation	0.680
root allocation	0.656
wood allocation	0.638
leaf residence time	0.678
root residence time	0.664
wood residence time	0.755

3.4. Reduced precipitation impacts on functional diversity facets

The alterations in the density distribution of functional traits drove changes in the three facets of functional diversity (Fig. 6). Functional richness and functional evenness increased in a level higher than 100% for all the six considered traits. Divergence had an increase of more than 200% for the leaf allocation trait, while the other traits displayed a reduction in this facet (Fig. 6c). From a multi-trait perspective, there was an increase in richness due to the enlargement in the volume occupied by the communities within the functional space (Fig. 5): under current climatic conditions, the size of the volume that the data occupied was equal to 1.71 while under reduced precipitation we found a volume size of 47.84.

On the finer scales, like in the whole basin, an increase in the range of trait values (Table SM.4) and in the volume occupied when considering the six traits together (Fig. SM.7) indicate a rise in functional richness. Beyond that, the curves from the trait probability density distributions (Fig. SM.5 and SM.6 and Table SM.4) showed a high distribution dissimilarity (~1) and the hypervolumes (regular climate and reduced precipitation) presented a small overlap for the three analyzed regions: 0.006, 0.001 and 0.007 for the northwest, the center and the southeast respectively.

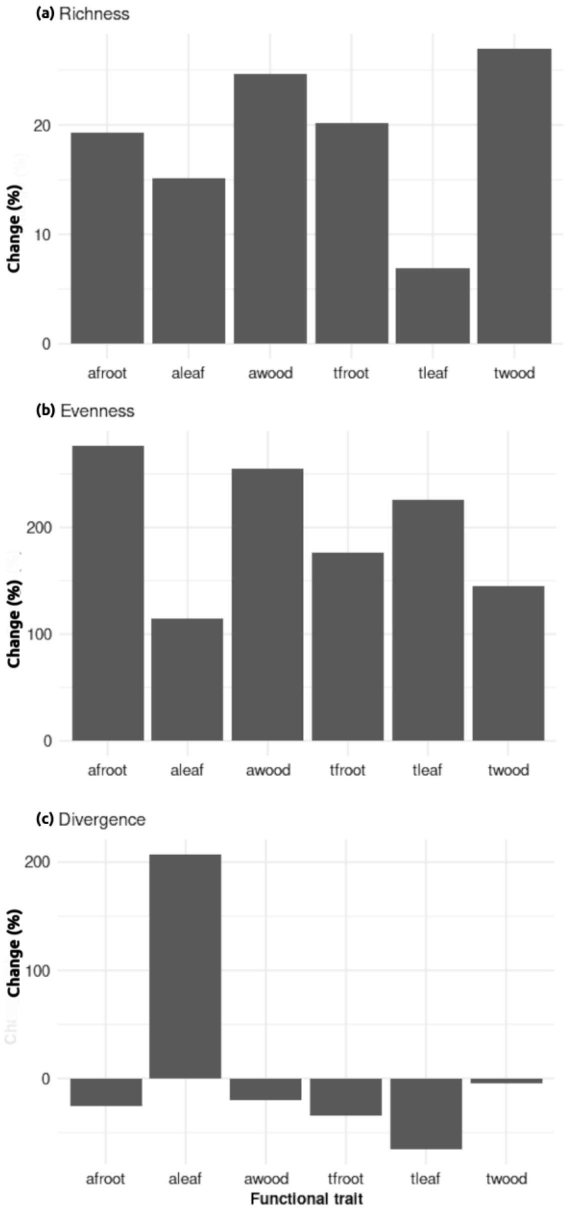

Figure 6. Percentage change in the functional diversity components (divergence, evenness and richness) with the applied precipitation reduction scenario (-50%) for trait-based approach. This results concern to the Amazon basin spatial scale. Allocation to fine roots (afroot), leaves (aleaf) and wood (awood). Carbon residence time for fine roots (tfroot), leaves (tleaf) and wood (twood).

4. Discussion

4.1. Model performance

Our results indicate that the inclusion of trait variability in vegetation models may lead to considerable improvement when simulating the vegetation C cycle with current climatic conditions. Compared to reference data (Fig. 2 and SM.3), our simulations with the PLS approach were able to represent NPP and vegetation C storage reasonably well and showed better agreement (spatial distribution and total values) than the PFT approach). Improved accuracy in biogeochemical variables has already been observed in other PFT-based models when trait variability was added (Fyllas et al., 2014; Sakschewski et al., 2015; Verheijen et al., 2013). Trait variability confers a higher diversity of community responses to environmental filtering through climatic heterogeneity, thereby allowing a more realistic simulation of plant community assembly (Keddy, 1992) avoiding a complete switch in vegetation state, such as a catastrophic Amazon dieback (Lapola et al., 2018), due to abrupt changes in plant performance and establishment success (Fyllas et al., 2014; Sakschewski et al., 2015; Scheiter et al., 2013).

Both modeling approaches show some mismatch with regard to the reference maps, such that there appears to be an overestimation of aboveground vegetation C storage and NPP, and especially so for the PFT approach (Fig. 2 and SM.3). This is because the PFTs (chosen from previous PFTs implemented in other vegetation models) are already parameterized to present a high performance (or optimal trait combination) in the climatic envelope found in regions dominated by tropical forests, which allowed a more frequent occurrence of PFTs with higher vegetation C storage (Scheiter et al., 2013; Verheijen et al., 2013). Furthermore, both approaches show a tendency to overestimate vegetation C storage and NPP at the edges and in the central/northwestern Amazon basin (Fig. 2 and SM.3). These inconsistencies could be attenuated through the improvement of some caveats of the CAETÊ model. First, such an overestimation can be linked to the lack of representation of human land use and fire for determining vegetation distribution in the model (Houghton et al., 2001; Saatchi et al., 2007). Another important caveat is that the model does not yet represent impacts on vulnerability to cavitation and embolism (Anderegg et al., 2016; Oliveira et al., 2021). The lack of representation of human land use, fire and plant hydraulics may be particularly important to achieve a more realistic representation of C storage in the edges of the basin (Eller et al., 2018; Joshi et al., 2020; Papastefanou et al., 2020, Rowland et al., 2015). Furthermore, nutrient cycling (nitrogen and phosphorus) is not represented in our model and low soil nutrient availability in the Amazon may limit vegetation C storage across the Amazon basin (Fleischer et al., 2019; Yang et al., 2019).

It is important to highlight that despite using the maps produced by Saatchi et al. (2011) and Baccini et al. (2012) as reference, these maps include other sources of uncertainties and therefore present different estimates of aboveground biomass across the Amazon basin.

4.2. Reduced precipitation impacts on vegetation carbon storage: comparing a PFT with a trait-based modeling approach

We found that, in accordance with previous literature (Enquist & Enquist, 2011; Fauset et al., 2012, 2015; Wieczynski et al., 2019), the inclusion of trait variability in vegetation models in fact matters for projecting the impacts of environmental change in ecosystems. Although the two approaches applied in this study (*i.e.*, PFT vs. PLS) show similar changes with regard to total basin vegetation C budget, spatial patterns showed that only considering this biogeochemical variable can hide important details about the mechanism in which trait diversity determines ecosystem functioning. For example, the inclusion of trait variability in the model avoided sharp boundaries (especially in naturally) in drier regions, showing a more subtle, less sensitive, and probably more realistic change in C stock across the basin (Fig. 3) when compared to models PFT based that commonly simulate the Amazon dieback (Cox et al., 2000, 2004; Lapola et al., 2009; Oyama and Nobre, 2003).

Disturbances are expected to trigger shifts in the occurrence and abundance of species/functional traits to adapt to the new environmental conditions (Aguirre-Gutiérrez et al., 2020; Barros et al., 2016; Esquivel-Muelbert et al., 2018). Such changes were well captured in our modeling experiment for the PLS approach: similarity/dissimilarity indices (for the single and multi-trait perspectives), together with centroid displacements, showed that the functional structure and composition of the plant communities were significantly modified by the climatic forcing scenario. This ability to functionally reorganize and cope with new climatic conditions in the PLS approach (allowed by trait variability) was decisive to the effects of reduced precipitation on both the total and the spatial distribution of C vegetation storage. Trait variability allows for functional density compensation process that counterbalances losses or decreases in the dominance of plant life strategies, thus decreasing the impact of perturbation on ecosystem functioning (Gonzalez & Loreau, 2009; Mori, Furukawa, & Sasaki, 2013; Sakschewski et al., 2016). On the other hand, in the PFT approach, alternative PFTs are too few to compensate for losses in establishments, hence, this model approach prevents better suited trait combinations to establish, leading to higher occurrence of grid cells in which none of the PFT's survived (Fig. 3). This severe effect of environmental change using a PFT approach corroborates other modeling studies (Huntingford et al., 2013; Sakschewski et al., 2016). Our results reinforce the importance of functional diversity for maintaining ecosystem functioning and give support for the "insurance hypothesis" (Mori, Furukawa, & Sasaki, 2013; Yachi & Loreau, 1999), thus strengthening the assumption that diversity can promote ecosystem stability (Tilman et al., 2006).

4.3. Functional composition and the selection of plant life strategies

The changes in functional composition and structure due to reduced precipitation in the PLS simulation is supported by the dissimilarity/similarity indices found between the trait probability density distributions and the hypervolumes, respectively. The centroids' displacements also showed that the dominant values (composition) were modified with the new climatic condition. This high capacity of communities in the PLS approach simulations to functionally reorganize enabled shifts in functional community composition, thus corroborating with the hypothesis of a selection toward plant strategies with higher investment in roots in drier climate conditions (Fig. 4b and e). The higher investment in roots simulated by the PLS approach was to the detriment of investment in leaves (Fig. 4a and d) and woody tissue (Fig. 4c and f), thus leading to higher root:shoot ratios. Higher root biomass enabled water uptake and allowed the community of the PLS simulation to better deal with the imposed moisture stress and maintain C stocks or reduce the degree of biomass loss when compared to the simulation using PFTs. The prioritization of root investment at the expense of other tissues in response to drought has been observed in manipulative ecosystem experiments and from monitoring forest inventory plots (Doughty et al., 2014; Kannenberg et al., 2019; Rowland et al., 2014). Given the limited trait variability, the PFT approach did not show these changes in C investment, increasing mortality rates and preventing the PFTs from establishing in some grid cells, thereby rendering the ecosystem more vulnerable in general (Fig. 3a), as predicted.

Notwithstanding, an unexpected result was that in some grid cells the amount of C stock in the PFT was higher than that in the PLS approach with the applied reduced precipitation (Fig. 3a and b). This occurred due to an increase in the root:shoot ratio in the simulations with high trait variability, that is, C was allocated toward pools with shorter turnover times (fine roots), which result in less total vegetation C storage (Chave et al., 2009; De Kauwe et al., 2014). Although the increase in fine roots in the PLS approach provides resistance to moisture stress, thereby preventing the total loss of carbon in several grid cells, it also led to lower vegetation C storage (in some locations) compared to the PFT approach. This result is contrary to the widely accepted paradigm that higher functional diversity maximizes ecosystem function (Cadotte, 2017; Tilman 1997; Tilman et al. 2014). Our findings of the community-wide reorganization and associated increase in trait variability in response to novel climatic conditions indicate that functional diversity *per se* does not necessarily maximize ecosystem functions and properties such as C storage (Chiang et al., 2016; Holzwarth et al., 2015) but that functional diversity can influence ecosystem functions in more than one direction (Hooper et al 2005; Shen et al 2016). In our study, the functional composition, and especially the dominant plant functional trait, was more critical in determining the C stock than functional richness, with other studies finding similar results (Chiang et al 2016; Finegan et al., 2015; Ruiz-Jaen and Potvin, 2011; Roscher et al., 2012). Overall, this suggests that trait-based modeling approaches can improve our mechanistic understanding of the linkage between functional diversity and ecosystem functioning.

4.4. Environmental changes modify functional diversity components

Our results from analyses of the PLS approach showed that a reduction of precipitation modified the way that traits occupy the functional space (Fig. 4 and 5) and, as consequence, the functional diversity facets (Fig. 6). For example, reduced precipitation led to a wider range of expressed trait values in functional space (Fig. 4 and 5) and thus increased the community's richness (Fig. 6a). This increase in functional richness contradicts the expected outcomes from the environmental filtering hypothesis (Keddy 1992, Grime 1998; Boersma et al., 2016; Funk et al., 2017; Perronne & Gaba, 2017). Our findings may be explained by a decrease in hyperdominance in response to simulated climate change, which allowed a higher range of ecological strategies to become viable, in accordance with the compensatory dynamics theory (Gonzales & Loreau, 2009; Walker et al., 1999). Importantly, these results provide further evidence that environmental filtering not always reduce trait diversity (Le Bagousse-Pinget et al. 2017, Laughlin & Laughlin 2013) and that functional richness can increase after disturbance, especially so if environmental change mainly affects the dominant plant functional strategies (Boersma et al., 2016; Funk et al., 2017; Mouillot et al., 2013a). Beyond that, it is necessary to consider that the role of the environmental filtering as a driver of functional structure will strongly depend on the traits being considered (de La Riva et al., 2017).

The observed increase in functional richness is also certainly linked to the CAETÊ functioning mechanism. Model experiment of reduced precipitation resulted in higher functional richness mainly to the increase in the range of traits values of traits related to roots C allocation and residence time, which in turn, thanks to the considered trade-offs, was metabolically balanced by increases in functional richness related to other traits. In addition, one could hypothesize that the overestimation of C storage in drier regions at the edges of the Amazon basin would be the cause of higher simulated functional richness under reduced precipitation. However, it is more reasonable to first consider that, at the community scale, higher C stock may not be directly linked to functional richness. For instance, we found that despite the model simulates higher value for total C in the northwest of the Amazon basin, this region also showed lower functional richness than the southeast for all the functional traits, beyond a smaller increase of functional richness with reduced precipitation (Table SM.4 and Fig. SM.5 and SM.6), and the concentration of trait values in certain restricted areas of the functional space/volume could be one of the causes of such pattern.

There was an increase in evenness in all traits considered in the PLS approach (Fig. 6b). The evenness increase is tightly related to the observed decrease in dominance and increase in the abundance of trait values that were very rare in regular climate condition. Evenness can also be interpreted as evidence of the effectiveness of using the functional niche space; the higher the evenness is, the higher the utilization of the total functional space is (De La Riva et al., 2017; Hillebrand et al., 2008; Mouillot et al., 2011). Therefore, our results indicate that a change in the environment can force the community to better occupy the functional niche space, thus providing a lower sensitivity to the applied reduced precipitation, if the community presents sufficient variability in its trait values.

We observed a general decrease in divergence (Fig. 6c), which was caused by the strong decrease in abundance of previous dominant trait values which tended to concentrate at the extremes of functional spaces with the regular climate condition. Consequently, other trait values, concentrated along the functional axis, that were not as abundant became significant for the community after the reduction in precipitation. Based on empirical evidence obtained by analyzing a disturbance gradient, Mouillot et al. (2013a) also found a decreasing divergence with greater disturbance, which was attributed to a declining in the abundance of specialist species that were the most impacted by the disturbance. In addition, this decrease in divergence can be additional evidence that the frequency distribution of trait values in the functional niche space maximizes the total community variation in functional characters (Mason et al., 2005).

It could be argued that the observed changes in functional diversity, especially the increase in functional richness, can be attributed to the fact that we considered the whole Amazon basin as a single ecological unit while it is known that a high environmental heterogeneity exists throughout the basin. However, a similar pattern was found across a gradient of precipitation sampled from the northwest, center and southeast of the Amazon basin (Fig. SM.5, SM.6 and SM.7). This finding highlight that our results are not dependent on the spatial scale of analysis or the degree of environmental heterogeneity. Nevertheless, to avoid a simplification of diversity when considering large spatial scales, we recommend that future studies should try to integrate functional diversity across spatial scales, in this case from grid cells to the whole Amazon basin, as described in Carmona et al. (2016).

5. Concluding remarks

In this study, we show that incorporating trait variability in a vegetation model improves accuracy in representing ecosystem functioning and also plays an import role on ecosystem response to climate change. The trait-based modeling approach allows for a more in dept analysis on the mechanisms that connect ecosystem functioning and the different components of functional diversity. With the PLS approach, we show that the traits diversity allows the community to functionally reorganize under environmental changes, occupying a greater amount of functional space and increasing the occurrence of strategies that deal better with the applied lower water availability (higher investment in fine roots). Investment in roots at the expense of investment in leaves and wood led to a relatively lower total carbon storage. Functional reorganization also triggered changes in the primary components of functional diversity: increase in richness and evenness, and decrease in divergence. On the other hand, the use of a small number of PFTs restrict changes in the functional structure of the community, leading to a more expressive impact of environmental change on ecosystem functioning. In addition, PFT approach hinders the assess to functional diversity analyses.

This study brings further evidence that the inclusion of trait variability may have implications for modeling the so-called Amazon tipping point (Lovejoy and Nobre, 2018) since a trait-based-like approach would potentially yield more subtle, but not necessarily less relevant, responses of the forest vegetation to extreme climate change (Sakschewski et al., 2015).

Acknowledgments

This study has been financed by Sao Paulo Research Foundation – FAPESP through grants to BFR (2019/04223-0), JPDF (2017/00005-3), and DML (2015/02537-7), related to the AmazonFACEʃME project (labterra.cpa.unicamp.br/amazonface-me/). This study was also financed in part by the Coordenação de Aperfeiçoamento de Pessoal de Nível Superior - Brasil (CAPES) through grants to BFR (88887.177275/2018-00). KF acknowledges funding from the German Research Foundation (DFG) project R2060/5-1. FH gratefully acknowledges funding from IIASA and the National Member Organizations that support the institute.

The authors of this manuscript have no conflict of interest to declare.

Data Availability Statement

The data that support the findings of this study are openly available on GitHub at https://github.com/BiancaRius/CAETE_Rius_etal_2021

6. References

Adler, P.B., Salguero-Gómez, R., Compagnoni, A., Hsu, J.S., Ray-Mukherjee, J., Mbeau-Ache, C., Franco, M., 2014. Functional traits explain variation in plant lifehistory strategies. *Proc. Natl. Acad. Sci. U. S. A.*, 111, 740–745. https://doi.org/10.1073/pnas.1315179111

Allen, C.D., Macalady, A.K., Chenchouni, H., Bachelet, D., McDowell, N., … Cobb, N., 2010. A global overview of drought and heat-induced tree mortality reveals emerging climate change risks for forests. *For. Ecol. Manage*. 259, 660–684. https://doi.org/10.1016/j.foreco.2009.09.001

Aguirre-Gutiérrez, J., Oliveras, I., Rifai, S., Fauset, S., Adu-Bredu, S., Affum-Baffoe, K., ... Malhi, Y.S., 2019. Drier tropical forests are susceptible to functional changes in response to a long- term drought. *Ecology Letters*. 855–865. https://doi.org/10.1111/ele.13243

Aguirre-Gutiérrez, J., Malhi, Y., Lewis, S.L., Fauset, S., Adu-Bredu, S., ... Oliveras, I., 2020. Long-term droughts may drive drier tropical forests towards increased functional, taxonomic and phylogenetic homogeneity. *Nat. Commun.* 11, 1–10. https://doi.org/10.1038/s41467-020-16973-4

Anderegg, W.R.L., Klein, T., Bartlett, M., Sack, L., Pellegrini, A.F.A., Choat, B., Jansen, S., 2016. Meta-analysis reveals that hydraulic traits explain cross-species patterns of drought-induced tree mortality across the globe. *Proc. Natl. Acad. Sci. U. S. A.* 113, 5024–5029. https://doi.org/10.1073/pnas.1525678113

Avitabile, V., Herold, M., Heuvelink, G.B.M., Lewis, S.L., Phillips, O.L., Asner, G.P., … Willcock, S., 2016. An integrated pan-tropical biomass map using multiple reference datasets. *Glob. Chang. Biol.* 22, 1406–1420. https://doi.org/10.1111/gcb.13139

Baccini, A., Goetz, S. J., Walker, W. S., Laporte, N. T., Sun, M., Sulla-Menashe, D., … Houghton, R. A., 2012. Estimated carbon dioxide emissions from tropical deforestation improved by carbon-density maps. *Nature Clim. Change*, *2*(3), 182–185. https://doi.org/10.1038/nclimate1354

Barros, C., Thuiller, W., Georges, D., Boulangeat, I., & Münkemüller, T., 2016. N-dimensional hypervolumes to study stability of complex ecosystems. *Ecology Letters*, *19*(7), 729–742. https://doi.org/10.1111/ele.12617

Berzaghi, F., Wright, I.J., Kramer, K., Oddou-Muratorio, S., Bohn, … Hartig, F., 2020. Towards a New Generation of Trait-Flexible Vegetation Models. *Trends Ecol. Evol.*, 35, 191–205. https://doi.org/10.1016/j.tree.2019.11.006

Betts, R.A., Cox, P.M., Collins, M., Harris, P.P., Huntingford, C., Jones, C.D., 2004. The role of ecosystem-atmosphere interactions in simulated Amazonian precipitation decrease and forest dieback under global climate warming. *Theor. Appl. Climatol.* 78, 157–175. https://doi.org/10.1007/S00704-004-0050-Y/METRICS

Blonder, B., 2017. Hypervolume concepts in niche- and trait-based ecology. *Ecography*, (August), 1–13. https://doi.org/10.1111/ecog.03187

Blonder, B., Lamanna, C., Violle, C., & Enquist, B. J., 2014. The n-dimensional hypervolume. *Global Ecology and Biogeography*, *23*(5), 595–609. https://doi.org/10.1111/geb.12146

Boersma, K. S., Dee, L. E., Miller, S. J., Bogan, M. T., Lytle, D. A., & Gitelman, A. I., 2016. Linking multidimensional functional diversity to quantitative methods: A graphical hypothesis-evaluation framework. *Ecology*, *97*(3), 583–593. https://doi.org/10.1890/15-0688

Bongers, F., Poorter, L., Hawthorne, W.D., Sheil, D., 2009. The intermediate disturbance hypothesis applies to tropical forests, but disturbance contributes little to tree diversity. *Ecol. Lett.* 12, 798–805. https://doi.org/10.1111/j.1461-0248.2009.01329.x

Cadotte, M. W., Carscadden, K., & Mirotchnick, N., 2011. Beyond species: Functional diversity and the maintenance of ecological processes and services. *Journal of Applied Ecology*, *48*(5), 1079–1087. https://doi.org/10.1111/j.1365-2664.2011.02048.x

Cadotte, M. W., 2017. Functional traits explain ecosystem function through opposing mechanisms. *Ecology Letters*, *20*(8), 989–996. https://doi.org/10.1111/ele.12796

Cannell, M. G. R., & Dewar, R. C., 1994. *Carbon Allocation in Trees - a Review of Concepts for Modeling*. *Advances in Ecological Research* (Vol. 25. https://doi.org/10.1016/s0065-2504(08)60213-5

Carmona, C. P., de Bello, F., Mason, N. W. H., & Lepš, J., 2016. Traits Without Borders: Integrating Functional Diversity Across Scales. *Trends in Ecology and Evolution*, *31*(5), 382–394. https://doi.org/10.1016/j.tree.2016.02.003

Carmona, C. P., de Bello, F., Mason, N. W. H., & Lepš, J., 2019. Trait probability density (TPD): measuring functional diversity across scales based on TPD with R. *Ecology*, *100*(12), 1–8. https://doi.org/10.1002/ecy.2876

Chave, J., Coomes, D., Jansen, S., Lewis, S. L., Swenson, N. G., & Zanne, A. E., 2009. Towards a worldwide wood economics spectrum. *Ecology Letters*, *12*(4), 351–366. https://doi.org/10.1111/j.1461-0248.2009.01285.x

Chiang, J.M., Spasojevic, M.J., Muller-Landau, H.C., Sun, I.F., Lin, Y., Su, S.H., Chen, Z.S., Chen, C.T., Swenson, N.G., McEwan, R.W., 2016. Functional composition drives ecosystem function through multiple mechanisms in a broadleaved subtropical forest. *Oecologia,* 182, 829–840. https://doi.org/10.1007/s00442-016-3717-z

Cornwell, W. K., Schwilk, D. W., & Ackerly, D. D., 2006. A Trait-Based Test for Habitat Filtering: Convex Hull Volume. *Ecology*, *87*(6), 1465–1471. http://www.jstor.org/stable/20069097

Cox, P M, Betts, R. a, Jones, C. D., Spall, S. a, & Totterdell, I. J., 2000. Acceleration of global warming due to carbon-cycle feedbacks in a coupled climate model. *Nature*, *408*(6809), 184–187. https://doi.org/10.1038/35041539

Cox, Peter M., Betts, R. a., Collins, M., Harris, P. P., Huntingford, C., & Jones, C. D., 2004. Amazonian forest dieback under climate-carbon cycle projections for the 21st century. *Theoretical and Applied Climatology*, *78*(1–3), 137–156. https://doi.org/10.1007/s00704-004-0049-4

Da Costa, A. C. L., Galbraith, D., Almeida, S., Portela, B. T. T., da Costa, M., de Athaydes Silva Junior, J., … Meir, P., 2010. Effect of 7 yr of experimental drought on vegetation dynamics and biomass storage of an eastern Amazonian rainforest. *New Phytologist*, *187*(3), 579–591. https://doi.org/10.1111/j.1469-8137.2010.03309.x

De Bello, F., Lavorel, S., Hallett, L. M., Valencia, E., Garnier, E., Roscher, C., … Lepš, J., 2021. Functional trait effects on ecosystem stability: assembling the jigsaw puzzle. *Trends in Ecology and Evolution*, *36*(9), 822–836. https://doi.org/10.1016/j.tree.2021.05.001

De Kauwe, M. G., Medlyn, B. E., Zaehle, S., Walker, A. P., Dietze, M. C., Wang, Y. P., … Norby, R. J., 2014. Where does the carbon go? A model-data intercomparison of vegetation carbon allocation and turnover processes at two temperate forest free-air CO2 enrichment sites. *New Phytologist*, *203*(3), 883–899. https://doi.org/10.1111/nph.12847

De La Riva, E. G., Lloret, F., Pérez-Ramos, I. M., Marañón, T., Saura-Mas, S., Díaz-Delgado, R., & Villar, R., 2017. The importance of functional diversity in the stability of Mediterranean shrubland communities after the impact of extreme climatic events. *Journal of Plant Ecology*, *10*(2), 281–293. https://doi.org/10.1093/jpe/rtw027

Díaz, S., & Cabido, M., 2001. Vive la difference: plant functional diversity matters to ecosystem processes. *Proceedings. Biological Sciences / The Royal Society*, *16*(4), 646–655. https://doi.org/10.1098/rspb.2010.1923

Díaz, S., Lavorel, S., de Bello, F., Quétier, F., Grigulis, K., Robson, T.M., 2007. Incorporating plant functional diversity effects in ecosystem service assessments. *Proc. Natl. Acad. Sci. U. S. A.,* 104, 20684–20689. https://doi.org/10.1073/pnas.0704716104

Doughty, C. E., Malhi, Y., Araujo-Murakami, A., Metcalfe, D. B., Silva-Espejo, J. E., Arroyo, L., … Ledezma, R., 2014. Allocation trade-offs dominate the response of tropical forest growth to seasonal and interannual drought. *Ecology*, *95*(8), 2192–2201. https://doi.org/10.1890/13-1507.1

Eller, C. B., Barros, F. de V., Bittencourt, P. R. L., Rowland, L., Mencuccini, M., & Oliveira, R. S., 2018. Xylem hydraulic safety and construction costs determine tropical tree growth. *Plant Cell and Environment*, *41*(3), 548–562. https://doi.org/10.1111/pce.13106

Enquist, B. J., & Enquist, C. A. F., 2011. Long-term change within a Neotropical forest: Assessing differential functional and floristic responses to disturbance and drought. *Global Change Biology*, *17*(3), 1408–1424. https://doi.org/10.1111/j.1365-2486.2010.02326.x

Enquist, B. J., Bentley, L. P., Shenkin, A., Maitner, B., Savage, V., Michaletz, S., … Malhi, Y., 2017. Assessing trait-based scaling theory in tropical forests spanning a broad temperature gradient. *Global Ecology and Biogeography*, *26*(12), 1357–1373. https://doi.org/10.1111/geb.12645

Esquivel-Muelbert, A., Galbraith, D., Dexter, K. G., Baker, T. R., Lewis, S. L., Meir, P., … Phillips, O. L., 2017. Biogeographic distributions of neotropical trees reflect their directly measured drought tolerances. *Scientific Reports*, *7*(1), 1–11. https://doi.org/10.1038/s41598-017-08105-8

Esquivel-Muelbert, A., Baker, T. R., Dexter, K. G., Lewis, S. L., Brienen, R. J. W., Feldpausch, T. R., … Phillips, O. L., 2018. Compositional response of Amazon forests to climate change. *Global Change Biology*, (June 2018), 39–56. https://doi.org/10.1111/gcb.14413

Fauset, S., Baker, T. R., Lewis, S. L., Feldpausch, T. R., Affum-Baffoe, K., Foli, E. G., … Etienne, R., 2012. Drought-induced shifts in the floristic and functional composition of tropical forests in Ghana. *Ecology Letters*. https://doi.org/10.1111/j.1461-0248.2012.01834.x

Fauset, S., Johnson, M. O., Gloor, M., Baker, T. R., Monteagudo M., A., Brienen, R. J. W., … Phillips, O. L., 2015. Hyperdominance in Amazonian forest carbon cycling. *Nature Communications*, *6*, 6857. https://doi.org/10.1038/ncomms7857

Finegan, B., Peña-Claros, M., de Oliveira, A., Ascarrunz, N., Bret-Harte, M.S., Carreño-Rocabado, G., ... Poorter, L., 2015. Does functional trait diversity predict above-ground biomass and productivity of tropical forests? Testing three alternative hypotheses. *J. Ecol.*, 103, 191–201. https://doi.org/10.1111/1365-2745.12346

Fisher, R.A., Koven, C.D., Anderegg, W.R.L., Christoffersen, B.O., Dietze, M.C., … T., Moorcroft, P.R., 2018. Vegetation demographics in Earth System Models: A review of progress and priorities. *Glob. Chang. Biol.*, 24, 35–54. https://doi.org/10.1111/gcb.13910

Fleischer, K., Rammig, A., De Kauwe, M. G., Walker, A. P., Domingues, T. F., Fuchslueger, L., … Lapola, D. M., 2019. Amazon forest response to CO2 fertilization dependent on plant phosphorus acquisition. *Nature Geoscience*, *12*(9), 736–741. https://doi.org/10.1038/s41561-019-0404-9

Funk, J. L., Larson, J. E., Ames, G. M., Butterfield, B. J., Cavender-Bares, J., Firn, J., … Wright, J., 2017. Revisiting the Holy Grail: using plant functional traits to understand ecological processes. *Biological Reviews*, *92*(2), 1156–1173. https://doi.org/10.1111/brv.12275

Fyllas, N. M., Gloor, E., Mercado, L. M., Sitch, S., Quesada, C. a., Domingues, T. F., … Lloyd, J., 2014. Analysing Amazonian forest productivity using a new individual and trait-based model (TFS v.1. *Geoscientific Model Development*, *7*, 1251–1269. https://doi.org/10.5194/gmd-7-1251-2014

Galbraith, D., Levy, P. E., Sitch, S., Huntingford, C., Cox, P., Williams, M., & Meir, P., 2010. Multiple mechanisms of Amazonian forest biomass losses in three dynamic global vegetation models under climate change. *The New Phytologist*, *187*, 647–665. https://doi.org/10.1111/j.1469-8137.2010.03350.x

Gonzalez, A., & Loreau, M., 2009. The Causes and Consequences of Compensatory Dynamics in Ecological Communities. *Annu.Rev.Ecol.Syst.*, *40*, 393–414. https://doi.org/10.1146/annurev.ecolsys.39.110707.173349

Grime, J. P., 1998. Benefits of plant diversity to ecosystems: Immediate, filter and founder effects. *Journal of Ecology*, *86*(6), 902–910. https://doi.org/10.1046/j.1365-2745.1998.00306.x

Haghtalab, N., Moore, N., Heerspink, B.P., Hyndman, D.W., 2020. Evaluating spatial patterns in precipitation trends across the Amazon basin driven by land cover and global scale forcings. *Theor. Appl. Climatol*. 140, 411–427. https://doi.org/10.1007/s00704-019-03085-3

Herben, T., Klimešová, J., Chytrý, M., 2018. Effects of disturbance frequency and severity on plant traits: An assessment across a temperate flora. *Funct. Ecol.*, 32, 799–808. https://doi.org/10.1111/1365-2435.13011

Hillebrand, H., Bennett, D. M., & Cadotte, M. W., 2008. Consequences of Dominance: a Review of Evenness Effects on Local and Regional Ecosystem Processes. *Ecology*, *89*(6), 1510–1520. https://doi.org/10.1890/07-1053.1

Hofhansl, F., Chacón-Madrigal, E., Brännström, Å., Dieckmann, U., & Franklin, O., 2021. Mechanisms driving plant functional trait variation in a tropical forest. *Ecology and Evolution*. https://doi.org/10.1097/bot.0000000000002145

Holzwarth, F., Rüger, N., Wirth, C., 2015. Taking a closer look: Disentangling effects of functional diversity on ecosystem functions with a trait-based model across hierarchy and time. *R. Soc. Open Sci.*, 2. https://doi.org/10.1098/rsos.140541

Hooper, D.U., Chapin, F.S., Ewel, J.J., Hector, A., Inchausti, P., Lavorel, S., … Wardle, D.A.,

2005. Effects of biodiversity on ecosystem functioning: A consensus of current knowledge. *Ecol. Monogr.*, 75, 3–35. https://doi.org/10.1890/04-0922

Houghton, R. a, Lawrence, K. T., Hackler, J. L., & Brown, S., 2001. The spatial distribution of forest biomass in the Brazilian Amazon: a comparison of estimates. *Global Change Biology*, *7*(7), 731–746. https://doi.org/DOI 10.1046/j.1365-2486.2001.00426.x

Hubau, W., Lewis, S. L., Phillips, O. L., Affum-Baffoe, K., Beeckman, H., Cuní-Sanchez, A., … Zemagho, L., 2020. Asynchronous carbon sink saturation in African and Amazonian tropical forests. *Nature*, *579*(7797), 80–87. https://doi.org/10.1038/s41586-020-2035-0

Huntingford, C., Zelazowski, P., Galbraith, D., Mercado, L. M., Sitch, S., Fisher, R., … Cox, P. M., 2013. Simulated resilience of tropical rainforests to CO2-induced climate change. *Nature Geoscience*, *6*(4), 268–273. https://doi.org/10.1038/ngeo1741

Hutyra, L. R., Munger, J. W., Nobre, C. A., Saleska, S. R., Vieira, S. A., & Wofsy, S. C., 2005. Climatic variability and vegetation vulnerability in Amazŏnia. *Geophysical Research Letters*, *32*(24), 1–4. https://doi.org/10.1029/2005GL024981

Joshi, J., Stocker, B. D., Hofhansl, F., Zhou, S., Dieckmann, U., & Prentice, I. C., 2020. Towards a unified theory of plant photosynthesis and hydraulics. *BioRxiv*. https://doi.org/10.1101/2020.12.17.423132

Joshi, J., Stocker, B.D., Hofhansl, F., Zhou, S., Dieckmann, U., & Prentice, I. C., 2022. Towards a unified theory of plant photosynthesis and hydraulics. *Nat. Plants,* 8, 1304–1316. https://doi.org/10.1038/s41477-022-01244-5

Kannenberg, S. A., Novick, K. A., Alexander, M. R., Maxwell, J. T., Moore, D. J. P., Phillips, R. P., & Anderegg, W. R. L., 2019. Linking drought legacy effects across scales: From leaves to tree rings to ecosystems. *Global Change Biology*, *25*(9), 2978–2992. https://doi.org/10.1111/gcb.14710

Keddy, P. A., 1992. Assembly and response rules: two goals for predictive community ecology. *Journal of Vegetation Science*, *3*(2), 157–164. https://doi.org/10.2307/3235676

Kleidon, A., Adams, J., Pavlick, R., & Reu, B., 2009. Simulated geographic variations of plant species richness, evenness and abundance using climatic constraints on plant functional diversity. *Environmental Research Letters*, *4*(1), 014007. https://doi.org/10.1088/1748-9326/4/1/014007

Koch, A., Hubau, W., & Lewis, S. L., 2021. Earth System Models Are Not Capturing Present-Day Tropical Forest Carbon Dynamics. *Earth's Future*, *9*(5), 1–19. https://doi.org/10.1029/2020EF001874

Lapola, D. M., Oyama, M. D., & Nobre, C. A., 2009. Exploring the range of climate biome projections for tropical South America: The role of CO2 fertilization and seasonality. *Global Biogeochemical Cycles*, *23*(3), 1–22. https://doi.org/10.1029/2008GB003357

Lapola, D.M., Pinho, P., Quesada, C.A., Strassburg, B.B.N., Rammig, A., ... Nobre, C.A., 2018. Limiting the high impacts of Amazon forest dieback with no-regrets science and policy action. *Proc. Natl. Acad. Sci. U. S. A.* 115, 11671–11679. https://doi.org/10.1073/pnas.1721770115

Law R., 1979. Ecological determinants in the evolution of life histories. In *Population dynamics* (eds R.M. Anderson, B.D. Turner & L.R. Taylor) pp. 267-292. Blackwell Scientific Publications, Oxford, UK.

Laughlin, D.C., Laughlin, D.E., 2013. Advances in modeling trait-based plant community assembly. *Trends Plant Sci.* ,18, 584–593. https://doi.org/10.1016/j.tplants.2013.04.012

Lavorel, S., & Garnier, E., 2002. Predicting changes in community composition and ecosystem functioning from plant traits: revisiting the Holy Grail. *Functional Ecology*, *16*(Essay Review), 545–556. https://doi.org/Doi 10.1046/J.1365-2435.2002.00664.X

Lee, J.-Y., Marotzke, J., Bala G., Cao, L., Corti, S., Dunne, J. P., … Zhou, T., 2021. Future Global Climate: Scenario-Based Projections and Near-Term Information. in: Masson-Delmotte, V., P. Zhai, A. Pirani, S.L. Connors, C. Péan, S. Berger, N. Caud, Y. Chen, L. Goldfarb, M.I. Gomis, M. Huang, K. Leitzell, E. Lonnoy, J.B.R. Matthews, T.K. Maycock, T. Waterfield, O. Yelekçi, R. Yu, and B. Zhou (Eds.), Climate Change 2021: The Physical Science Basis. Contribution of Working Group I to the Sixth Assessment Report of the Intergovernmental Panel on Climate Change Cambridge University Press. In Press.

Le Bagousse-Pinguet, Y., Gross, N., Maestre, F.T., Maire, V., de Bello, F., Fonseca, C.R., Kattge, J., Valencia, E., Leps, J., Liancourt, P., 2017. Testing the environmental filtering concept in global drylands. *J. Ecol.* ,105, 1058–1069. https://doi.org/10.1111/1365-2745.12735

Levine, N. M., Zhang, K., Longo, M., Baccini, A., Phillips, O. L., Lewis, S. L., … Moorcroft, P. R., 2016. Ecosystem heterogeneity determines the ecological resilience of the Amazon to climate change. *Proceedings of the National Academy of Sciences*, *113*(3), 793–797. https://doi.org/10.1073/pnas.1511344112

Lohbeck, M., Bongers, F., Martinez-Ramos, M., & Poorter, L., 2016. The importance of biodiversity and dominance for multiple ecosystem functions in a human- modified tropical landscape. *Ecology*, *97*(10), 2772–2779. http://onlinelibrary.wiley.com/journal/10.1002/(ISSN)1939-9170/issues

Longo, M., Knox, R.G., Levine, N.M., Alves, L.F., Bonal, D., Camargo, P.B... Moorcroft, P.R., 2018. Ecosystem heterogeneity and diversity mitigate Amazon forest resilience to frequent extreme droughts. *New Phytol.*, 219, 914–931. https://doi.org/10.1111/nph.15185

Lovejoy, T.E., Nobre, C., 2018. Amazon tipping point. *Sci. Adv.*, 4, 1–2. https://doi.org/10.1126/sciadv.aat2340

Malhi, Y., Aragao, L.E.O.C., Galbraith, D., Huntingford, C., Fisher, R., Zelazowski, P., Sitch, S., McSweeney, C., Meir, P., 2009. Exploring the likelihood and mechanism of a climate-change-induced dieback of the Amazon rainforest. *Proc. Natl. Acad. Sci.* 106, 20610–20615. https://doi.org/10.1073/pnas.0804619106

Malhi, Y., Rowland, L., Aragão, L.E.O.C., Fisher, R.A., 2018. New insights into the variability of the tropical land carbon cycle from the El Niño of 2015/2016. *Philos. Trans. R. Soc. B Biol. Sci.* 373. https://doi.org/10.1098/rstb.2017.0298

Marengo, J.A., Nobre, C.A., Tomasella, J., Oyama, M.D., de Oliveira, ... Brown, I.F., 2008. The drought of Amazonia in 2005. J. Clim. 21, 495–516. https://doi.org/10.1175/2007JCLI1600.1

Mason, N. W. H., Mouillot, D., Lee, W. G., & Wilson, J. B., 2005. Functional richness, functional evenness and functional divergence: The primary components of functional diversity. *Oikos*, *111*(1), 112–118. https://doi.org/10.1111/j.0030-1299.2005.13886.x

Metcalfe, D. B., Meir, P., Aragão, L. E. O. C., Lobo-do-Vale, R., Galbraith, D., Fisher, R. A., … Williams, M., 2010. Shifts in plant respiration and carbon use efficiency at a large-scale drought experiment in the eastern Amazon. *New Phytologist*, *187*(3), 608–621. https://doi.org/10.1111/j.1469-8137.2010.03319.x

Mitchard, E.T., Saatchi, S.S., Baccini, A., Asner, G.P., Goetz, S.J., Harris, N.L., Brown, S., 2013. Uncertainty in the spatial distribution of tropical forest biomass: a comparison of pan-tropical maps. *Carbon Balance Manag.*, 8, 10. https://doi.org/10.1186/1750-0680-8-10

Mori, A. S., Furukawa, T., & Sasaki, T., 2013. Response diversity determines the resilience of ecosystems to environmental change. *Biological Reviews*, *88*(2), 349–364. https://doi.org/10.1111/brv.12004

Morton, D.C., Le Page, Y., DeFries, R., Collatz, G.J., Hurtt, G.C., 2013. Understorey fire frequency and the fate of burned forests in southern Amazonia. Philos. Trans. R. Soc. B Biol. Sci. 368, 20120163. https://doi.org/10.1098/rstb.2012.0163

Mouillot, D., Graham, N. A. J., Villéger, S., Mason, N. W. H., & Bellwood, D. R., 2013a. A functional approach reveals community responses to disturbances. *Trends in Ecology and Evolution*, *28*(3), 167–177. https://doi.org/10.1016/j.tree.2012.10.004

Mouillot, D., Bellwood, D. R., Baraloto, C., Chave, J., Galzin, R., Harmelin-Vivien, M., … Thuiller, W., 2013b. Rare Species Support Vulnerable Functions in High-Diversity Ecosystems. *PLoS Biology*, *11*(5). https://doi.org/10.1371/journal.pbio.1001569

Mouillot, D., Villéger, S., Scherer-Lorenzen, M., & Mason, N. W. H., 2011. Functional structure of biological communities predicts ecosystem multifunctionality. *PLoS ONE*, *6*(3). https://doi.org/10.1371/journal.pone.0017476

Nobre, C.A., Sampaio, G., Borma, L.S., Castilla-Rubio, J.C., Silva, J.S., Cardoso, M., 2016. Land-use and climate change risks in the amazon and the need of a novel sustainable development paradigm. *Proc. Natl. Acad. Sci.* U. S. A. 113, 10759–10768.

https://doi.org/10.1073/PNAS.1605516113/-/DCSUPPLEMENTAL

Oliveira, R.S., Eller, C.B., Barros, F. de V., Hirota, M., Brum, M., Bittencourt, P., 2021. Linking plant hydraulics and the fast-slow continuum to understand resilience to drought in tropical ecosystems. *New Phytol*. 230, 904–923. https://doi.org/10.1111/NPH.17266

Papastefanou, P., Zang, C. S., Pugh, T. A. M., Liu, D., Grams, T. E. E., Hickler, T., & Rammig, A., 2020. A Dynamic Model for Strategies and Dynamics of Plant Water-Potential Regulation Under Drought Conditions. *Frontiers in Plant Science*, *11*(April), 1–13. https://doi.org/10.3389/fpls.2020.00373

Pappas, C., Fatichi, S., Rimkus, S., Burlando, P., Huber, M., 2015. The role of local scale heterogeneities in terrestrial ecosystem modeling. *J. Geophys. Res. Biogeosciences*, 120, 341–360. https://doi.org/10.1002/2014JG002735

Pavlick, R., Drewry, D. T., Bohn, K., Reu, B., & Kleidon, A., 2013. The Jena Diversity-Dynamic Global Vegetation Model (JeDi-DGVM): a diverse approach to representing terrestrial biogeography and biogeochemistry based on plant functional trade-offs. *Biogeosciences*, *10*(6), 4137–4177. https://doi.org/10.5194/bg-10-4137-2013

Perronne, R., & Gaba, S., 2017. How to design trait-based analyzes of community assembly mechanisms: Insights and guidelines from a literature review, *25*, 29–44. https://doi.org/10.1016/j.ppees.2017.01.004

Poorter, L., van der Sande, M. T., Thompson, J., Arets, E. J. M. M., Alarcón, A., Álvarez-Sánchez, J., … Peña-Claros, M., 2015. Diversity enhances carbon storage in tropical forests. *Global Ecology and Biogeography*, *24*(11), 1314–1328. https://doi.org/10.1111/geb.12364

Prentice, I. C., Bondeau, A., Cramer, W., Harrison, S. P., Hickler, T., Lucht, W., … Sykes, M. T., 2007. Dynamic Global Vegetation Modeling: Quantifying Terrestrial Ecosystem Responses to Large-Scale Environmental Change. *Terrestrial Ecosystems in a Changing World*, 175–192. https://doi.org/10.1007/978-3-540-32730-1_15

Quesada, C.A., Phillips, O.L., Schwarz, M., Czimczik, C.I., Baker, T.R., Patiño, S., … Lloyd, J., 2012. Basin-wide variations in Amazon forest structure and function are mediated by both soils and climate. *Biogeosciences*, 9, 2203–2246. https://doi.org/10.5194/bg-9-2203-2012

Rammig, A., Jupp, T., Thonicke, K., Tietjen, B., Heinke, J., Ostberg, S., … Shukla, J., 2010. Amazon deforestation and climate change. *Global Change Biology*, *4*(3), 957–988. https://doi.org/10.1111/j.1365-2486.2009.02157.x

Reich, A.P.B., Wright, I.J., Bares, J.C., Craine, J.M., Oleksyn, J., Westoby, M., Walters, M.B., 2003. The Evolution of Plant Functional Variation: Traits, Spectra, and Strategies. *Int. J. Plant Sci*. 164, S143–S164. https://doi.org/10.1086/374368

Reu, B., Proulx, R., Bohn, K., Dyke, J. G., Kleidon, A., Pavlick, R., & Schmidtlein, S., 2011. The role of climate and plant functional trade-offs in shaping global biome and biodiversity patterns. *Global Ecology and Biogeography*, *20*(4), 570–581. https://doi.org/10.1111/j.1466-8238.2010.00621.x

Reu, B., Zaehle, S., Bohn, K., Pavlick, R., Schmidtlein, S., Williams, J. W., & Kleidon, A., 2014. Future no-analogue vegetation produced by no-analogue combinations of temperature and insolation. *Global Ecology and Biogeography*, *23*(2), 156–167. https://doi.org/10.1111/geb.12110

Roscher, C., Schumacher, J., Gubsch, M., Lipowsky, A., Weigelt, A., Buchmann, N., Schmid, B., Schulze, E.D., 2012. Using plant functional traits to explain diversity-productivity relationships. *PLoS One*, 7. https://doi.org/10.1371/journal.pone.0036760

Rowland, L., da Costa, A. C. L., Galbraith, D. R., Oliveira, R. S., Binks, O. J., Oliveira, A. A. R., … Meir, P., 2015. Death from drought in tropical forests is triggered by hydraulics not carbon starvation. *Nature*, 1–13. https://doi.org/10.1038/nature15539

Rowland, Lucy, Hill, T. C., Stahl, C., Siebicke, L., Burban, B., Zaragoza-Castells, J., … Williams, M., 2014. Evidence for strong seasonality in the carbon storage and carbon use efficiency of an Amazonian forest. *Global Change Biology*, *20*(3), 979–991. https://doi.org/10.1111/gcb.12375

Ruiz-Jaen, M.C., Potvin, C., 2011. Can we predict carbon stocks in tropical ecosystems from tree diversity? Comparing species and functional diversity in a plantation and a natural forest. *New Phytol.*, 189, 978–987. https://doi.org/10.1111/j.1469-8137.2010.03501.x

Running, S., Zhao, M., 2021. *MODIS/Terra Net Primary Production Gap-Filled Yearly L4 Global 500m SIN Grid V061* [Data set]. NASA EOSDIS Land Processes DAAC. Accessed 2021-09-01 from https://doi.org/10.5067/MODIS/MOD17A3HGF.061

Saatchi, S., Houghton, R. A., Dos Santos Alval??, R. C., Soares, J. V., & Yu, Y., 2007. Distribution of aboveground live biomass in the Amazon basin. *Global Change Biology*, *13*(4), 816–837. https://doi.org/10.1111/j.1365-2486.2007.01323.x

Saatchi, S. S., Harris, N. L., Brown, S., Lefsky, M., Mitchard, E. T. A., Salas, W., … Morel, A., 2011. Benchmark map of forest carbon stocks in tropical regions across three continents. *Proceedings of the National Academy of Sciences*, *108*(24), 9899–9904. https://doi.org/10.1073/pnas.1019576108

Sakschewski, B., von Bloh, W., Boit, A., Poorter, L., Peña-Claros, M., Heinke, J., … Thonicke, K., 2016. Resilience of Amazon forests emerges from plant trait diversity. *Nature Climate Change*, *1*(August). https://doi.org/10.1038/nclimate3109

Sakschewski, B., von Bloh, W., Boit, A., Rammig, A., Kattge, J., Poorter, L., … Thonicke, K., 2015. Leaf and stem economics spectra drive diversity of functional plant traits in a dynamic global vegetation model. *Global Change Biology*, 2711–2725. https://doi.org/10.1111/gcb.12870

Salazar, L. F., Nobre, C. A., & Oyama, M. D., 2007. Climate change consequences on the biome distribution in tropical South America. *Geophysical Research Letters*, *34*(9), 2–7. https://doi.org/10.1029/2007GL029695

Scheiter, S., Langan, L., & Higgins, S. I., 2013. Next-generation dynamic global vegetation models: learning from community ecology. *The New Phytologist*. https://doi.org/10.1111/nph.12210

Schmitt, S., Maréchaux, I., Chave, J., Fischer, F. J., Piponiot, C., Traissac, S., & Hérault, B., 2019. Functional diversity improves tropical forest resilience: Insights from a long-term virtual experiment. *Journal of Ecology*, (October), 1–13. https://doi.org/10.1111/1365-2745.13320

Shen, Y., Yu, S., Lian, J., Shen, H., Cao, H., Lu, H., Ye, W., 2016. Tree aboveground carbon storage correlates with environmental gradients and functional diversity in a tropical forest. *Sci. Rep.*, 6. https://doi.org/10.1038/srep25304

Sitch, S., Smith, B., Prentice, I. C., Arneth, A., Bondeau, A., Cramer, W., … Venevsky, S. (2003). Evaluation of ecosystem dynamics, plant geography and terrestrial carbon cycling in the LPJ dynamic global vegetation model. *Global Change Biology*. https://doi.org/10.1046/j.1365-2486.2003.00569.x

Smith, E.A., Holden, E.M., Brown, C., Cahill, J.F., 2022. Disturbance has lasting effects on functional traits and diversity of grassland plant communities. *PeerJ.*, 10. https://doi.org/10.7717/peerj.13179

Sombroek, W., 2000. Amazon landforms and soils in relation to biological diversity. *Acta Amaz.*, 30, 81–81. https://doi.org/10.1590/1809-43922000301100

Song, Y., Wang, P., Li, G., & Zhou, D., 2014. Relationships between functional diversity and ecosystem functioning: A review. *Acta Ecologica Sinica*, *34*(2), 85–91. https://doi.org/10.1016/j.chnaes.2014.01.001

Ter Steege, H., Pitman, N.C.A., Phillips, O.L., Chave, J., Sabatier, D., Duque, A., … Vásquez, R., 2006. Continental-scale patterns of canopy tree composition and function across Amazonia. *Nature*, 443, 444–447. https://doi.org/10.1038/nature05134

Thomas, S. C., & Martin, A. R., 2012. Carbon content of tree tissues: A synthesis. *Forests*, *3*(2), 332–352. https://doi.org/10.3390/f3020332

Thornley, J. H. M., 1972. A balanced quantitative model for root: Shoot ratios in vegetative plants. *Annals of Botany*, *36*(2), 431–441. https://doi.org/10.1093/oxfordjournals.aob.a084602

Tilman, D., Isbell, F., Cowles, J.M., 2014. Biodiversity and Ecosystem Functioning. *Annu. Rev. Ecol. Evol. Syst.*, 45, 471–493. https://doi.org/10.1146/annurev-ecolsys-120213-091917

Tilman, D., Knops, J., Wedin, D., Reich, P., Ritchie, M., Siemann, E., 1997. The influence of functional diversity and composition on ecosystem processes. *Science*, 277, 1300–1302.

https://doi.org/10.1126/science.277.5330.1300

Tilman, D., Reich, P.B., Knops, J.M.H., 2006. Biodiversity and ecosystem stability in a decade-long grassland experiment. *Nature,* 441, 629–632. https://doi.org/10.1038/nature04742

Verheijen, L. M., Brovkin, V., Aerts, R., Bönisch, G., Cornelissen, J. H. C., Kattge, J., … Van Bodegom, P. M., 2013. Impacts of trait variation through observed trait-climate relationships on performance of an Earth system model: A conceptual analysis. *Biogeosciences*, *10*(8), 5497–5515. https://doi.org/10.5194/bg-10-5497-2013

Verheijen, L. M., Aerts, R., Brovkin, V., Cavender-Bares, J., Cornelissen, J. H. C., Kattge, J., & van Bodegom, P. M., 2015. Inclusion of ecologically based trait variation in plant functional types reduces the projected land carbon sink in an earth system model. *Global Change Biology*, 3074–3086. https://doi.org/10.1111/gcb.12871

Villéger, S., Mason, N. W. H., & Mouillot, D., 2008. New Multidimensional Functional Diversity Indices for a Multifaceted Framework in Functional Ecology. *America*, *89*(8), 2290–2301. https://doi.org/10.1890/07-1206.1

Villéger, S., Miranda, J. R., Hernández, D. F., & Mouillot, D., 2010. Contrasting changes in taxonomie vs. functional diversity of tropical fish communities after habitat degradation. *Ecological Applications*, *20*(6), 1512–1522. https://doi.org/10.1890/09-1310.1

Violle, C., Navas, M., Vile, D., Kazakou, E., Fortunel, C., Hummel, I., & Garnier, E., 2007. Let the concept of trait be functional! *Oikos*, *116*(5), 882–892. https://doi.org/10.1111/j.2007.0030-1299.15559.x

Walker, B., Kinzig, A., & Langridge, J., 1999. Plant attribute diversity, resilience, and ecosystem function: The nature and significance of dominant and minor species. *Ecosystems*, *2*(2), 95–113. https://doi.org/10.1007/s100219900062

Webb, C. T., Hoeting, J. a., Ames, G. M., Pyne, M. I., & LeRoy Poff, N., 2010. A structured and dynamic framework to advance traits-based theory and prediction in ecology. *Ecology Letters*, *13*(3), 267–283. https://doi.org/10.1111/j.1461-0248.2010.01444.x

Wieczynski, D. J., Boyle, B., Buzzard, V., Duran, S. M., Henderson, A. N., Hulshof, C. M., … Savage, V. M., 2019. Climate shapes and shifts functional biodiversity in forests worldwide. *Proceedings of the National Academy of Sciences*, *116*(15), 7591–7591. https://doi.org/10.1073/pnas.1904390116

Wullschleger, S. D., Epstein, H. E., Box, E. O., Euskirchen, E. S., Goswami, S., Iversen, C. M., … Xu, X., 2014. Plant functional types in Earth system models: Past experiences and future directions for application of dynamic vegetation models in high-latitude ecosystems. *Annals of Botany*, *114*(1), 1–16. https://doi.org/10.1093/aob/mcu077

Yachi, S., & Loreau, M., 1999. Biodiversity and ecosystem productivity in a fluctuating environment: The insurance hypothesis. *Proceedings of the National Academy of*

Sciences of the United States of America, *96*, 1463–1468. https://doi.org/10.1073/pnas.96.4.1463

Yang, X., Ricciuto, D.M., Thornton, P.E., Shi, X., Xu, M., …Norby, R.J., 2019. The Effects of Phosphorus Cycle Dynamics on Carbon Sources and Sinks in the Amazon Region: A Modeling Study Using ELM v1. *J. Geophys. Res. Biogeosciences*, 124, 3686–3698. https://doi.org/10.1029/2019JG005082

Zakharova, L., Meyer, K.M., Seifan, M., 2019. Trait-based modelling in ecology: lessons from two decades of research. *PeerJ Preprints*, 1–9. https://doi.org/.1037//0033-2909.I26.1.78

7. Supplementary Material

Higher functional diversity improves modeling of Amazon forest carbon storage

Authors: Bianca Fazio Rius, João Paulo Darela Filho, Katrin Fleischer, Florian Hofhansl, Carolina Casagrande Blanco, Anja Rammig, Tomas Domingues, David Montenegro Lapola

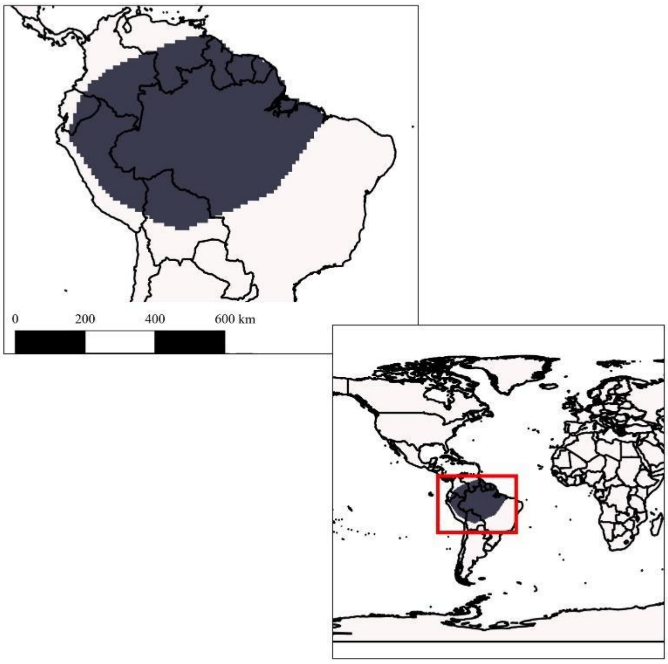

Figure SM.1. Delimitation of the studied region in gray, representing the Amazon basin.

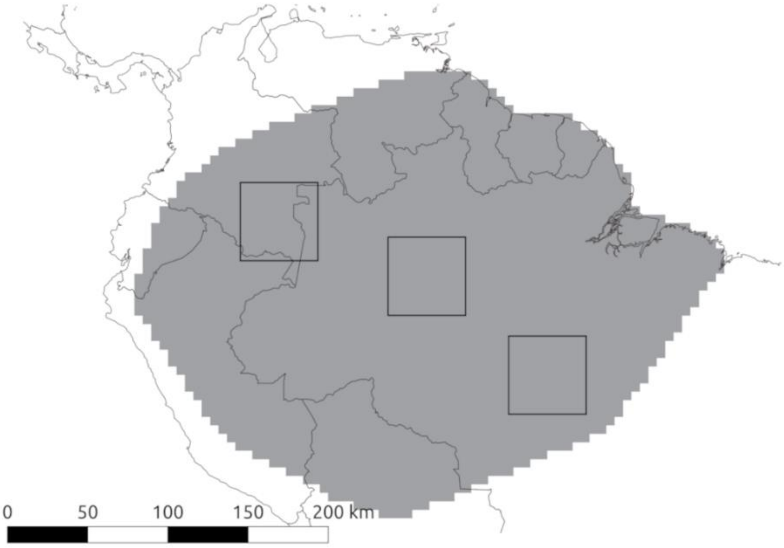

Figure SM.2. The three (northwest, center and southeast) spatial windows along a northwest to southeast axis used to the functional analyzes in a finer scale. The size of the windows is 10x10 grid cells each.

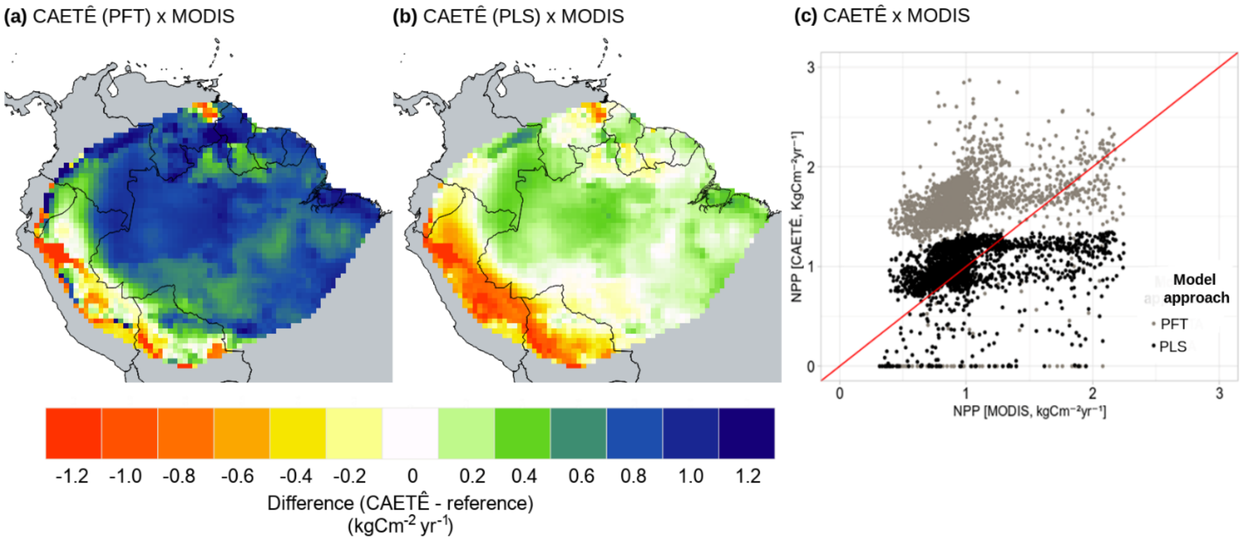

Figure SM.3. Evaluation of CAETÊ performance in representing net primary productivity for both modeling approaches: trait-based and PFT approach, when compared to the reference map generated by the MODIS NPP Project. The plots (a) and (b) show the spatial absolute difference between values simulated by CAETÊ and those simulated by reference. The plot (c) shows the linear regression between CAETÊ and reference map for all the simulated grid cells. The 1:1 line is represented in red. NPP: net primary productivity. PFT: PFT approach. PLS: trait-based approach.

Table SM.1. Range of functional trait values from which values are sampled and its combinations create the different plant life strategies (PLSs). These values are used in the trait-based modeling approach. α: allocation; τ: residence time. *months; **years.

	Functional trait range values					
	Allocation (%)			**Residence time**		
	α_{Leaf}	α_{Wood}	$\alpha_{Fineroots}$	τ_{Leaf}	τ_{Wood}	$\tau_{Fineroots}$
Grasses	15 - 85	-	15 - 85	1 (m*) - 8 (y**)	-	1 (m) - 8 (y)
Woody strategies	15 - 85	15 - 85	15 - 85	1 (m*) - 8 (y**)	1 (y) – 80 (y)	1 (m) - 8 (y)

Table SM.2. Functional trait values for each plant functional type (PFT) used in the PFT modeling approach. The values were chosen based on previous literature: Enquist & Niklas, 2002, Foley, 1996; Krinner et al., 2005; Kucharik et al., 2000; Malhi et al., 2009; Malhi, Doughty, Galbraith, 2011; Sitch et al., 2003. α: allocation; τ: residence time.

	Functional trait value					
	Allocation (%)			**Residence time (years)**		
	α_{Leaf}	α_{Wood}	$\alpha_{Fineroots}$	τ_{Leaf}	τ_{Wood}	$\tau_{Fineroots}$
Tropical evergreen tree	30	35	35	3	30	3
Tropical deciduous tree	35	35	30	2	30	2
Tropical grass	45	0	55	2	0	2

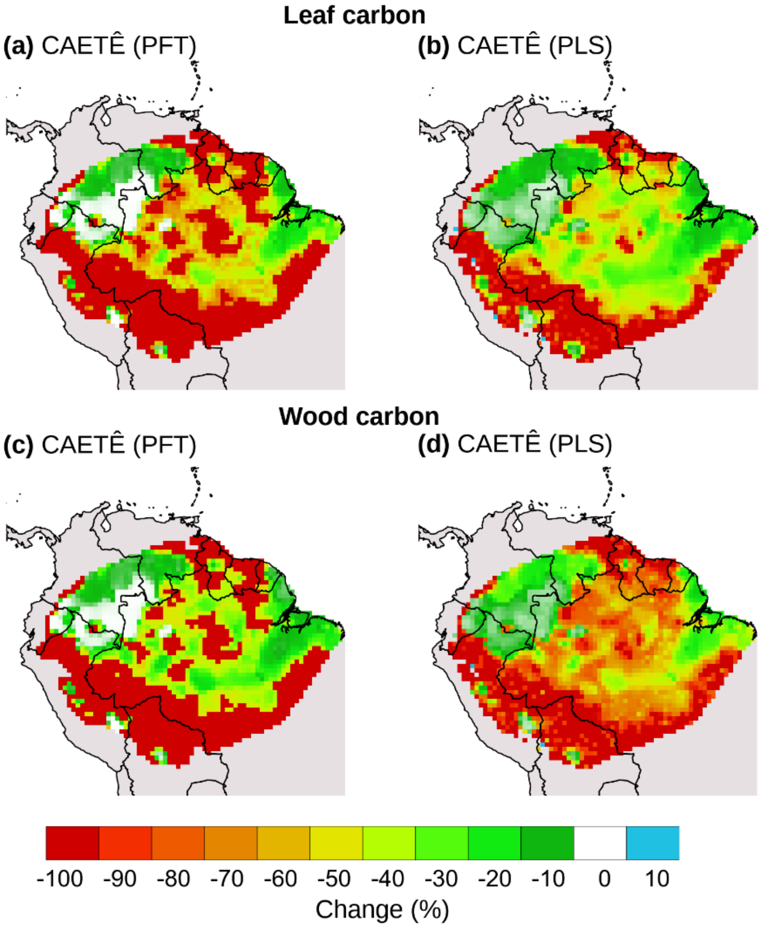

Figure SM.4. Percentage change of carbon storage in (a) wood and in (b) leaves with reduced precipitation (-50%) for the two employed modeling approaches. PFT: PFT approach. PLS: trait-based approach.

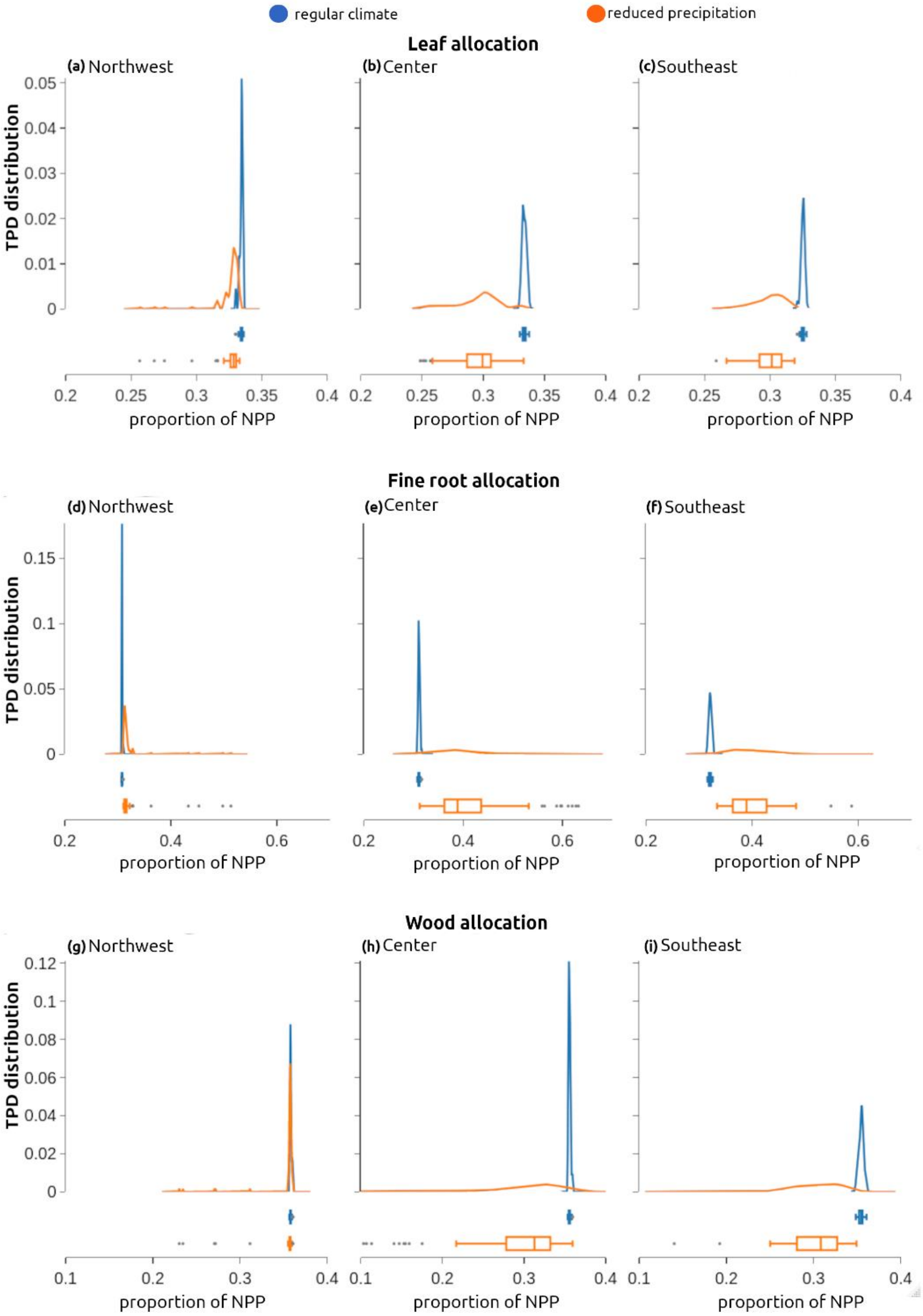

Figure SM.5. Density distributions of functional traits associated to carbon residence time using the trait probability density method (Carmona et al., 2016). This analysis regards to the trait-based approach simulated in each of the three spatial windows along amazon basin (Fig. SM.2). The curves correspond to the probability density distribution of the trait values. Each boxplot represents the median value and variance for each trait in each climatic condition. The boxes extend from the first to the third quartiles, and the whiskers extend from the minimum and maximum data. The outliers are shown in grey dots. The orange curves/boxplots represent the results with the applied low precipitation scenario, and the blue curves/boxplots represent the results concerning the regular climate conditions. NPP: net primary productivity. The dissimilarities between the distributions before and after the reduced precipitation are presented in Table SM.4. Note that the scales of the y and x axes are different for each spatial location. The graphs are presented in this way to improve readability

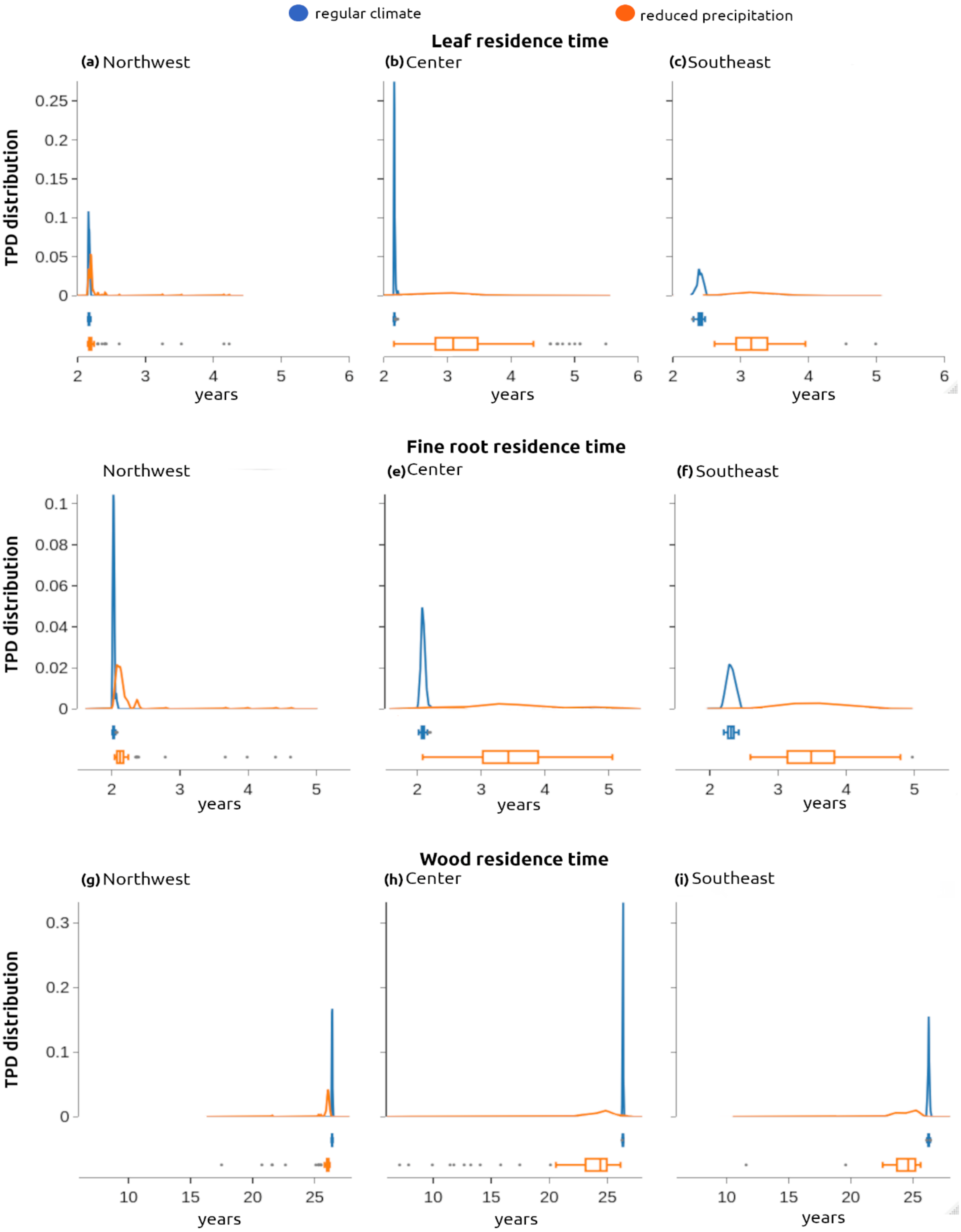

Figure SM.6. Density distributions of functional traits associated to carbon residence time using the trait probability density method (Carmona et al., 2016). This analysis regards to the trait-based approach simulated in each of the three spatial windows along amazon basin (Fig. SM.2). The curves correspond to the probability density distribution of the trait values. Each boxplot represents the median value and variance for each trait in each climatic condition. The boxes extend from the first to the third quartiles, and the whiskers extend from the minimum and maximum data. The outliers are shown in grey dots. The orange curves/boxplots represent the results with the applied low precipitation scenario, and the blue curves/boxplots represent the results concerning the regular climate conditions. NPP: net primary productivity. The dissimilarities between the distributions before and after the reduced precipitation are presented in Table SM.4. Note that the scales of the y and x axes are different for each spatial location. The graphs are presented in this way to improve readability.

(a) Northwest

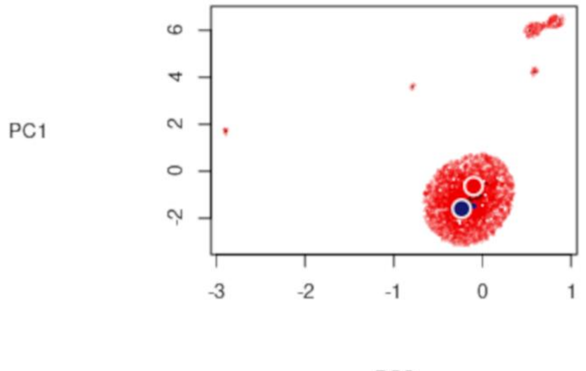

(b) Center

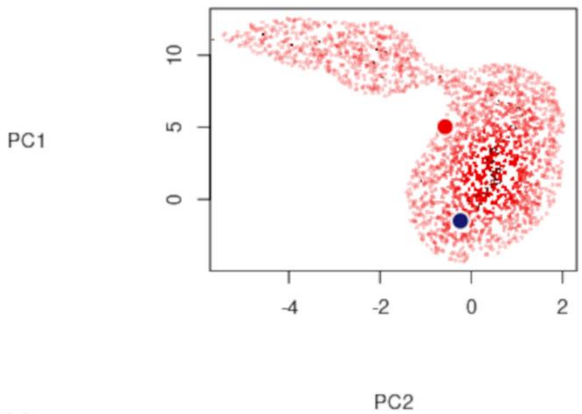

(c) Southeast

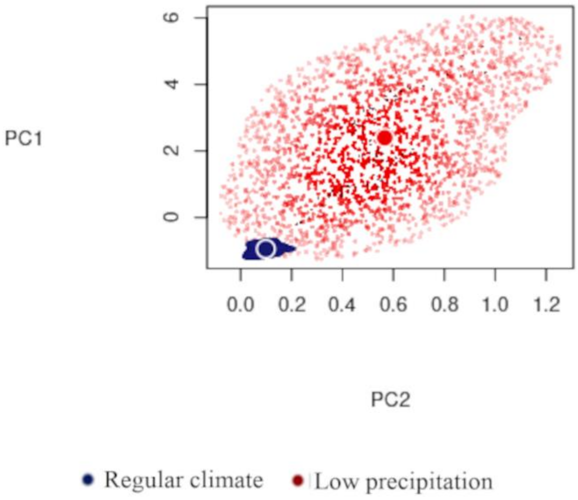

Figure SM.7: Hypervolumes of created with the six functional traits for the trait-based modeling approach in the three spatial windows along amazon basin (Fig. SM.2). We used the method of Blonder et al. (2018) in which the hypervolumes are created after the data were submitted to a PCA (see Fig. SM.11). The blue points indicate the data in a regular climate scenario, and the red points indicate the scenario of -50% of precipitation in the study area. The darker the color of the point is, the higher the density of the value within the functional space is. The bigger circles represent the centroid (*i.e.*, the mean values) of data distribution. Here, the volumes of the different locations are shown separately to improve readability; hence, they are not presented on the same scale.

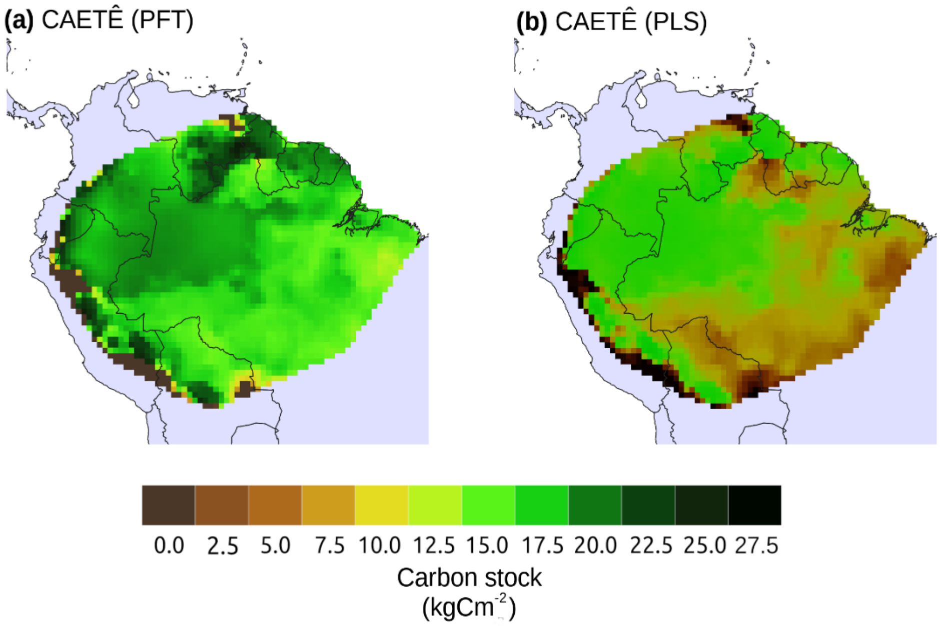

Figure SM.8: Total carbon storage simulated by CAETÊ along the amazon basin. Here we show the simulation performed by both employed approaches. PFT: PFT approach. PLS: trait-based approach.

Table SM.3. Functional traits (carbon allocation and residence time for leaves, woody tissues and fine roots), their respective trade-offs and associated equations. The equations are described in Supplementary Material SM.1 together with the model description.

Functional trait	**Trade-offs**	**Equation**
Leaves allocation	Leaves carbon content	3
	Total plant carbon stock	2
	Leaf area index	SM 18
	Maintenance respiration	SM 24
	Growth respiration	SM 23
Wood allocation	Wood carbon content	3
	Total plant carbon stock	2
	Light capture	section SM.1.8
	Maintenance respiration	SM 24
	Growth respiration	SM 23
Fine roots allocation	Fine roots carbon content	3
	Total plant carbon stock	2
	Water stress	SM 30
	Maintenance respiration	SM 24
	Growth respiration	SM 23
Leaves residence time	Leaves carbon content	3
	Total plant carbon stock	2
	Leaf area index	SM 18
	Specific leaf area	SM 19
	Maintenance respiration	SM 24
	Growth respiration	SM 23
Wood residence time	Wood carbon content	3
	Total plant carbon stock	2
	Light capture	section SM.1.8
	Maintenance respiration	SM 24
	Growth respiration	SM 23
Fine roots residence time	Fine roots carbon content	3
	Total plant carbon stock	2
	Water stress	SM 30
	Maintenance respiration	SM 24
	Growth respiration	SM 23

Table SM.4. Change in richness and dissimilarities of trait distributions (Fig. SM5 and SM6) with the applied reduction in precipitation (-50%) for the trait-based approach in the 3 different locations along Amazon basin (Fig. SM.2) The closer the value is to 1, the more dissimilar the curves are to each other. reg. clim: regular climate. red. prec.: reduced precipitation.

Location	Functional trait	Scenario	Richness	Richness change (%)	Distribution Dissimilarity
Northwest	leaf allocation	reg. clim.	0.0048	286.95	0.89
		red. prec.	0.0184		
	root allocation	reg. clim.	0.0030	636.36	0.99
		red. prec.	0.0218		
	wood allocation	reg. clim.	0.0041	75	0.25
		red. prec.	0.0071		
	leaf residence time	reg. clim.	0.0406	419.99	0.59
		red. prec.	0.2113		
	root residence time	reg. clim.	0.0544	637.5	0.90
		red. prec.	0.4012		
	wood residence time	reg. clim.	0.0933	974.99	1.00
		red. prec.	1.0027		
Center	leaf allocation	reg. clim.	0.0071	1040.98	0.97
		red. prec.	0.0806		
	root allocation	reg. clim.	0.0072	4176.47	0.98
		red. prec.	0.3072		
	wood allocation	reg. clim.	0.0051	4414.28	0.97
		red. prec.	0.2303		
	leaf residence time	reg. clim.	0.0391	7466.66	0.99
		red. prec.	2.9573		
	root residence time	reg. clim.	0.1382	2137.14	0.97
		red. prec.	3.0916		
	wood residence time	reg. clim.	0.1254	8659.99	0.99
		red. prec.	10.9834		
Southeast	leaf allocation	reg. clim.	0.0058	763.07	1.00
		red. prec.	0.0505		
	root allocation	reg. clim.	0.0106	1323.33	1.00
		red. prec.	0.1511		
	wood allocation	reg. clim.	0.0115	775	0.99
		red. prec.	0.1004		
	leaf residence time	reg. clim.	0.1720	667.34	1.00
		red. prec.	1.3200		
	root residence time	reg. clim.	0.2337	718.46	1.00
		red. prec.	1.9128		
	wood residence time	reg. clim.	0.2708	1071.42	1.00
		red. prec.	3.1725		

Supplementary Material SM.1 - Description of CAETÊ (Carbon and Ecosystem functional Trait Evaluation Model)

Here we fully describe the model CAETÊ, including all the ecophysiological equations. These equations are mainly based on the CPTEC Potential Vegetation Model 2 (CPTEC-PVM2; Lapola, Oyama, & Nobre, 2009), otherwise the references are detailed together with the respective equation. The symbols used for each variable, its description, unit and associated equations can be found in Table SM.5. The constant parameters with its respective values are shown in Table SM.6. Hereafter, the symbols i, y and z correspond, respectively, to a PLS/PFT, a grid cell and a plant compartment [leaves, wood and fine roots]. It is important to highlight that all ecosystem parameters and properties are aggregated to grid cell scale according to the method described in section 2.1 in the main text.

Table SM.5. Descriptions, units and the respective equation number of the variables used in the CAETÊ model. *see Oyama & Nobre (2004).

Symbol	Variable	Unit	Equation
A_r	Relative abundance	unitless	1
C	Total carbon in a plant	$KgCm^{-2}$	3
C_T	Total carbon in a grid cell	$KgCm^{-2}$	2
C_z	Carbon content in a plant compartment	$KgCm^{-2}$	4
C_a	Atmospheric CO_2 concentration	ppmv	Input
C_{init_z}	Initial carbon content in a plant compartment	$KgCm^{-2}$	SM 1
C_{equi_z}	Amount of carbon in equilibrium in each plant compartment	$KgCm^{-2}$	SM 2
C_{press}	Partial CO_2 pressure at leaf interior	Pa	SM 9
C_r	Canopy resistance	sm^{-1}	SM 26
D	Atmospheric demand for transpiration	mmH_2Oday^{-1}	SM 33

$E_{vap_{pot}}$	Potential evapotranspiration	mmH_2Oday^{-1}	*
E_{evap}	Evapotranspiration	mmH_2Oday^{-1}	*
f_1	leaf level gross photosynthesis	$molCO_2m^{-2}s^{-1}$	SM 4
f_2	Michaelis-Menten constant for CO_2	Pa	SM 7
f_3	Michaelis-Menten constant for O_2	Pa	SM 8
f_4	Function for upscaling the leaf level photosynthesis to the canopy level	unitless	SM 17/18
f_4^{sun}	Canopy portion in which solar radiation reaches it in a 90° angle	unitless	SM 17
f_4^{shade}	Canopy portion that receives diffuse radiation in a 20° angle	unitless	SM 18
f_5	Water stress factor	unitless	SM 31
GPP	Gross primary productivity	$kgCm^{-2}yr^{-1}$	SM 3
g_{pot}	Canopy potential conductance	mms^{-1}	SM 34
g_s	Stomatal conductance	$molCO_2m^{-2}s^{-1}$	SM 27
H	Relative humidity	gkg^{-1}	Input
H_y	Actual soil water content in a grid cell	mm	SM 29
$IPAR$	Incident photosynthetic active radiation	$Einm^{-2}s^{-1}$	Input
J_C	Rubisco carboxylation limiting factor for photosynthesis	$molCO_2m^{-2}s^{-1}$	SM 6
J_E	Electron limiting factor for photosynthesis	$molCO_2m^{-2}s^{-1}$	SM 15
J_L	Light limiting factor for photosynthesis	$molCO_2m^{-2}s^{-1}$	SM 14
J_P	The minimum between J_C and J_L	$molCO_2m^{-2}s^{-1}$	SM 5
L	Water supply for transpiration	mmH_2Oday^{-1}	SM 32
LAI	Leaf area index	unitless	SM 19
LAI_{sun}	Leaf area index in the canopy portion in which solar radiation reaches it in a 90° angle	unitless	SM 21
LAI_{shade}	Leaf area index in the canopy portion in which solar radiation reaches it in a 90° angle	unitless	SM 22
NPP	Net primary productivity	$kgCm^{-2}yr^{-1}$	5
NPP_{grid}	Net primary productivity aggregated to the grid cell scale	$kgCm^{-2}yr^{-1}$	6
NPP_{pot}	Potential net primary productivity	$kgCm^{-2}yr^{-1}$	Input

P_{rec}	Precipitation	mmm^{-1}	Input
P_{surf}	Surface water vapor pressure	atm	Input
R_a	Autotrophic respiration	kgCm^{-2}yr^{-1}	SM 23
R_g	Growth respiration	kgCm^{-2}yr^{-1}	SM 24
R_m	Maintenance respiration	kgCm^{-2}yr^{-1}	SM 25
R	Leaf level moisture deficit	kgkg^{-1}	SM 11
r_{max}	Saturated mixing ratio	kgkg^{-1}	SM 12
R_{off}	Runoff	mmH_2O	*
S	Number of alive PLSs/PFTs in the grid cell	unitless	*
SLA	Specific leaf area	m^{2}KgC^{-1}	SM 20
T	Temperature	ºC	Input
T_{soil}	Soil temperature	ºC	Input
V_m	Rubisco carboxylation rate	molCO^{2}m^{-2}s^{-1}	SM 16
VPD	Deficit of vapor pressure on the leaf surface	kPa	SM 28
W_{press}	Partial pressure of water vapor	hPa	SM 13
W_{sat}	Degree of water soil saturation	unitless	SM 30
Γ	Photorespiration compensation point	Pa	SM 10

Table SM.6. Descriptions, values and units of constant parameters used in the CAETÊ equations. IPAR: incident photosynthetically active radiation.

Parameter	**Description**	**Value/units**
c_{sru}	Water uptake capacity	0.0005 mmH_2OkgC^{-1}day^{-1}
g_0	Minimal stomatal conductance	0.001 molm^{-2}s^{-1}
g_1	Conductance sensibility to the carbon assimilation	kPa$^{1/2}$
g_m	Upscaling of stomatal conductance to canopy	3.26 mms^{-1}
H_{max}	Water maximum holding capacity	500 mm
k_1	Photosynthesis co-limitation coefficient	0.93
k_{10}	Function Q_{10} parameter	0.57
k_{11}	Function Q_{10} reference temperature	25 ºC
k_{12}	CO_2 Michaelis-Menten constant parameter	30 Pa
k_{13}	CO_2 Michaelis-Menten constant parameter	2.1
k_{14}	O_2 Michaelis-Menten constant parameter	30.000 Pa
k_{15}	O_2 Michaelis-Menten constant parameter	1.2

k_{16}	Maximum ratio between intern and extern CO$_2$	0.9
k_{17}	Critical moisture deficit	0.1
k_{18}	Rubisco carboxylation rate parameter	2
k_{19}	Rubisco carboxylation rate parameter	0.3
k_2	Photosynthesis co-limitation coefficient	0.83
k_{20}	Rubisco carboxylation rate parameter	36 °C
k_{21}	Light extinction coefficient for direct IPAR (sun)	0.5/sen(90º)
k_{22}	Light extinction coefficient for direct IPAR (shade)	0.5/sen(20º)
k_3	Oxygen atmospheric concentration	21.200 Pa
k_4	Quantum efficiency	0.08 mol electrons/Ein
k_5	Light scattering rate	0.15
k_6	J$_L$ parameter	2
k_7	Ratio between photosynthesis limited by light and by rubisco carboxylation	0.5
k_8	Photorespiration point compensation parameter	5.2
k_9	Photosynthesis co-limitation coefficient	0.1
nc_{leaves}	N:C ratio for leaves	0.034
$nc_{sapwood}$	N:C ratio for sapwood	0.003
$nc_{fineroots}$	N:C ratio for fine roots	0.034
rc_{min5}	The minimum stomatal resistance	100 sm^{-1}
$V_{c_{max}}$	Maximum rate of Rubisco carboxylation	0.00004 molCO^{2}m^{-2}s^{-1}
γ_m	Maximum Priestley-Taylor coefficient	1.391

SM.1.1. Model structure

For the next sections the symbols symbol i, y and z refer to a PLS/PFT, to a grid cell and to a plant compartment, respectively.

SM.1.1.1. Creating and sampling plant life strategies (PLSs)

To create the hypervolume that contains the possible combinations of functional traits and, hence, the PLSs, each trait owns a range of values that determines the minimum and the maximum value that will be sampled (Table SM.1). From this initial range, trait values are uniformly sampled and are combined to create the potential functional trait space. From this potential space some combinations are excluded following a viability standard: first, the combination of values for allocation functional traits, necessarily, must sum 100%, otherwise this combination is excluded from the functional space. Also, before model initialization, all the combinations are submitted to a procedure to check their viability, that is, their capacity to maintain a minimal value of carbon content (0.001 kgCm^{-2}) on both fine roots and leaves considering a low input of carbon (NPP equals to 0.001 kgCm^{-2}yr^{-1}). For this, we use a simple iterative module that resolves numerically the carbon balance at each time step and runs until the stability attainment of the total carbon stock (i.e., the sum of carbon in all plant compartments) in all the grid cells, with a sensibility of 10% of difference between t_x and t_{x-1}. Thus, from the minimum NPP (NPP_{min_y}), the amount of carbon in equilibrium ($C_{equi_{i,y,z}}$) in each plant compartment in a time t_x:

$$\frac{dC_{equi_{i,y,z}}}{dt_x} = \alpha_{i,z} NPP_{min_y} - \frac{C_{equi_{i,y,z}}}{\tau_{i,z}} \qquad \text{(SM 1)}$$

From the combinations that respect the established pattern of viability, 3000 PLSs are sampled and seeded in each grid cell. The number of sampled PLSs was defined through a sensitivity test (see Supplementary Material SM.2).

SM.1.1.2. Model initialization

After seeding the PLSs/PFTs, we determine the initial carbon content on plant compartments by using a module analogous to a model spin-up in a dynamical process-based vegetation modeling framework. The module is described in section SM.1.1.1, but other than using a minimum value of NPP, we use a potential value of NPP for each grid-cell which is obtained from a map that is previously simulated by a precursor model of CAETÊ, the CPTEC Potential Vegetation Model 2 (CPTEC-PVM2; Lapola, Oyama, & Nobre, 2009), using the same climatology applied to CAETÊ running.

Thus, from a target potential NPP (NPP_{pot_y}), the initial amount of carbon ($C_{init_{i,y,z}}$) in each plant compartment in a specific PFT or PLS, in a time t_x:

$$\frac{dC_{init_{i,y,z}}}{dt_x} = \alpha_{i,z} NPP_{pot_y} - \frac{C_{init_{i,y,z}}}{\tau_{i,z}} \tag{SM 2}$$

where α_{i_z} (Table SM.1 and SM.2) is the fraction of NPP allocated to a plant compartment in each PLS/PFT and $\tau_{i,z}$ (Table SM.1 and SM.2) represents the carbon residence time in a compartment. The module is run until equilibrium, as described in previous section.

SM.1.2. Input Data

The following climatic data were used as inputs for the model: air surface temperature, precipitation, shortwave radiation, relative humidity and atmospheric CO_2 concentration. The first four variables were obtained from mean monthly data for the period between 1980 to 2010, which are available in the Inter-Sectoral Impact Model Intercomparison Project 2 (ISI-MIP2; Warszawski et al., 2014). Atmospheric CO_2 concentration was obtained from the CO_2 Earth website (Mc. Gee, 2020), employing the mean value of [CO2] for the same period used for the other climatic data.

SM.1.3. Photosynthesis

The photosynthesis equation ($GPP_{i,y}$) and the ones associated with it are based on Farquhar, Caemmerer, & Berry (1980) formulation, which takes into account three limiting factors: rubisco carboxylation (J_c), light (J_{L_i}) and electron transport (J_E). We also included water stress limitation (f_{5_i}).

$$GPP_{i,y} = 0.012 * 31557600 * f_{1_i} f_{4_{i,y}}^{sun} f_{4_{i,y}}^{shade} f_{5_i} \tag{SM 3}$$

where $f_{1_{i,y}}$ is the leaf level gross photosynthesis and $f_{4_{i,y}}^{sun}$ and $f_{4_{i,y}}^{shade}$ are functions for upscaling the leaf level photosynthesis to the canopy level.

In the following equations k_n are constants summarized in Table SM.6. The $f_{1_{i,y}}$is calculated as the smallest root between the three limiting rates: $J_{C_{i,y}}$, $J_{L_i}$and J_E:

$$f_{1_{i,y}} = smallestrootof: k_1 J^2 - J\left(J_{P_{i,y}} + J_E\right) + J_{P_{i,y}} J_E = 0 \tag{SM 4}$$

where $J_{P_{i,y}}$ is the minimum between $J_{C_{i,y}}$ and $J_{L_{i,y}}$:

$$J_{P_{i,y}} = smallest\ root\ of: k_2 {J_{P_{i,y}}}^2 - J_{P_{i,y}}\left(J_{C_{i,y}} + J_{L_{i,y}}\right) + J_{C_{i,y}} J_{L_{i,y}} = 0 \tag{SM 5}$$

$J_{C_{i,y}}$ is the photosynthesis rate limited by the Rubisco carboxylation capacity:

$$J_{C_{i,y}} = V_{m_{i,y}}\left\{C_{press_{i,y}} - \frac{\Gamma_{i,y}}{C_{press_{i,y}}} + f_{2_{i,y}}\left[1 + \left(\frac{k_3}{f_{3_{i,y}}}\right)\right]\right\} \tag{SM 6}$$

Where $V_{m_{i,y}}$ is the rate of Rubisco carboxylation, $C_{press_{i,y}}$ is the partial CO2 pressure at leaf interior, $\Gamma_{i,y}$ is the photorespiration compensation point, $f_{2_{i,y}}$ is the Michaelis-Menten constant for CO2 and $f_{3_{i,y}}$ the Michaelis-Menten constant for O2.

$$f_{2_{i,y}} = k_{12} k_{13}^{k_{10}(T_y - k_{11})} \tag{SM 7}$$

$$f_{3_{i,y}} = k_{14} k_{15}^{k_{10}(T_y - k_{11})} \tag{SM 8}$$

$$C_{press_{i,y}} = k_{16} * \left[1 - \left(\frac{r_{i,y}}{k_{17}}\right)\right] * \left(C_{a_y} - \Gamma_{i,y}\right) + \Gamma_{i,y} \tag{SM 9}$$

where $r_{i,y}$ is the leaf level moisture deficit and C_{a_y} is the atmospheric CO2 concentration (input).

$$\Gamma_{i,y} = \left(\frac{k_3}{k_8}\right) * k_9^{k_{10}(T_y - k_{11})} \tag{SM 10}$$

$r_{i,y}$ is obtained by the actual mixing ratio on leaf level and the saturated mixing ratio ($r_{max_{i,y}}$):

$$r_i = -0.315 r_{max_i} \tag{SM 11}$$

$r_{max_{i,y}}$ is a function of partial pressure of water vapor ($w_{press_{i,y}}$) and the surface pressure (P_{surf_y}):

$$r_{max_{i,y}} = 0.622 \frac{w_{press_{i,y}}}{P_{surf_y} - w_{press_{i,y}}} \tag{SM 12}$$

$$w_{press_{i,y}} = 6.1121 * exp\left\{\left[18.678 - \left(\frac{T_y}{234.5}\right)\right] * \left[\frac{T_y}{\left(257.14 + T_y\right)}\right]\right\} \tag{SM 13}$$

$J_{L_{i,y}}$ is the photosynthetic rate limited by light as a function of the incident photosynthetically active radiation [$IPAR_{i,y}$; here we considered $IPAR$ as 50% of the shortwave radiation (input)]:

$$J_{L_{i,y}} = k_4(1 - k_5)IPAR_{i,y} \tag{SM 14}$$

The photosynthetic rate limited by the electron transport $J_{E_{i,y}}$ is given by:

$$J_{E_{i,y}} = k_7 V_{m_i,y} \tag{SM 15}$$

$$V_{m_i,y} = V_{cmax_i,y} \frac{\left(k_{18}^{k_{10}(T_y - k_{11})}\right)}{1} + exp\left(k_{19}\left(T_y - k_{20}\right)\right) \tag{SM 16}$$

where $V_{cmax_{i,y}}$ (Table SM.6) is the maximum rate of Rubisco carboxylation and T_y (input) is temperature.

The function $f_{4_{i,y}}$ is used in the canopy scaling of photosynthesis. Since we assume a canopy division in sun and shade parts this function is subdivided in $f_{4_{i,y}}^{sun}$ and $f_{4_{i,y}}^{shade}$. The sun part aims to represent the canopy portion in which solar radiation reaches it directly in a 90º angle, while the shade part receives diffuse radiation in a 20º angle.

$$f_{4_{i,y}}^{sun} = \frac{\left(1 - e^{-k_{21}LAI_{sun_{i,y}}}\right)}{k_{21}} \tag{SM 17}$$

$$f_{4_{i,y}}^{shade} = \frac{\left(1 - e^{-k_{22}LAI_{shade_{i,y}}}\right)}{k_{22}} \tag{SM 18}$$

where $LAI_{i,y}$ is the leaf area index also splitted in $LAI_{sun_{i,y}}$ and $LAI_{shade_{i,y}}$ in order to follow the canopy subdivision. Then, following Beer-Lambert's Law (see De Pury & Farquhar, 1997):

$$LAI_{i,y} = C_{leaves_{i,y}} SLA_{i,y} \tag{SM 19}$$

The calculation of $SLA_{i,y}$ (specific leaf area) is based on the approach used by Pavlick et al. (2013):

$$SLA_{i,y} = 30\left(\frac{4380}{\tau_{leaves_{i,y}}}\right) exp(-0.46) \tag{SM 20}$$

where $\tau_{leaves_{i,y}}$ (Table SM.1 and SM.2) is the carbon residence time on leaves for a PLS/PFT. This equation uses an empirical relationship derived from Reich, Walters, & Ellsworth (1997) and aims to represents the leaf economic spectrum (Wright et al., 2004).

$$LAI_{sun_{i,y}} = 1 - exp\frac{\left(-k_{21}LAI_{i,y}\right)}{k_{21}} \quad \text{(SM 21)}$$

$$LAI_{shade_{i,y}} = LAI_{i,y} - LAI_{sun_{i,y}} \quad \text{(SM 22)}$$

SM.1.4. Respiration

The autotrophic respiration ($R_{a_{i,y}}$) is divided in growth respiration ($R_{g_{i,y}}$) and maintenance respiration ($R_{m_{i,y}}$) following Ryan (1991a; 1991b).

$$R_{a_{i,y}} = R_{g_{i,y}} + R_{m_{i,y}} \quad \text{(SM 23)}$$

SM.1.4.1. Growth Respiration

The $R_{g_{i,y}}$ formulation is based on Ryan et al. (1991a; 1991b), which postulates that a reasonable growth respiration estimate can be done assuming that its metabolic costs in each tissue consumes an amount of carbon equal to a quarter of the carbon incorporated in the new tissue (i.e. the difference between the carbon content in a compartment in a time t ($C_{z_{i,y_t}}$) and the carbon content in the same compartment in a time $t-1$ ($C_{z_{i,y_{t-1}}}$). Total growth respiration is the sum of growth respiration in all the three plant compartments considered.

$$R_{g_{i,y}} = \sum_{z=1}^{3}\left[0.25\left(C_{z_{i,y_t}} - C_{z_{i,y_{t-1}}}\right)\right] \quad \text{(SM 24)}$$

SM.1.4.2. Maintenance Respiration

The maintenance respiration is calculated according to the nitrogen and carbon content in each compartment. The nitrogen content on plant tissues is intimately connected to the maintenance respiration since about 60% of it is used to protein repair and substitution (Ryan, 1991a, 1991b). Yet, the nitrogen supply is not here considered as a limiting factor.

$$R_{m_{i,y}} = \sum_{z=1}^{3} \left[nc_z C_{z_i} 27 \, exp\left(0.07 T_y\right) \right] \qquad \text{(SM 25)}$$

where nc_z represents the N:C ratio for each plant compartment z and T_y(ºC) is the mean annual temperature. A considerable amount of the wood tissues does not respire (the so-called heartwood; Ryan, 1991b), and then we consider only 5% of the aboveground woody tissues carbon content on the maintenance respiration for this compartment. This 5% aims to represent the sapwood (Pavlick et al., 2013). The N:C ratio is equal to 0.034, 0.003 and 0.034 for leaves, sapwood and fine roots, respectively (Levis et al., 2004; Sitch et al., 2003). The parameter 0.07 is a sensibility factor of the maintenance respiration to temperature. Because in tropical forests the soil temperature is lower than the air temperature, then for calculating the fine roots maintenance respiration we used the soil temperature (T_{soil_y}; see Oyama & Nobre, 2004).

SM.1.5. Stomatal conductance and canopy resistance

Stomatal conductance ($gs_{i,y}$) and canopy resistance ($C_{r_{i,y}}$) link the carbon cycle (through $GPP_{i,y}$) with the water balance sub-model (see SM.1.7.):

$$C_{r_{i,y}} = \frac{1}{g_{s_{i,y}}} \qquad \text{(SM 26)}$$

$$gs_{i,y} = g_0 + 1.6\left(1 + \frac{g1}{\sqrt{VPD_y}}\right) * \frac{GPP_{i,y}}{C_{a_y}} \qquad \text{(SM 27)}$$

g_0 is the stomatal conductance with a fix value of 0.001, g_1 is the conductance sensibility to the carbon assimilation (Medlyn et al., 2011) and has a constant value of 3.77. Lastly, VPD_y is the deficit of vapor pressure on the leaf surface:

$$VPD_y = \frac{\left(E_{vap_y} h_y\right)}{10} \qquad \text{(SM 28)}$$

where h_y (input) is the relative humidity and $E_{vap_{i,y}}$is the evapotranspiration (see SM.1.7.).

SM.1.6. Light capture for distinct PLSs/PFTs

The carbon stored on aboveground wood tissues are highly correlated to light competition (Reich, 2014). However, the model CAETÊ is still not able to represent the competition ecological process mechanistically, since there is no representation of shading of PLSs/PFTs that resemble understory plants by the ones that resemble trees with higher height and higher canopy area, for example. The majority of models represents the plants' competitive ability for light associated with woody tissues through variables that describe height, wood density and canopy ratio [*e.g.*, aDGVM (Scheiter, Langan, & Higgins, 2013) and LPJ (Sitch et al., 2003). These variables are estimated via allometric relationships that were not used by CAETÊ in this study. So, in order to implement a trade-off for the traits (allocation and residence time) that determines the carbon content on wood tissues (C_{wood_i}), we used a simplified approach for the sake of representing the differential light capture between the different PLSs/PFTs in a grid cell. We considered that 5% of the PLSs/PFTs that present the higher relative carbon content on wood tissue in a grid cell can capture 100% of the incident $IPAR$ while the other ones can capture 80% of the IPAR.

SM.1.7. Water balance sub-model

The CAETÊ uses a sub-model to calculate the water balance in a grid cell scale. This sub-model is based on Oyama & Nobre (2004) and is evaluated over a homogeneous soil layer with a unique water maximum holding capacity (H_{max_y}) equal to 500 mm. In the present study different types of soil are not considered. Developments on CAETÊ have being done in order to increase the amount of soil layers and to implement different soil types with different water holding capacity and different nutrients availability.

SM.1.7.1. Soil water content and saturation

The model here employed calculates soil water and snow budgets separately, however given the climatic conditions of the study area we do not present here the soil snow budget formulation [see Oyama & Nobre (2004) for accessing it]. The actual soil water content (H_{y_t}) in a grid cell y in a certain time step t depends on the precipitation (P_{rec_y}), the evapotranspiration ($E_{vap_{i,y}}$; see Oyama & Nobre, 2004) and the runoff ($R_{off_{i,y}}$; see Oyama & Nobre, 2004) on this grid cell:

$$\frac{\partial H_y}{\partial_t} = P_{rec_y} - E_{vap_{i,y}} - R_{off_{i,y}} \quad \text{(SM 29)}$$

Then, the degree of water soil saturation in the grid cell (w_{sat_y}) can be calculated:

$$w_{sat_y} = \frac{H_y}{H_{max}} \quad \text{(SM 30)}$$

SM.1.7.2. Water stress

In order to include the limitation of photosynthesis by water availability and to comprise a trade-off for the fine roots' traits investment, we added to the photosynthesis ($GPP_{i,y}$) equation a water stress factor ($f_{5_{i,y}}$). This factor is calculated in function of the ratio between the potential water supply for transpiration ($L_{i,y}$) and the atmospheric demand for transpiration ($D_{i,y}$). This approach is based on Pavlick et al. (2013).

$$f_{5_{i,y}} = 1 - exp\left(\frac{L_{i,y}}{D_{i,y}}\right) \quad \text{(SM 31)}$$

$L_{i,y}$ is a function of the carbon stock on fine roots compartment ($C_{root_{i,y}}$) multiplied by a constant water uptake capacity (c_{sru}) with a value of 0.0005 mmH2OkgC^{-1}day^{-1}, and by the degree of water soil saturation in the grid cell (w_{sat_y}). It is important to highlight that the value for $w_{sat_y}$is correspondent to that of the previous day.

$$L_{i,y} = c_{sru} C_{root_{i,y}} w_{sat_{y_{t-1}}} \quad \text{(SM 32)}$$

Following Gerten et al. (2004), D_i represents the condition of a "unstressed transpiration" which occurs when stomatal opening is not limited by reduced water potential in the plant:

$$D_{i,y} = \left[\left(1 - w_{sat_y}\right) E_{vap_{pot_y}} \frac{\gamma_m}{\left(1 + \frac{g_m}{g_{pot_{i,y}}}\right)} \right] \quad \text{(SM 33)}$$

where $E_{vap_{pot_y}}$ is the potential evapotranspiration (see Oyama & Nobre, 2004); γ_m is a coefficient with fixed value equal to 1.391, g_m is the canopy scaling stomatal conductance and presents a value equal to 3.26 mms^{-1}. $g_{pot_{i,y}}$ is the canopy potential conductance when there is not water limitation and is calculated through minimum stomatal resistance (rc_{min}) with a value equal to 100:

$$g_{pot_{i,y}} = \frac{1}{rc_{min}} \quad \text{(SM 34)}$$

Supplementary Material SM.2 - **Sensitivity test for the number of sampled PLSs**

After creating the potential functional space with thousands of PLSs a problem emerges: how many PLSs are enough in order to make meaningful representation of the entire trait space created? To answer this question a set of 6 ensembles with different numbers of sampled PLSs (number of PLSs = 50, 100, 200, 500, 1000, 3000) was run to test the model sensitivity. Each ensemble contains 10 runs, this is required because of the random nature of the initial sampling process. The only difference between the ensembles is the number of initialized PLS.

To explore the sensitivity of the model for the number of sampled PLSs we assessed the mean values and the variance in each of the 10 runs for the 6 ensembles for total plant carbon storage and for all the six functional traits (Fig. SM.4). With this strategy we sought to understand how the mean and the variances change between the runs for each ensemble of PLS numbers. Our idea is that since the sampling of functional trait values is random, we expect that the higher the number of PLSs the lower the difference in mean and variance between the runs. It would ensure that the results that emerge from the model, both for biogeochemical and functional diversity variables, are not a product of a “forged” diversity derived from the simple difference between the runs.

As expected, it is notable that the number of PLSs sampled from all the possible combinations presents a meaningful influence on estimating the mean value and variance between the runs, both for the total plant carbon stock and the functional traits. We observed that as more PLSs are sampled, the greater the convergence in the mean values (orange ticks on Fig. SM.4) and in the variance between the 10 runs. These results emerge from the fact that the increase in the

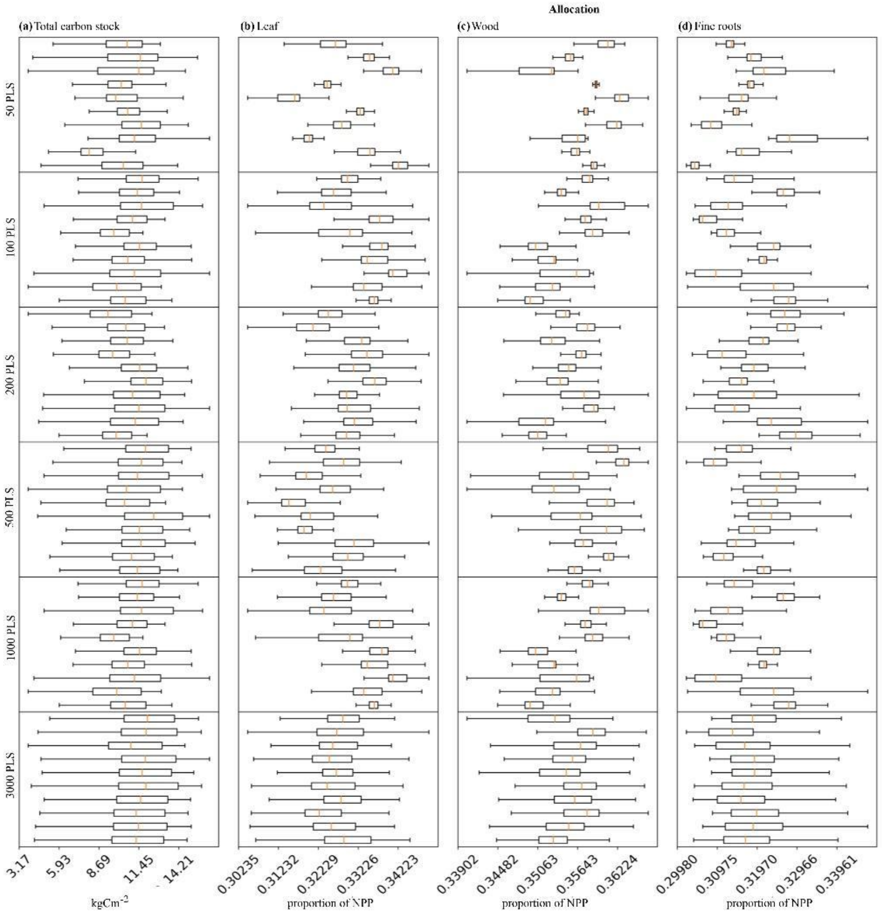
Allocation
(a) Total carbon stock
(b) Leaf
(c) Wood
(d) Fine roots
50 PLS
100 PLS
200 PLS
500 PLS
1000 PLS
3000 PLS
3.17
5.93
8.69
11.45
14.21
kgCm-2
0.30235
0.31232
0.32229
0.33226
0.34223
proportion of NPP
0.33902
0.34482
0.35063
0.35643
0.36224
proportion of NPP
0.29980
0.30975
0.31970
0.32966
0.33961
proportion of NPP

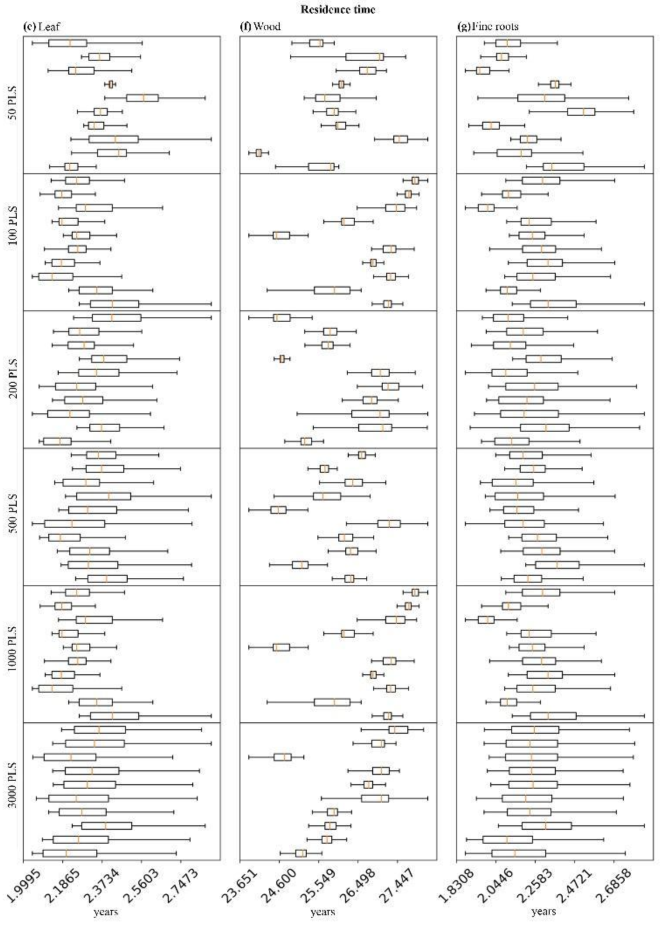
Residence time
(e) Leaf
(f) Wood
(g) Fine roots
50 PLS
100 PLS
200 PLS
500 PLS
1000 PLS
3000 PLS
1.9995
2.1865
2.3734
2.5603
2.7473
years
23.651
24.600
25.549
26.498
27.447
years
1.8308
2.0446
2.2583
2.4721
2.6858
years

Figure SM.9. Box plots representing the values of the six functional traits and of the total plant carbon storage simulated by CAETÊ in its trait-based approach**.** Each boxplot represents the median value (orange tick) and variance for each of the 10 runs. The boxes extend from the first to the third quartiles, and the whiskers extend from the minimum and maximum data. The outliers are not shown. Each represented simulation ensemble contains 10 simulations with the same number of PLSs (50, 100, 200, 500, 1000, 3000) randomly sampled from the potential functional space (see Appendix SM.2). Total C.: total plant carbon storage; F. roots allocation: fine roots allocation; res. time: residence time. PLS: plant life strategy.

number of sampled PLSs improves the ability in representing the total traits combinations in the potential functional space.

Supplementary Material SM.3 - **Building hypervolumes**

The method to analyze functional diversity from a multi-trait perspective is the hypervolume metric from Blonder et al. (2014). To use this method, the components entering the analysis need to be in comparable units (e.g., centered and scaled), uncorrelated and the number of variables should not exceed 5-8 (Barros et al., 2016; Blonder et al., 2014). In this study we used six variable functional traits that present distinct units and are correlated (mainly the allocation ones). In that sense, in order to overcome these limitations, we performed, as recommended by Barros et al. (2016), a scaled principal component analysis (PCA; Fig. SM.10) and selected to perform the hypervolumes the factor scores of the first three orthogonal principal components PCs which retained a cumulative variance explanation > 95% (Barros et al., 2016). Since our interest was to assess differences in the hypervolumes with the applied low precipitation scenario, the PCA was calculated using regular climate and low precipitation datasets together (Barros et al., 2016). After that, separate hypervolumes were calculated from the factor scores corresponding to each dataset (Fig. 5). The same procedure was made considering the dataset corresponded to the three spatial windows (Fig. SM.11)

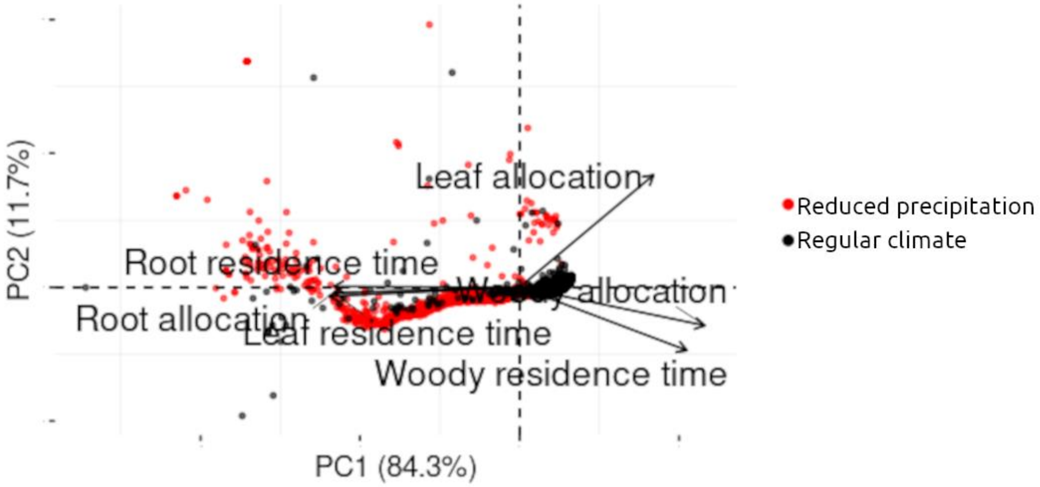

Figure SM.10. Principal component analysis of the trait values used to produce the hypervolumes (Fig. 5). The dataset is composed of the model results regarding the six functional traits for trait-based approach and for both climate scenarios (reduced precipitation and regular climate).

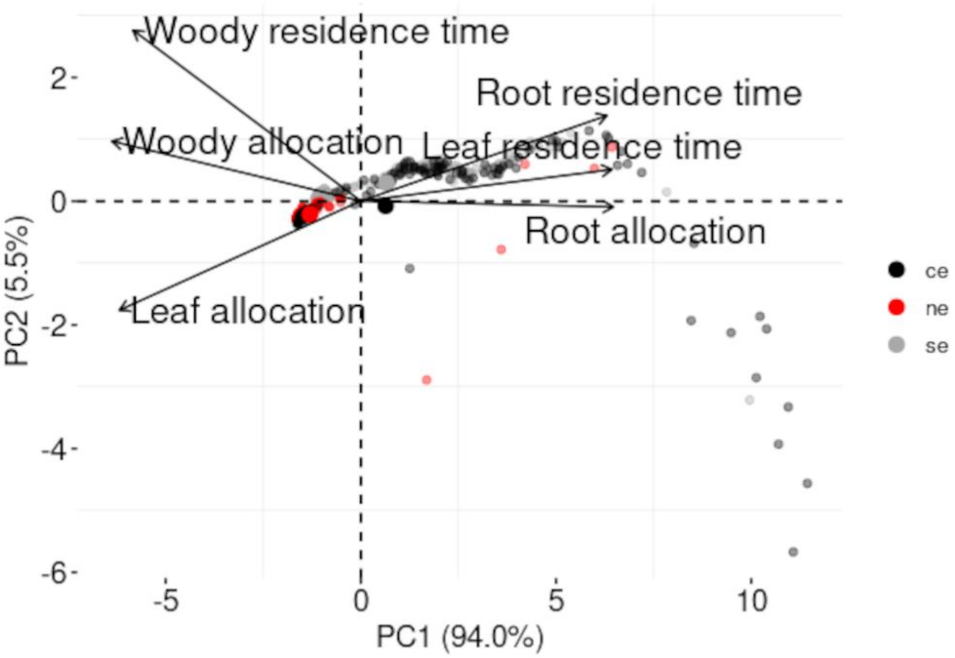

Figure SM.11. Principal component analysis of the trait values used to produce the hypervolumes (Fig. SM.7). The dataset is composed of the model results regarding the six functional traits for trait-based approach in the three spatial windows along amazon basin in the two used climatic scenarios (reduced precipitation and regular climate). ce: center. ne: northwest. se: southeast.

References

Barros, C., Thuiller, W., Georges, D., Boulangeat, I., & Münkemüller, T. (2016). N-dimensional hypervolumes to study stability of complex ecosystems. *Ecology Letters*, *19*(7), 729–742. https://doi.org/10.1111/ele.12617

Blonder, B., Lamanna, C., Violle, C., & Enquist, B. J. (2014). The n-dimensional hypervolume. *Global Ecology and Biogeography*, *23*(5), 595–609. https://doi.org/10.1111/geb.12146

De Pury, D. G. G., & Farquhar, G. D. (1997). Simple scaling of photosynthesis from leaves to canopies without the errors of big-leaf models. *Plant, Cell and Environment*, *20*(5), 537–557. https://doi.org/10.1111/j.1365-3040.1997.00094.x

Farquhar, G. D., Caemmerer, S. Von, & Berry, J. a. (1980). A biochemical model of photosynthetic CO2 assimilation in leaves of C3 species. *Planta*, *90*, 78–90. https://doi.org/10.1007/BF00386231

Gerten, D., Schaphoff, S., Haberlandt, U., Lucht, W., & Sitch, S. (2004). Terrestrial vegetation and water balance - Hydrological evaluation of a dynamic global vegetation model. *Journal of Hydrology*, *286*(1–4), 249–270. https://doi.org/10.1016/j.jhydrol.2003.09.029

Grime, J. P. (1998). Benefits of plant diversity to ecosystems: Immediate, filter and founder effects. *Journal of Ecology*, *86*(6), 902–910. https://doi.org/10.1046/j.1365-2745.1998.00306.x

Lapola, D. M., Oyama, M. D., & Nobre, C. A. (2009). Exploring the range of climate biome projections for tropical South America: The role of CO2 fertilization and seasonality. *Global Biogeochemical Cycles*, *23*(3), 1–22. https://doi.org/10.1029/2008GB003357

Levis, S., Bonan, G. B., Vertenstein, M., & Oleson, K. W. (2004). The Community Land Model's Dynamic Global Vegetation Model (CLM-DGVM). *Ncar/Tn-459+Ia*, 50. https://doi.org/10.5065/D6P26W36

McGee, M. (2020, March 2). *Monthly CO2.* CO2.Earth. https://www.co2.earth/monthly-co2

Medlyn, B. E., Duursma, R. A., Eamus, D., Ellsworth, D. S., Prentice, I. C., Barton, C. V. M., … Wingate, L. (2011). Reconciling the optimal and empirical approaches to modelling stomatal conductance. *Global Change Biology*, *17*(6), 2134–2144. https://doi.org/10.1111/j.1365-2486.2010.02375.x

Oyama, M. D., & Nobre, C. a. (2004). A simple potential vegetation model for coupling with the Simple Biosphere Model (SiB). *Rev. Bras. Meteorol.*, *19*, 203–216.

Pavlick, R., Drewry, D. T., Bohn, K., Reu, B., & Kleidon, A. (2013). The Jena Diversity-Dynamic Global Vegetation Model (JeDi-DGVM): a diverse approach to representing terrestrial biogeography and biogeochemistry based on plant functional trade-offs. *Biogeosciences*, *10*(6), 4137–4177. https://doi.org/10.5194/bg-10-4137-2013

Reich, P B, Walters, M. B., & Ellsworth, D. S. (1997). From tropics to tundra: global convergence in plant functioning. *Proceedings of the National Academy of Sciences of the United States of America*, *94*(25), 13730–13734. https://doi.org/10.1073/pnas.94.25.13730

Reich, Peter B. (2014). The world-wide “fast-slow” plant economics spectrum: A traits manifesto. *Journal of Ecology*, *102*(2), 275–301. https://doi.org/10.1111/1365-2745.12211

Reu, B., Proulx, R., Bohn, K., Dyke, J. G., Kleidon, A., Pavlick, R., & Schmidtlein, S. (2011). The role of climate and plant functional trade-offs in shaping global biome and biodiversity patterns. *Global Ecology and Biogeography*, *20*(4), 570–581. https://doi.org/10.1111/j.1466-8238.2010.00621.x

Ryan, M. G. (1991a). A simple method for estimating gross carbon budgets for vegetation in forest ecosystems. *Tree Physiology*, *9*(1_2), 255–266. https://doi.org/10.1093/treephys/9.1-2.255

Ryan, M. G. (1991b). Effects of Climate Change on Plant Respiration, *1*(2), 157–167.

Scheiter, S., Langan, L., & Higgins, S. I. (2013). Next-generation dynamic global vegetation models: learning from community ecology. *The New Phytologist*. https://doi.org/10.1111/nph.12210

Sitch, S., Smith, B., Prentice, I. C., Arneth, A., Bondeau, A., Cramer, W., … Venevsky, S. (2003). Evaluation of ecosystem dynamics, plant geography and terrestrial carbon cycling in the LPJ dynamic global vegetation model. *Global Change Biology*. https://doi.org/10.1046/j.1365-2486.2003.00569.x

Warszawski, L., Frieler, K., Huber, V., Piontek, F., Serdeczny, O., & Schewe, J. (2014). The inter-sectoral impact model intercomparison project (ISI-MIP): Project framework. *Proceedings of the National Academy of Sciences of the United States of America*, *111*(9), 3228–3232. https://doi.org/10.1073/pnas.1312330110

Wright, I. J., Reich, P. B., Westoby, M., Ackerly, D. D., Baruch, Z., Bongers, F., … Gulias, J. (2004). The worldwide leaf economics spectrum. *Nature*, *428*, 821–827

CHAPTER II - Tropical forest resilience under increased drought frequency: insights from ecosystem indicators beyondcarbon stocks

Abstract

Given the threats tropical forests face due to climate change, particularly the projected increase in drought frequency and intensity in the Amazon region, understanding the resilience of these forests is fundamental. In this study, we conducted modeling experiments using a varying-trait-based vegetation model (CAETÊ) to assess the impacts of a 30% reduction in precipitation on Amazon forest resilience applied at two different frequencies: every eight years (7-year frequency) and alternately every other year (2-year frequency). Control group simulations ran under normal climate with no reduction. Here, we simulated 6,000 plant life strategies (PLSs), each defined by varying combinations of functional traits: wood density (*WD*), specific leaf area (*SLA*), and stomatal conductance sensitivity to CO_2 assimilation (*g1*). In addition to traditional carbon stock assessments, we explored ecosystem resilience by examining other ecosystem state indicators: net primary productivity (NPP), evapotranspiration, water use efficiency (WUE), and the diversity of surviving plant life strategies (PLSs). Our findings unveiled a complete collapse under the 2-year frequency scenario in 2006 and diminished resilience in the 8-year frequency scenario, leading to changes in ecosystem configuration with lower NPP, carbon stock, evapotranspiration, and surviving strategies, but increased WUE. Despite these changes, the system maintained its states effectively during at least three instances of reduced precipitation for both frequency applications. However, the recurring droughts gradually reduced ecosystem resilience, rendering it more vulnerable to minor fluctuations. For instance, after the relatively stable period of 3 droughts, just one additional drought event was enough to trigger a sharp decline in the ecosystem indicator, ultimately resulting in system collapse under the 2-year precipitation reduction scenario, and a shift in ecosystem configuration under the 8-year climate condition. Each ecosystem indicator exhibited a unique response to drought events, with NPP being identified as the most sensitive, followed by evapotranspiration. This highlights the importance of considering multiple indicators when analyzing resilience, and not only carbon stocks. The low resilience of evapotranspiration is particularly significant, given its crucial role in the Amazon rainforest, as it is involved in precipitation feedback loops. The functional composition did not change prominently under the 8-year frequency condition, whereas under the 2-year frequency, there was a significant shift in the selection of surviving strategies during drought events: a decrease in wood density, an increase in specific leaf area (*SLA*), and a decrease in *g1*. The changes in wood density and *SLA*

contradicted expectations and previous observations. This discrepancy can be justified by the functioning of the model, as it tends to select strategies with faster biomass accumulation capacity due to its grid cell occupation scheme. On the other hand, the response of *g1* was as expected. The decrease in *g1* is associated with the selection of strategies that maximize water use efficiency, but it simultaneously reduces carbon assimilation, which contributes to the long-term decrease in resilience. This study underscores the vulnerability of tropical forests to climate change-induced disturbances and the need for comprehensive conservation strategies that account for the diverse responses of ecosystem components. Our results show that ecosystem processes and properties can be less resilient than carbon stocks, suggesting that terrestrial ecosystems worldwide may be even more vulnerable than previously thought.

1. Introduction

Climate change poses significant threats to tropical forests worldwide, endangering their biodiversity, ecological functions, and the livelihoods of millions who rely on them (Bennett et al., 2023). The escalating temperatures, shifting precipitation patterns, and more frequent extreme weather events, such as droughts, have the potential to induce alterations in forest structure, species composition, and distribution (Malhi et al., 2008; Corlett, 2011). These transformations can disrupt crucial ecological processes, including carbon cycling and water regulation, which are vital for sustaining the vitality and resilience of tropical forest ecosystems (Bonan, 2008; Malhi et al., 2014). Furthermore, they can push ecosystems beyond their typical range of variability (Keane et al., 2009), triggering unexpected and nonlinear responses, such as abrupt transitions to alternative ecosystem states (Albrich et al., 2020; Ratajczak et al., 2018). An ecosystem state can be defined as a particular configuration of an ecosystem that is characterized by its structure, composition, and functional processes and properties. This scenario not only poses a challenge for ecosystem managers but also presents a formidable obstacle for researchers striving to comprehend and evaluate reactions to unprecedented conditions (Albrich et al., 2020).

Tropical forests play a critical role in mitigating climate change by sequestering carbon dioxide and providing essential ecosystem services, such as regulating climate and preserving biodiversity (Artaxo et al., 2022; Bonan, 2008; Malhi et al., 2014). Given the importance of these ecosystems, it is paramount to assess the impacts of climate change and bridge existing knowledge gaps (Malhi et al., 2014; Corlett, 2016). Among the world's largest tropical forests, the Amazon plays a pivotal role in the carbon and water cycles, owing to its exceptional productivity, carbon storage capacity, and diverse biodiversity. However, the resilience of the Amazon forest faces escalating threats from climate change and human interventions, prompting concerns about its capacity to adapt to environmental shifts (Boulton et al., 2022; Flores et al., 2024). Comprehending the resilience of the Amazon holds critical importance for regional ecosystems, global climate stability (Ciemer et al., 2019), and the conservation of biodiversity (Boulton et al., 2022). A decline in the Amazon's resilience could trigger significant repercussions, including diminished CO_2 absorption, reduced global carbon storage and potentially leading to a positive feedback loop that accelerates global warming (Poulter et al., 2010; Rowland et al., 2015; Phillips et al., 2009). The uncertainties surrounding the Amazon forest's resilience (Doughty et al., 2015; Hollunder et al., 2022; Huntingford et al., 2013; 2008) underscore the urgent necessity to address environmental threats and unravel the mechanisms governing the Amazon's ability to confront these challenges.

Recent research indicates that natural ecosystems, such as the Amazon forest, are facing a decline in resilience (Boulton et al., 2022; Flores et al., 2024; Forzieri et al., 2022; Hubau et al., 2020; Liu et al., 2019). This diminishing resilience can contract the Amazon's "attraction basin," representing the range of conditions the forest can endure without transitioning to an alternative state (Scheffer et al., 2009). As resilience weakens, the forest becomes increasingly susceptible to disturbances and minor disruptions that could unsettle its equilibrium, potentially leading to critical thresholds (Forzieri et al., 2022) and triggering shifts in ecosystem dynamics or transitions to alternate states (Scheffer et al., 2009). For instance, a reduction in the Amazon forest's resilience could drive the ecosystem towards a critical threshold of rainforest dieback (Boulton et al., 2022).

Of particular concern is the significant impact of climate change on the Amazon's precipitation patterns, resulting in heightened variability in rainfall and more frequent and severe drought events across the region (Flores et al., 2024; Phillips et al., 2009). While consistent directional trends in total rainfall remain elusive for the region as a whole (Artaxo & Marengo et al., 2020), specific areas within the Amazon Basin have encountered recurring periods of abnormal dryness over the past two decades (Feldpausch et al., 2016; Marengo et al., 2011). These prolonged drought episodes pose a substantial threat to the Amazon ecosystem's resilience, as demonstrated by studies linking events like those in 2005 and 2010 to a decline in resilience (Boulton et al., 2022) and subsequent reductions in the forest's carbon sequestration capacity (Brienen et al., 2015; Feldpausch et al., 2016). Water scarcity, a primary driver behind these occurrences, can erode resilience through a complex interplay of mechanisms, exacerbating the impacts of drought. These mechanisms include increased mortality rates, reduced productivity, compromised growth capacity, and alterations in species and functional composition (Aguirre-Gutiérrez et al., 2019; Fauset et al., 2012; Doughty et al., 2015; Phillips et al., 2009). Consequently, climate change, deforestation, and other human-induced disturbances are disrupting the Amazon's self-sustaining water cycle and carbon storage functions (Artaxo et al., 2022; Malhi et al., 2009).

Despite increasing recognition of climate change's impact on the resilience of the Amazon in recent years (Allen et al., 2010; Chave et al., 2008), persistent uncertainties remain regarding vegetation response (Aleixo et al., 2019; Brienen et al., 2015; Chave et al., 2008; Levine et al., 2016). The bulk of studies on forest resilience concentrate on changes in carbon stocks/biomass as the main ecosystem indicator (e.g., Boulton et al., 2022; Cox et al., 2000; Huntingford et al., 2013; Isbell et al., 2015; Sakschewski et al., 2016; Huntingford et al., 2013), operating under the assumption that carbon stock serves as a crucial indicator of ecosystem health and functionality (Yang et al., 2024; Poorter et al., 2016). However, the response of Amazon forests' carbon stock, both present and future, remains highly uncertain with no consensus: while some studies indicate a decrease in carbon stock (Boulton et al., 2022; Brienen et al., 2015; Enquist & Enquist 2011; Phillips et al., 2009; Saatchi et al., 2021), others report an increase in biomass in recent years within the Amazon forest (Baker et al., 2004; Chave et al., 2008; Phillips et al., 1998).

Detecting changes in the resilience of natural ecosystems can be challenging, and focusing solely on one ecosystem indicator, such as biomass, may obscure other crucial processes and properties essential for ecosystem functioning (Hu et al., 2022; Dakos et al., 2019). Moreover, even if carbon is maintained or increased in a system, other properties and processes may have been compromised (Mori et al 2013; de Bello et al., 2021). Conversely, if carbon decreases, other processes could indicate a loss of resilience even before changes in carbon stocks become apparent (Hu et al., 2022). This suggests that the resilience of the system can deteriorate or be compromised without immediate or noticeable changes in its overall condition, such as in carbon stocks (Boulton et al., 2022; Jones et al., 2009; Dakos et al., 2019). The ecosystem functioning as a whole is multifunctional, that is, it is sustained by several processes (Mouillot et al., 2011; Reiss et al., 2009) that can be as important as carbon stock for climate feedbacks (e.g., through the intricate process of evapotranspiration, the forest contributes to regional and global climate regulation by releasing moisture into the atmosphere; Flores et al., 2024; Staal et al., 2018). Thus, the determination of resilience through the biomass response to disturbances does not seem enough to comprehensively understand ecosystem response in the long term (de Bello et al., 2021; Ferreira et al., 2018; Manning et al., 2018).

Although it has been widely neglected in the resilience studies (Dakos et al., 2019), assessing ecosystem resilience also requires considering potential shifts in functional composition (Dakos et al., 2019; Sakschewski et al., 2016), particularly in response to drought events (Aguirre-Gutiérrez et al., 2022; Brum et al., 2019), Such events can significantly alter plant species' traits and strategies, consequently affecting functional composition (Enquist & Enquist, 2011; Esquivel-Muelbert et al., 2017; González-M. et al., 2021; Umaña et al., 2023) and ultimately the ecosystem functioning (Diaz & Cabido, 2001; Holzwarth et al., 2015). The response of species to extreme drought varies depending on their unique combinations of functional traits (Aguirre-Gutiérrez et al., 2022; Brum et al., 2019; González-M. et al., 2021; Allen et al., 2017), which are critical for tree survival and growth during water scarcity (Allen et al., 2017; González-M. et al., 2021; Oliveira et al., 2021). Traits like specific leaf area, wood density, and stomatal conductance play vital roles in trees' ability to thrive under drought conditions (González-M. et al., 2021). Some species prioritize hydraulic safety and efficiency, while others invest more in leaf and wood tissues (González-M. et al., 2021). This shift towards drought-tolerant traits may alter species composition, favoring drought-resistant species over water-sensitive ones. This type of change have already been observed in tropical forests (Enquist & Enquist et al., 2011; Esquivel-Muelbert et al., 2017; Fauset et al., 2012; Umaña et al., 2023). Because of this adaptation the ecosystems might be more resilient than previously taught (Fauset et al., 2012; Sakschewski et al., 2016). Understanding these responses is essential for predicting the impacts of future drought scenarios on tropical forests (Enquist & Enquist, 2011; González-M. et al., 2021; Umaña et al., 2023) and its resilience (Aguirre-Gutiérrez et al., 2022).

Vegetation models play a crucial role in enhancing our understanding of the impacts of drought on vegetation (Xu et al., 2013; Fisher et al., 2010). These models offer unparalleled flexibility and freedom from spatial and temporal limitations (Albrich et al., 2020). Experimental studies on resilience in forest ecosystems face challenges due to the extensive timeframes and spatial dimensions required for meaningful insights (Albrich et al., 2020). Another key advantage of these models is their ability to isolate individual variables, allowing researchers to differentiate the specific effects of climate change-induced factors, such as drought frequency and intensity. Moreover, vegetation models provide a platform to simulate extremely rare events that may be impractical to study solely through experiments or field observations (Egli et al., 2018; Seidl et al., 2014). They enable the exploration of the impacts of environmental changes that lack historical precedents (Albrich et al., 2020), allowing researchers to simulate severe weather events like droughts and evaluate how ecosystems respond and adapt to such disturbances over time. For example, the majority of observations regarding the impact of drought on ecosystem functioning, with only a few exceptions, are derived from a single drought occurrence (Bonal et al., 2016). However, the frequency seems to play a very important role and models can be used to test the role of the frequency in the sensitivity. Additionally, over the past decade, vegetation models have increasingly sought to incorporate the diversity of plant strategies found in nature through trait-based models. This approach has been pivotal in advancing our understanding of the role of functional diversity in ecosystem resilience to climate change (Sakschewski et al., 2016), although it remains relatively underexplored (Rius et al., 2023; Sakschewski et al., 2016). Trait-based models allow for a detailed examination of functional diversity and its connections to ecosystem functioning. By integrating these approaches into vegetation models, we can more accurately predict how ecosystems will respond to changing environmental conditions and human disturbances, and assess their resilience in the face of unprecedented conditions.

2. Objectives

Drawing from recent studies and collective efforts to expand our understanding, this essay utilizes the trait-based vegetation model CAETÊ to delve deeper into the repercussions of severe and recurrent droughts on Amazon forest resilience. This model aims to encapsulate a high degree of functional diversity by incorporating 6000 distinct combinations of trait values, thereby striving to reflect the wide-ranging variability of plant life strategies (PLSs) observed in nature. To assess the significance of severity and frequency, we conducted simulations under three different climatic conditions: regular climate, and a 30% reduction in precipitation applied at two distinct frequencies – once every 8 years, and alternately each year. In order to comprehensively evaluate forest resilience, we expanded our analysis beyond the traditional carbon stock indicator. We incorporated additional ecosystem properties and processes as indicators of forest resilience, including net primary productivity (NPP), evapotranspiration, water use efficiency (WUE), and the diversity of surviving plant life strategies (PLSs). Furthermore, we examined how drought applications influenced functional traits composition of the PLSs, encompassing wood density (*WD*), specific leaf area (SLA), stomatal conductance sensitivity to CO_2 assimilation (*g1*). In our analyses, we assessed resilience by examining various aspects. Firstly, we investigated the system's capacity to maintain its different properties and processes despite the disturbance application. Secondly, we identified changes in the time series by detecting critical thresholds (breakpoints) and determining their occurrence times along the time series. We also assessed changes in functional composition to better understand the changes in ecosystem processes and properties.

More specifically we seeked to advance in the following questions:

1. How do different ecosystem resilience indicators respond to changes in reduced precipitation concerning temporal dynamics compared to regular climate? Have breakpoints been identified, and if so, what is their timing in relation to the shifts in precipitation patterns?

2. Do any ecosystem indicators exhibit signs of declining resilience prior to changes in carbon stock?
3. What role does drought frequency play in influencing ecosystem resilience?
4. Are there observable changes in the system's state or configuration in response to the applied disturbances?
5. How does functional diversity within the plant strategies respond to a drier climate and more frequent drought events?

3. Methods

3.1. The model CAETÊ

3.1.1. General model description

The CAETÊ (Carbon and Ecosystem Functional-Trait Evaluation) model is a trait-based vegetation model designed that seeks to represent the diversity of plant strategies and its functional traits observed in nature (Rius et al., 2023). It achieves this by simulating various plant life strategies (PLSs) through the random assignment of functional trait values, rather than representing vegetation through a small amount of Plant Functional Types (PFTs), as is usually done in most vegetation models. This approach differs from conventional models by emphasizing the variability of plant functional traits. In CAETÊ, plant functional traits that, in the model, are parameters that ends up defining the plant eco-physiological behavior and its interaction with the environment, are randomly assigned within specified ranges obtained from literature, controlling eco-physiological characteristics such as carbon acquisition via photosynthesis, carbon distribution within plant compartments, and evapotranspiration. Each PLS is represented by a unique combination of values for each functional trait. These diverse plant strategies are simulated simultaneously using the same eco-physiological parameterizations and climatic forcings, with only the values of functional traits varying from one strategy to another.

The creation of PLSs hinges on the notion that the observed range of values for a functional trait in nature constitutes one axis of a multidimensional hypervolume formed by the combination of *n* chosen functional traits. Each point within this hypervolume represents a unique combination of trait values, delineating a PLS. These trait values are sampled from the entire range used as a reference. The resultant volume forms a potential functional space with myriad trait combinations. Analogous to other trait-based models, such as Pavlick et al. (2013) and Reu et al. (2011), CAETÊ posits that sampling an adequate number of PLSs from this potential space, coupled with an environmental filtering mechanism, enables the model to generate realistic biogeochemical and functional diversity patterns.

During each iteration, at a daily time step, the distinct performances of PLSs/PFTs dictate ecosystem-scale processes and properties, such as gross primary productivity (GPP), evapotranspiration, and C storage. Together with environmental conditions, these factors determine the composition of PLSs and PFTs in each grid cell for subsequent iterations. Performance is quantified as the relative abundance of a PLS/PFT in a specific grid cell.

3.1.2. Input data and initial conditions

The input data for observed and projected atmospheric climate variables are sourced from the ISIMIP repository (The Inter-Sectoral Impact Model Intercomparison Project). The selected observed data span a period of 38 years between January 1st, 1979, and December 31st, 2016, consisting of daily estimates for four variables: 2-meter surface temperature, relative humidity, atmospheric pressure, precipitation, and incident shortwave radiation. The temporal resolution of the data is daily, and the spatial resolution is 0.5° latitude by 0.5° longitude (Weedon et al., 2014). Annual atmospheric [CO_2] data are also provided by ISIMIP along with the atmospheric data.

A spin-up phase was conducted to achieve a stable dynamic equilibrium state, establishing initial values for vegetation carbon pools and the PLSs to be simulated. Given the significant influence of initial conditions on model outcomes, the spin-up performed under regular climate conditions served as the baseline for all runs, including experiments (see section 3.3). Subsequently, the model was applied using these initial conditions to historical climatology for regular climate conditions and various disturbance scenarios spanning the period from 1979 to 2016. In this model version, ontogenetic growth is not incorporated, necessitating initial conditions for each PLS to fulfill requirements for allocation (see section 3.2.2) on the first day of spin-up and accurately represent typical Amazon forest individuals in terms of structure (height, canopy size, diameter, etc). After rigorous trial and error testing, initial carbon pool combinations were determined for the first day for each plant compartment: 1.0 $kgCm^{-2}$ for leaves, 0.8 $kgCm^{-2}$ for fine roots, 80 $kgCm^{-2}$ in heartwood, 20 $kgCm^{-2}$ for sapwood and 15 $kgCm^{-2}$ for the storage. All PLSs were initialized with equal carbon amounts in their vegetation pools, while exhibiting distinct structural characteristics due to variant traits and respective trade-offs (see section 3.2.1. for details). To establish initial conditions for carbon and water soil pools, a pre-spin-up phase employed the same formulations as those utilized in Darela (2022).

The CAETÊ model operates on a daily time step: on any given day or time step, the flows and rates are calculated, and the reservoirs are updated using the daily average values derived from the input variables for that day and the current state of the model.

3.1.3. Model formulations

Here, we present some formulations for the model. Detailed information on model formulations, including photosynthesis, autotrophic respiration, evapotranspiration, and stomatal conductance, can be found in Rius et al. (2023).

3.1.3.1. Gridcell occupation and performance

The functional trait values assigned to each PLS/PFT determine its ecophysiological behavior and its responses and effects to the environ-ment. For example, each PLS, as a distinct combination of functional traits, constitutes a differential way of storing carbon and capturing water and light. Thus, the functional traits of a PLS or a PFT ultimately determine its performance and survivorship.

In each grid cell, an identical set of PLSs is initialized, determined during the spin-up phase. Consequently, all trait combinations have equal likelihood of occupying a grid cell initially. However, the differential capture of carbon, water, and light through the diverse combination of functional traits can lead to variations in abundance among PLSs. The initialization assumes an initial condition akin to bare soil, indicating the absence of any PLS in the grid cell before initialization. Once a PLS is excluded from a grid cell, it is no longer considered as a potential occupant. Therefore, an environmental filter is applied to assess a PLS's suitability for a specific grid cell. Changes in environmental conditions may render certain trait combinations more productive and capable of storing carbon effectively, leading to their increased relative abundance (Eq. 1). Conversely, other combinations may be unsuitable under altered conditions and are thus excluded.

The performance of an average individual of a PLS i is evaluated through its relative abundance ($A_{r_{i,j}}$) within a grid cell y, which relies on the PLS's relative contribution to the total carbon storage (C_{T_y}) within the grid cell considering the number of living PLSs (S) at a specific time step. Grid cells are represented as a mosaic of PLSs, where each PLS occupies space proportional to its abundance, expressed as a percentage.

Hereafter, the symbol i denotes an average individual of a PLS, represents a grid cell, and z refers to a plant compartment.

$$A_{r_{i,j}} = \frac{C_{i,y}}{C_{T_y}} \tag{Eq. 1}$$

$$C_{T_y} = \sum_{i=1}^{S} \square \, C_{i,y} \tag{Eq. 2}$$

where $C_{i,y}$ is the carbon stock of a PLS, a result of the sum of carbon stored in each plant compartment ($C_{z_{i,y}}$), in its turn determined following allometric constraints (section 3.2.2.).

$$C_{i,y} = \sum_{z=1}^{5} C_{z_{i,y}} \tag{Eq. 3}$$

The survival of a PLS in a given grid cell is contingent upon the simultaneous presence of a minimum amount of carbon (>1 -12 kgCm -2) in the leaf and fine root compartments, as these two compartments are strictly necessary for the photosynthetic process. Additionally, we developed a mortality based on growth efficiency (see section 3.2.2.)

3.1.3.2. Ecosystem-scale processes and properties

The scaling of biogeochemical fluxes from each PLS to the ecosystem level follows the "biomass-ratio" hypothesis (Grime, 1998), which posits that the immediate effects of functional traits of a species are proportional to its relative contribution to the total biomass of the community. Grime (1998) suggests that both theoretical and experimental evidence supports the notion that the extent to which a plant species affects ecosystem functioning can be predicted by its contribution to the total community biomass. Based on this premise, scaling up to the grid cell level involves summing up each property or process performed by each PLS and multiplying it by its relative abundance. Therefore, in each simulation, each PLS is simulated independently, without considering competition, resulting in a potential value for its properties and processes, such as NPP. This value is then multiplied by the PLSs relative abundance, yielding the "actual" value of each property or process. For example, the NPP in a given gridcell y is:

$$NPP_y = \sum_{z=1}^{S} (NPP_{i,y} A_{r_{i,j}}) \qquad \text{(Eq. 4)}$$

This procedure is performed for all biogeochemical fluxes and stocks at each time step.

3.1.3.3. Functional composition in a grid cell and temporal dynamics

The functional composition of a grid cell y in a time step t is given by the values of each variant functional trait used in the simulation. Each functional trait (F) is represented in a grid cell scale (F_{y_t}) by a unique value, which is the sum of this trait value (F_{i,y_t}) calculated for each PLS i alive in the grid cell, weighted by their relative abundances in the time t.

$$F_{y_t} = \sum_{i=1}^{S} (F_{i,y_t} A_{r_{i,j_t}}) \qquad \text{(Eq. 5)}$$

This community weighted mean value can be understood as the dominant trait value in a community (Díaz et al., 2007) in a given time. It allows us to identify the temporal dynamics of each functional trait of interest.

3.2. Model version

The CAETÊ model undergoes continual development and refinement, resulting in various versions of the model. In the chapter I of this thesis, a stationary version of the model (CAETÊ-v1.0; Rius et al., 2023) was utilized. Darela (2022) subsequently introduced the dynamic version of the model, integrating the N and P cycles (CAETÊ-CNP). For this current chapter, we adopt the dynamic version of the model, albeit excluding consideration of the nutrient cycle. Notably, a significant departure from prior versions lies in our approach to carbon allocation. Here, rather than employing fixed percentages of NPP for each plant carbon compartment in each PLS, we've implemented a methodology that incorporates carbon allocation constrained by allometric principles. In this approach, carbon distribution varies in response to environmental conditions and plant performance. Comprehensive details regarding this development can be found in section 3.2.2 where we also offer a concise overview of this and other enhancements made in the current version of the model. It is crucial to emphasize that this latest version lays the groundwork for further refinements and implementations aimed at enhancing the model's utility and applicability to a broader array of ecological inquiries.

3.2.1. Variant traits and associated trade-offs

To refine the specific variant traits in this version, we transformed traits previously considered as variants (in Rius et al. (2023) and Darela et al. (2022)) into fixed values, defined as formula parameters. In the present study, we defined as variant traits the following: wood density (*WD*), specific leaf area (*SLA*) and stomatal conductance sensitivity to CO_2 assimilation (*g1*). The range of values for each trait primarily derives from literature sources (Table 1). From this comprehensive range of trait values, those that will constitute the PLSs are randomly and uniformly sampled (Fig. SM1). These traits are crucial due to their impact on the ability of species to capture energy for growth and conserve resources, such as water, essential for survival under challenging environmental conditions like droughts. Moreover, these traits have been demonstrated to undergo changes in response to shifting climatic conditions (Aguirre-Gutiérrez et al., 2022; 2019; Esquivel-Muelbert et al., 2019).

In CAETÊ, it is common for a significant portion of initially initialized PLSs to perish. On average, approximately 1% of the 6,000 PLSs initiated do not survive. Consequently, extreme trait values are rarely encountered. Using only the observed range of values could lead to undersampling and subsequent incongruence. To address this issue, we established slightly broader ranges of values than those found in the literature (Table 1). It is important to note that a master's student will be dedicated to understanding why so few strategies survive and to determining the best approach for sampling values within these ranges and combining them to obtain a functional diversity representation that aligns with reality.

Table 1. Overview of Variant Functional Traits: The table presents the minimum and maximum values for each trait, indicating the range utilized for model simulations as well as the original range sourced from literature. *SLA*: specific leaf area; *WD*: wood density.

Functional trait	**Range adopted (min-max)**	**Original range (min-max)**	**Unit**	**Reference**
SLA	0.006 - 0.05	0.009 - 0.04	m^2g^{-1}	TRY database (Kattge et al., 2020)
g1	0.1 - 19.0	1.0 - 15.0	$kPa^{1/2}$	Medlyn et al., 2011
WD	0.3 - 1.0	0.5 - 0.9	gcm^{-3}	WD database (Zanne et al., 2009

To avoid the creation of “Darwinian demons” (Law, 1979), that is, optimal but rather unrealistic strategies that maximize all the functions that contribute to plant fitness and survival (Pavlick et al., 2013; Scheiter et al., 2013), each variant functional trait is connected to at least one trade-off (Rius et al., 2023). Theoretically, WD can be connected to the concept of stem economics spectrum that encompasses a range of interconnected stem traits that collectively influence various growth strategies (Baraloto et al., 2010; Chave et al., 2009). These traits include wood density, vessel lengths and diameter, water conductivity, cavitation risk, mechanical properties like resilience to breakage, growth rate, and survival rate. For example, high water conductivity is correlated with increased vessel number and diameter, leading to reduced wood density. However, this association also results in a heightened risk of cavitation during periods of drought or cold, as well as increased susceptibility to breakage. Conversely, lower wood density can enhance growth rates, a characteristic particularly advantageous in highly competitive environments (Sakschewski et al., 2016). However, in the model CAETÊ not all connections of WD with other traits and with plant processes described are represented. Here, the trait WD is associated with carbon investment in sapwood, constraints on carbon distribution, plant growth efficiency, and plant structure (e.g., diameter ($Diam$; m); height (H, m)). For instance, high WD can limit growth due to the increased carbon investment required for leaves and roots. WD is also used in calculating leaf requirements and root requirements in allocation and plays a role in allocation formulations itself (see next section).

$$Diam_{i,y_t} = \left[\left(C_{sapwood_{i,y_t}}/WD_{i,y}\right) * \pi * k_{allom2}\right]^{(1/(2+k_{allom3})} \qquad \text{(Eq. 6)}$$

where $C_{sapwood}$ (kgCm^{-2}) represents the carbon content in the sapwood compartment (see section 3.2.2). k_{allom2} and k_{allom3} are constants equal to 20.0 and 0.8, respectively.
For the height formulation see Eq. 16.

SLA influences how plants allocate resources between leaf construction and other vital functions, impacting growth strategies (Reich et al., 2014; Wright et al., 2004). Species with high SLA invest resources in quickly produced, short-lived leaves for rapid growth, while low SLA species prioritize longer leaf lifespans at the expense of growth rates. High SLA facilitates light capture due to thin leaves but may compromise structural support, while low SLA species maintain robustness at the expense of some light-capturing efficiency. But as for WD not all traits and processes linked to *SLA* are represented. In our model *SLA* is connected to carbon investment in leaves and constraints to the other compartments, photosynthesis, and growth efficiency (see section 3.2.2).

SLA is linked to photosynthesis (see SM.1.3 in Rius et al. 2023 for the respective formulations formulations) through the calculation of leaf area index (LAI):

$$LAI_{i,y_t} = C_{leaf_{i,y_t}} * \ SLA_{i,y} \qquad \text{(Eq. 8)}$$

where C_{leaf} (kgCm^{-2}) represents the carbon content in the leaf compartment (see section 3.2.2). *SLA* (m^{2}kgC$^{-1)}$ also plays a crucial role in carbon distribution, as it determines the leaf area needed to meet allometric constraints. From these leaf requirements, the corresponding root requirements can be derived (see section 3.2.2).

The *g1* parameter represents the stomatal conductance sensitivity to CO$_2$ assimilation, a crucial trait influencing a plant's ability to regulate gas exchange and water loss (Medlyn et al., 2011). High *g1* values indicate a plant's capacity for greater gas exchange, promoting higher photosynthetic rates but also increasing water loss through transpiration. Conversely, lower *g1* values suggest more conservative water use, enhancing WUE but potentially limiting carbon assimilation. The balance of these trade-offs is critical for plant survival and performance under varying environmental conditions. In CAETÊ *g1* is connected to the calculation of stomatal conductance (gs_{i,y_t}; molCO$_2$m^{-2}s^{-1}):

$$gs_{i,y_t} = 1.6 * [1 + (g1/\sqrt{VPD_{y_t}})] * (f_{1_{i,y_t}}/C_{a_y}) \qquad \text{(Eq. 9)}$$

where VPD is the deficit of vapor pressure on the leaf surface (kPa), f_1 is the leaf level gross photosynthesis (molCO$_2$m^{-2}s^{-1}) and C_a is the atmospheric CO$_2$ concentration (ppmv), a model input. As gs determines canopy resistance, evapotranspiration, WUE, and the water stress modifier parameter (*f*5), *g1* also indirectly influences these processes. Detailed formulations for VPD, f_1, canopy resistance, evapotranspiration, WUE, and *f5* are available in the supplementary material of Rius et al. (2023).

3.2.2. Model developments

Most of the developments made for this thesis are presented in this section. Other advancements were also undertaken, albeit offline, and were not integrated into the model. These developments were initially planned for inclusion in this doctoral work; however, despite having been completed, they were not implemented into the model due to time constraints and underestimation of the complexity involved in incorporating these modules into the code. The unimplemented developments can be found in supplementary material SM1. It is important to emphasize that such developments will be crucial for future model enhancements.

The primary distinction in the current model version lies in the revised allocation strategy, which previously relied on fixed percentages for allocation across each compartment within each PLS (Rius et al., 2023). These percentages were treated as variable traits. Now, however, the allocation is determined by allometric constraints. This shift in the model's carbon allocation scheme from a uniform fraction for each plant compartment to an allometric scheme aims to more accurately represent the spatial distribution of biomass. The majority of the new allocation scheme draws inspiration from the Lund-Potsdam-Jena Model (LPJ; Sitch et al., 2003; Smith, Prentice & Sykes, 2001).

The allocation module of CAETÊ is responsible for allocate the carbon originating from NPP between the plant compartments: leaves, fine roots, sapwood, heartwood and storage. Essentially, it calculates the carbon increment, or growth, in each compartment while accounting for carbon losses due to tissue turnover. The carbon lost through turnover is subsequently transferred to the litter pool. The following equations illustrate this process:

The amount of carbon ($C_{t,z}$; kgCm^{-2}) in a time step (t; year) in a compartment (z) is given by the its previous carbon content ($C_{t-1,z}$; kgCm^{-2}), the carbon increment ($C_{inc_{t,z}}$; kgCm^{-2}y^{-1}) and the loss of carbon by turnover (τ_z; kgCy^{-1}) and by autotrophic respiration divided in growth ($R_{g_{t,z}}$; kgCm^{-2}y^{-1}) and maintenance ($R_{m_{t,z}}$; kgCm^{-2}y^{-1}) respiration:

$$C_{t,z} = C_{t-1,z} + C_{inc_{t,z}} - (\tau_z + R_{g_{t,z}} + R_{m_{t,z}}) \qquad \text{(Eq. 10)}$$

Each compartment presents its own turnover rate: 0.5 kgCyear^{-1} for leaves and roots and 0.05 kgCyear^{-1} for sapwood. The carbon lost from leaves and roots go directly to compose the litter, while the carbon turned over in sapwood is converted to heartwood. In that sense, carbon in heartwood ($C_{t,heartwood}$; kgCm^{-2}) is given by:

$$C_{t,heartwood} = C_{t-1,heartwood} + (C_{t,sapwood} * \tau_{sawood}) \qquad \text{(Eq. 11)}$$

Growth respiration, that is, the metabolic costs of constructing new tissue, is assumed to be a quarter of the carbon incorporated in the tissue (Ryan et al. 1991a; 1991b). The carbon incorporated in the tissue is represented by the difference between the carbon content in a compartment in a time t and the carbon content in the same compartment in a time $t - 1$. Total growth respiration is the sum of growth respiration in all the plant compartments considered except for the heartwood once it is considered as a dead tissue.

$$R_{g_{t,z}} = \sum_{z=1}^{4}[1.25(\, C_{t,z} - C_{t-1,z})] \qquad \text{(Eq. 12)}$$

Maintenance respiration is determined based on the nitrogen and carbon content present in each compartment. Nitrogen content in plant tissues significantly influences maintenance respiration, as approximately 60% of nitrogen is allocated to protein repair and replacement (Ryan, 1991a, 1991b). However, it's important to note that nitrogen supply is not currently considered a limiting factor in this context.

$$R_{m_{t,z}} = \sum_{z=1}^{4}[nc_z C_{t,z} 15 * exp(0.03 * T)] \qquad \text{(Eq. 13)}$$

where nc_z represents the N:C ratio for each plant compartment and (T; ºC) is the mean annual temperature. For the fine roots compartment the temperature used is the soil temperature.

The carbon increment ($C_{inc_{t,z}}$; kgCm^{-2}y^{-1}), representing the amount of carbon allocated to a compartment, is distributed in a manner that satisfies the allometric relations:

$$LA = k_{latosa} * SA \qquad \text{(Eq. 14)}$$

where LA is the average individual leaf area (m^2), SA (m^2) is the sapwood cross sectional area and k_{latosa} constant equal to 10000. This relationship is grounded in several studies that suggest a one-to-one correspondence between leaf area and the supporting transport tissue area (Sitch et al., 2003).

Another correlation involves the allocation of resources to fine roots in comparison to leaves, particularly in water-limited environments where plants are compelled to invest a higher proportion of resources in fine root biomass. This allocation strategy leads to elevated maintenance respiration costs and a reduction in potential photosynthetic tissue due to the increased expenditure associated with water and nutrient acquisition (Sitch et al., 2003).

$$C_{leaf} = ltor * f5 * C_{root} \qquad \text{(Eq. 15)}$$

where $f5$ is a value in the range 0-1 representing the current degree of water stress facing the PLS (see supplementary material of Rius et al. (2023)) and $ltor$ is a fixed parameter that represents the leaf to root ratio and is equal to 0.773.

A standard allometry relates vegetation height to stem diameter (e.g. Huang et al., 1992):

$$H_{i,y_t} = k_{allom2} * (Diam_{i,y_t}{}^{k_{allom3}}) \qquad \text{(Eq. 16)}$$

Based on the mathematical derivations of the equations above described, the allocation scheme prioritizes increasing the carbon in the leaf and fine root compartments (see the flowchart in Fig. 1). Initially, it assesses whether the sum of the minimum required increments for leaves ($Leaf_{inc_{min}}$; gC) and roots ($Root_{inc_{min}}$; gC) exceeds zero in the specific time step.

$$Leaf_{inc_{min}} = Leaf_{req_{i,y_t}} - C_{leaf_{i,y_t}} \qquad \text{(Eq. 14)}$$

where $Leaf_{req_{i,y_t}}$is the leaf requirement considering the carbon in sapwood ($C_{sapwood_{i,y_t}}$), *WD*, *H* and *SLA*.

$$Root_{inc_{min}} = Leaf_{req_{i,y_t}}/ltor - C_{root_{i,y_t}} \qquad \text{(Eq. 15)}$$

where $ltor$ is a fixed parameter that represents the leaf to root ratio and is equal to 0.773.

$$Leaf_{req_{i,y_t}} = k_{latosa} * C_{sapwood_{i,y_t}}/WD_{i,y} * H_{i,y} * SLA_{i,y} \qquad \text{(Eq. 16)}$$

k_{latosa} is a fixed parameter that denotes the ratio between leaf area and sapwood and is equal to 10000.

If the sum of the minimum increments for leaves and roots is greater than zero, it indicates that leaf and root tissues must be constructed (i.e., grow) to satisfy the constraints outlined in equations 14 to 16. Then, the allocation follows as in Eq. 17. However, if there is no requirement for leaves and roots, the NPP is fully allocated to storage, serving as a reserve for periods of low productivity. When sufficient NPP is available to meet the leaf and root requirements, it is utilized accordingly. If the available NPP is insufficient, the model assesses whether combining the available NPP with stored carbon can fulfill the requirements. In cases where there is no NPP or the NPP is negative (indicating that respiratory costs exceed the photosynthesis rate), the PLS will use the carbon stored in storage, provided it is sufficient. If it is not, allocation does not occur (see flowchart in Fig. 1). The NPP is calculated in the productivity module of the model, which is also responsible to compute photosynthesis and respiration.

The allocation process, referred to as the increment for each plant compartment, begins with determining the allocation to leaves. This requires the use of a mathematical algorithm known as the bisection method, a root-finding technique for functions within a specified interval (Burden & Douglas, 1985). The function to be resolved for the bisection method is described below, utilizing variables that ensure allometric restrictions and relationships between plant compartments are respected.

The allocation to leaves ($C_{inc_{leaf_{i,y_t}}}$) is determined by the bisection method within the interval [0, 10]:

$$C_{inc_{leaf_{i,y_t}}} = bisection\ method(0{,}10) \quad \text{(Eq. 17)}$$

In the bisection method, the function to be resolved is:

$$x_{searched} = tau_1 * [((SS - x - x)/ltor)/(C_{t,leaf} + x) * tau_3]^{tau_2} \quad \text{(Eq. 18)}$$

where x represents the values in the chosen interval (0 to 10) used in each iteration of the algorithm. The parameters tau_1, tau_2, tau_3 and SS ensure that the allometric constraints are respected:

$$tau_1 = [k_{allom_2}{}^{(2/k_{allom_3})}] * [(4/\pi)/WD] \quad \text{(Eq. 19)}$$

where k_{allom_2} and k_{allom_3} are allometric constants equal to 20.0 and 0.8, respectively, π is the mathematical constant pi, and *WD* is the wood density.

$$tau_2 = 3/k_{allom_3} \qquad \text{(Eq. 20)}$$

$$tau_3 = (k_{latosa}/WD)/SLA \qquad \text{(Eq. 21)}$$

$$SS = (C_{sapwood_{i,y_{t-1}}} + NPP_t + C_{leaf_{i,y_{t-1}}})/ltor + C_{root_{i,y_{t-1}}} \qquad \text{(Eq. 22)}$$

By applying the bisection method iteratively, the model systematically narrows down the interval to find the optimal allocation value for leaves. This ensures that the allocation process adheres to the plant's allometric constraints, optimizing growth and resource distribution across compartments. This iterative process is crucial for accurately determining the increment for each plant compartment, starting with leaves, based on the specified functional and structural relationships.

After $C_{inc_{leaf}}$ is known, we can calculate increment in fine roots and in sapwood:

$$C_{inc_{root_{i,y_t}}} = (C_{inc_{leaf_{i,y_t}}} + C_{leaf_{i,y_{t-1}}})/(ltor - C_{root_{i,y_{t-1}}}) \qquad \text{(Eq. 23)}$$

$$C_{inc_{sapwood_{i,y_t}}} = NPP_{i,y_t} - C_{inc_{leaf_{i,y_t}}} - C_{inc_{root_{i,y_t}}} \qquad \text{(Eq. 24)}$$

In addition to allocation, we also incorporated mortality based on growth efficiency. This ensures that carbon distribution between compartments is ecologically reliable and establishes a connection between the implemented trait variations and the trade-off with mortality. This development is also based on Lund-Potsdam-Jena Model (LPJ; Sitch et al., 2003; Smith, Prentice & Sykes, 2001).

Mortality by growth efficiency ($mort_{groweff_{i,y_t}}$) is calculated considering the growth efficiency of a PLS ($groweff_{i,y_t}$) and other two fixed parameters k_{mort_1} and k_{mort_2} equal to 0.01 and 0.3, respectively.

$$mort_{groweff_{i,y_t}} = k_{mort1}/1 + (k_{mort2} * groweff_{i,y_t}) \qquad \text{(Eq. 25)}$$

$$groweff_{i,y_t} = C_{total_{inc_{i,y_t}}}/C_{leaf_{i,y_t}} * SLA_{i,y} \qquad \text{(Eq. 26)}$$

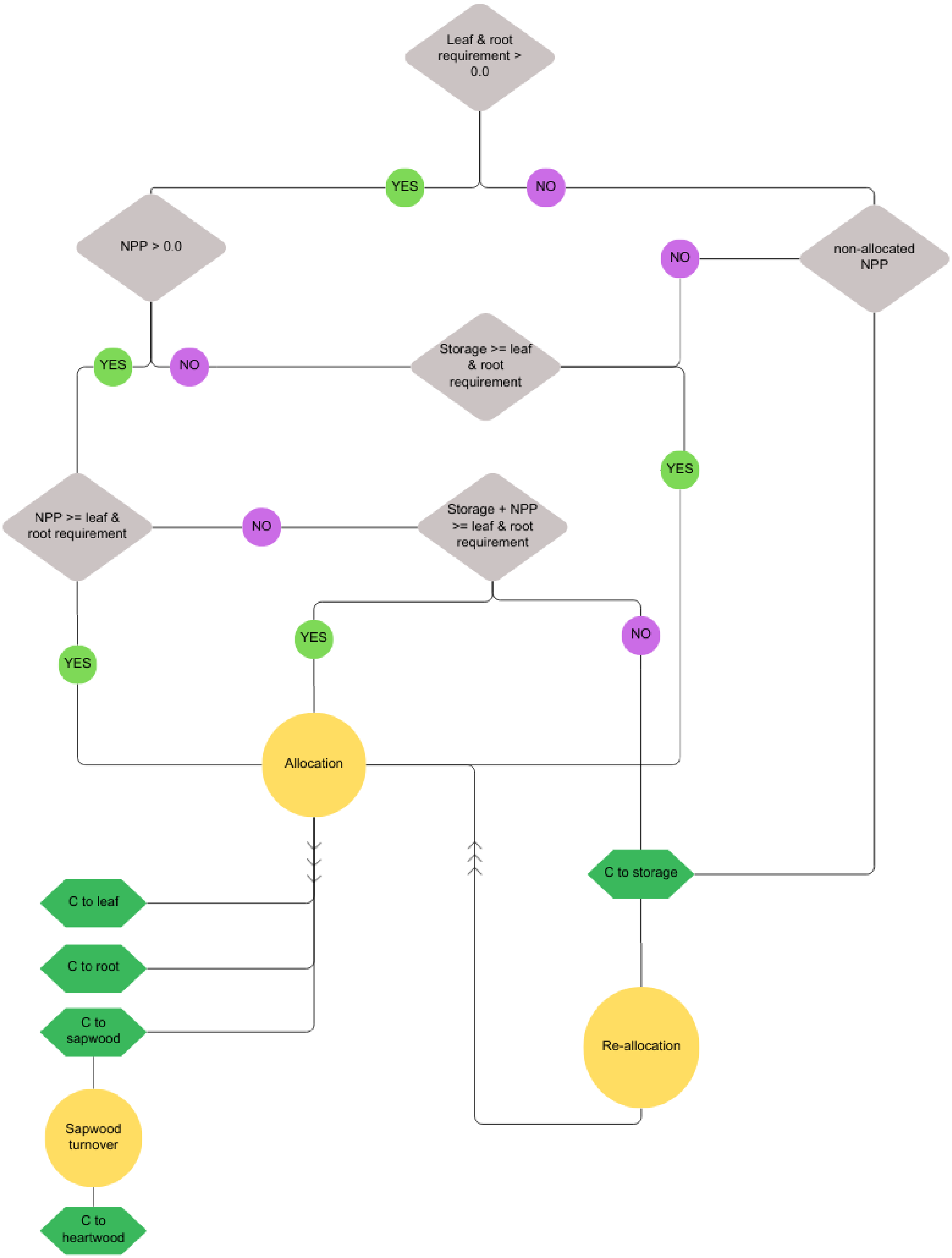

Fig. 1. Arrows indicate the direction of carbon allocation to different plant compartments. Green symbols represent compartments, while grey symbols represent decision evaluations for allocation. NPP: net primary productivity. C: carbon.

3.3. Virtual experiment

To investigate the impacts of projected increases in drought frequency and severity on Amazon forest resilience, a series of virtual experiments was conducted using the model CAETÊ. In accordance with the framework outlined by Albrich et al. (2020), our comprehension of resilience is informed by the foundational contributions of Holling (1973) and Holling & Gunderson (2002). Within this framework, resilience is defined as "...the ability of a system to maintain its functions, structures and feedback in the face of disturbance. It acknowledges the presence of multiple equilibrium states, and the possibility that a system will not return to its state prior to disturbance but rather shifts to an alternative state" (Albrich et al., 2020). These experiments entailed a consistent 30% reduction in precipitation across the entire year of disturbance. The treatments varied based on the frequency of this precipitation reduction, with disturbances occurring at intervals of 2 and 8 years. In the 8-year frequency treatment, the disturbance was implemented for a full year, followed by 7 years of normal climate conditions, and then another year of disturbance. In the case of the 2-year frequency treatment, the disturbance lasted for a full year, also followed by 1 year of regular climate conditions, and then another year of disturbance. This alternating pattern of disturbance and normal climate conditions persisted throughout the simulation period. Simulations for the control group were conducted under regular climate conditions throughout the entire simulated period, as outlined in previous sections. Notably, the reduction applications were made to the time series of regular climate conditions, without the use of projections. Essentially, the model was run three times for the same period (1979 to 2016), each representing a different climatic condition. Each simulation began from the same steady state (see section 3.1.2) and employed identical 6000 PLS. Furthermore, all simulations were conducted within a single grid cell corresponding to Manaus, Amazonas, Brazil.

We acknowledge that a 30% reduction in precipitation represents a significant decrease, particularly concerning the 2-year frequency treatment. Nevertheless, the prediction of changes in precipitation patterns for the Amazon remains highly uncertain, with outcomes varying significantly across different regions of the Amazon basin. Certain areas, such as the southern region, exhibit more pronounced reductions in precipitation (Fu et al., 2013; Marengo et al., 2018). Despite being an extreme scenario, a 30% reduction in precipitation in the Amazon region is within the realm of possibility based on scientific studies and projections (Malhi & Wright, 2004). For instance, projections indicate that by the end of the century (2071-2100), precipitation in the Amazon basin could decrease by about 20% or more (Marengo et al., 2012). The frequency of drought events in the Amazon Basin also varies. On average, the Amazon basin experiences an extreme event, either a flood or a drought, approximately every 10 years. However, in recent years, these events have occurred more frequently, with occurrences within a shorter span of five years (Marengo et al., 2011). Additionally, historical records reveal that the Amazon has encountered mega-droughts in the past, such as those in 1925–1926, 1982–1983, and 1997–1998, primarily associated with El Niño events (Artaxo & Marengo, 2020). Some projections also suggest that severe drought events could occur in up to 9 out of every 10 years by 2060 (Cox et al., 2008; Duffy et al., 2015; Parsons, 2020).

We have opted for these extreme conditions to fully exploit the potential of modeling, as replicating such scenarios in experiments is practically unfeasible and rarely verifiable in observed data (Albrich et al., 2020). For instance, by simulating drastic changes in precipitation, models provide valuable insights into the vegetation's capacity to adapt or withstand such alterations. This is crucial for understanding the extent to which ecosystems may be impacted and what adaptation measures may be necessary. Extreme conditions also aid in identifying vulnerability points in vegetation, revealing areas where it may be more susceptible to significant damage or decline. Examining vegetation responses under such conditions allows us to discern patterns of behavior, aiding in forecasting reactions in various climatic scenarios. Furthermore, testing these extreme conditions is essential for understanding and addressing limitations within vegetation models themselves. Comparing modeling results with real-world observations during extreme events enables us to validate the accuracy and reliability of the models. It also helps in pinpointing potential flaws in the representations of vegetation's biophysical processes, model parameterizations, spatial and temporal resolutions, and the assumptions and hypotheses assumed, thereby contributing to ongoing improvements in modeling and understanding terrestrial ecosystems.

In this experiment, we focused solely on reducing precipitation. We acknowledge that climate change encompasses various other changes, such as temperature increase and CO_2 concentration rise, which interact and may affect vegetation response. This experimental design was chosen to isolate and better understand the effect of water availability reduction. It's challenging to disentangle the effects when multiple aspects change simultaneously, as would be the case with projections.

3.4. Ecosystem state indicators

As recommended by Hu et al. (2022), two sets of variables were selected to assess ecosystem state. One set pertains to the carbon cycle, including net primary productivity and total carbon storage. The other set relates to the water cycle, comprising evapotranspiration and WUE. Furthermore, the evaluation of ecosystem state extended to each carbon stock compartment, namely leaf, root, wood, heartwood, sapwood, and storage. The results for these compartments can be found in Figure SM3. We also used as an ecosystem indicator the number of surviving PLSs as a proxy for species diversity. Our analysis was extended to alterations in functional composition, monitoring shifts in traits to deeply understand ecosystem response to climate dynamics.

3.5. Breakpoints identification

3.5.1. Method overview

Breakpoints are points in time where a significant shift in time series values is detected, indicating a notable change or deviation in the behavior or state of an ecological system (Verbesselt et al., 2010a; 2010b; Almeida, 2017). They mark moments when the system undergoes a notable transition, often signaling a loss of stability or resilience. Breakpoints can manifest as sudden alterations in crucial ecosystem properties or processes, including shifts in species composition, changes in productivity, or disruptions to ecological functions. Identifying breakpoints is crucial for understanding how ecosystems respond to environmental stressors and disturbances, as they can signify critical thresholds beyond which the system may struggle to recover or maintain its previous state. To identify breakpoints in the time series of the ecosystem indicators we used the *bfast* package in R (Verbesselt et al., 2010a; 2010b). "BFAST" stands for Breaks For Additive Season and Trend, which is an additive decomposition model that iteratively fits a piecewise linear trend and seasonal model. In BFAST analysis, the time series data undergoes decomposition into seasonal, trend, and remainder components. The first one accounts for the periodic fluctuations of fixed duration, such as temperature variations and rainfall patterns. The trend factor captures long-term changes in the time series signal. The remainder is the difference between the actual time series and the combined effect of its trend and seasonal components, in other words, a stochastic element of error.

The procedures for detecting breakpoints involve testing or evaluating deviations from the traditional linear regression model:

$$y_i = x_i \beta_i + \epsilon_i, \quad i = 1,2,\dots,n \qquad \text{(Eq. 27)}$$

y_i represents the value of the dependent variable for the i-th observation, while x_i is the value of the independent variable for the i-th observation. The parameter β_i is the slope coefficient, indicating the expected change in y_i for a unit change in x_i. Lastly, ϵ_i is the error term for the i-th observation, representing the variation in y_i that is not explained by the linear model. Here, the i represents segment size between potentially detected breaks in the trend model given as a fraction relative to the sample size, that is, the minimal number of observations in each segment divided by the total length of the timeseries (see section 3.5.3 for the sensitivity of the segment size). n is the total number of observations.

When a breakpoint is identified, the regression coefficients transition from one stable regression to another. If a total of bp breakpoints are detected, there will be bp+1 segments where the regression coefficients remain constant. Consequently, the regression model can be reformulated as the piecewise linear model:

$$y_i = x_i\beta_j + \epsilon_i, \quad i = j_{i-1} + 1, \dots, i_j, \quad j = 1,2, \dots bp \qquad \text{(Eq. 28)}$$

where j represents the segment index and i_j are the breakpoints. The estimation of the breakpoints is accomplished by minimizing the sum of squared residuals of that adjusted regression model.

To be processed by the BFAST algorithm, the time series must be regularly spaced; hence, the datasets used for this analysis were monthly aggregated by a median summarization.

We used this technique to identify breakpoints for all ecosystem indicators except for the surviving number of strategies. This variable is categorical rather than continuous, making BFAST not directly applicable to categorical data analysis.

3.5.2. Resilience evaluation

The overall model of the time series is represented as $Y_t = T_t + S_t + e_t$, where Y_t denotes the observed data at time t. Here, T_t signifies the trend component, S_t represents the seasonal component, and e_t the error component. The method performs structural change detection separately on the trend and seasonal components.In this study, our focus was on the trend component to discern shifts in resilience, as no breakpoints were detected in the seasonal component for any variable analyzed. The trend component T_t is assumed to follow a piecewise linear pattern. This means that the trend is modeled as a series of linear segments, with each segment defined by specific break points denoted as t_1^*, t_2^*, up to t_m^*. The trend component is expressed as following for each segment j ($j = 1, \dots, m$):

$$T_t = \alpha_j + \beta_j t \qquad \text{(Eq. 29)}$$

where α_j represents the intercept and β_j represents the slope of the linear trend within the time interval from t_{j-1}^* to t_j^*. This formulation allows for the trend to exhibit different linear behaviors between consecutive break points, enabling the detection of changes in the trend over time.

The slopes (β_j) of the fitted trend model between the breakpoints can be used to infer the resilience of the system once it indicates the rate of change in the data between these breakpoints (Verbesselt et al., 2010a). In other words, the slope represents the speed at which the values of the time series are changing within a specific interval. A positive slope indicates an increase in the series values, while a negative slope indicates a decrease. Therefore, analyzing the slope between breakpoints can provide insights into the trends and patterns of change in the data over time. The greater the absolute value of the slope (positive or negative), the larger the magnitude of the change in the data between the break points. A positive slope with a high value indicates a sharp increase in the time series values, while a negative slope with a high value indicates a significant decrease. Thus, the magnitude of the slope can be used as a measure of the intensity of the change between breakpoints in a time series. A change in the slope between segments of a time series may indicate changes in the system's ability to recover from disruptive events or adapt to new conditions. For example, a smoother or gradual slope may suggest greater stability and resilience of the system, while abrupt changes in the slope may indicate periods of transition or instability. Therefore, by analyzing the slope between breakpoints in a time series, it is possible to infer the resilience of the system under study and how it responds to changes and disturbances over time.

The bfast algorithm provides users with p-values from ANOVA to evaluate the statistical significance of abrupt changes in trend and seasonal components of a time series. These p-values assess the significance of estimated slopes between breakpoints, indicating whether the observed variances in slopes between segments are statistically significant or due to chance.

3.5.3. Sensitivity analysis for parameter "h"

Usually, a minimal segment size h is also parametrized, which is further used to limit the minimal distance between consecutive breakpoints (Almeida, 2017). The "h" parameter in BFAST analysis acts as a pivotal factor in identifying breaks or sudden shifts within the trend model of a time series. It signifies the minimum segment size between potentially detected breaks within the trend model, presented as a fraction relative to the total sample size. Essentially, "h" dictates the smallest length a segment of the time series must possess to be deemed eligible for a potential breakpoint, with this minimum segment length scaling in proportion to the entire time series. This parameter exerts control over the model's adaptability in discerning alterations in the data. A higher "h" value empowers the algorithm to recognize more potential breakpoints, rendering the model more adaptable, albeit potentially susceptible to overfitting noise in the data. Conversely, a lower "h" value restricts the model to detecting fewer breakpoints, possibly disregarding smaller fluctuations in the time series.

Selecting an appropriate "h" value necessitates a balancing act between model intricacy and sensitivity to data alterations. This decision-making process is critical as it harmonizes the analysis's sensitivity in detecting changes with the risk of overfitting noise in the data. It often demands experimentation and contemplation of the unique characteristics of the time series under scrutiny. Generally, larger and more intricate datasets might thrive with a higher "h" value, while smaller datasets or those exhibiting less variability may warrant a lower value.

During our investigation, we tested various "h" values, including 0.15, 0.2, 0.25, and 0.3. We scrutinized breakpoint identification in correspondence with the original time series. Given the multitude of variables (3 climatic conditions*4 ecosystem indicators = 12 variables) to be analyzed, we determined the "h" value that best aligned with the overall considerations of all variables. Considering the results presented in Fig. SM2 we opted to use the value of 0.25 for the parameter "h". That is, considering the study period, the minimal time span between consecutive breakpoints must be 25% of the data.

4. Results

4.1. Ecosystem indicators and climatic conditions

Figure 2 displays the time series of all selected ecosystem indicators across different climatic conditions. Additionally, Figure 3 complements these time series by incorporating precipitation data. These visualizations illustrate the dependency of the impact of reduced precipitation on the chosen ecosystem indicators, as well as on the frequency of reduced precipitation application.

Under regular climate conditions (Fig. 2 and Fig. 3a), all variables serving as ecosystem indicators demonstrate a consistent pattern in their time series, maintaining the structure of the ecosystem with occasional oscillations. The fluctuations observed in precipitation and the variables exhibit a moderate relationship, suggesting an incomplete temporal coupling between them.

Implementing reduced precipitation at a frequency of eight years (Fig. 2 and Fig. 3b) leads to noticeable alterations in the patterns of all variables when compared to the regular climate curve (Fig. 4a). Notably, NPP emerges as the most sensitive variable to changes, diverging from the reference series as early as 2004 with a deviation exceeding 10%, closely followed by evapotranspiration in 2010 with a similar deviation. This heightened sensitivity is reflected in NPP's substantial impact, reaching its lowest value in 2015 at -56.9% relative to the regular climate. Interestingly, NPP exhibited a notable decline in deviation starting in 2007 (-16.9%), which, however, was only sustained until 2008 (-7.4%). From 2009 (-13%), the difference sharply increased once more. This recovery is preceded by a natural increase in precipitation between 2005, 2006, and 2007 (Fig. 3). However, this increase in precipitation is followed by a reduction, also natural, in precipitation in the years 2008, 2009, and 2010, which may explain the no sustained recovery in NPP. It is important to highlight that these decreases/increases in precipitation are not related to the disturbances applications and can be observed in the regular climatology (Fig. 3). Conversely, the number of plant life strategies and total carbon exhibit greater resilience, requiring more time to deviate from their values compared to those under regular climate conditions (as depicted in Fig. 4a). For instance, the difference exceeds 10% for total carbon in 2012, while the number of PLSs shows a decrease of only -7.5% in the final year of simulation. It's noteworthy that although the number of strategies shows minimal deviation from the regular climate, biogeochemical variables demonstrate more pronounced effects.

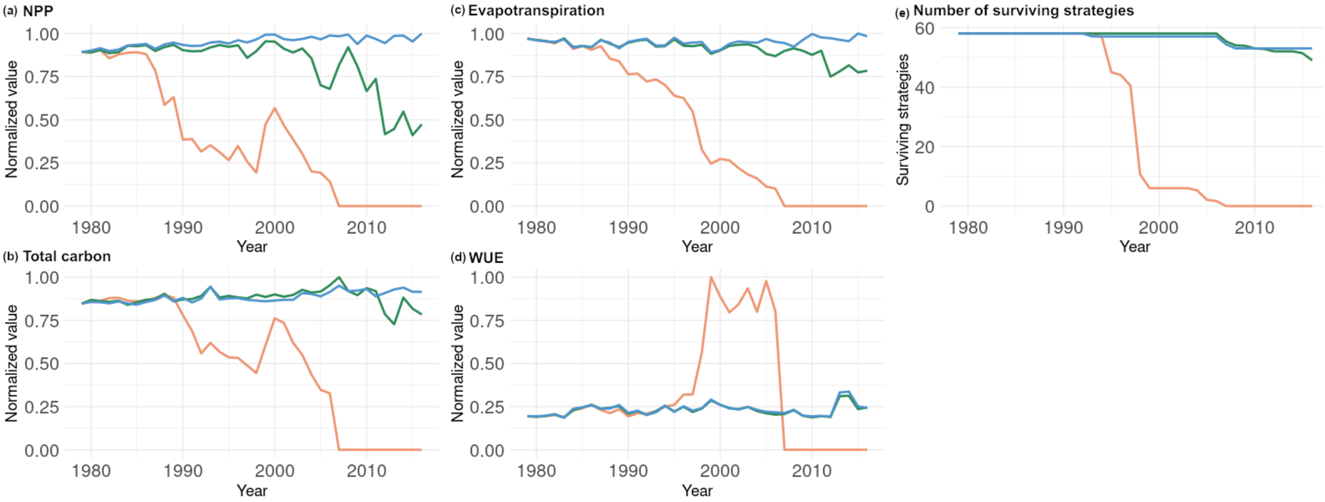

Fig. 2. Time series data spanning from 1979 to 2016 regarding ecosystem indicators (a-d) and the survival strategies of plant life (e) under three distinct climate scenarios: regular conditions (blue line), reduced precipitation (30% less) occurring every 8 years (green line), and alternately every other year (orange line). In detail, (a) and (b) are related to carbon cycle variables, encompassing NPP and total carbon, while (b) and (c) focus on water cycle variables, including evapotranspiration and WUE. The y-axis is normalized from 0 to 1, simplifying comparison across variables and conditions. NPP: net primary productivity; WUE: water use efficiency.

As expected, the application of reduced precipitation at a frequency of two years proved to be the most detrimental for all variables (Fig. 2 and Fig. 3c), resulting in complete system collapse across all the metrics. Notably, the initial indications of resilience loss were most conspicuous in NPP, where it exhibited a remarkable 60% decline compared to the reference (regular climate) after a decade of simulation (Fig. 4). Following closely, evapotranspiration demonstrated the second highest rate of decrease, trailed by total carbon and the number of PLSs (Fig. 4b). However, WUE displayed a distinct behavior, initially experiencing a significant increase approximately 16 years into the simulation, followed by a rapid decline after 10 years, ultimately leading to total collapse (Fig. 4c). This shift in WUE's trajectory may be attributed to the change in the strategies that survived with the reduced precipitation. We observed that after 8 pulse applications, the number of strategies decreased at a very high rate (Fig. 3): in 1995 there was a decrease in 20% of the number of strategies, while in the next couple of years it attended -80% of the number of surviving strategies (Fig. 4). This phenomenon could be attributed to the selective pressure favoring trait combinations, or strategies, that demonstrate enhanced performance under the new climatic conditions, such as more efficient water usage. This aspect warrants further exploration in subsequent discussions.

We observed an intriguing phenomenon with NPP and total carbon that, notably, was not mirrored in evapotranspiration: following a significant decline in their values starting around 1985 for NPP and 1990 for total carbon, both indicators displayed a remarkable recovery (Fig. 2 and 4b). Within less than 5 years, the percentage change relative to normal climate conditions shifted from -80% to -42% for NPP and from -48% to -11% for total carbon. As observed in Figure 2e and in Figure 4b, this is tightly connected to the decrease in the number of surviving strategies. This can be justified by the fact that the selection of strategies that deal better with the condition are the ones that present higher productivity and total carbon, also the decrease in the number of strategies is necessarily linked to an increase in the abundance of the ones that survived decreased leading to an increase in the abundance of strategies that deal better with the new climatic condition a topic to be explored further in subsequent sections. However this recovery does not preclude the system from fully collapsing right after.

Both in the 8-year and 2-year frequency applications, the ecosystem response to pulse disturbance is not immediate. In the case of the 8-year frequency, it takes at least four applications of reduced precipitation to initiate a decline in the variables, yet none experience complete collapse (Fig. 3b). Similarly, for the 2-year application, it requires between 4 and 5 pulses of reduced precipitation for the variable values to begin decreasing and for the system to exhibit structural changes (Fig. 3c). These findings underscore the necessity of accumulating disturbance pulses, emphasizing the significance of disturbance frequency. They also indicate a degree of resilience within the communities. However, even during the intervals between disturbances when the impact of reduced precipitation is mitigated, the indicators used to assess the system's state fail to return to their initial levels.

Fig. 3. Time series plots showing precipitation (blue bars) and ecosystem indicators (red lines). Each column corresponds to a different climatic condition: (a) regular climate, (b) reduced precipitation applied every 8 years, and (c) every 2 years. Each row represents a different ecosystem indicator: 1-NPP, 2-Total Carbon, 3-Evapotranspiration, 4-WUE and 5-Number of surviving PLSs. Light blue bars indicate years without reduced precipitation, while dark blue bars indicate years with reduced precipitation (30%). NPP: Net Primary Productivity; Evap.: Evapotranspiration; WUE: Water Use Efficiency; PLS: Plant Life Strategies; Num. PLSs: number of surviving PLSs.

4.2. Detecting breakpoints

Breakpoints were identified in all variables across various climatic conditions, as illustrated in Figure 5. However, the response of each variable varied uniquely across different climatic scenarios. Notably, in instances where the frequency of reduced precipitation increased, breakpoints occurred earlier, except for WUE. Detailed information regarding the specific dates of these breakpoints can be found in Table 2, while Table 3 presents the corresponding beta coefficients and associated p-values.

In the case of NPP under regular climatic conditions (Fig. 5a.1), a single breakpoint occurred in June 1998, 19 years into the simulation. Before this breakpoint, beta was positive at 0.009 with $p < 0.05$, indicating increasing resilience. After the breakpoint, beta turned negative (-0.001) with a non-significant p-value of 0.608. Total carbon had its first breakpoint (bp1) in December 1992 and the second (bp2) in September 2002, approximately 10 years apart (Fig. 5b.1). Prior to bp1, beta was positive at 0.006 with $p < 0.005$, showing resilience growth. Following bp1, beta turned negative (-0.0160) with $p < 0.005$, suggesting decreased resilience. After bp2, beta was positive at 0.0040 hinting at potential resilience recovery but not statistically significant ($p = 0.0380$). Evapotranspiration experienced a single breakpoint in 1998, with a slightly negative trend before (beta = -0.0001), although not statistically significant ($p = 0.8400$; Fig. 5c.1). Post-breakpoint, resilience significantly increased as indicated by a positive beta of 0.0110 with statistical significance. WUE had two breakpoints: one after ten years in 1989 and another 13 years after bp1 in 2004 (Fig. 5d.1). Before bp1, beta was positive at 0.0203 with $p < 0.05$ showing increased resilience. Between bp1 and bp2, beta remained positive at 0.006 with $p < 0.05$. After bp2, beta was positive at 0.016 suggesting potential resilience recovery with $p < .05$ for both cases of increased post-breakpoint.

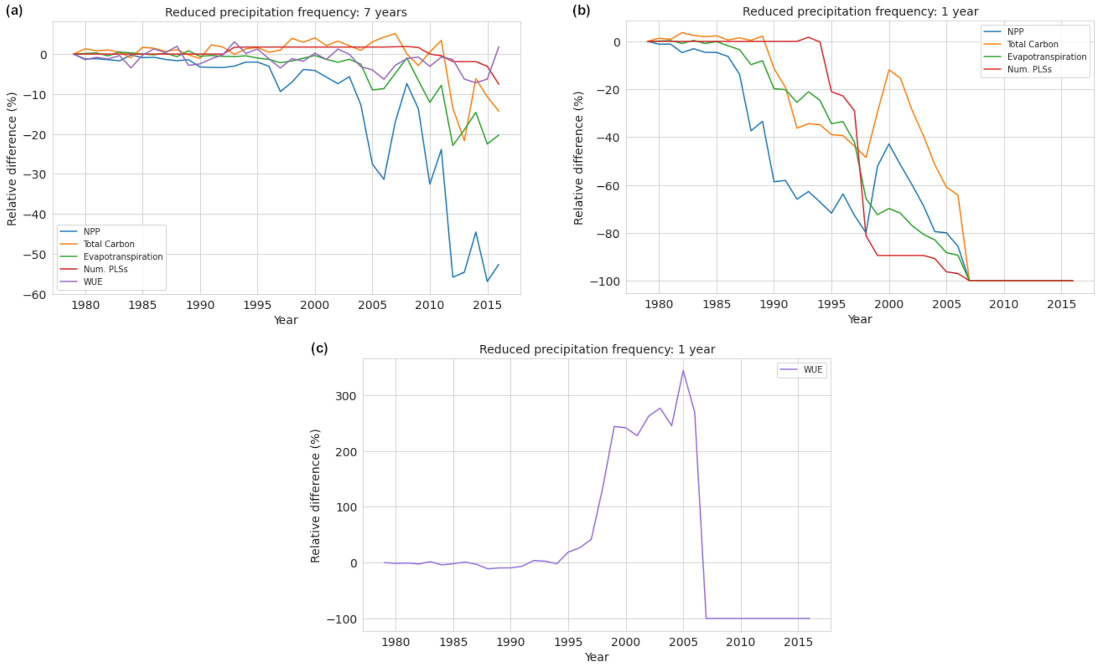

Fig. 4. Time series plots depicting the relative difference (%) of each ecosystem indicator variable compared to the regular climate condition, under different frequencies of reduced precipitation application: every 8 years (a) and every 2 years (b and c). For clarity, WUE is presented separately for the 2-year scenario.
NPP: Net Primary Productivity; Num. PLSs: number of surviving PLSs; WUE: water use efficiency.

In the analysis of reduced precipitation occurring every 8 years, two breakpoints were observed for NPP (Fig. 5a.2). The first breakpoint occurred in 1997, 18 years after the simulation began, and the second breakpoint occurred in 2007, 9 years after the first one. Before the first breakpoint, beta was positive (0.0010) with a non-significant p-value (p1 = 0.1650). However, after the first breakpoint, beta became negative (-0.0327; $p < 0.05$), indicating a significant decline in resilience and slower recovery. Following the second breakpoint, beta remained negative and decreased further (-0.0670, $p < 0.05$), suggesting a continued decrease in resilience and a slower recovery rate. For total carbon, there was a single breakpoint identified in 2006, 27 years after the start of the simulation (Fig. 5b.2). Prior to this point, beta was positive (0.0040; $p < 0.05$), indicating an increase in total carbon resilience over time despite reduced precipitation application. After the breakpoint, beta turned negative (-0.0380; $p < 0.05$), pointing towards a sharp decline in total carbon resilience or a reduced capacity for recovery. Evapotranspiration exhibited a single identified breakpoint in 2007 (Fig. 5c.2). Before this point, the beta value was negative (-0.0048) with a significant p-value, showing a declining trend in resilience. Post-breakpoint, the beta value further

Table 2. Breakpoint dates identified using the *bfast* algorithm for each climatic condition and each indicator of ecosystem state. The "Frequency" column indicates the interval of reduced precipitation application. NA indicates cases where a second breakpoint event was not detected for a given indicator.

Frequency (years)	Ecosystem indicator	Breakpoint 1	Breakpoint 2
Reg clim	NPP	1998-06	NA
Reg clim	Evapotranspiration	1998-05	NA
Reg clim	Total carbon	1992-12	2002-09
Reg clim	WUE	1989-07	2004-10
8	NPP	1997-11	2007-05
8	Evapotranspiration	2007-06	NA
8	Total carbon	2006-01	NA
8	WUE	1989-07	2004-10
2	NPP	1988-06	1999-02
2	Evapotranspiration	1997-11	2007-05
2	Total carbon	1990-08	2006-10
2	WUE	1997-06	2006-12

Reg clim: regular climate; NPP: net primary productivity; WUE: water use efficiency; NA: not applicable.

decreased (-0.0425; $p < 0.05$), implying a substantial reduction in resilience. WUE showed two breakpoints in 1989 and 2004 respectively (Fig. 5d.2). Before the first breakpoint, beta was positive (0.0230; $p < 0.05$), indicating increased resilience. Between both breakpoints, the beta value remained positive (0.0070) with a significant p-value ($p = 0.017$), suggesting continued improvement but less pronounced than before. After the last breakpoint, no significant change in resilience was observed.

The NPP showed two breakpoints for the frequency of 2 years of reduced precipitation

(Fig. 5a.3). The bp1 occurred in 1988, about 9 years into the simulation. Before bp1, the beta value was negative (-0.0120), indicating a change in resilience that was statistically significant. Between bp1 and bp2, the beta value decreased further (-0.03; $p < 0.05$), suggesting a significant decline in resilience. After bp2 in 1999, the beta value continued to decrease (-0.033), indicating a further decline in resilience, which was statistically significant. For the total carbon, two breakpoints were identified: one in 1990 (11 years into the simulation) and another 9 years later (2006; Fig. 5b.3). Before the first breakpoint, the beta value was positive (0.001) but not statistically significant (p1 = 0.071). Between the two breakpoints, the beta value decreased significantly (-0.011; $p < 0.05$), suggesting a decrease in resilience. After the second breakpoint, the beta value continued negative (-0.01), but not significant. Evapotranspiration also exhibited two breakpoints: one in 1997 and another in 2007, occurring at approximately 18 years and then again at around 10 years into the simulation respectively (Fig. 5c.3). Before the first breakpoint, the beta value was negative (-0.02; $p < 0.05$), signaling a decrease in resilience. Between these two points, there was a significant decrease in beta value (-0.027), suggesting a further decline in resilience. After the second breakpoint, beta assumed the value of 0.0, because of the collapse. WUE had two identified breakpoints: one in 1997 (18 years into simulation) and another in 2006 (Fig. 5d.3). Before the first breakpoint, showed an increase in WUE (beta = 0.003, $p < 0.05$). Between both breakpoints significant increase of beta happened (0.028). Afterward, there is no indication of resilience change, once the beta was not significant.

4.3. Number of surviving strategies

As expected, we found that the drought application, particularly its frequency, plays a significant role in determining the number of surviving strategies (Fig. 2e). The change in the number of surviving strategies can primarily be attributed to fluctuations in biomass, as grid cell occupation is determined by the percentage contribution of biomass relative to the total biomass. Accordingly, strategies that exhibit a greater propensity for biomass

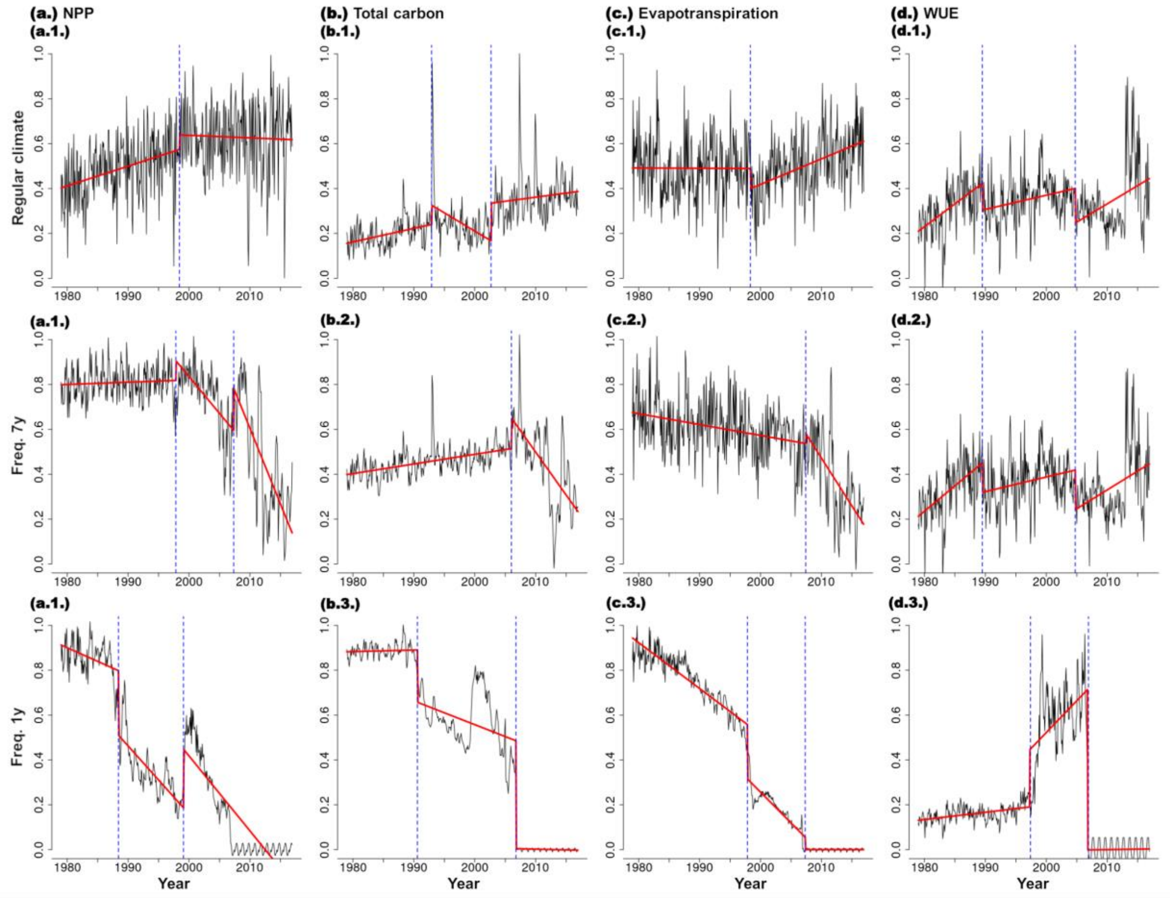

Fig. 5. Graphs representing the time series (black line), the fitted model (red line) that represents the trend between two breakpoints, identified breakpoints (dashed blue). Each column in the figure has graphs for different variables that represent ecosystems indicators: NPP (a, e, i), total carbon (b, f, j), evapotranspiration (c, g, k), and water use efficiency (d, h, l). Rows organize the graphs based on the frequency of reduced precipitation: regular climate (a-d), 8-year frequency (e-h), and 2-year frequency (i-l). All variables are shown in normalized (0 to 1) values on the y-axis for easy comparison.

accumulation under specific environmental conditions tend to increase their relative contribution and overall performance in the model. Among the strategies that endure in various climatic conditions, accounting for natural climate variability under regular conditions and drought applications, are those with functional trait combinations that optimize biomass accumulation. The exploration of these trait combinations, or functional composition, is elaborated upon in the subsequent section.

Table 3. Slopes (β) of segments from the trend component of the time series between the breakpoints. β_1 corresponds to the segment before the first breakpoint; β_2 corresponds to the segment after the second breakpoint (if present) or after the first breakpoint (if only one exists); and β_3 is the segment after the second breakpoint (if present). Breakpoint dates were identified using the BFAST algorithm for each climatic condition and ecosystem state indicator. The "Frequency" column indicates the interval of reduced precipitation application. In cases where a second breakpoint event was not detected for a specific indicator, denoted as NA, there is no third segment available for analysis.

Frequency (years)	**Ecosystem indicator**	β_1	β_2	β_3
Reg clim	NPP	0.009^*	-0.001	NA
Reg clim	Evapotranspiration	-0.0001	0.011^*	NA
Reg clim	Total carbon	0.006^*	-0.016^*	0.004^*
Reg clim	WUE	0.0203^*	0.00634^*	0.0163^*
8	NPP	0.0010	-0.0327^*	-0.0670^*
8	Evapotranspiration	-0.0048^*	-0.0425^*	NA
8	Total carbon	0.0040^*	-0.038^*	NA
8	WUE	0.0230^*	0.007^*	0.0170^*
2	NPP	-0.012^*	-0.03^*	-0.003^*
2	Evapotranspiration	-0.02^*	-0.027^*	0.0
2	Total carbon	0.0007	-0.011^*	-0.01^*
2	WUE	0.003^*	0.028^*	0.0

Reg clim: regular climate; NPP: net primary productivity; WUE: water use efficiency; NA: not applicable.

For regular climate conditions, we observed a consistent maintenance in the number of surviving strategies from 1979 to 1992, totaling 58 surviving strategies. From 1993 onwards, there was a slight change, with the number of surviving strategies decreasing to 57 and remaining stable until 2006. However, in 2007, this number declined to 54, ultimately reaching 53 by the end of the simulation. In the case of the 8-year frequency application, we unexpectedly noted a similar consistent maintenance in the number of surviving strategies from 1979 to 2006, totaling 58 strategies. However, a decline became apparent in 2007, reducing the number to 55, and ultimately dwindling to 49 by the simulation's conclusion. Despite this reduction, the overall change in the number of surviving strategies did not significantly deviate from conditions under regular climate (Fig. 4a). By the simulation's conclusion, there was merely a 7.55% difference compared to the number observed under regular climate conditions. Regarding the 2-year frequency application, we observed a degree of resilience over 15 years, indicated by the maintenance in the number of surviving strategies at 58 (Fig. 2e). However, a decline commenced in 1995, with a notable drop to 45 strategies. In the subsequent two years, there was a significant decrease, dropping to 44 in 1996 (-22.8%), and then sharply declining to 10 in 1998 (-81.2%). Following this substantial reduction, the number of strategies stabilized at 6 from 1999 to 2004, representing an approximate 90% reduction. Starting in 2005, the number continued to decrease, reaching 2 strategies, ultimately resulting in 0 by 2007, indicating a complete collapse. Before the total collapse in 2007, the percentage deviation from the regular climate was -97%.

4.4. Functional composition

We observed temporal variations in all three traits across the three applied climatic conditions (Fig. 6). These variations are attributed to changes in the relative abundance of surviving life strategies and the values of their traits that may reflect adaptive responses of the ecosystem to the imposed disturbances or the climatic fluctuations in the regular climate condition, with the favoring of strategies that enhance their survival through time and under the altered conditions. In the regular climate, the values for the last year do not significantly differ from those of the first year for any of the traits in this climate condition, despite a small decrease in the *SLA* value (-4.6%). The relative differences (%) from the beginning to the end of the simulation are 0.5, -4.6, and 2.5 for *g1*, *SLA*, and *WD*, respectively, suggesting that the regular climate condition maintains relatively stable trait values over time, with minor fluctuations. Under the disturbance scenarios, particularly with more frequent disruptions,

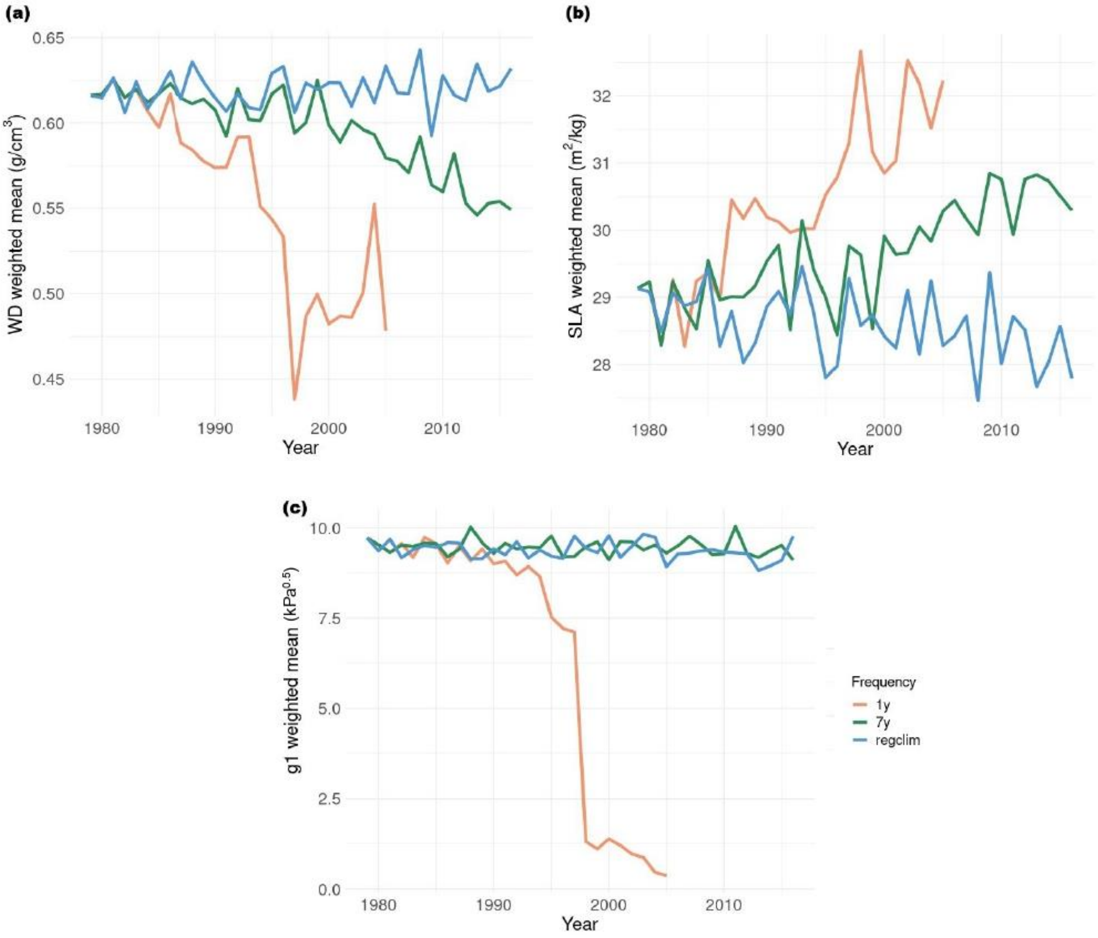

Fig. 6. Time series data spanning from 1979 to 2016 regarding the community weighted mean of three functional traits: wood density (a), specific leaf area (b) and g1 (c) under three distinct climate scenarios: regular conditions (regclim), reduced precipitation (30% less) occurring every 8 years (8y), and every 2 years (2y). *WD:* wood density; *SLA*: specific leaf area; *g1:* stomatal conductance sensitivity to CO_2 assimilation

there are observable shifts in trait values, indicating potential changes in the composition and functioning of the ecosystem. When assessing the disturbance application at an 8-year frequency, in comparison to the regular climate conditions, *WD* exhibited a variance of -13%, *g1* showed a difference of -6.7%, and *SLA* indicated an increase of 9%. In contrast, for the disturbance application at a 2-year frequency, due to the system collapse, all traits attained a value of 0. Before the collapse in 2006, we observed a decreasing trend in the trait value for g1 (-95.8%) and *WD* (-24.5%), and an increasing trend for *SLA* (+13%) when compared to regular climate conditions (Fig. 7). However, *WD* showed a recovery in values between the years 1998 and 2004, transitioning from a value 27% lower (the largest relative difference) in 1997 to -9%

in 2004. After 2004, *WD* experienced a sharp and permanent decline, reaching a decrease of -24% in 2006. Thus, the sensitivity of the traits varied for each of the environmental conditions: *WD* was the most sensitive trait, showing the greatest changes for the 8-year frequency, while *g1* was the most sensitive for the 2-year frequency.

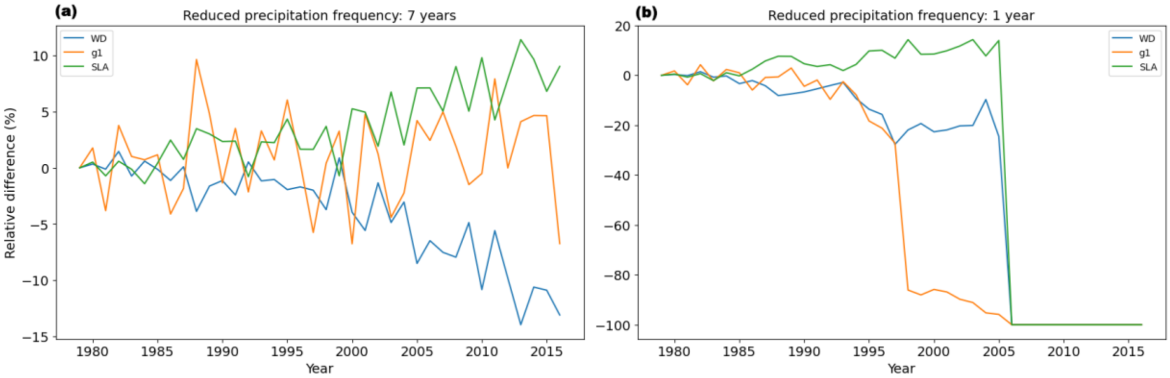

Fig. 7. Time series plots depicting the relative difference (%) of each functional trait compared to the regular climate condition, under different frequencies of reduced precipitation application (30% less): every 8 years (a) and every 2 years (b). *WD*: wood density; *SLA*: specific leaf area; *g1:* stomatal conductance sensitivity to CO_2 assimilation

5. Discussion

In the present study, we investigated how the magnitude and frequency of droughts influence the resilience of ecosystems. In summary, we found:

- Not only the magnitude but also the frequency of droughts can be critical as it decreases resilience, bringing the system closer to critical thresholds.
- All ecosystem indicators show some degree of resilience due to functional composition adaptation, but this adaptation is not sufficient to prevent collapse at a 2-year frequency or configuration changes at an 8-year frequency.
- Evapotranspiration and NPP emerged as the most sensitive variables under scrutiny, contradicting the commonly used carbon stock to evaluate resilience.
- Contrary to expectations, drought events led to changes in functional composition towards acquisitive strategies characterized by higher SLA and lower WD. However, we also found a decrease in g1, linked to strategies that are more conservative in terms of water use.

In this section, we discuss the key findings concerning the application of drought. Further details on the results under regular climate conditions can be found in the supplementary material in section SM.2.

5.1. The importance of drought frequency

Prior studies primarily focused on assessing forest responses to individual drought events, overlooking the potential long-term implications of previous drought occurrences (Phillips et al., 2009; Saatchi et al., 2013; Silva et al., 2013; Yang et al., 2018). It is anticipated that recurrent droughts could prompt forests to either develop adaptive mechanisms to withstand drought conditions (Cole et al., 2014) or gradually diminish their functionality. The cumulative effects of multiple drought episodes over time might lead to a more substantial decline in forest functionality than what could be anticipated from a single drought event (Anderegg et al., 2020; Mitchell et al., 2016; van Passel et al., 2022). All the variables examined exhibited a delayed response to drought treatments (Fig. 2 and Fig. 3), suggesting a level of resilience within the Amazon forest. This initial resilience to drought has been documented in extensive long-term plot studies (e.g., Feldpausch et al., 2016) and experimental drought simulations in forest ecosystems (Brando et al., 2008; da Costa et al., 2010). Such results are to be expected, as ecosystems can often show insensitivity within certain ranges of external conditions (Scheffer et al., 2009). Experimental studies on drought effects have revealed that the consequences of drought may take several years to materialize (da Costa et al., 2010; Feldpausch et al., 2016). For instance, the mortality effects of two drought experiments in eastern Amazonia became evident only after two or three seasons of experimental moisture reduction (Brando et al., 2008; da Costa et al., 2010; Rowland et al., 2015). Additionally, consecutive droughts may act together, leading to cumulative effects such as repeated episodes of irreversible damage from embolism (Anderegg et al., 2014) and hydraulic failure (Rowland et al., 2015), or the continual depletion of carbohydrate reserves (non-structural carbons) due to reduced photosynthetic rates (Doughty et al., 2014; 2015). Although our model does not currently incorporate embolism or hydraulic failure, we observed a decrease in storage compartments as the photosynthetic rate declined (Fig. SM3).

Our results underscore the understanding, and observations (Meir et al., 2015; Rowland et al., 2015), that not only the magnitude but also the frequency of droughts can be as critical as their intensity (Feldpausch et al., 2016; Phillips et al., 2009; Wunderling et al., 2022). This outcome further emphasizes the cumulative impacts of drought and that the rainforest might be able to withstand incidental although severe droughts (Wunderling et al., 2022). While the initial drought may weaken the system, it may not immediately provoke a response, making it vulnerable to subsequent droughts of similar intensity (Brando et al., 2008; Wundereling et al., 2022). This is known as the "degradation" hypothesis, wherein the initial drought diminishes trees' capacity to cope with subsequent physiological challenges (Feldpausch et al., 2016). This aligns with the idea that repeated droughts could diminish the basin of attraction of the system, eventually leading to collapse (Scheffer 2009; Ciemer et al., 2019). Our results support this viewpoint, as we observed a decrease in resilience, suggesting a reduction in the size of the basin of attraction. After several droughts, only one or a few events were needed to trigger collapse in the case of the 2-year frequency (Fig. 3c) or to alter the system's configuration in the case of the 8-year frequency (Fig. 3b). This is especially notable in the context of the 2-year frequency, where successive drought events pushed the system toward a critical threshold followed by complete collapse, as expected by a system that reached a tipping point (Forzieri et al., 2022; Scheffer et al., 2015).

While total collapse was not observed in the 8-year frequency, we did notice a change in the ecosystem's configuration (Fig. 2 and Fig. 3b), indicating a loss of structural integrity (Holling, 1973; Scheffer et al., 2015), which could lead to a further decrease in resilience and maybe a future system collapse. It's worth noting that a 8-year frequency of drought is less frequent than what has been observed for Amazon forest historically. Therefore, our findings may indicate that, over the long term, even with a relatively low frequency of drought, the system can undergo significant shifts. This holds particular significance considering the potential trajectory of Amazon climate, where drought events could become the predominant pattern in the latter half of this century (Wunderling et al., 2022).

5.2. Drought impacts on ecosystem state indicators

The results obtained from the drought experiments demonstrate the central role of precipitation in determining ecosystem functioning, influencing both the carbon and water cycles. Despite the general tendency to decrease resilience, in accordance with other studies (Ciemer et al., 2019), the variables showed different responses to drought applications regarding the amount of change, the timing of differing from regular climate, the breakpoints and the slopes (Fig. 5, Table 2 and Table 3).

Carbon stock and NPP tended to decrease with the drier conditions (Fig. 5a and Fig. 4). A decrease in total carbon stock due to drought events was observed (Phillips et al., 2009; Nepstad et al., 2007) and also predicted by model simulations (Friedlingstein et al 2006). The observed decline in total carbon stock aligns with previous research indicating that drought events can transition the Amazon forest from a carbon sink to a carbon-neutral or carbon source state, shifting from a net carbon sink in wet years to a carbon-neutral/source status during severe drought years such as 2005, 2010, and 2015/2016 (Hubau et al., 2020; Gatti et al. 2014). This shift can be attributed to alterations in air temperature, vapor pressure deficit, and notably reduced soil water availability (Bonal et al., 2016). The projected increase in the frequency of such extreme drought occurrences in the future is anticipated to disrupt the vital role of intact tropical rainforests in carbon sequestration and may counteract the positive fertilization effect of elevated CO_2 levels (Cox et al. 2013). Our findings demonstrate that even under a low-frequency scenario (e.g., every 8 years), the capacity for carbon storage can undergo significant changes, with the most substantial alteration revealing a 20% decrease in total carbon content (Fig. 4).

Partially, the decline in biomass observed in our results may be linked to reduced NPP, as observed in various studies (Bonal et al., 2016; Feldpausch et al., 2016; Wunderling et al., 2022). However, it is important to note that some research indicates that the NPP response to drier conditions can vary, with instances of increase, decrease, and stability reported (Bonal et al., 2016). This variability in NPP under drought conditions could be influenced by factors such as increased solar radiation resulting from reduced cloud cover compared to wet periods (Huete et al., 2006; Samanta et al., 2010; Saleska et al., 2007), phenological patterns and action of deep roots to access deep soil layers (Markewitz et al., 2010; Nepstad et al., 1994), which cannot be investigated with CAETÊ at the present moment. Nevertheless, this response is typically observed in moderate drought scenarios (Bonal et al., 2016), and prolonged water deficit can ultimately override any initial productivity gains, diminishing the ecosystem's capacity to sequester carbon effectively (Samanta et al., 2010), leading to decreased NPP.

Droughts of different magnitudes and frequency have the potential to alter the hydrological cycle (Gloor et al., 2013). In our study, evapotranspiration emerges as one of the most sensitive variables under scrutiny (Fig. 4 and Fig. 5), exhibiting notably steep slopes in breakpoint analysis across both 8-year and 2-year frequencies (Fig. 5, Table 2 and Table 3) with a strong tendency to decrease. A decrease in evapotranspiration is commonly observed with drought (Stahl et al. 2013), and the harsher the drought, the stronger is the decrease (Fisher et al., 2007). It can be primarily expected that this can be explained by: (i) intense solar radiation in dry periods increases evaporative demand, resulting in drier and warmer atmospheric air, theoretically leading to higher evapotranspiration rates (Fisher et al., 2007) and (ii) the fact that a reduction in soil water availability results in the regulation of stomatal conductance (Bonal et al. 2016; Stahl et al. 2013). As plants experience water scarcity, they close their stomata to conserve water, which in turn reduces transpiration rates. This reduction in transpiration affects the overall evapotranspiration from the ecosystem.

A decrease in forest evapotranspiration is extremely important. Its significance lies in its potential impact on the system's sensitivity; a reduction in evapotranspiration could severely hamper the Amazon forest's moisture recycling capacity, triggering secondary ramifications and escalating the risk of nearing critical thresholds (Ruíz-Vasquez et al., 2020; Wunderling et al., 2022). The decrease in atmospheric recycling potential has been forecasted for the Amazon basin (Swann et al., 2015) and observed in the southern Amazon basin (Ruiz-Vásquez et al., 2020). Even over the eight-year timeframe, though the system hasn't faced complete collapse, the decline in evapotranspiration remains notable, nearing a reduction of approximately 20% (Fig. 4). This finding aligns with Wundersling et al.'s (2022) study, which recorded an average evapotranspiration decrease ranging from -10% to 25%. In a real-world scenario, such reduction could worsen drought impacts by potentially diminishing regional precipitation levels, thereby extending the repercussions to other Amazon basin areas (Wunderling et al., 2022). However, there is still no clear trend of decrease or increase in evapotranspiration in the Amazon (Baker et al., 2021). A possible precipitation reduction situation poses a potential threat of forest transformations, even in regions where reduced precipitation hasn't been directly observed (Aragão, 2012; Staal et al., 2018; Wunderling et al., 2022). Although our model doesn't yet incorporate this feedback loop, the rapid responsiveness of evapotranspiration serves as a crucial alert for future considerations. For example, Unlike NPP and total carbon, it has not shown a recovery akin to the levels observed in the 2000s, particularly evident in the 2-year frequency. Moreover, among all variables, evapotranspiration demonstrates the swiftest changes in the time series, following closely behind NPP.

Contrary to the decrease in evapotranspiration, we observed an increase in WUE in both the 8-year and 2-year applications, with a significant rise in WUE during the first 20 years followed by a sharp decline after 2005. WUE typically increases during droughts as the system adapts to new conditions, and our model reflects this expectation. This increase in WUE can be seen as a sign of the system's resilience due to its adaptive responses. However, this resilience comes at a cost, affecting both evapotranspiration and overall system productivity. The rise in

WUE is also anticipated due to the selection of functional strategies that reduce water loss, characterized by lower *g1* values, which will be further explored in the following sections.

5.3. The number of surviving strategies

Variation in soil moisture due to decreased precipitation is a significant driver of functional composition changes in tropical forests (Aguirre-Gutiérrez et al., 2019; Fauset et al., 2012; Enquist & Enquist, 2011; Rius et al., 2023), influencing the number of species and the functional identity present in an ecosystem (Papastefanou et al., 2022). The observed variation in surviving strategies (Fig. 4) is closely linked to changes in functional traits, as these strategies are tailored to specific environmental conditions. This phenomenon is evident in natural ecosystems, where tree species exhibit varying sensitivities to climate variations based on their functional traits (Diaz & Cabido, 2001; Townsend et al., 2008). These variations result in nonrandom, short-term shifts in species composition or changes in dominance (Enquist & Enquist, 2011; Fauset et al., 2012). For example, rare species or unique functional trait combinations may increase in dominance (Enquist & Enquist, 2011; Rius et al., 2023), while some species may be unable to cope with new climatic conditions and become extinct, thereby the ecosystem can adapt to changing conditions, allowing species with previously minor functional roles to assume functional dominance, and vice versa (Sakschewski et al., 2016) altering species number and diversity in the species composition. This phenomenon is nominated as compensatory dynamics and is important for ecosystem resilience.

Interestingly, we found that the 2-year frequency treatment maintained the number of strategies over the long term better than both the 8-year frequency treatment and the regular climate condition (Fig. 2 and Fig. 4). Meanwhile, the 8-year frequency treatment preserved the number of surviving strategies for a longer period compared to the regular climate condition (Fig. 2 and Fig. 4). This does not mean the system was static or that the strategies did not change in terms of functional composition or abundance. For example, from the beginning of the time series, functional traits already showed fluctuations in their values (Fig. 6 and Fig. 7). This indicates that even if the number of surviving strategies remains the same, the functional composition can differ in terms of trait values or relative abundances, as the trait values are weighted by the abundances of the surviving strategies. This phenomenon is particularly notable under the 2-year reduced precipitation condition. In nature, the number (diversity) of species can differ from functional diversity—being higher, equal, or lower. Therefore, the diversity of functional traits in our system appears to be crucial for defining resilience. Since the number of surviving strategies remained constant for a relatively long period, it underscores the importance of functional trait diversity as a source of ecosystem resilience, also determining the resilience of the other ecosystem indicators such as NPP and total carbon stock. This concept has been observed in other studies as well (Allen et al., 2017; Anderegg et al., 2018; Poorter et al., 2015; Sakschewski et al., 2016; Schmitt et al., 2020).

This result can be explained by the fact that diversity ensures partial resilience. The diversity of strategies appears to be even more crucial under more extreme conditions, such as the 2-year frequency scenario. However, these adaptations in functional composition may become insufficient to withstand permanent, prolonged, or very frequent drier conditions. In such cases, changes in functional composition might lag behind the rapid shifts in climatic conditions (Boulton et al., 2022; Esquivel-Muelbert et al., 2019; Wunderling et al., 2020; 2022). This was evident in the 2-year scenario, where we observed a total collapse of the system in terms of the number of surviving strategies and all other ecosystem indicators. This reinforces the idea that changes in functional composition can have cascading effects on ecosystem processes, such as carbon and water cycling, ultimately influencing the resilience and stability of the ecosystem in the face of future drought events.

5.4. Functional composition

We observed a change in the functional composition in the three climatic conditions but it was more expressive, as expected, the 2-year frequency drought application. The temporal variation in the three applied climatic conditions was anticipated due to the favored combination of traits despite others. The observed changes in regular climate conditions can be attributed to natural climate fluctuations. Previous studies indicate that climate changes documented in historical climatology have already led to alterations in functional composition. However, in our model, the regular climate did not show the same level of sensitivity as seen in earlier studies, which connected changes in functional composition to historical drought events (Phillips et al., 2009). On the other hand, other studies show some conservation on traits (Esquivel-Muelbert et al., 2018).

Studies show that hydrological conditions are important for selecting wood density in tropical forests (Cosme et al., 2017; Feldpausch et al., 2011; Ferry et al., 2010; Kraft et al. 2008; Oliveira et al., 2019). Drier conditions are expected to increase wood density in tropical forests, as verified by various studies (Chave et al., 2006; Marca-Zevallos et al., 2022; Oliveira et al., 2019; Phillips et al., 2009; Rowland et al., 2015). Research shows that fast-growing, light-wooded trees are particularly susceptible to drought due to potential issues such as cavitation or carbon starvation (Phillips et al., 2009; Rowland et al., 2015). Drought-induced mortality disproportionately affects trees with lower wood density, leading to a higher proportion of denser-wood trees over time (Phillips et al., 2009). Denser wood offers several advantages: it has smaller and fewer vessels, reducing the risk of embolism during dry periods (Hacke et al. 2001; Hoeber et al., 2014; Marca-Zevallos et al., 2022), and provides greater structural support under mechanical stress. Hence, higher wood density increases plant survival during drought. However, denser wood requires more time to grow, leading to reduced growth rates (Umaña et al., 2023). Some studies, although fewer, indicate a decrease in wood density under certain conditions (Aguirre-Gutiérrez et al., 2019; Johnson et al., 2016; Esquivel-Muelbert et al., 2020). This decrease can favor the development of fast-growing species, as lower wood density might confer competitive advantages in obtaining light and occupying space. Additionally, producing lower-density wood requires less energy and resources compared to high-density wood, which can be advantageous in resource-limited environments.

In this study, we observed a decrease in wood density (Fig. 6 and Fig. 7) for both the 2-year and 8-year frequencies, contradicting initial expectations. The change was more pronounced at the 2-year frequency, aligning with our predictions. However, wood density also demonstrated significant sensitivity to drought conditions over the 8-year period. Under these conditions, wood density emerged as the most sensitive trait, exhibiting the earliest and most substantial changes. In our model, growth (biomass accumulation) tends to be favored due to the rules governing gridcell space occupation. Consequently, strategies favoring lower wood density are expected, as they increase growth rates. In contrast, higher wood density can lead to mortality due to lower growth efficiency. Additionally, higher wood density requires greater carbon allocation to these tissues, which, in dry conditions, reduces allocation to other critical tissues such as leaves and roots. It is also important to note that in the model, wood density is not linked to hydraulics. Hydraulics, which have a significant correlation with wood density, generally favor higher wood density. The implementation of hydraulics in the model is essential for future development, as the current lack of hydraulic representation may reduce the reliability of the model in accurately depicting wood density response patterns to drought.

SLA is an important leaf trait for tropical forest responses to a drying climate (Aguirre-Gutiérrez et al., 2022). It reflects a trade-off describing the range from conservative to acquisitive aboveground resource uptake strategies (González-M. et al., 2021; Wright et al., 2004). Conservative strategies, characterized by lower *SLA*, involve plants investing in thicker, denser leaves that are more durable and efficient in water use. These leaves minimize water loss through transpiration, making them better suited for survival in water-limited conditions. On the other hand, acquisitive strategies are marked by higher *SLA*, where plants produce thinner, larger leaves that maximize light capture and photosynthesis but are less durable and more vulnerable to drought (González-M. et al., 2021; Wright et al., 2004). Typically, *SLA* is expected to decrease with drier conditions, and this pattern has been observed. However, a few studies show no significant change or a slight increase in *SLA* under dry conditions (Anderegg et al., 2018; Aguirre-Gutiérrez et al., 2019; González-M. et al., 2021; Sakschewski et al., 2016). Higher *SLA* means thinner and larger leaves relative to their weight, increasing the surface area for light capture. In drier conditions, where water availability limits photosynthesis, maximizing light capture helps optimize the limited resources for energy production (Feng et al., 2008). Leaves with higher *SLA* tend to have a larger surface area to volume ratio, enhancing the efficiency of gas exchange and water use (Sakschewski et al., 2016). High *SLA* is often associated with fast-growing species that can quickly capitalize on favorable conditions. Additionally, higher *SLA* requires less investment per unit leaf area, which is crucial in resource-limited environments (Wright et al., 2004). Some studies suggest that higher *SLA* in dry conditions may be an adaptive response to stress, allowing plants to maintain metabolic functions at a lower cost (Sakschewski et al., 2016.

Our results indicate a preference for acquisitive strategies characterized by higher *SLA* with drier conditions. We observed an increase in *SLA* for both the 2-year and 8-year frequencies, with a more pronounced increase at the 2-year frequency due to the severity of the climate conditions. This trend suggests that plants are adapting by producing thinner, larger leaves to maximize light capture and photosynthesis in response to drought stress. In our model, higher *SLA* enhances light capture, favoring these strategies by increasing productivity. This increased productivity is reflected in the model by greater occupation of gridcells, indicating a competitive advantage. The increase in *SLA* is also supported by the lower required investment per unit leaf area, which is crucial under resource-limited conditions. This means that plants can allocate fewer resources to leaf construction while still maintaining a relatively high photosynthetic capacity, which is particularly beneficial in drier environments where water and nutrients are scarce. This result was also found by Sakschewski et al. (2016). These factors help explain the discrepancy between the majority of observations and our model results. Observations typically suggest that lower *SLA*, associated with more durable leaves that minimize water loss, would be favored under drought conditions. However, the CAETÊ model does not represent certain physiological processes such as leaf durability and water conservation strategies, which could lead to a bias towards higher *SLA* in the model's simulations. Thus, the observed increase in *SLA* can be attributed to the model's emphasis on maximizing light capture and productivity under stress conditions, whereas the potential advantage of lower *SLA* with more durable, water-efficient leaves is not accounted for in the current version of the model. Future improvements in the CAETÊ model should aim to incorporate these physiological processes to provide a more comprehensive understanding of plant responses to drought.

The functional trait g1, or stomatal conductance sensitivity to CO_2 assimilation, is crucial for understanding and modeling plant physiology, particularly in relation to photosynthesis and water use (Lin et al., 2015; Medlyn et al., 2011). This trait determines the upper limit of stomatal conductance to water vapor under optimal conditions, playing a key role in regulating gas exchange between the leaf interior and the atmosphere (Anderegg et al., 2016). Higher *g1* values can enhance photosynthetic rates by increasing CO_2 uptake but also lead to increased water loss through transpiration. Therefore, plants must optimize *g1* to balance maximizing photosynthesis and minimizing water loss, especially in water-limited environments (Lin et al., 2015). In dry conditions, lower *g1* values are beneficial as they limit water loss, although they may restrict CO_2 uptake and reduce photosynthetic efficiency (Medlyn et al., 2011).

In our model, for regular climate conditions and the 8-year frequency scenario, *g1* oscillated throughout the time series but, on average, did not differ significantly from the initial values (Fig. 6c and Fig. 7a). A more prominent reduction in *g1* was observed during the last 5 years of the 8-year frequency scenario, though similar values had been reached at other times. The maintenance of *g1* values in this scenario can be explained by the longer intervals between precipitation reductions, which allow plants to recover between periods of water stress and restore physiological processes (Gupta et al., 2020; Zhang et al., 2024), recovering for example the carbon on storage compartment (O'Brien et al., 2014; Sala, Woodruff & Meinzer, 2012), allowing the strategies to invest in water regulation. In contrast, for the 2-year frequency scenario, we observed a selection of strategies with lower *g1* values. Decreased *g1* is associated with reduced stomatal conductance, effectively minimizing water loss through transpiration. This adaptation enhances WUE, as seen in Fig. 4c, allowing plants to conserve water more effectively. However, lower *g1* values can lead to decreased photosynthetic rates, potentially causing a depletion in carbon in the storage compartment and consequently the carbon starvation (Hartmann et al., 2015; McDowell et al., 2013; Sala et al., 2010). In CAETÊ, photosynthesis is also penalized under water-limited conditions (through the f5 parameter; see section SM.1.3. in Supplementary Material in Rius et al., 2023). It reinforces the reduced photosynthetic rates, pushing the system towards its tipping point and eventual collapse.

6. Conclusions

Here we assessed the impacts of recurrent drought events (-30%) on the Amazon forest at two frequencies every 2 years and every 8 years. We examined their effects on five ecosystem state indicators, including two related to the carbon cycle (total carbon and NPP), two linked to the water cycle (evapotranspiration and WUE), and the number of surviving strategies as a proxy for species diversity. Additionally, we sought to understand changes in functional composition through the analysis of a time series of three functional attributes: *WD*, *SLA*, and *g1*.

Our results underscore the critical importance of drought frequency on the resilience of the Amazon rainforest. Recurrent droughts, especially those occurring annually, exert a significant toll on the forest's functionality compared to less frequent events (every 8 years). While the Amazon initially demonstrates resilience to drought, the cumulative effects lead to substantial declines in ecosystem indicators such as carbon storage, primary productivity, and evapotranspiration. These findings suggest a potential transition of the Amazon forest from a carbon sink to a carbon source under severe drought conditions, with profound implications for global carbon sequestration. Particularly noteworthy is the observed change in evapotranspiration, signaling a severe impact on the ecosystem's water functionality, further compromising its resilience.

The diversity of functional strategies proves vital for ecosystem resilience, as changes in functional composition through shifts in relative abundances and exclusions of strategies play a crucial role in the initially observed resilience. For instance, we noted a tendency for wood density to decrease under drought conditions, indicating a functional adaptation favoring rapid growth and space occupation, albeit with trade-offs in terms of carbon allocation and water use efficiency. Additionally, the increase in specific leaf area (*SLA*) suggests an adaptive strategy to maximize light capture and photosynthesis while minimizing water loss. Meanwhile, stomatal conductance sensitivity to CO_2 assimilation (*g1*) exhibited significant variations, with initial values maintained under regular climate conditions and an 8-year frequency but notably reduced under a two year frequency, reflecting an adaptation to minimize water loss and enhance water use efficiency.

However, the adaptation of functional composition alone proves insufficient to withstand permanent, prolonged, or very frequent drought conditions. Under the annual drought condition, we observed a complete collapse of the system in terms of the number of survival strategies and all other ecosystem indicators. This collapse underscores how changes in functional composition can trigger cascading effects on ecosystem processes, such as carbon and water cycles, significantly impacting resilience and stability in the face of future drought events. Furthermore, while lower frequency reduced precipitation did not lead to a total collapse, the observed change in functional composition was insufficient to prevent the system from altering its configuration.

These findings suggest that repeated droughts weaken the forest, rendering it vulnerable to collapse, especially as climate change forecasts predict more frequent droughts in the future. Consequently, the long-term impacts of increasing drought frequency could drive the Amazon towards significant ecological shifts and potential collapse. Ultimately, our study emphasizes the importance of assessing various ecosystem indicators, as carbon alone cannot adequately gauge resilience, as commonly practiced in studies. Our results reveal that ecosystem processes and properties may prove less resilient than carbon stocks, indicating that terrestrial ecosystems worldwide could be even more vulnerable than previously assumed.

7. References

Aguirre-Gutiérrez, J., Oliveras, I., Rifai, S., Fauset, S., Adu-Bredu, S., Affum-Baffoe, K., Baker, T. R., Feldpausch, T. R., Gvozdevaite, A., Hubau, W., Kraft, N. J. B., Lewis, S. L., Moore, S., Niinemets, Ü., Peprah, T., Phillips, O. L., Ziemińska, K., Enquist, B., & Malhi, Y. (2019). Drier tropical forests are susceptible to functional changes in response to a long-term drought. *Ecology Letters*, *22*(5), 855–865. https://doi.org/10.1111/ele.13243

Aguirre-Gutiérrez, J., Berenguer, E., Oliveras Menor, I., Bauman, D., Corral-Rivas, J. J., Nava-Miranda, M. G., Both, S., Ndong, J. E., Ondo, F. E., Bengone, N. N., Mihinhou, V., Dalling, J. W., Heineman, K., Figueiredo, A., González-M, R., Norden, N., Hurtado-M, A. B., González, D., Salgado-Negret, B., … Malhi, Y. (2022). Functional susceptibility of tropical forests to climate change. *Nature Ecology & Evolution*, *6*(7), 878–889. https://doi.org/10.1038/s41559-022-01747-6

Aguirre-Gutiérrez, J. et al. (2020) Long-term droughts may drive drier tropical forests towards increased functional, taxonomic and phylogenetic homogeneity. Nat. Commun. 11, 3346.

Albrich, K., Rammer, W., Turner, M. G., Ratajczak, Z., Braziunas, K. H., Hansen, W. D., & Seidl, R. (2020). Simulating forest resilience: A review. *Global Ecology and Biogeography*, *29*(12), 2082–2096. https://doi.org/10.1111/geb.13197

Aleixo, I., Norris, D., Hemerik, L., Barbosa, A., Prata, E., Costa, F., & Poorter, L. (2019). Amazonian rainforest tree mortality driven by climate and functional traits. *Nature Climate Change*, *9*(5), 384–388. https://doi.org/10.1038/s41558-019-0458-0

Allen, C. D., Macalady, A. K., Chenchouni, H., Bachelet, D., McDowell, N., Vennetier, M., Kitzberger, T., Rigling, A., Breshears, D. D., Hogg, E. H. (Ted., Gonzalez, P., Fensham, R., Zhang, Z., Castro, J., Demidova, N., Lim, J. H., Allard, G., Running, S. W., Semerci, A., & Cobb, N. (2010). A global overview of drought and heat-induced tree mortality reveals emerging climate change risks for forests. *Forest Ecology and Management*, *259*(4), 660–684. https://doi.org/10.1016/j.foreco.2009.09.001

Allen, K., Dupuy, J. M., Gei, M. G., Hulshof, C., Medvigy, D., Pizano, C., Salgado-Negret, B., Smith, C. M., Trierweiler, A., Van Bloem, S. J., Waring, B. G., Xu, X., & Powers, J. S. (2017). Will seasonally dry tropical forests be sensitive or resistant to future changes in rainfall regimes? Environmental Research Letters, 12(2), 023001. https://doi.org/10.1088/1748-9326/AA5968

Almeida, Alexandre Esteves. "Time Series Components and Breakpoints in Remote Sensing Image Analysis." Universidade Estadual de Campinas, Instituto de Computação, 2017.

Anderegg, W. R. L., L. D. L. Anderegg, J. A. Berry, and C. B. Field (2014), Loss of whole-tree hydraulic conductance during severe drought and multi-year forest die-off, Oecologia, 175, 11–23.

Anderegg, W. R. L., Trugman, A. T., Badgley, G., Konings, A. G., & Shaw, J. (2020). Divergent forest sensitivity to repeated extreme droughts. Nature Climate Change, 10(12), 1091–1095. https://doi.org/10.1038/s41558-020-00919-1

Anderegg, W. R. L., Konings, A. G., Trugman, A. T., Yu, K., Bowling, D. R., Gabbitas, R., Karp, D. S., Pacala, S., Sperry, J. S., Sulman, B. N., & Zenes, N. (2018). Hydraulic diversity of forests regulates ecosystem resilience during drought. Nature, 561(7724), 538–541. https://doi.org/10.1038/S41586-018-0539-7

Aragão, L. E. O. C. (2012). The rainforest's water pump. *Nature 2012 489:7415*, *489*(7415), 217–218. https://doi.org/10.1038/nature11485

Artaxo, P., & Marengo, J. A. (2020). Climate change in the Amazon: tendencies, impacts and ecological consequences. In *Thermodynamics and Phase Transformations* (pp. 479–506). EDP Sciences. https://doi.org/10.1051/978-2-7598-0247-0.c025

Artaxo P, Hansson HC, Machado LAT, Rizzo LV (2022) Tropical forests are crucial in regulating the climate on Earth. PLOS Clim 1(8): e0000054. https://doi.org/10.1371/journal.pclm.0000054

Baker, T.R., Phillips, O.L., Malhi, Y., Almeida, S., Arroyo, L., Di Fiore, A. et al. (2004a). Increasing biomass in Amazonian forest plots. Philos. T. Roy. Soc. B, 359, 353–365.

Baker, T.R., Phillips, O.L., Malhi, Y., Almeida, S., Arroyo, L., Di Fiore, A. et al. (2004b). Variation in wood density determines spatial patterns in Amazonian forest biomass. Glob. Change Biol., 10, 545–562.

Baker, J. C. A., Garcia-Carreras, L., Gloor, M., Marsham, J. H., Buermann, W., Da Rocha, H. R., Nobre, A. D., De Carioca Araujo, A., & Spracklen, D. V. (2021). Evapotranspiration in the Amazon: Spatial patterns, seasonality, and recent trends in observations, reanalysis, and climate models. *Hydrology and Earth System Sciences*, *25*(4), 2279–2300. https://doi.org/10.5194/hess-25-2279-2021

Baraloto, C., Paine, C. E. T., Poorter, L., Beauchene, J., Bonal, D., Domenach, A. M., Hérault, B., Patiño, S., Roggy, J. C., & Chave, J. (2010). Decoupled leaf and stem economics in rain forest trees. Ecology Letters, 13(11), 1338–1347. https://doi.org/10.1111/j.1461-0248.2010.01517.x

Bennett, A. C., Rodrigues de Sousa, T., Monteagudo-Mendoza, A., Esquivel-Muelbert, A., Morandi, P. S., Coelho de Souza, F., Castro, W., Duque, L. F., Flores Llampazo, G., Manoel dos Santos, R., Ramos, E., Vilanova Torre, E., Alvarez-Davila, E., Baker, T. R., Costa, F. R. C., Lewis, S. L., Marimon, B. S., Schietti, J., Burban, B., … Phillips, O. L. (2023). Sensitivity of South American tropical forests to an extreme climate anomaly. *Nature Climate Change*. https://doi.org/10.1038/s41558-023-01776-4

Bonal, D., Burban, B., Stahl, C., Wagner, F., & Hérault, B. (2016). The response of tropical rainforests to drought—lessons from recent research and future prospects. *Annals of Forest Science*, *73*(1), 27–44. https://doi.org/10.1007/s13595-015-0522-5

Bonan, G. B. (2008). Forests and climate change: Forcings, feedbacks, and the climate benefits of forests. Science, 320(5882), 1444-1449. doi:10.1126/science.1155121

Boulton, C. A., Lenton, T. M., & Boers, N. (2022). Pronounced loss of Amazon rainforest resilience since the early 2000s. *Nature Climate Change*, *12*(3), 271–278. https://doi.org/10.1038/s41558-022-01287-8

Brando, P. M., D. C. Nepstad, E. A. Davidson, S. E. Trumbore, D. Ray, and P. Camargo (2008). Drought effects on litterfall, wood production and belowground carbon cycling in an Amazon forest: Results of a throughfall reduction experiment. Philos. Trans. R. Soc. London B Biol. Sci., 363(1498), 1839–1848.

Brienen, R. J. W., Phillips, O. L., Feldpausch, T. R., & et al. (2015). Long-term decline of the Amazon carbon sink. *Nature*, *519*(7543), 344–348. https://doi.org/10.1038/nature14283

Brum, M. et al. (2019). Hydrological niche segregation defines forest structure and drought tolerance strategies in a seasonal Amazon forest. J. Ecol. 107, 318–333.

Carmona, C. P., Tamme, R., Pärtel, M., De Bello, F., Brosse, S., Capdevila, P., González, R. M., González-Suárez, M., Salguero-Gómez, R., Vásquez-Valderrama, M., & Toussaint, A. (2021). Erosion of global functional diversity across the tree of life. *Science Advances*, *7*(13), 1–13. https://doi.org/10.1126/sciadv.abf2675

Cernusak, L. a., Winter, K., Dalling, J. W., Holtum, J. a M., Jaramillo, C., Körner, C., Leakey, A. D. B., Norby, R. J., Poulter, B., Turner, B. L., & Wright, S. J. (2013). Tropical forest responses to increasing atmospheric CO2: Current knowledge and opportunities for future research. *Functional Plant Biology*, *40*, 531–551. https://doi.org/10.1071/FP12309

Chave, J., Condit, R., Muller-Landau, H. C., Thomas, S. C., Ashton, P. S., Bunyavejchewin, S., Co, L. L., Dattaraja, H. S., Davies, S. J., Esufali, S., Ewango, C. E. N., Feeley, K. J., Foster, R. B., Gunatilleke, N., Gunatilleke, S., Hall, P., Hart, T. B., Hernández, C., Hubbell, S. P., … Losos, E. C. (2008). Assessing evidence for a pervasive alteration in tropical tree communities. *PLoS Biology*, *6*(3), 0455–0462. https://doi.org/10.1371/journal.pbio.0060045

Chave, J., Coomes, D., Jansen, S., Lewis, S. L., Swenson, N. G., & Zanne, A. E. (2009). Towards a worldwide wood economics spectrum. *Ecology Letters*, *12*(4), 351–366. https://doi.org/10.1111/j.1461-0248.2009.01285.x

Choat, B., Brodribb, T. J., Brodersen, C. R., Duursma, R. A., López, R., & Medlyn, B. E. (2018). Triggers of tree mortality under drought. Nature, 558(7711), 531-539.

Ciemer, C., Boers, N., Hirota, M., Kurths, J., Müller-Hansen, F., Oliveira, R. S., & Winkelmann, R. (2019). Higher resilience to climatic disturbances in tropical vegetation exposed to more variable rainfall. *Nature Geoscience 2019 12:3*, *12*(3), 174–179. https://doi.org/10.1038/s41561-019-0312-z

Cole, L. E. S., Bhagwat, S. A., & Willis, K. J. (2014). Recovery and resilience of tropical forests after disturbance. Nature Communications, 5, 1– 7. https://doi.org/10.1038/ncomms4906

Corlett, R. T. (2011). Impacts of warming on tropical lowland rainforests. Trends in Ecology & Evolution, 26(11), 606-613. doi:10.1016/j.tree.2011.06.015

Corlett, R. T. (2016). The impacts of climate change in the tropics. Annual Review of Environment and Resources, 41, 501-518. doi:10.1146/annurev-environ-110615-085711

Cosme, L. H. M. et al. 2017. The importance of hydraulic architecture to the distribution patterns of trees in a central Amazonian forest. New Phytol. 215: 113–125.

Cox, P. M., Betts, R. a, Jones, C. D., Spall, S. a, & Totterdell, I. J. (2000). Acceleration of global warming due to carbon-cycle feedbacks in a coupled climate model. *Nature*, *408*(6809), 184–187. https://doi.org/10.1038/35041539

Cox et al., Increasing risk of Amazonian drought due to decreasing aerosol pollution. Nature 453, 212–215 (2008).

Cox, P. M., Pearson, D., Booth, B. B., Friedlingstein, P., Huntingford, C., Jones, C. D., & Luke, C. M. (2013). Sensitivity of tropical carbon to climate change constrained by carbon dioxide variability. Nature, 494(7437), 341–344. https://doi.org/http://www.nature.com/nature/journal/v494/n7437/abs/nature11882.html#supplementary-information

da Costa, A. C. L., Galbraith, D., Almeida, S., Portela, B. T. T., da Costa, M., de Athaydes Silva Junior, J., Braga, A. P., de Gonçalves, P. H. L., de Oliveira, A. A., Fisher, R., Phillips, O.

L., Metcalfe, D. B., Levy, P., & Meir, P. (2010). Effect of 7 yr of experimental drought on vegetation dynamics and biomass storage of an eastern Amazonian rainforest. *New Phytologist*, *187*(3), 579–591. https://doi.org/10.1111/j.1469-8137.2010.03309.x

Darela Filho, J. P. (2022). Modelagem dos impactos do aumento da concentração de CO2 e nutrientes sobre a composição funcional na floresta amazônica. Tese de Doutorado, Universidade Estadual Paulista "Júlio de Mesquita Filho", Instituto de Biociências, Rio Claro.

Dakos, V., Matthews, B., Hendry, A. P., Levine, J., Loeuille, N., Norberg, J., Nosil, P., Scheffer, M., & De Meester, L. (2019). Ecosystem tipping points in an evolving world. *Nature Ecology and Evolution*, *3*(3), 355–362. https://doi.org/10.1038/s41559-019-0797-2

de Bello, F., Lavorel, S., Hallett, L. M., Valencia, E., Garnier, E., Roscher, C., Conti, L., Galland, T., Goberna, M., Májeková, M., Montesinos-Navarro, A., Pausas, J. G., Verdú, M., E-Vojtkó, A., Götzenberger, L., & Lepš, J. (2021). Functional trait effects on ecosystem stability: assembling the jigsaw puzzle. Trends in Ecology & Evolution, 36(9), 822–836. https://doi.org/10.1016/j.tree.2021.05.001

Díaz, S., & Cabido, M. (2001). Vive la difference: plant functional diversity matters to ecosystem processes. *Proceedings. Biological Sciences / The Royal Society*, *16*(4), 646–655. http://rspb.royalsocietypublishing.org/content/278/1713/1894.abstract%5Cnhttp://www.ncbi.nlm.nih.gov/pubmed/19019785%5Cnhttp://www.pnas.org/content/100/13/7650.short

Díaz, S., Lavorel, S., de Bello, F., Quétier, F., Grigulis, K., & Robson, T. M. (2007). Incorporating plant functional diversity effects in ecosystem service assessments. Proceedings of the National Academy of Sciences of the United States of America, 104(52), 20684–20689. https://doi.org/10.1073/pnas.0704716104

Doughty, C. E., Malhi, Y., Araujo-Murakami, A., Metcalfe, D. B., Silva-Espejo, J. E., Arroyo, L., Heredia, J. P., Pardo-Toledo, E., Mendizabal, L. M., Rojas-Landivar, V. D., Vega-Martinez, M., Flores-Valencia, M., Sibler-Rivero, R., Moreno-Vare, L., Jessica Viscarra, L., Chuviru-Castro, T., Osinaga-Becerra, M., & Ledezma, R. (2014). Allocation trade-offs dominate the response of tropical forest growth to seasonal and interannual drought. Ecology, 95(8), 2192–2201. https://doi.org/10.1890/13-1507.1

Doughty, C. E., Metcalfe, D. B., Girardin, C. A. J., Amézquita, F. F., Cabrera, D. G., Huasco, W. H., Silva-Espejo, J. E., Araujo-Murakami, A., da Costa, M. C., Rocha, W., Feldpausch, T. R., Mendoza, A. L. M., da Costa, A. C. L., Meir, P., Phillips, O. L., & Malhi, Y. (2015).

Drought impact on forest carbon dynamics and fluxes in Amazonia. *Nature*, *519*(7541), 78–82. https://doi.org/10.1038/nature14213

Duffy, P. B., Brando, P., Asner, G. P., & Field, C. B. (2015). Projections of future meteorological drought and wet periods in the Amazon. Proc. Natl. Acad. Sci. U.S.A. 112, 13172–13177

Egli, L., Weise, H., Radchuk, V., Seppelt, R., & Grimm, V. (2018). Exploring resilience with agent-based models: State of the art, knowledge gaps and recommendations for coping with multidimensionality. Ecological Complexity. 40 Part B, 1–7.

Enquist, B. J., & Enquist, C. A. F. (2011). Long-term change within a Neotropical forest: Assessing differential functional and floristic responses to disturbance and drought. *Global Change Biology*, *17*(3), 1408–1424. https://doi.org/10.1111/j.1365-2486.2010.02326.x

Esquivel-Muelbert, A., Baker, T. R., Dexter, K. G., Lewis, S. L., Brienen, R. J. W., Feldpausch, T. R., Lloyd, J., Monteagudo-Mendoza, A., Arroyo, L., Álvarez-Dávila, E., Higuchi, N., Marimon, B. S., Marimon-Junior, B. H., Silveira, M., Vilanova, E., Gloor, E., Malhi, Y., Chave, J., Barlow, J., … Phillips, O. L. (2018). Compositional response of Amazon forests to climate change. *Global Change Biology*, *June 2018*, 39–56. https://doi.org/10.1111/gcb.14413

Esquivel-Muelbert, A., Baker, T. R., Dexter, K. G., Lewis, S. L., Brienen, R. J. W., Feldpausch, T. R., Lloyd, J., Monteagudo-Mendoza, A., Arroyo, L., Álvarez-Dávila, E., Higuchi, N., Marimon, B. S., Marimon-Junior, B. H., Silveira, M., Vilanova, E., Gloor, E., Malhi, Y., Chave, J., Barlow, J., … Phillips, O. L. (2019). Compositional response of Amazon forests to climate change. Global Change Biology, 25(1), 39–56. https://doi.org/10.1111/gcb.14413

Esquivel-Muelbert, A., Baker, T. R., Dexter, K. G., Lewis, S. L., ter Steege, H., Lopez-Gonzalez, G., Monteagudo Mendoza, A., Brienen, R., Feldpausch, T. R., Pitman, N., Alonso, A., van der Heijden, G., Peña-Claros, M., Ahuite, M., Alexiaides, M., Álvarez Dávila, E., Murakami, A. A., Arroyo, L., Aulestia, M., … Phillips, O. L. (2017). Seasonal drought limits tree species across the Neotropics. *Ecography*, *40*(5), 618–629. https://doi.org/10.1111/ECOG.01904

Esquivel-Muelbert, A., Phillips, O. L., Brienen, R. J. W., Fauset, S., Sullivan, M. J. P., Baker, T. R., Chao, K. J., Feldpausch, T. R., Gloor, E., Higuchi, N., Houwing-Duistermaat, J., Lloyd, J., Liu, H., Malhi, Y., Marimon, B., Marimon Junior, B. H., Monteagudo-Mendoza, A., Poorter, L., Silveira, M., … Galbraith, D. (2020). Tree mode of death and mortality risk factors across Amazon forests. *Nature Communications*, *11*(1). https://doi.org/10.1038/s41467-020-18996-3

Esquivel-Muelbert, A., Baker, T. R., Dexter, K. G., Lewis, S. L., Brienen, R. J. W., Feldpausch, T. R., Lloyd, J., Monteagudo-Mendoza, A., Arroyo, L., Álvarez-Dávila, E., Higuchi, N., Marimon, B. S., Marimon-Junior, B. H., Silveira, M., Vilanova, E., Gloor, E., Malhi, Y., Chave, J., Barlow, J., … Phillips, O. L. (2019). Compositional response of Amazon forests to climate change. *Global Change Biology, 25*(1), 39–56. https://doi.org/10.1111/gcb.14413

Fauset, S., Baker, T. R., Lewis, S. L., Feldpausch, T. R., Affum-Baffoe, K., Foli, E. G., Hamer, K. C., Swaine, M. D., & Etienne, R. (2012). Drought-induced shifts in the floristic and functional composition of tropical forests in Ghana. *Ecology Letters*. https://doi.org/10.1111/j.1461-0248.2012.01834.x

Feldpausch, T. R. et al. (2011). Height-diameter allometry of tropical forest trees. Biogeosciences 8: 1081–1106.

Feldpausch, T. R., Phillips, O. L., Brienen, R. J. W., Gloor, E., Lloyd, J., Lopez-Gonzalez, G., Monteagudo-Mendoza, A., Malhi, Y., Alarcón, A., Álvarez Dávila, E., Alvarez-Loayza, P., Andrade, A., Aragao, L. E. O. C., Arroyo, L., Aymard C., G. A., Baker, T. R., Baraloto, C., Barroso, J., Bonal, D., … Vos, V. A. (2016). Amazon forest response to repeated droughts. *Global Biogeochemical Cycles*, *30*(7), 964–982. https://doi.org/10.1002/2015GB005133

Ferreira, J., Lennox, G. D., Gardner, T. A., Thomson, J. R., Berenguer, E., Lees, A. C., Mac Nally, R., Aragão, L. E. O. C., Ferraz, S. F. B., Louzada, J., Moura, N. G., Oliveira, V. H. F., Pardini, R., Solar, R. R. C., Vieira, I. C. G., & Barlow, J. (2018). Carbon-focused conservation may fail to protect the most biodiverse tropical forests. *Nature Climate Change*. https://doi.org/10.1038/s41558-018-0225-7

Ferry, B. et al. 2010. Higher treefall rates on slopes and waterlogged soils result in lower stand biomass and productivity in a tropical rain forest. J. Ecol. 98: 106–116.

Fisher RA, Williams M, Da Costa AL, Malhi Y, da Costa RF, Almeida S, Meir P (2007) The response of an Eastern Amazonian rain forest to drought stress: results and modelling analyses from a throughfall exclusion experiment. Glob Change Biol 13:2361–2378

Fisher, R., McDowell, N., Purves, D., Moorcroft, P., Sitch, S., Cox, P., Huntingford, C., Meir, P., & Ian Woodward, F. (2010). Assessing uncertainties in a second-generation dynamic vegetation model caused by ecological scale limitations. *New Phytologist*, *187*(3), 666–681. https://doi.org/10.1111/j.1469-8137.2010.03340.x

Flores, B. M., Montoya, E., Sakschewski, B., Nascimento, N., Staal, A., Betts, R. A., Levis, C., Lapola, D. M., Esquível-Muelbert, A., Jakovac, C., Nobre, C. A., Oliveira, R. S., Borma, L. S., Nian, D., Boers, N., Hecht, S. B., ter Steege, H., Arieira, J., Lucas, I. L., … Hirota, M. (2024). Critical transitions in the Amazon forest system. *Nature*, *626*(7999), 555–564. https://doi.org/10.1038/s41586-023-06970-0

Forzieri, G., Dakos, V., McDowell, N. G., Ramdane, A., & Cescatti, A. (2022). Emerging signals of declining forest resilience under climate change. *Nature*, *608*(7923), 534–539. https://doi.org/10.1038/s41586-022-04959-9

Friedlingstein P, Cox P, Betts R et al. (2006) Climate – carbon cycle feedback analysis: results from the C4MIP model intercom- parison. Journal of Climate, 14, 3337–3353.

Fu, R., Yin, L., Li, W., Arias, P. A., Dickinson, R. E., Huang, L., ... & Myneni, R. B. (2013). Increased dry-season length over southern Amazonia in recent decades and its implication for future climate projection. Proceedings of the National Academy of Sciences, 110(45), 18110-18115.

Gatti, L. V, Gloor, M., Miller, J. B., Doughty, C. E., Malhi, Y., Domingues, L. G., Basso, L. S., Martinewski, a, Correia, C. S. C., Borges, V. F., Freitas, S., Braz, R., Anderson, L. O., Rocha, H., Grace, J., Phillips, O. L., & Lloyd, J. (2014). Drought sensitivity of Amazonian carbon balance revealed by atmospheric measurements. Nature, 506(7486), 76–80. https://doi.org/10.1038/nature12957

Gloor M, Brienen RJW, Galbraith D, Feldpausch TR, Schöngart J, Guyot JL, Espinoza JC, Lloyd J, Phillips OL (2013) Intensification of the Amazon hydrological cycle over the last two decades. Geophys Res Lett 40:1729–1733

González-M., R., Posada, J. M., Carmona, C. P., Garzón, F., Salinas, V., Idárraga-Piedrahita, Á., Pizano, C., Avella, A., López-Camacho, R., Norden, N., Nieto, J., Medina, S. P., Rodríguez-M., G. M., Franke-Ante, R., Torres, A. M., Jurado, R., Cuadros, H., Castaño-Naranjo, A., García, H., & Salgado-Negret, B. (2021). Diverging functional strategies but high sensitivity to an extreme drought in tropical dry forests. *Ecology Letters*, *24*(3), 451–463. https://doi.org/10.1111/ELE.13659

Grime, J.P., 1998. Benefits of plant diversity to ecosystems: immediate, filter and founder effects. J. Ecol. 86 (6), 902–910. https://doi.org/10.1046/j.1365-2745.1998.00306. x.

Gupta, A., Rico-Medina, A., & Caño-Delgado, A. I. (2020). The physiology of plant responses to drought. Science, 368(6488), 266-269.

Hacke, U. G. et al. 2001. Trends in wood density and structure are linked to prevention of xylem implosion by negative pressure. Oecologia 126: 457–461.

Hartmann, H. (2015). Carbon starvation during drought-induced tree mortality – are we chasing a myth?. Journal of Plant Hydraulics, 2, e005.

Harris PP, Huntingford C, Gash JHC, Hodnett MG, Cox PM, Malhi Y, Araujo AC (2004) Calibration of a land-surface model using data from primary forest sites in Amazonia. Theoretical and Applied Climatology, 78, 27–45

Hoeber S, Leuschner C, K€oler L, Arias-Aguilar D, Schuldt B. (2014). The importance ofhydraulic conductivityand wood density to growth performance in eight tree species from a tropical semi-dry climate. ForestEcologyandManagement 330: 126–136.

Holling, C. S. (1973). Resilience and stability of ecological systems. Annual Review of Ecology and Systematics, 4, 1–23. https://doi.org/10.1146/annur ev.es.04.110173.000245

Holling, C. S., & Gunderson, L. H. (2002). Resilience and adaptive cycles. In L. H. Gunderson & C. S. Holling (Eds.), Panarchy: Understanding the transformations in human and natural systems (pp. 25–62). Island Press.

Holzwarth, F., Rüger, N., & Wirth, C. (2015). Taking a closer look: Disentangling effects of functional diversity on ecosystem functions with a trait-based model across hierarchy and time. *Royal Society Open Science*, *2*(3). https://doi.org/10.1098/rsos.140541

Hu, Z., Dakos, V., & Rietkerk, M. (2022). Using functional indicators to detect state changes in terrestrial ecosystems. Trends in Ecology & Evolution, 37(12), 1036–1045. https://doi.org/10.1016/j.tree.2022.07.011

Hubau, W., Lewis, S. L., Phillips, O. L., Affum-Baffoe, K., Beeckman, H., Cuní-Sanchez, A., Daniels, A. K., Ewango, C. E. N., Fauset, S., Mukinzi, J. M., Sheil, D., Sonké, B., Sullivan,

M. J. P., Sunderland, T. C. H., Taedoumg, H., Thomas, S. C., White, L. J. T., Abernethy, K. A., Adu-Bredu, S., … Zemagho, L. (2020). Asynchronous carbon sink saturation in African and Amazonian tropical forests. *Nature*, *579*(7797), 80–87. https://doi.org/10.1038/s41586-020-2035-0

Huete AR, Didan K, Shimabukuro YE, Ratana P, Saleska SR, Hutyra LR, Yang W, Nemani RR, Myneni R (2006) Amazon rainforests green- up with sunlight in dry season. Geophys Res Lett 33:L06405. doi: 10.1029/2005GL025583

Huntingford, C., Fisher, R. A., Mercado, L., Booth, B. B. B., Sitch, S., Harris, P. P., Cox, P. M., Jones, C. D., Betts, R. A., Malhi, Y., Harris, G. R., Collins, M., & Moorcroft, P. (2008). Towards quantifying uncertainty in predictions of Amazon "dieback." *Philosophical Transactions of the Royal Society B: Biological Sciences*, *363*(1498), 1857–1864. https://doi.org/10.1098/rstb.2007.0028

Huntingford, C., Zelazowski, P., Galbraith, D., Mercado, L. M., Sitch, S., Fisher, R., Lomas, M., Walker, A. P., Jones, C. D., Booth, B. B. B., Malhi, Y., Hemming, D., Kay, G., Good, P., Lewis, S. L., Phillips, O. L., Atkin, O. K., Lloyd, J., Gloor, E., … Cox, P. M. (2013). Simulated resilience of tropical rainforests to CO2-induced climate change. *Nature Geoscience*, *6*(4), 268–273. https://doi.org/10.1038/ngeo1741

Levine, N. M., Zhang, K., Longo, M., Baccini, A., Phillips, O. L., Lewis, S. L., Alvarez-Dávila, E., Segalin de Andrade, A. C., Brienen, R. J. W., Erwin, T. L., Feldpausch, T. R., Monteagudo Mendoza, A. L., Nuñez Vargas, P., Prieto, A., Silva-Espejo, J. E., Malhi, Y., & Moorcroft, P. R. (2016). Ecosystem heterogeneity determines the ecological resilience of the Amazon to climate change. *Proceedings of the National Academy of Sciences*, *113*(3), 793–797. https://doi.org/10.1073/pnas.1511344112

Jones, C., Lowe, J., Liddicoat, S., & Betts, R. (2009). Committed terrestrial ecosystem changes due to climate change. *Nature Geoscience*, *2*(7), 484–487. https://doi.org/10.1038/ngeo555

Johnson, M. O., Galbraith, D., Gloor, M., De Deurwaerder, H., Guimberteau, M., Rammig, A., Thonicke, K., Verbeeck, H., von Randow, C., Monteagudo, A., Phillips, O. L., Brienen, R. J. W., Feldpausch, T. R., Lopez Gonzalez, G., Fauset, S., Quesada, C. A., Christoffersen, B., Ciais, P., Sampaio, G., … Baker, T. R. (2016). Variation in stem mortality rates determines patterns of above-ground biomass in Amazonian forests: Implications for dynamic global vegetation models. Global Change Biology, 44, 1–18. https://doi.org/10.1111/gcb.13315

Keane, R. E., Hessburg, P. F., Landres, P. B., & Swanson, F. J. (2009). The use of historical range and variability (HRV) in landscape management. Forest Ecology and Management, 258, 1025–1037. https://doi.org/10.1016/j.foreco.2009.05.035

Köpp Hollunder, R., Garbin, M. L., Rubio Scarano, F., & Mariotte, P. (2022). Regional and local determinants of drought resilience in tropical forests. In *Ecology and Evolution* (Vol. 12, Issue 5). https://doi.org/10.1002/ece3.8943

Kraft, N. J. B. et al. 2008. Functional traits and niche-based tree community assembly in an Amazonian forest. Science 322: 580–582.

Laurance, W.F. & Peres, C.A. (eds.) (2006). Emerging Threats to Tropical Forests. The University of Chicago Press, Chicago.

Levine, N. M., Zhang, K., Longo, M., Baccini, A., Phillips, O. L., Lewis, S. L., Alvarez-Dávila, E., Segalin de Andrade, A. C., Brienen, R. J. W., Erwin, T. L., Feldpausch, T. R., Monteagudo Mendoza, A. L., Nuñez Vargas, P., Prieto, A., Silva-Espejo, J. E., Malhi, Y., & Moorcroft, P. R. (2016). Ecosystem heterogeneity determines the ecological resilience of the Amazon to climate change. *Proceedings of the National Academy of Sciences*, *113*(3), 793–797. https://doi.org/10.1073/pnas.1511344112

Lewis, S.L., Lopez-Gonzalez, G., Sonke´, B., Affum-Baffoe, K., Baker, T.R., Ojo, L.O. et al. (2009). Increasing carbon storage in intact African tropical forests. Nature, 457, 1003–1006.

Lin, Y. S., Medlyn, B. E., Duursma, R. A., Prentice, I. C., Wang, H., Baig, S., ... & Wingate, L. (2015). Optimal stomatal behaviour around the world. Nature Climate Change, 5(5), 459-464.

Liu, Y., Kumar, M., Katul, G. G., & Porporato, A. (2019). Reduced resilience as an early warning signal of forest mortality. *Nature Climate Change*, *9*(11), 880–885. https://doi.org/10.1038/s41558-019-0583-9

Malhi, Y. & Wright, J. (2004). Spatial patterns and recent trends in the climate of tropical rainforest regions. Philos. T. Roy. Soc. B, 359, 311–329.

Malhi, Y., Roberts, J. T., Betts, R. A., Killeen, T. J., Li, W., & Nobre, C. A. (2008). Climate change, deforestation, and the fate of the Amazon. Science, 319(5860), 169-172. doi:10.1126/science.1146961

Malhi, Y., Aragao, L. E. O. C., Galbraith, D., Huntingford, C., Fisher, R., Zelazowski, P., Sitch, S., McSweeney, C., & Meir, P. (2009). Exploring the likelihood and mechanism of a climate-change-induced dieback of the Amazon rainforest. *Proceedings of the National Academy of Sciences*, *106*(49), 20610–20615. https://doi.org/10.1073/pnas.0804619106

Malhi, Y., Gardner, T. A., Goldsmith, G. R., Silman, M. R., & Zelazowski, P. (2014). Tropical forests in the Anthropocene. Annual Review of Environment and Resources, 39, 125-159. doi:10.1146/annurev-environ-030713-155141

Manning, P., Van Der Plas, F., Soliveres, S., Allan, E., Maestre, F. T., Mace, G., Whittingham, M. J., & Fischer, M. (2018). Redefining ecosystem multifunctionality. *Nature Ecology and Evolution*, *2*(3), 427–436. https://doi.org/10.1038/s41559-017-0461-7

Marengo, J. A., Souza, C. M., Thonicke, K., Burton, C., Halladay, K., Betts, R. A., Alves, L. M., & Soares, W. R. (2018). Changes in Climate and Land Use Over the Amazon Region: Current and Future Variability and Trends. In Frontiers in Earth Science (Vol. 6, p. 228). Frontiers Media S.A. https://doi.org/10.3389/feart.2018.00228

Marengo, J. A., Tomasella, J., Alves, L. M., Soares, W. R., & Rodriguez, D. A. (2011). The drought of 2010 in the context of historical droughts in the Amazon region. *Geophysical Research Letters*, *38*(12). https://doi.org/10.1029/2011GL047436

Marengo, J. A., Tomasella, J., Soares, W. R., Alves, L. M., & Nobre, C. A. (2012). Extreme climatic events in the Amazon basin. *Theoretical and Applied Climatology*, *107*(1–2), 73–85. https://doi.org/10.1007/s00704-011-0465-1

Marca-Zevallos, M. J., Moulatlet, G. M., Sousa, T. R., Schietti, J., Coelho, L. de S., Ramos, J. F., Lima Filho, D. de A., Amaral, I. L., de Almeida Matos, F. D., Rincón, L. M., Cardenas Revilla, J. D., Pansonato, M. P., Gribel, R., Barbosa, E. M., Miranda, I. P. de A., Bonates, L. C. de M., Guevara, J. E., Salomão, R. P., Ferreira, L. V., … Costa, F. R. C. (2022). Local hydrological conditions influence tree diversity and composition across the Amazon basin. Ecography, 2022(11). https://doi.org/10.1111/ecog.06125

Markewitz D, Devine S, Davidson E, Brando PM, Nepstad DC (2010) Soil moisture depletion under simulated drought in the Amazon: impacts on deep root uptake. New Phytol 187:592–607

McDowell, N. G., Allen, C. D., Anderson-Teixeira, K., Aukema, B. H., Bond-Lamberty, B., Chini, L., ... & Williams, A. P. (2020). "Pervasive shifts in forest dynamics in a changing world." Science, 368(6494), eaaz9463.

McDowell, N. G., Fisher, R. A., Xu, C., Domec, J., Hölttä, T., Mackay, D. S., ... & Middleton, R. S. (2013). Evaluating theories of drought-induced vegetation mortality using a multimodel-experiment framework. New Phytologist, 200(2), 304-321.

Meir, P. et al. (2015). Threshold responses to soil moisture deficit by trees and soil in tropical rain forests: Insights from field experiments. Bioscience 65, 882–892.

Mori, A. S., Furukawa, T., & Sasaki, T. (2013). Response diversity determines the resilience of ecosystems to environmental change. Biological Reviews, 88(2), 349–364. https://doi.org/10.1111/brv.12004

Mouillot, D., Villéger, S., Scherer-Lorenzen, M., & Mason, N. W. H. (2011). Functional structure of biological communities predicts ecosystem multifunctionality. *PLoS ONE*, *6*(3). https://doi.org/10.1371/journal.pone.0017476

Mitchell, P. J., O'Grady, A. P., Pinkard, E. A., Brodribb, T. J., Arndt, S. K., Blackman, C. J., Duursma, R. A., Fensham, R. J., Hilbert, D. W., Nitschke, C. R., Norris, J., Roxburgh, S. H., Ruthrof, K. X., & Tissue, D. T. (2016). An ecoclimatic framework for evaluating the resilience of vegetation to water deficit. Global Change Biology, 22(5), 1677– 1689. https://doi.org/10.1111/gcb.13177

Nepstad DC, De Carvalho CR, Davidson EA, Jipp PH, Lefebvre PA, Negreiros GH, Da Silva ED, Stone TA, Trumbore SE, Vieira S (1994) The role of deep roots in the hydrological and carbon cycles of Amazonian forests and pastures. Nature 372:666–669

Nepstad, D. C., Tohver, I. M., Ray, D., Moutinho, P., & Cardinot, G. (2007). Mortality of large trees and lianas following experimental drought in an amazon forest. Ecological Society of America, 88(9), 2259–2269. https://doi.org/10.1038/aps.2015.36

Niinemets Ü (2010) Responses of forest trees to single and multiple environmental stresses from seedlings to mature plants: past stress history, stress interactions, tolerance and acclimation. For Ecol Manag 260:1623–1639

O'Brien, M. J., Leuzinger, S., Philipson, C. D., Tay, J., & Hector, A. (2014). Drought survival of tropical tree seedlings enhanced by non-structural carbohydrate levels. Nature Climate Change, 4(8), 710-714.

Oliveira, R. S., Costa, F. R. C., van Baalen, E., de Jonge, A., Bittencourt, P. R., Almanza, Y., Barros, F. de V., Cordoba, E. C., Fagundes, M. V., Garcia, S., Guimaraes, Z. T. M., Hertel, M., Schietti, J., Rodrigues-Souza, J., & Poorter, L. (2019). Embolism resistance drives the distribution of Amazonian rainforest tree species along hydro-topographic gradients. New Phytologist, 221(3), 1457–1465. https://doi.org/10.1111/NPH.15463

Oliveira, R. S., Eller, C. B., Barros, F. de V., Hirota, M., Brum, M., & Bittencourt, P. (2021). Linking plant hydraulics and the fast-slow continuum to understand resilience to drought in tropical ecosystems. The New Phytologist, 230(3), 904–923. https://doi.org/10.1111/NPH.17266

Parsons, L. (2020). Implications of CMIP6 projected drying trends for 21st century Amazonian drought risk. Earth's Futur. 8, e2020EF001608.

Sala, A., Woodruff, D. R., & Meinzer, F. C. (2012). Carbon dynamics in trees: feast or famine? Tree Physiology, 32(6), 764-775.

Sala, A., Piper, F., & Hoch, G. (2010). Physiological mechanisms of drought-induced tree mortality are far from being resolved. New Phytologist, 186(2), 274-281.

Scheiter, S., Langan, L., & Higgins, S. I. (2013). Next-generation dynamic global vegetation models: learning from community ecology. In The New phytologist (Vol. 198, Issue 3, pp. 957–969). https://doi.org/10.1111/nph.12210

Pavlick, R., Drewry, D. T., Bohn, K., Reu, B., & Kleidon, A. (2013). The Jena Diversity-Dynamic Global Vegetation Model (JeDi-DGVM): a diverse approach to representing terrestrial biogeography and biogeochemistry based on plant functional trade-offs. Biogeosciences, 10(6), 4137–4177. https://doi.org/10.5194/bg-10-4137-2013

Phillips OL, Malhi Y, Higuchi N, Laurance WF, Nunez PV, et al. (1998) Changes in the carbon balance of tropical forests: evidence from long-term plots. Science 282: 439–442.

Phillips, O. L., Aragão, L. E. O. C., Lewis, S. L., Fisher, J. B., Lloyd, J., López-González, G., Malhi, Y., Monteagudo, A., Peacock, J., Quesada, C. A., Van Der Heijden, G., Almeida, S., Amaral, I., Arroyo, L., Aymard, G., Baker, T. R., Bánki, O., Blanc, L., Bonal, D., … Torres-Lezama, A. (2009). Drought sensitivity of the amazon rainforest. *Science*, *323*(5919), 1344–1347. https://doi.org/10.1126/SCIENCE.1164033

Poorter, L., van der Sande, M. T., Thompson, J., Arets, E. J. M. M., Alarcón, A., Álvarez-Sánchez, J., Ascarrunz, N., Balvanera, P., Barajas-Guzmán, G., Boit, A., Bongers, F., Carvalho, F. A., Casanoves, F., Cornejo-Tenorio, G., Costa, F. R. C., de Castilho, C. V., Duivenvoorden, J. F., Dutrieux, L. P., Enquist, B. J., … Peña-Claros, M. (2015). Diversity enhances carbon storage in tropical forests. *Global Ecology and Biogeography*, *24*(11), 1314–1328. https://doi.org/10.1111/geb.12364

Poorter, L., van der Sande, M. T., Thompson, J., Arets, E. J. M. M., Alarcón, A., Álvarez-Sánchez, J., Ascarrunz, N., Balvanera, P., Barajas-Guzmán, G., Boit, A., Bongers, F., Carvalho, F. A., Casanoves, F., Cornejo-Tenorio, G., Costa, F. R. C., de Castilho, C. V., Duivenvoorden, J. F., Dutrieux, L. P., Enquist, B. J., … Peña-Claros, M. (2015). Diversity enhances carbon storage in tropical forests. *Global Ecology and Biogeography*, *24*(11), 1314–1328.

Poulter, B., Hattermann, F., Hawkins, E., Zaehle, S., Sitch, S., Restrepo-Coupe, N., Heyder, U., & Cramer, W. (2010). Robust dynamics of Amazon dieback to climate change with perturbed ecosystem model parameters. *Global Change Biology*, *16*(9), 2476–2495. https://doi.org/10.1111/j.1365-2486.2009.02157.x

Ratajczak, Z., Carpenter, S. R., Ives, A. R., Kucharik, C. J., Ramiadantsoa, T., Stegner, M. A., Williams, J. W., Zhang, J., & Turner, M. G. (2018). Abrupt change in ecological systems: Inference and diagnosis. Trends in Ecology and Evolution, 33, 513–526. https://doi.org/10.1016/j.tree.2018.04.013

Reich, P. B. (2014). The world-wide “fast-slow” plant economics spectrum: A traits manifesto. *Journal of Ecology*, *102*(2), 275–301. https://doi.org/10.1111/1365-2745.12211

Reiss, J., Bridle, J. R., Montoya, J. M., & Woodward, G. (2009). Emerging horizons in biodiversity and ecosystem functioning research. *Trends in Ecology and Evolution*, *24*(9), 505–514. https://doi.org/10.1016/j.tree.2009.03.018

Reu, B., Proulx, R., Bohn, K., Dyke, J. G., Kleidon, A., Pavlick, R., & Schmidtlein, S. (2011). The role of climate and plant functional trade-offs in shaping global biome and biodiversity patterns. Global Ecology and Biogeography, 20(4), 570–581. https://doi.org/10.1111/j.1466-8238.2010.00621.x

Rius, B. F., Filho, J. P. D., Fleischer, K., Hofhansl, F., Blanco, C. C., Rammig, A., Domingues, T. F., & Lapola, D. M. (2023). Higher functional diversity improves modeling of Amazon forest carbon storage. Ecological Modelling, 481(March 2022), 110323. https://doi.org/10.1016/j.ecolmodel.2023.110323

Ruiz-Vásquez, M. et al. (2020) Effects of Amazon basin deforestation on regional atmospheric circulation and water vapor transport towards tropical South America. Clim. Dyn., v. 54, p. 4169–4189.

Rowland, L., da Costa, A. C. L., Galbraith, D. R., Oliveira, R. S., Binks, O. J., Oliveira, A. A. R., Pullen, A. M., Doughty, C. E., Metcalfe, D. B., Vasconcelos, S. S., Ferreira, L. V., Malhi, Y., Grace, J., Mencuccini, M., & Meir, P. (2015). Death from drought in tropical forests is triggered by hydraulics not carbon starvation. *Nature*, 1–13. https://doi.org/10.1038/nature15539

Ryan, M. G. (1991a). A simple method for estimating gross carbon budgets for vegetation in forest ecosystems. Tree Physiology, 9(1_2), 255–266. https://doi.org/10.1093/treephys/9.1-2.255

Ryan, M. G. (1991b). Effects of Climate Change on Plant Respiration, 1(2), 157–167.

Saatchi, S., Asefi-Najafabady, S., Malhi, Y., Aragão, L. E. O. C., Anderson, L. O., Myneni, R. B., & Nemani, R. (2013). Persistent effects of a severe drought on Amazonian forest canopy. *Proceedings of the National Academy of Sciences of the United States of America*, *110*(2), 565–570. https://doi.org/10.1073/PNAS.1204651110/SUPPL_FILE/PNAS.201204651SI.PDF

Saatchi, S., Longo, M., Xu, L., Yang, Y., Abe, H., André, M., Aukema, J. E., Carvalhais, N., Cadillo-Quiroz, H., Cerbu, G. A., Chernela, J. M., Covey, K., Sánchez-Clavijo, L. M., Cubillos, I. V., Davies, S. J., De Sy, V., De Vleeschouwer, F., Duque, A., Sybille Durieux, A. M., … Elmore, A. C. (2021). Detecting vulnerability of humid tropical forests to multiple stressors. *One Earth*, *4*(7), 988–1003. https://doi.org/10.1016/j.oneear.2021.06.002

Sakschewski, B., von Bloh, W., Boit, A., Rammig, A., Kattge, J., Poorter, L., Pe??uelas, J., & Thonicke, K. (2015). Leaf and stem economics spectra drive diversity of functional plant traits in a dynamic global vegetation model. Global Change Biology, 2711–2725. https://doi.org/10.1111/gcb.12870

Sakschewski, B., von Bloh, W., Boit, A., Poorter, L., Peña-Claros, M., Heinke, J., Joshi, J., & Thonicke, K. (2016). Resilience of Amazon forests emerges from plant trait diversity. *Nature Climate Change*, *1*(August). https://doi.org/10.1038/nclimate3109

Saleska SR, Didan K, Huete AR, da Rocha HR (2007) Amazon forests green-up during 2005 drought. Science (80) 318 612

Samanta A, Ganguly S, Hashimoto H, Devadiga S, Vermote E, Knyazikhin Y, Nemani RR, Myneni RB (2010) Amazon forests did not green-up during the 2005 drought. Geophys Res Lett 37: L05401. doi:10.1029/2009GL042154

Scheffer M. 2009. Critical Transitions in Nature and Society. Princeton, NJ: Princeton Univ. Press

Scheffer, M., Carpenter, S. R., Dakos, V., & Van Nes, E. H. (2015). Generic Indicators of Ecological Resilience: Inferring the Chance of a Critical Transition. Https://Doi.Org/10.1146/Annurev-Ecolsys-112414-054242, 46, 145–167. https://doi.org/10.1146/ANNUREV-ECOLSYS-112414-054242

Schmitt, S., Maréchaux, I., Chave, J., Fischer, F. J., Piponiot, C., Traissac, S., & Hérault, B. (2020). Functional diversity improves tropical forest resilience: Insights from a long-term virtual experiment. Journal of Ecology, 108(3), 831–843. https://doi.org/10.1111/1365-2745.13320

Seidl, R., Rammer, W., & Spies, T. A. (2014). Disturbance legacies increase the resilience of forest ecosystem structure, composition, and functioning. Ecological Applications, 24, 2063–2077. https://doi.org/10.1890/14-0255.1

Silva, C. E., Kellner, J. R., Clark, D. B., & Clark, D. A. (2013). Response of an old- growth tropical rainforest to transient high temperature and drought. Global Change Biology, 19(11), 3423– 3434. https://doi. org/10.1111/gcb.12312

Sitch, S., Huntingford, C., Gedney, N., Levy, P. E., Lomas, M., Piao, S. L., Betts, R., Ciais, P., Cox, P., Friedlingstein, P., Jones, C. D., Prentice, I. C., & Woodward, F. I. (2008). Evaluation of the terrestrial carbon cycle, future plant geography and climate-carbon cycle feedbacks using five Dynamic Global Vegetation Models (DGVMs). *Global Change Biology*, *14*(9), 2015–2039. https://doi.org/10.1111/j.1365-2486.2008.01626.x

Sitch, S., Smith, B., Prentice, I. C., Arneth, A., Bondeau, A., Cramer, W., Kaplan, J. O., Levis, S., Lucht, W., Sykes, M. T., Thonicke, K., & Venevsky, S. (2003). Evaluation of ecosystem dynamics, plant geography and terrestrial carbon cycling in the LPJ dynamic global vegetation model. In *Global Change Biology* (Vol. 9, Issue 2, pp. 161–185). https://doi.org/10.1046/j.1365-2486.2003.00569.x

Staal, A., Tuinenburg, O. A., Bosmans, J. H. C., Holmgren, M., Van Nes, E. H., Scheffer, M., Zemp, D. C., & Dekker, S. C. (2018). Forest-rainfall cascades buffer against drought across the Amazon. *Nature Climate Change 2018 8:6*, *8*(6), 539–543. https://doi.org/10.1038/s41558-018-0177-y

Stahl C, Burban B, Wagner F, Goret JY, Bompy F, Bonal D (2013) Influence of seasonal variations in soil water availability on gas exchange of tropical canopy trees. Biotropica 45:155–164

Swann, A. L. et al. (2015). Future deforestation in the Amazon and consequences for South American climate. Agric. For. Meteorol., v. 214, p. 12–24.

Townsend AR, Asner GP, Cleveland CC (2008) The biogeochemical heterogeneity of tropical forests. Trends in Ecology & Evolution, 23, 424–431

Umaña, M. N., Salgado-Negret, B., Norden, N., Salinas, V., Garzón, F., Medina, S. P., Rodríguez-M, G. M., López-Camacho, R., Castaño-Naranjo, A., Cuadros, H., Franke-Ante, R., Avella, A., Idárraga-Piedrahita, Á., Jurado, R., Nieto, J., Pizano, C., Torres, A. M., García, H., & González-M, R. (2023). Upscaling the effect of traits in response to drought: The relative importance of safety–efficiency and acquisitive–conservation functional axes. *Ecology Letters*, *September*, 2098–2109. https://doi.org/10.1111/ele.14328

Van Passel, J., de Keersmaecker, W., Bernardino, P. N., Jing, X., Umlauf, N., Van Meerbeek, K., & Somers, B. (2022). Climatic legacy effects on the drought response of the Amazon rainforest. *Global Change Biology*, *July*, 5808–5819. https://doi.org/10.1111/gcb.16336

Verbesselt, J., Hyndman, R., Newnham, G., & Culvenor, D. (2010a). Detecting trend and seasonal changes in satellite image time series. *Remote Sensing of Environment*, *114*(1), 106–115. https://doi.org/10.1016/j.rse.2009.08.014

Verbesselt J, Hyndman R, Zeileis A, Culvenor D (2010a). “Phenological Change Detection while Accounting for Abrupt and Gradual Trends in Satellite Image Time Series.” Remote Sensing of Environment, 114(12), 2970–2980. doi:10.1016/j.rse.2010.08.003.

Weedon, Graham P.; Balsamo, Gianpaolo; Bellouin, Nicolas; Gomes, Sandra; Best, Martin J.; Viterbo, Pedro. The WFDEI meteorological forcing data set: WATCH Forcing Data methodology applied to ERA-Interim reanalysis data. Water Resources Research, [S. l.], v. 50, n. 9, p. 7505–7514, 2014. http://doi.wiley.com/10.1002/2014WR015638.

Wright, I. J., Reich, P. B., Westoby, M., Ackerly, D. D., Baruch, Z., Bongers, F., Cavender-bares, J., Chapin, T., Cornelissen, J. H. C., Diemer, M., Flexas, J., Garnier, E., Groom, P. K., & Gulias, J. (2004). The worldwide leaf economics spectrum. *Nature*, *428*, 821–827.

Wunderling, N., Staal, A., Sakschewski, B., Hirota, M., Tuinenburg, O. A., Donges, J. F., Barbosa, H. M. J., & Winkelmann, R. (2022). Recurrent droughts increase risk of cascading tipping events by outpacing adaptive capacities in the Amazon rainforest. *Proceedings of the National Academy of Sciences of the United States of America*, *119*(32), e2120777119. https://doi.org/10.1073/pnas.2120777119

Xu, C., Mcdowell, N. G., Sevanto, S., & Fisher, R. A. (2013). Our limited ability to predict vegetation dynamics under water stress. *New Phytologist*, *200*(2), 298–300. https://doi.org/10.1111/nph.12450

Yang, J., Tian, H., Pan, S., Chen, G., Zhang, B., & Dangal, S. (2018). Amazon drought and forest response: Largely reduced forest photosynthesis but slightly increased canopy greenness during the extreme drought of 2015/2016. Global Change Biology, 24(5), 1919–1934. https://doi.org/10.1111/gcb.14056

Yang, Q., Huang, Z., Wu, L., Guo, B., Liu, M., Xue, X., Li, X., & Liu, X. (2024). Resilience changes of carbon stocks to quantify the long-term effects of ecological engineering projects in subtropical forests of China based on satellite-derived net ecosystem production time series and inventory data. *Land Degradation & Development*, *35*(7), 2329–2344. https://doi.org/10.1002/ldr.5063

Zhang, R. Q., Xiong, Q., Wu, L., Wang, P., Kong, J. Y., Shi, X., & Sun, Z. Y. (2024). Water supply following drought: Effects on drougt legacy and resilience in a tropical forest - A case study in Xishuangbanna, China. Ecological Informatics, 79(October 2023), 102422. https://doi.org/10.1016/j.ecoinf.2023.102422

8. Supplementary Material

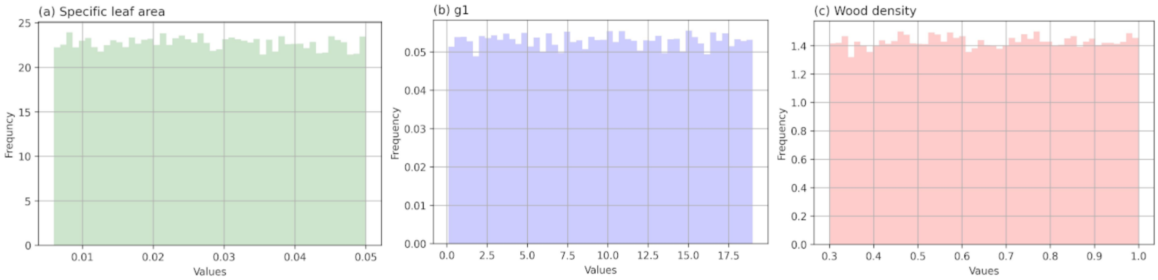

Fig. SM1. Initial distribution of variant traits to be sampled in the creation of the 6000 PLSs

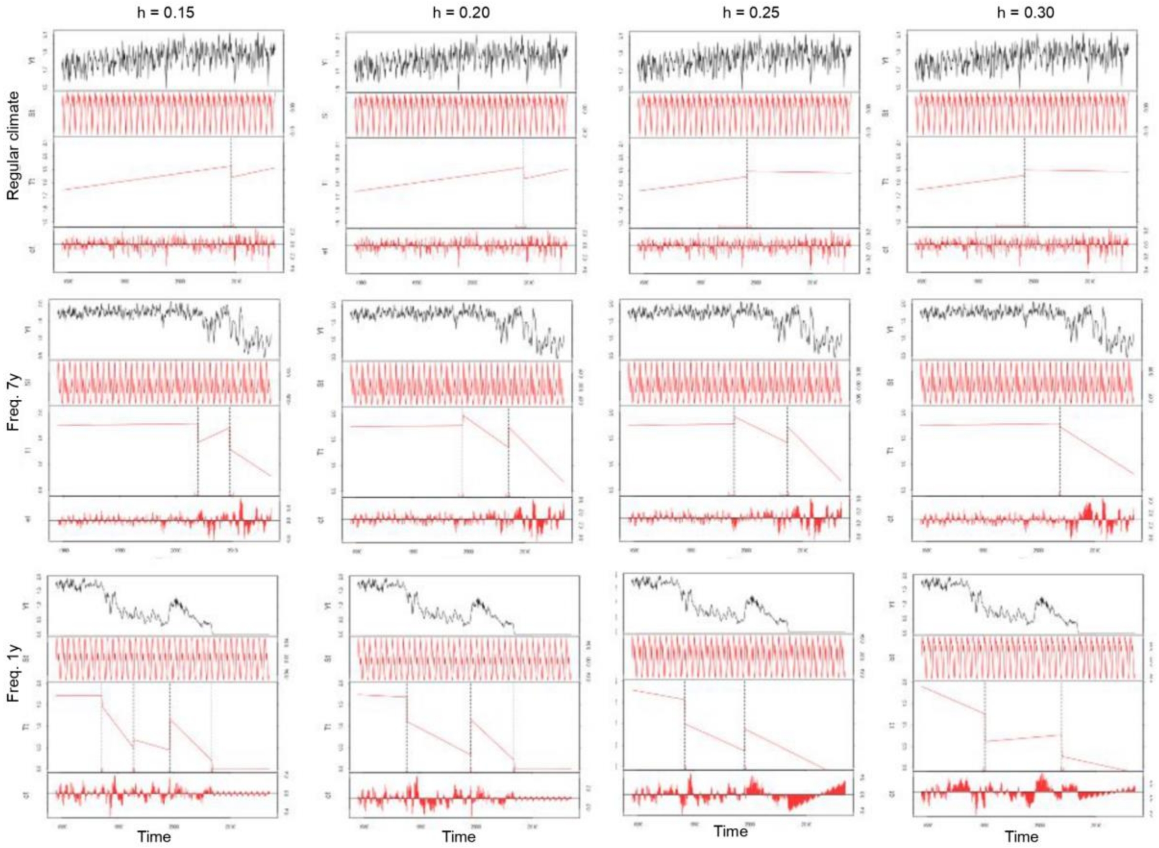

Fig. SM2. Sensitivity analysis of the "h" parameter for the bfast algorithm across varied climate scenarios. Each plot comprises three subplots: the first displays the original time series without decomposition; the second showcases the seasonal component; the third illustrates the fitted model; and the fourth depicts the error component. The analysis was conducted for "h" values of 0.15, 0.2, 0.25, and 0.3, exploring three distinct climate scenarios: regular conditions (Regular climate), reduced precipitation (30% less) occurring every 8 years (Freq. 8y), and every years (Freq. 2y).

Fig. SM3. Time series data spanning from 1979 to 2016 showcases changes in the plant carbon compartments under three distinct climate scenarios: regular conditions (blue line), reduced precipitation (30% less) occurring every 8 years (green line), and every 2 years (orange line).

SM.1. Model developments not implemented

SM.1.1. Area based occupation of grid cell

In order to use an area-based scheme for grid cell occupation we implemented the use of the Fractional Projective Cover developed by LPJ. From the allometry constraints of a PLS is now possible to determine its grid-cell occupation in an area-based approach instead of the biomass-based approach used in the CAETÊ previous version, which employed biomass-ratio hypothesis (Grime, 1998; Pavlick et al., 2013). Using biomass-ratio approach may overfavour the PLSs with high biomass (especially the ones with high carbon storage on stem) and lead to the hyperdominance of certain traits combinations that affect the community assemblage as well as the ecosystem processes. In the present version, a grid-cell is occupied by a mosaic of PLSs (each one represented by a single average individual), being that the area that each one occupies is called as fractional projective cover (Fractional PC, m^{-2}) that is based on the projection of the leaf area of a PLS, the so called foliar projective cover (FPC ;unitless) and on the estimation of the density of average individuals (N_{ind}, ind/m^2) of a certain PLS given its diameter (Smith, 2001). The use of the diameter for calculating the density of individuals is based on the the self-thinning rule (the number of trees per unit area decrease as average tree size increases; WELLER, 1987; WESTOBY, 1984); here we consider the "size" of the PLS as its diameter and, indirectly, its crown area. As in the LPJ model, we assume canopy closure but no overlap between crowns, hence, the sum of the Fractional PC of all PLSs in a grid cell cannot exceed 1, also meaning that there is no vertical overlap among PLSs. At least 5% of the grid cell is intended for grasses, in that sense, the sum of all woody PLS occupation can not exceed 95%. If so, all the PLSs present a percentage reduction in its occupation in order to respect the maximum occupation area.

$$Foliar_{PC} = 1 - exp(-0.5 * LAI) \qquad \text{(Eq. SM1)}$$

$$N_{ind} = Diam^{-1.6} \qquad \text{(Eq. SM2)}$$

$$Fractional_{PC} = crown_{area} N_{ind} Foliar_{PC} \qquad \text{(Eq. SM3)}$$

SM.1.2. Establishment

During the implementation of mortality by space competition (see section, we realized that it would be necessary to develop a module of establishment of new individuals sapling, otherwise, the areas of occupation of the PLS would continuously decrease and the PLS would become increasingly larger due to a self-thinning process (when individuals become larger as the population density declines; Westoby, 1984). The establishment of saplings occurs only if the sum of occupation of all PLS is lower than 95%. All the PLSs present the same rate of establishment that depends on the amount of area available and the number of survival strategies.

$$estab_{PLS} = estab_{max} * (1 - FPC_{total})/n_{PLS} \qquad \text{(Eq. SM4)}$$

With the saplings' establishment the density of individuals for each PLS is updated:

$$dens_{PLS_{new}} = dens_{PLS_{new}} + estab_{PLS} \qquad \text{(Eq. SM5)}$$

All the saplings have the same leaf area index (LAI) and according to allometric rules the carbon is allocated to each carbon pool.

SM.1.3. Self-thinning

To maintain the correct carbon balance, as the density population of a PLS increases the average individuals go through a process of "shrink" once that the saplings are invariably smaller than the average individual. Then, the new amount of carbon of an average individual of a PLS ($C_{\alpha PLS_{new}}$) is giving by the carbon ($C_{\alpha PLS_{old}}$) and the density ($dens_{PLS_{old}}$) in the previous time step, the carbon invested in saplings ($C_{\alpha\, sapling_{PLS}}$), the establishment rate ($estab_{PLS}$) and the density of individuals considering the amount of sapling established ($dens_{PLS_{new}}$)

$$C_{\alpha PLS_{new}} = [(C_{\alpha PLS_{old}} dens_{PLS_{old}}) + (C_{\alpha\, sapling_{PLS}} * \quad estab_{PLS})]/ \quad + dens_{PLS_{new}} \qquad \text{(Eq. SM6)}$$

SM.1.4. Mortality by space

In the previous version of CAETÊ, mortality was overly simplistic, considering only a negative carbon balance as a factor. Now, in addition to this, PLS mortality also depends on grid cell space occupation. If the fractional projective cover of the woody PLSs ($Fractional_{PC_{woody}}$ exceeds 95%, the number of average individuals is reduced, consequently decreasing the occupied area. Then, the mortality due to space ($mort_{space}$):

$$mort_{space} = [1 - (0.95/Fractional_{PC_{woody}})] * N_{ind} \qquad \text{Eq. SM7}$$

$$Fractional_{PC_{woody}} = Diam(N_{ind} * mort_{space}) Folir_{PC} \qquad \text{Eq. SM8}$$

This formulation is based on Zeng, Li & Song (2014)

Besides, the height of a PLS must obey a mechanical stability that imposes a critical height H_{crit}. This formulation is derived from the model aDGVM2 (Langan, Higgins & Scheiter, 2017):

$$H_{crit} = 0.79\{[(11.852 * WD + 37)/9.81] * WD\}^{1/3} * Diam^{2/3} \qquad \text{Eq. SM9}$$

SM.2. The regular climate conditions

Despite the already observed historical climate changes, such as the droughts in 2005 and 2010, we did not detect a significant alteration in resilience under regular climate conditions. Despite fluctuations in precipitation, there was a consistent maintenance of the ecosystem structure and functioning across all indicators (Fig. 2 and Fig. 3). However, we identified one breakpoint for NPP and evapotranspiration, and two breakpoints for total carbon and WUE, with a trend towards an increase in these ecosystem indicators (Fig. 5). This upward trend aligns with studies indicating long-term increases in productivity and biomass (e.g., Baker et al., 2004a; Lewis et al., 2009; Phillips et al., 2009). These results contradict studies suggesting a decrease in resilience or no change in resilience when biomass is considered a proxy for resilience (Feldpausch et al., 2016).

Regarding evapotranspiration, we observed a slight increase in this variable. Typically, during drought periods, the reduction in soil moisture availability can lead to decreased evapotranspiration as plants close their stomata to conserve water, resulting in lower transpiration rates (Liu et al., 2020; Zhao et al., 2022). This decrease in evapotranspiration is more pronounced during severe or prolonged drought events when soil water availability is severely limited (Bonal et al., 2016). However, in some cases, evapotranspiration may actually increase during drought periods due to the elevated atmospheric moisture demand associated with such conditions (Zhao et al., 2022). This increase in evapotranspiration during drought can accelerate water resource depletion, trigger flash droughts, and exacerbate stress on ecosystems (Brodribb et al., 2020; Zhao et al., 2022). The effects of non-severe drought on evapotranspiration remain largely unknown.

SM.2. Reduced precipitation conditions

Despite the already observed historical climate changes, such as the droughts in 2005 and 2010, we did not detect a significant alteration in resilience under regular climate conditions. Despite fluctuations in precipitation, there was a consistent maintenance of the ecosystem structure and functioning across all indicators (Fig. 2 and Fig. 3). However, we identified one breakpoint for NPP and evapotranspiration, and two breakpoints for total carbon and WUE, with a trend towards an increase in these ecosystem indicators (Fig. 5, Table 2 and Table 3). This upward trend aligns with studies indicating long-term increases in productivity and biomass (e.g., Baker et al., 2004a; Lewis et al., 2009; Phillips et al., 2009) and contradicts studies suggesting a decrease in resilience or no change in resilience when biomass is considered a proxy for resilience (Feldpausch et al., 2016).

Regarding evapotranspiration, we observed a slight increase in this variable (Fig. 2, Fig. 3). Typically, during drought periods, the reduction in soil moisture availability can lead to decreased evapotranspiration as plants close their stomata to conserve water, resulting in lower transpiration rates (Liu et al., 2020; Zhao et al., 2022). This decrease in evapotranspiration is more pronounced during severe or prolonged drought events when soil water availability is severely limited (Bonal et al., 2016). However, in some cases, evapotranspiration may actually increase during drought periods due to the elevated atmospheric moisture demand associated with such conditions (Zhao et al., 2022). This increase in evapotranspiration during drought can accelerate water resource depletion, trigger flash droughts, and exacerbate stress on ecosystems (Brodribb et al., 2020; Zhao et al., 2022). The effects of non-severe drought on evapotranspiration remain largely unknown.

Concerning WUE, we observed an increasing trend (Fig. 2, Fig. 3), although not highly prominent. Typically, WUE increases with drier conditions as plants tend to close their stomata to prevent water loss, thereby enhancing their WUE. However, if the drought becomes too severe, it can lead to a reduction in WUE because although the plant is losing less water, this can also result in a decrease in carbon uptake. WUE during dry periods can lead to changes in the relationship between the amount of carbon fixed by the plant and the amount of water lost through transpiration. In dry conditions, plants may close their stomata to reduce water loss, potentially decreasing the photosynthesis rate. This can result in a reduction in WUE as the plant is losing less water but also fixing less carbon. However, the response of WUE to drought can vary depending on plant species, soil conditions, and the intensity of the drought. In some cases, plants may exhibit higher water use efficiency during drought, indicating they can maintain a relatively high photosynthesis rate compared to the amount of water lost through transpiration.

GENERAL CONCLUSION

This thesis delved into the resilience of the Amazon rainforest in the face of climate change, utilizing a trait-based approach to model functional diversity and assess the impacts of drought. Our research underscores the critical role of trait variability in enhancing the precision of ecosystem function representation and understanding ecosystem responses to changing environmental conditions.

In the initial chapter, we demonstrated that incorporating trait variability not only enhances the accuracy of ecosystem function representation but also enables a more profound exploration of the connections between ecosystem functioning and different facets of functional diversity. Our findings revealed that trait diversity empowers plant communities to undergo functional reorganization in response to challenging environmental conditions, such as decreased water availability, leading to shifts towards strategies favoring root investment over leaves and wood. This reorganization resulted in a decline in total carbon storage but an increase in community richness and evenness. Conversely, the plant functional type (PFT) approach constrained changes in community functional structure, amplifying the impacts of environmental shifts on ecosystem functioning and impeding comprehensive functional diversity analyses.

In the subsequent chapter, we evaluated the repercussions of recurring drought events (30% precipitation reduction) on the Amazon forest at varying frequencies: every two years and every eight years. Our results underscore the pivotal influence of drought frequency on the Amazon rainforest's resilience. Recurrent droughts, particularly those occurring annually, exert a substantial toll on forest functionality compared to less frequent occurrences. While the Amazon initially exhibits resilience to drought, the cumulative effects culminate in significant declines in ecosystem indicators like carbon storage, primary productivity, and evapotranspiration. These outcomes hint at a potential transition of the Amazon forest from a carbon sink to a carbon source under severe drought conditions, with far-reaching implications for global carbon sequestration.

Moreover, the diversity of functional strategies emerges as a linchpin for ecosystem resilience, with alterations in functional composition through shifts in relative abundances and exclusions of strategies playing a pivotal role in the initial observed resilience. Nonetheless, the adaptation of functional composition alone proves inadequate to withstand enduring, frequent, or very severe drought conditions. Under the 2- year drought scenario, we witnessed a complete system collapse in terms of surviving strategies and all other ecosystem indicators. This collapse underscores how shifts in functional composition can trigger cascading effects on ecosystem processes, such as carbon and water cycles, significantly impacting resilience and stability in the face of forthcoming drought events.

Our findings underscore the significance of evaluating diverse ecosystem indicators, as carbon alone may not sufficiently gauge resilience. We unveil that ecosystem processes and properties may exhibit less resilience than carbon stocks, suggesting that terrestrial ecosystems globally could be even more susceptible than previously assumed.

GENERAL REFERENCES

Aguirre-Gutiérrez, J., Oliveras, I., Rifai, S., Fauset, S., Adu-Bredu, S., Affum-Baffoe, K., Baker, T. R., Feldpausch, T. R., Gvozdevaite, A., Hubau, W., Kraft, N. J. B., Lewis, S. L., Moore, S., Niinemets, Ü., Peprah, T., Phillips, O. L., Ziemińska, K., Enquist, B., & Malhi, Y. (2019). Drier tropical forests are susceptible to functional changes in response to a long-term drought. *Ecology Letters*, *22*(5), 855–865. https://doi.org/10.1111/ele.13243

Aguirre-Gutiérrez, J., Berenguer, E., Oliveras Menor, I., Bauman, D., Corral-Rivas, J. J., Nava-Miranda, M. G., Both, S., Ndong, J. E., Ondo, F. E., Bengone, N. N., Mihinhou, V., Dalling, J. W., Heineman, K., Figueiredo, A., González-M, R., Norden, N., Hurtado-M, A. B., González, D., Salgado-Negret, B., … Malhi, Y. (2022). Functional susceptibility of tropical forests to climate change. *Nature Ecology & Evolution*, *6*(7), 878–889. https://doi.org/10.1038/s41559-022-01747-6

Aguirre-Gutiérrez, J. et al. (2020) Long-term droughts may drive drier tropical forests towards increased functional, taxonomic and phylogenetic homogeneity. Nat. Commun. 11, 3346.

Albrich, K., Rammer, W., Turner, M. G., Ratajczak, Z., Braziunas, K. H., Hansen, W. D., & Seidl, R. (2020). Simulating forest resilience: A review. *Global Ecology and Biogeography*, *29*(12), 2082–2096. https://doi.org/10.1111/geb.13197

Aleixo, I., Norris, D., Hemerik, L., Barbosa, A., Prata, E., Costa, F., & Poorter, L. (2019). Amazonian rainforest tree mortality driven by climate and functional traits. *Nature Climate Change*, *9*(5), 384–388. https://doi.org/10.1038/s41558-019-0458-0

Allen, C. D., Macalady, A. K., Chenchouni, H., Bachelet, D., McDowell, N., Vennetier, M., Kitzberger, T., Rigling, A., Breshears, D. D., Hogg, E. H. (Ted., Gonzalez, P., Fensham, R., Zhang, Z., Castro, J., Demidova, N., Lim, J. H., Allard, G., Running, S. W., Semerci, A., & Cobb, N. (2010). A global overview of drought and heat-induced tree mortality reveals emerging climate change risks for forests. *Forest Ecology and Management*, *259*(4), 660–684. https://doi.org/10.1016/j.foreco.2009.09.001

Allen, K., Dupuy, J. M., Gei, M. G., Hulshof, C., Medvigy, D., Pizano, C., Salgado-Negret, B., Smith, C. M., Trierweiler, A., Van Bloem, S. J., Waring, B. G., Xu, X., & Powers, J. S. (2017). Will seasonally dry tropical forests be sensitive or resistant to future changes in rainfall regimes? Environmental Research Letters, 12(2), 023001. https://doi.org/10.1088/1748-9326/AA5968

Almeida, Alexandre Esteves. "Time Series Components and Breakpoints in Remote Sensing Image Analysis." Universidade Estadual de Campinas, Instituto de Computação, 2017.

Anderegg, W. R. L., L. D. L. Anderegg, J. A. Berry, and C. B. Field (2014), Loss of whole-tree hydraulic conductance during severe drought and multi-year forest die-off, Oecologia, 175, 11–23.

Anderegg, W. R. L., Trugman, A. T., Badgley, G., Konings, A. G., & Shaw, J. (2020). Divergent forest sensitivity to repeated extreme droughts. Nature Climate Change, 10(12), 1091–1095. https://doi.org/10.1038/s41558-020-00919-1

Anderegg, W. R. L., Konings, A. G., Trugman, A. T., Yu, K., Bowling, D. R., Gabbitas, R., Karp, D. S., Pacala, S., Sperry, J. S., Sulman, B. N., & Zenes, N. (2018). Hydraulic diversity of forests regulates ecosystem resilience during drought. Nature, 561(7724), 538–541. https://doi.org/10.1038/S41586-018-0539-7

Aragăo, L. E. O. C. (2012). The rainforest's water pump. *Nature 2012 489:7415*, *489*(7415), 217–218. https://doi.org/10.1038/nature11485

Artaxo, P., & Marengo, J. A. (2020). Climate change in the Amazon: tendencies, impacts and ecological consequences. In *Thermodynamics and Phase Transformations* (pp. 479–506). EDP Sciences. https://doi.org/10.1051/978-2-7598-0247-0.c025

Artaxo P, Hansson HC, Machado LAT, Rizzo LV (2022) Tropical forests are crucial in regulating the climate on Earth. PLOS Clim 1(8): e0000054. https://doi.org/10.1371/journal.pclm.0000054

Baker, T.R., Phillips, O.L., Malhi, Y., Almeida, S., Arroyo, L., Di Fiore, A. et al. (2004a). Increasing biomass in Amazonian forest plots. Philos. T. Roy. Soc. B, 359, 353–365.

Baker, T.R., Phillips, O.L., Malhi, Y., Almeida, S., Arroyo, L., Di Fiore, A. et al. (2004b). Variation in wood density determines spatial patterns in Amazonian forest biomass. Glob. Change Biol., 10, 545–562.

Baker, J. C. A., Garcia-Carreras, L., Gloor, M., Marsham, J. H., Buermann, W., Da Rocha, H. R., Nobre, A. D., De Carioca Araujo, A., & Spracklen, D. V. (2021). Evapotranspiration in the Amazon: Spatial patterns, seasonality, and recent trends in observations, reanalysis, and climate models. *Hydrology and Earth System Sciences*, *25*(4), 2279–2300. https://doi.org/10.5194/hess-25-2279-2021

Baraloto, C., Paine, C. E. T., Poorter, L., Beauchene, J., Bonal, D., Domenach, A. M., Hérault, B., Patiño, S., Roggy, J. C., & Chave, J. (2010). Decoupled leaf and stem economics in rain forest trees. Ecology Letters, 13(11), 1338–1347. https://doi.org/10.1111/j.1461-0248.2010.01517.x

Bellard, C., Bertelsmeier, C., Leadley, P., Thuiller, W., & Courchamp, F. (2012). Impacts of climate change on the future of biodiversity. In *Ecology Letters* (Vol. 15, Issue 4, pp. 365–377). https://doi.org/10.1111/j.1461-0248.2011.01736.x

Bennett, A. C., Rodrigues de Sousa, T., Monteagudo-Mendoza, A., Esquivel-Muelbert, A., Morandi, P. S., Coelho de Souza, F., Castro, W., Duque, L. F., Flores Llampazo, G., Manoel dos Santos, R., Ramos, E., Vilanova Torre, E., Alvarez-Davila, E., Baker, T. R., Costa, F. R.

C., Lewis, S. L., Marimon, B. S., Schietti, J., Burban, B., … Phillips, O. L. (2023). Sensitivity of South American tropical forests to an extreme climate anomaly. *Nature Climate Change*. https://doi.org/10.1038/s41558-023-01776-4

Bonal, D., Burban, B., Stahl, C., Wagner, F., & Hérault, B. (2016). The response of tropical rainforests to drought—lessons from recent research and future prospects. *Annals of Forest Science*, *73*(1), 27–44. https://doi.org/10.1007/s13595-015-0522-5

Bonan, G. B. (2008). Forests and climate change: Forcings, feedbacks, and the climate benefits of forests. Science, 320(5882), 1444-1449. doi:10.1126/science.1155121

Boulton, C. A., Lenton, T. M., & Boers, N. (2022). Pronounced loss of Amazon rainforest resilience since the early 2000s. *Nature Climate Change*, *12*(3), 271–278. https://doi.org/10.1038/s41558-022-01287-8

Brando, P. M., D. C. Nepstad, E. A. Davidson, S. E. Trumbore, D. Ray, and P. Camargo (2008). Drought effects on litterfall, wood production and belowground carbon cycling in an Amazon forest: Results of a throughfall reduction experiment. Philos. Trans. R. Soc. London B Biol. Sci., 363(1498), 1839–1848.

Brienen, R. J. W., Phillips, O. L., Feldpausch, T. R., & et al. (2015). Long-term decline of the Amazon carbon sink. *Nature*, *519*(7543), 344–348. https://doi.org/10.1038/nature14283

Breshears, D. D., Myers, O. B., Meyer, C. W., Barnes, F. J., Zou, C. B., Allen, C. D., McDowell, N. G., & Pockman, W. T. (2009). Tree die-off in response to global change-type drought: mortality insights from a decade of plant water potential measurements. *Frontiers in Ecology and the Environment*, *7*(4), 185–189. https://doi.org/10.1890/080016

Brum, M. et al. (2019). Hydrological niche segregation defines forest structure and drought tolerance strategies in a seasonal Amazon forest. J. Ecol. 107, 318–333.

Cadotte, M. W., Carscadden, K., & Mirotchnick, N. (2011). Beyond species: Functional diversity and the maintenance of ecological processes and services. *Journal of Applied Ecology*, *48*(5), 1079–1087. https://doi.org/10.1111/j.1365-2664.2011.02048.x

Carmona, C. P., de Bello, F., Mason, N. W. H., & Lepš, J. (2016). Traits Without Borders: Integrating Functional Diversity Across Scales. *Trends in Ecology and Evolution*, *31*(5), 382–394. https://doi.org/10.1016/j.tree.2016.02.003

Carmona, C. P., Tamme, R., Pärtel, M., De Bello, F., Brosse, S., Capdevila, P., González, R. M., González-Suárez, M., Salguero-Gómez, R., Vásquez-Valderrama, M., & Toussaint, A. (2021). Erosion of global functional diversity across the tree of life. *Science Advances*, *7*(13), 1–13. https://doi.org/10.1126/sciadv.abf2675

Cavin, L., Mountford, E. P., Peterken, G. F., & Jump, A. S. (2013). Extreme drought alters competitive dominance within and between tree species in a mixed forest stand. *Functional Ecology*, *27*(6), 1424–1435. https://doi.org/10.1111/1365-2435.12126

Cernusak, L. a., Winter, K., Dalling, J. W., Holtum, J. a M., Jaramillo, C., Körner, C., Leakey, A. D. B., Norby, R. J., Poulter, B., Turner, B. L., & Wright, S. J. (2013). Tropical forest responses to increasing atmospheric CO2: Current knowledge and opportunities for future research. *Functional Plant Biology*, *40*, 531–551. https://doi.org/10.1071/FP12309

Chave, J., Condit, R., Muller-Landau, H. C., Thomas, S. C., Ashton, P. S., Bunyavejchewin, S., Co, L. L., Dattaraja, H. S., Davies, S. J., Esufali, S., Ewango, C. E. N., Feeley, K. J., Foster, R. B., Gunatilleke, N., Gunatilleke, S., Hall, P., Hart, T. B., Hernández, C., Hubbell, S. P., … Losos, E. C. (2008). Assessing evidence for a pervasive alteration in tropical tree communities. *PLoS Biology*, *6*(3), 0455–0462. https://doi.org/10.1371/journal.pbio.0060045

Chave, J., Coomes, D., Jansen, S., Lewis, S. L., Swenson, N. G., & Zanne, A. E. (2009). Towards a worldwide wood economics spectrum. *Ecology Letters*, *12*(4), 351–366. https://doi.org/10.1111/j.1461-0248.2009.01285.x

Choat, B., Brodribb, T. J., Brodersen, C. R., Duursma, R. A., López, R., & Medlyn, B. E. (2018). Triggers of tree mortality under drought. Nature, 558(7711), 531-539.

Ciemer, C., Boers, N., Hirota, M., Kurths, J., Müller-Hansen, F., Oliveira, R. S., & Winkelmann, R. (2019). Higher resilience to climatic disturbances in tropical vegetation exposed to more variable rainfall. *Nature Geoscience 2019 12:3*, *12*(3), 174–179. https://doi.org/10.1038/s41561-019-0312-z

Cole, L. E. S., Bhagwat, S. A., & Willis, K. J. (2014). Recovery and resilience of tropical forests after disturbance. Nature Communications, 5, 1– 7. https://doi.org/10.1038/ncomms4906

Corlett, R. T. (2011). Impacts of warming on tropical lowland rainforests. Trends in Ecology & Evolution, 26(11), 606-613. doi:10.1016/j.tree.2011.06.015

Corlett, R. T. (2016). The impacts of climate change in the tropics. Annual Review of Environment and Resources, 41, 501-518. doi:10.1146/annurev-environ-110615-085711

Cosme, L. H. M. et al. 2017. The importance of hydraulic architecture to the distribution patterns of trees in a central Amazonian forest. New Phytol. 215: 113–125.

Cox, P. M., Betts, R. a, Jones, C. D., Spall, S. a, & Totterdell, I. J. (2000). Acceleration of global warming due to carbon-cycle feedbacks in a coupled climate model. *Nature*, *408*(6809), 184–187. https://doi.org/10.1038/35041539

Cox et al., Increasing risk of Amazonian drought due to decreasing aerosol pollution. Nature 453, 212–215 (2008).

Cox, P. M., Pearson, D., Booth, B. B., Friedlingstein, P., Huntingford, C., Jones, C. D., & Luke, C. M. (2013). Sensitivity of tropical carbon to climate change constrained by carbon dioxide variability. Nature, 494(7437), 341–344.

https://doi.org/http://www.nature.com/nature/journal/v494/n7437/abs/nature11882.html#supplementary-information

da Costa, A. C. L., Galbraith, D., Almeida, S., Portela, B. T. T., da Costa, M., de Athaydes Silva Junior, J., Braga, A. P., de Gonçalves, P. H. L., de Oliveira, A. A., Fisher, R., Phillips, O. L., Metcalfe, D. B., Levy, P., & Meir, P. (2010). Effect of 7 yr of experimental drought on vegetation dynamics and biomass storage of an eastern Amazonian rainforest. *New Phytologist*, *187*(3), 579–591. https://doi.org/10.1111/j.1469-8137.2010.03309.x

Darela Filho, J. P. (2022). Modelagem dos impactos do aumento da concentração de CO2 e nutrientes sobre a composição funcional na floresta amazônica. Tese de Doutorado, Universidade Estadual Paulista "Júlio de Mesquita Filho", Instituto de Biociências, Rio Claro.

Dakos, V., Matthews, B., Hendry, A. P., Levine, J., Loeuille, N., Norberg, J., Nosil, P., Scheffer, M., & De Meester, L. (2019). Ecosystem tipping points in an evolving world. *Nature Ecology and Evolution*, *3*(3), 355–362. https://doi.org/10.1038/s41559-019-0797-2

de Bello, F., Lavorel, S., Hallett, L. M., Valencia, E., Garnier, E., Roscher, C., Conti, L., Galland, T., Goberna, M., Májeková, M., Montesinos-Navarro, A., Pausas, J. G., Verdú, M., E-Vojtkó, A., Götzenberger, L., & Lepš, J. (2021). Functional trait effects on ecosystem stability: assembling the jigsaw puzzle. Trends in Ecology & Evolution, 36(9), 822–836. https://doi.org/10.1016/j.tree.2021.05.001

Díaz, S., & Cabido, M. (2001). Vive la difference: plant functional diversity matters to ecosystem processes. *Proceedings. Biological Sciences / The Royal Society*, *16*(4), 646–655. http://rspb.royalsocietypublishing.org/content/278/1713/1894.abstract%5Cnhttp://www.ncbi.nlm.nih.gov/pubmed/19019785%5Cnhttp://www.pnas.org/content/100/13/7650.short

Díaz, S., Lavorel, S., de Bello, F., Quétier, F., Grigulis, K., & Robson, T. M. (2007). Incorporating plant functional diversity effects in ecosystem service assessments. Proceedings of the National Academy of Sciences of the United States of America, 104(52), 20684–20689. https://doi.org/10.1073/pnas.0704716104

Díaz, S., Purvis, A., Cornelissen, J. H. C., Mace, G. M., Donoghue, M. J., Ewers, R. M., Jordano, P., & Pearse, W. D. (2013). Functional traits, the phylogeny of function, and ecosystem service vulnerability. *Ecology and Evolution*, *3*(9), 2958–2975. https://doi.org/10.1002/ece3.601

Doughty, C. E., Malhi, Y., Araujo-Murakami, A., Metcalfe, D. B., Silva-Espejo, J. E., Arroyo, L., Heredia, J. P., Pardo-Toledo, E., Mendizabal, L. M., Rojas-Landivar, V. D., Vega-Martinez, M., Flores-Valencia, M., Sibler-Rivero, R., Moreno-Vare, L., Jessica Viscarra, L., Chuviru-Castro, T., Osinaga-Becerra, M., & Ledezma, R. (2014). Allocation trade-offs dominate the response of tropical forest growth to seasonal and interannual drought. Ecology, 95(8), 2192–2201. https://doi.org/10.1890/13-1507.1

Doughty, C. E., Metcalfe, D. B., Girardin, C. A. J., Amézquita, F. F., Cabrera, D. G., Huasco, W. H., Silva-Espejo, J. E., Araujo-Murakami, A., da Costa, M. C., Rocha, W., Feldpausch, T. R., Mendoza, A. L. M., da Costa, A. C. L., Meir, P., Phillips, O. L., & Malhi, Y. (2015). Drought impact on forest carbon dynamics and fluxes in Amazonia. *Nature*, *519*(7541), 78–82. https://doi.org/10.1038/nature14213

Duffy, P. B., Brando, P., Asner, G. P., & Field, C. B. (2015). Projections of future meteorological drought and wet periods in the Amazon. Proc. Natl. Acad. Sci. U.S.A. 112, 13172–13177

Egli, L., Weise, H., Radchuk, V., Seppelt, R., & Grimm, V. (2018). Exploring resilience with agent-based models: State of the art, knowledge gaps and recommendations for coping with multidimensionality. Ecological Complexity. 40 Part B, 1–7.

Elmqvist, T., Folke, C., Nyström, M., Peterson, G., Bengtsson, J., Walker, B., & Norberg, J. (2003). Response diversity, ecosystem change, and resilience. *Frontiers in Ecology and the Environment*, *1*(9), 488–494. https://doi.org/10.1890/1540-9295(2003)001[0488:RDECAR]2.0.CO;2

Enquist, B. J., & Enquist, C. A. F. (2011). Long-term change within a Neotropical forest: Assessing differential functional and floristic responses to disturbance and drought. *Global Change Biology*, *17*(3), 1408–1424. https://doi.org/10.1111/j.1365-2486.2010.02326.x

Esquivel-Muelbert, A., Baker, T. R., Dexter, K. G., Lewis, S. L., Brienen, R. J. W., Feldpausch, T. R., Lloyd, J., Monteagudo-Mendoza, A., Arroyo, L., Álvarez-Dávila, E., Higuchi, N., Marimon, B. S., Marimon-Junior, B. H., Silveira, M., Vilanova, E., Gloor, E., Malhi, Y., Chave, J., Barlow, J., … Phillips, O. L. (2018). Compositional response of Amazon forests to climate change. *Global Change Biology*, *June 2018*, 39–56. https://doi.org/10.1111/gcb.14413

Esquivel-Muelbert, A., Baker, T. R., Dexter, K. G., Lewis, S. L., Brienen, R. J. W., Feldpausch, T. R., Lloyd, J., Monteagudo-Mendoza, A., Arroyo, L., Álvarez-Dávila, E., Higuchi, N., Marimon, B. S., Marimon-Junior, B. H., Silveira, M., Vilanova, E., Gloor, E., Malhi, Y., Chave, J., Barlow, J., … Phillips, O. L. (2019). Compositional response of Amazon forests to climate change. Global Change Biology, 25(1), 39–56. https://doi.org/10.1111/gcb.14413

Esquivel-Muelbert, A., Baker, T. R., Dexter, K. G., Lewis, S. L., ter Steege, H., Lopez-Gonzalez, G., Monteagudo Mendoza, A., Brienen, R., Feldpausch, T. R., Pitman, N., Alonso, A., van der Heijden, G., Peña-Claros, M., Ahuite, M., Alexiaides, M., Álvarez Dávila, E., Murakami, A. A., Arroyo, L., Aulestia, M., … Phillips, O. L. (2017). Seasonal drought limits tree species across the Neotropics. *Ecography*, *40*(5), 618–629. https://doi.org/10.1111/ECOG.01904

Esquivel-Muelbert, A., Phillips, O. L., Brienen, R. J. W., Fauset, S., Sullivan, M. J. P., Baker, T. R., Chao, K. J., Feldpausch, T. R., Gloor, E., Higuchi, N., Houwing-Duistermaat, J., Lloyd, J., Liu, H., Malhi, Y., Marimon, B., Marimon Junior, B. H., Monteagudo-Mendoza, A., Poorter, L., Silveira, M., … Galbraith, D. (2020). Tree mode of death and mortality risk factors across Amazon forests. *Nature Communications*, *11*(1). https://doi.org/10.1038/s41467-020-18996-3

Esquivel-Muelbert, A., Baker, T. R., Dexter, K. G., Lewis, S. L., Brienen, R. J. W., Feldpausch, T. R., Lloyd, J., Monteagudo-Mendoza, A., Arroyo, L., Álvarez-Dávila, E., Higuchi, N., Marimon, B. S., Marimon-Junior, B. H., Silveira, M., Vilanova, E., Gloor, E., Malhi, Y., Chave, J., Barlow, J., … Phillips, O. L. (2019). Compositional response of Amazon forests to climate change. *Global Change Biology*, *25*(1), 39–56. https://doi.org/10.1111/gcb.14413

Fauset, S., Baker, T. R., Lewis, S. L., Feldpausch, T. R., Affum-Baffoe, K., Foli, E. G., Hamer, K. C., Swaine, M. D., & Etienne, R. (2012). Drought-induced shifts in the floristic and functional composition of tropical forests in Ghana. *Ecology Letters*. https://doi.org/10.1111/j.1461-0248.2012.01834.x

Feldpausch, T. R. et al. (2011). Height-diameter allometry of tropical forest trees. Biogeosciences 8: 1081–1106.

Feldpausch, T. R., Phillips, O. L., Brienen, R. J. W., Gloor, E., Lloyd, J., Lopez-Gonzalez, G., Monteagudo-Mendoza, A., Malhi, Y., Alarcón, A., Álvarez Dávila, E., Alvarez-Loayza, P., Andrade, A., Aragao, L. E. O. C., Arroyo, L., Aymard C., G. A., Baker, T. R., Baraloto, C., Barroso, J., Bonal, D., … Vos, V. A. (2016). Amazon forest response to repeated droughts. *Global Biogeochemical Cycles*, *30*(7), 964–982. https://doi.org/10.1002/2015GB005133

Ferreira, J., Lennox, G. D., Gardner, T. A., Thomson, J. R., Berenguer, E., Lees, A. C., Mac Nally, R., Aragão, L. E. O. C., Ferraz, S. F. B., Louzada, J., Moura, N. G., Oliveira, V. H. F., Pardini, R., Solar, R. R. C., Vieira, I. C. G., & Barlow, J. (2018). Carbon-focused conservation may fail to protect the most biodiverse tropical forests. *Nature Climate Change*. https://doi.org/10.1038/s41558-018-0225-7

Ferry, B. et al. 2010. Higher treefall rates on slopes and waterlogged soils result in lower stand biomass and productivity in a tropical rain forest. J. Ecol. 98: 106–116.

Fisher RA, Williams M, Da Costa AL, Malhi Y, da Costa RF, Almeida S, Meir P (2007) The response of an Eastern Amazonian rain forest to drought stress: results and modelling analyses from a throughfall exclusion experiment. Glob Change Biol 13:2361–2378

Fisher, R., McDowell, N., Purves, D., Moorcroft, P., Sitch, S., Cox, P., Huntingford, C., Meir, P., & Ian Woodward, F. (2010). Assessing uncertainties in a second-generation dynamic vegetation model caused by ecological scale limitations. *New Phytologist*, *187*(3), 666–681. https://doi.org/10.1111/j.1469-8137.2010.03340.x

Flores, B. M., Montoya, E., Sakschewski, B., Nascimento, N., Staal, A., Betts, R. A., Levis, C., Lapola, D. M., Esquível-Muelbert, A., Jakovac, C., Nobre, C. A., Oliveira, R. S., Borma, L. S., Nian, D., Boers, N., Hecht, S. B., ter Steege, H., Arieira, J., Lucas, I. L., … Hirota, M.

(2024). Critical transitions in the Amazon forest system. *Nature*, *626*(7999), 555–564. https://doi.org/10.1038/s41586-023-06970-0

Forzieri, G., Dakos, V., McDowell, N. G., Ramdane, A., & Cescatti, A. (2022). Emerging signals of declining forest resilience under climate change. *Nature, 608*(7923), 534–539. https://doi.org/10.1038/s41586-022-04959-9

Friedlingstein P, Cox P, Betts R et al. (2006) Climate – carbon cycle feedback analysis: results from the C4MIP model intercom- parison. Journal of Climate, 14, 3337–3353.

Fu, R., Yin, L., Li, W., Arias, P. A., Dickinson, R. E., Huang, L., ... & Myneni, R. B. (2013). Increased dry-season length over southern Amazonia in recent decades and its implication for future climate projection. Proceedings of the National Academy of Sciences, 110(45), 18110-18115.

Fyllas, N. M., Gloor, E., Mercado, L. M., Sitch, S., Quesada, C. a., Domingues, T. F., Galbraith, D. R., Torre-Lezama, A., Vilanova, E., Ramírez-Angulo, H., Higuchi, N., Neill, D. a., Silveira, M., Ferreira, L., Aymard C., G. a., Malhi, Y., Phillips, O. L., & Lloyd, J. (2014). Analysing Amazonian forest productivity using a new individual and trait-based model (TFS v.1). *Geoscientific Model Development*, *7*, 1251–1269. https://doi.org/10.5194/gmd-7-1251-2014

Gatti, L. V, Gloor, M., Miller, J. B., Doughty, C. E., Malhi, Y., Domingues, L. G., Basso, L. S., Martinewski, a, Correia, C. S. C., Borges, V. F., Freitas, S., Braz, R., Anderson, L. O., Rocha, H., Grace, J., Phillips, O. L., & Lloyd, J. (2014). Drought sensitivity of Amazonian carbon balance revealed by atmospheric measurements. Nature, 506(7486), 76–80. https://doi.org/10.1038/nature12957

Gloor M, Brienen RJW, Galbraith D, Feldpausch TR, Schöngart J, Guyot JL, Espinoza JC, Lloyd J, Phillips OL (2013) Intensification of the Amazon hydrological cycle over the last two decades. Geophys Res Lett 40:1729–1733

González-M., R., Posada, J. M., Carmona, C. P., Garzón, F., Salinas, V., Idárraga-Piedrahita, Á., Pizano, C., Avella, A., López-Camacho, R., Norden, N., Nieto, J., Medina, S. P., Rodríguez-M., G. M., Franke-Ante, R., Torres, A. M., Jurado, R., Cuadros, H., Castaño-Naranjo, A., García, H., & Salgado-Negret, B. (2021). Diverging functional strategies but high sensitivity to an extreme drought in tropical dry forests. *Ecology Letters*, *24*(3), 451–463. https://doi.org/10.1111/ELE.13659

Grime, J.P., 1998. Benefits of plant diversity to ecosystems: immediate, filter and founder effects. J. Ecol. 86 (6), 902–910. https://doi.org/10.1046/j.1365-2745.1998.00306. x.

Gupta, A., Rico-Medina, A., & Caño-Delgado, A. I. (2020). The physiology of plant responses to drought. Science, 368(6488), 266-269.

Hacke, U. G. et al. 2001. Trends in wood density and structure are linked to prevention of xylem implosion by negative pressure. Oecologia 126: 457–461.

Hare, B., & Meinshausen, M. (2006). How much warming are we committed to and how much can be avoided? In *Climatic Change* (Vol. 75, Issues 1–2). https://doi.org/10.1007/s10584-005-9027-9

Hartmann, H. (2015). Carbon starvation during drought-induced tree mortality – are we chasing a myth?. Journal of Plant Hydraulics, 2, e005.

Harris PP, Huntingford C, Gash JHC, Hodnett MG, Cox PM, Malhi Y, Araujo AC (2004) Calibration of a land-surface model using data from primary forest sites in Amazonia. Theoretical and Applied Climatology, 78, 27–45

Hirota, M., Holmgren, M., Van Nes, E. H., & Scheffer, M. (2011). Global resilience of tropical forest and savanna to critical transitions. *Science*, *334*(6053), 232–235. https://doi.org/10.1126/science.1210657

Hoeber S, Leuschner C, K€oler L, Arias-Aguilar D, Schuldt B. (2014). The importance ofhydraulic conductivityand wood density to growth performance in eight tree species from a tropical semi-dry climate. ForestEcologyandManagement 330: 126–136.

Holling, C. S. (1973). Resilience and stability of ecological systems. Annual Review of Ecology and Systematics, 4, 1–23. https://doi.org/10.1146/annur ev.es.04.110173.000245

Holling, C. S., & Gunderson, L. H. (2002). Resilience and adaptive cycles. In L. H. Gunderson & C. S. Holling (Eds.), Panarchy: Understanding the transformations in human and natural systems (pp. 25–62). Island Press.

Holzwarth, F., Rüger, N., & Wirth, C. (2015). Taking a closer look: Disentangling effects of functional diversity on ecosystem functions with a trait-based model across hierarchy and time. *Royal Society Open Science*, *2*(3). https://doi.org/10.1098/rsos.140541

Hu, Z., Dakos, V., & Rietkerk, M. (2022). Using functional indicators to detect state changes in terrestrial ecosystems. Trends in Ecology & Evolution, 37(12), 1036–1045. https://doi.org/10.1016/j.tree.2022.07.011

Hubau, W., Lewis, S. L., Phillips, O. L., Affum-Baffoe, K., Beeckman, H., Cuní-Sanchez, A., Daniels, A. K., Ewango, C. E. N., Fauset, S., Mukinzi, J. M., Sheil, D., Sonké, B., Sullivan, M. J. P., Sunderland, T. C. H., Taedoumg, H., Thomas, S. C., White, L. J. T., Abernethy, K. A., Adu-Bredu, S., … Zemagho, L. (2020). Asynchronous carbon sink saturation in African and Amazonian tropical forests. *Nature*, *579*(7797), 80–87. https://doi.org/10.1038/s41586-020-2035-0

Huete AR, Didan K, Shimabukuro YE, Ratana P, Saleska SR, Hutyra LR, Yang W, Nemani RR, Myneni R (2006) Amazon rainforests green- up with sunlight in dry season. Geophys Res Lett 33:L06405. doi: 10.1029/2005GL025583

Huntingford, C., Fisher, R. A., Mercado, L., Booth, B. B. B., Sitch, S., Harris, P. P., Cox, P. M., Jones, C. D., Betts, R. A., Malhi, Y., Harris, G. R., Collins, M., & Moorcroft, P. (2008). Towards quantifying uncertainty in predictions of Amazon “dieback.” *Philosophical*

Transactions of the Royal Society B: Biological Sciences, *363*(1498), 1857–1864. https://doi.org/10.1098/rstb.2007.0028

Huntingford, C., Zelazowski, P., Galbraith, D., Mercado, L. M., Sitch, S., Fisher, R., Lomas, M., Walker, A. P., Jones, C. D., Booth, B. B. B., Malhi, Y., Hemming, D., Kay, G., Good, P., Lewis, S. L., Phillips, O. L., Atkin, O. K., Lloyd, J., Gloor, E., … Cox, P. M. (2013). Simulated resilience of tropical rainforests to CO2-induced climate change. *Nature Geoscience*, *6*(4), 268–273. https://doi.org/10.1038/ngeo1741

Levine, N. M., Zhang, K., Longo, M., Baccini, A., Phillips, O. L., Lewis, S. L., Alvarez-Dávila, E., Segalin de Andrade, A. C., Brienen, R. J. W., Erwin, T. L., Feldpausch, T. R., Monteagudo Mendoza, A. L., Nuñez Vargas, P., Prieto, A., Silva-Espejo, J. E., Malhi, Y., & Moorcroft, P. R. (2016). Ecosystem heterogeneity determines the ecological resilience of the Amazon to climate change. *Proceedings of the National Academy of Sciences*, *113*(3), 793–797. https://doi.org/10.1073/pnas.1511344112

Jones, C., Lowe, J., Liddicoat, S., & Betts, R. (2009). Committed terrestrial ecosystem changes due to climate change. *Nature Geoscience*, *2*(7), 484–487. https://doi.org/10.1038/ngeo555

Johnson, M. O., Galbraith, D., Gloor, M., De Deurwaerder, H., Guimberteau, M., Rammig, A., Thonicke, K., Verbeeck, H., von Randow, C., Monteagudo, A., Phillips, O. L., Brienen, R. J. W., Feldpausch, T. R., Lopez Gonzalez, G., Fauset, S., Quesada, C. A., Christoffersen, B., Ciais, P., Sampaio, G., … Baker, T. R. (2016). Variation in stem mortality rates determines patterns of above-ground biomass in Amazonian forests: Implications for dynamic global vegetation models. Global Change Biology, 44, 1–18. https://doi.org/10.1111/gcb.13315

Kannenberg, S. A., Schwalm, C. R., & Anderegg, W. R. L. (2020). Ghosts of the past: how drought legacy effects shape forest functioning and carbon cycling. *Ecology Letters*, *23*(5), 891–901. https://doi.org/10.1111/ele.13485

Keane, R. E., Hessburg, P. F., Landres, P. B., & Swanson, F. J. (2009). The use of historical range and variability (HRV) in landscape management. Forest Ecology and Management, 258, 1025–1037. https://doi.org/10.1016/j.foreco.2009.05.035

Köpp Hollunder, R., Garbin, M. L., Rubio Scarano, F., & Mariotte, P. (2022). Regional and local determinants of drought resilience in tropical forests. In *Ecology and Evolution* (Vol. 12, Issue 5). https://doi.org/10.1002/ece3.8943

Kraft, N. J. B. et al. 2008. Functional traits and niche-based tree community assembly in an Amazonian forest. Science 322: 580–582.

Laurance, W.F. & Peres, C.A. (eds.) (2006). Emerging Threats to Tropical Forests. The University of Chicago Press, Chicago.

Levine, N. M., Zhang, K., Longo, M., Baccini, A., Phillips, O. L., Lewis, S. L., Alvarez-Dávila, E., Segalin de Andrade, A. C., Brienen, R. J. W., Erwin, T. L., Feldpausch, T. R., Monteagudo Mendoza, A. L., Nuñez Vargas, P., Prieto, A., Silva-Espejo, J. E., Malhi, Y., & Moorcroft, P.

R. (2016). Ecosystem heterogeneity determines the ecological resilience of the Amazon to climate change. *Proceedings of the National Academy of Sciences*, *113*(3), 793–797. https://doi.org/10.1073/pnas.1511344112

Lewis, S.L., Lopez-Gonzalez, G., Sonke´, B., Affum-Baffoe, K., Baker, T.R., Ojo, L.O. et al. (2009). Increasing carbon storage in intact African tropical forests. Nature, 457, 1003–1006.

Lin, Y. S., Medlyn, B. E., Duursma, R. A., Prentice, I. C., Wang, H., Baig, S., ... & Wingate, L. (2015). Optimal stomatal behaviour around the world. Nature Climate Change, 5(5), 459-464.

Liu, Y., Kumar, M., Katul, G. G., & Porporato, A. (2019). Reduced resilience as an early warning signal of forest mortality. *Nature Climate Change*, *9*(11), 880–885. https://doi.org/10.1038/s41558-019-0583-9

Malhi, Y. & Wright, J. (2004). Spatial patterns and recent trends in the climate of tropical rainforest regions. Philos. T. Roy. Soc. B, 359, 311–329.

Malhi, Y., & Phillips, O. L. (2004). Tropical forests and global atmospheric change: A synthesis. *Philosophical Transactions of the Royal Society B: Biological Sciences*, *359*(1443), 549–555. https://doi.org/10.1098/rstb.2003.1449

Malhi, Y., Roberts, J. T., Betts, R. A., Killeen, T. J., Li, W., & Nobre, C. A. (2008). Climate change, deforestation, and the fate of the Amazon. Science, 319(5860), 169-172. doi:10.1126/science.1146961

Malhi, Y., Aragao, L. E. O. C., Galbraith, D., Huntingford, C., Fisher, R., Zelazowski, P., Sitch, S., McSweeney, C., & Meir, P. (2009). Exploring the likelihood and mechanism of a climate-change-induced dieback of the Amazon rainforest. *Proceedings of the National Academy of Sciences*, *106*(49), 20610–20615. https://doi.org/10.1073/pnas.0804619106

Malhi, Y., Doughty, C., & Galbraith, D. (2011). The allocation of ecosystem net primary productivity in tropical forests. *Philosophical Transactions of the Royal Society B: Biological Sciences*, *366*(1582), 3225–3245. https://doi.org/10.1098/rstb.2011.0062

Malhi, Y., Gardner, T. A., Goldsmith, G. R., Silman, M. R., & Zelazowski, P. (2014). Tropical forests in the Anthropocene. Annual Review of Environment and Resources, 39, 125-159. doi:10.1146/annurev-environ-030713-155141

Manning, P., Van Der Plas, F., Soliveres, S., Allan, E., Maestre, F. T., Mace, G., Whittingham, M. J., & Fischer, M. (2018). Redefining ecosystem multifunctionality. *Nature Ecology and Evolution*, *2*(3), 427–436. https://doi.org/10.1038/s41559-017-0461-7

Marengo, J. A., Souza, C. M., Thonicke, K., Burton, C., Halladay, K., Betts, R. A., Alves, L. M., & Soares, W. R. (2018). Changes in Climate and Land Use Over the Amazon Region: Current and Future Variability and Trends. In Frontiers in Earth Science (Vol. 6, p. 228). Frontiers Media S.A. https://doi.org/10.3389/feart.2018.00228

Marengo, J. A., Tomasella, J., Alves, L. M., Soares, W. R., & Rodriguez, D. A. (2011). The drought of 2010 in the context of historical droughts in the Amazon region. *Geophysical Research Letters*, *38*(12). https://doi.org/10.1029/2011GL047436

Marengo, J. A., Tomasella, J., Soares, W. R., Alves, L. M., & Nobre, C. A. (2012). Extreme climatic events in the Amazon basin. *Theoretical and Applied Climatology*, *107*(1–2), 73–85. https://doi.org/10.1007/s00704-011-0465-1

Marca-Zevallos, M. J., Moulatlet, G. M., Sousa, T. R., Schietti, J., Coelho, L. de S., Ramos, J. F., Lima Filho, D. de A., Amaral, I. L., de Almeida Matos, F. D., Rincón, L. M., Cardenas Revilla, J. D., Pansonato, M. P., Gribel, R., Barbosa, E. M., Miranda, I. P. de A., Bonates, L. C. de M., Guevara, J. E., Salomão, R. P., Ferreira, L. V., … Costa, F. R. C. (2022). Local hydrological conditions influence tree diversity and composition across the Amazon basin. Ecography, 2022(11). https://doi.org/10.1111/ecog.06125

Markewitz D, Devine S, Davidson E, Brando PM, Nepstad DC (2010) Soil moisture depletion under simulated drought in the Amazon: impacts on deep root uptake. New Phytol 187:592–607

McDowell, N. G., Allen, C. D., Anderson-Teixeira, K., Aukema, B. H., Bond-Lamberty, B., Chini, L., ... & Williams, A. P. (2020). "Pervasive shifts in forest dynamics in a changing world." Science, 368(6494), eaaz9463.

McDowell, N. G., Fisher, R. A., Xu, C., Domec, J., Hölttä, T., Mackay, D. S., ... & Middleton, R. S. (2013). Evaluating theories of drought-induced vegetation mortality using a multimodel-experiment framework. New Phytologist, 200(2), 304-321.

Meir, P. et al. (2015). Threshold responses to soil moisture deficit by trees and soil in tropical rain forests: Insights from field experiments. Bioscience 65, 882–892.

Mori, A. S., Furukawa, T., & Sasaki, T. (2013). Response diversity determines the resilience of ecosystems to environmental change. Biological Reviews, 88(2), 349–364. https://doi.org/10.1111/brv.12004

Mouillot, D., Villéger, S., Scherer-Lorenzen, M., & Mason, N. W. H. (2011). Functional structure of biological communities predicts ecosystem multifunctionality. *PLoS ONE*, *6*(3). https://doi.org/10.1371/journal.pone.0017476

Mitchell, P. J., O'Grady, A. P., Pinkard, E. A., Brodribb, T. J., Arndt, S. K., Blackman, C. J., Duursma, R. A., Fensham, R. J., Hilbert, D. W., Nitschke, C. R., Norris, J., Roxburgh, S. H., Ruthrof, K. X., & Tissue, D. T. (2016). An ecoclimatic framework for evaluating the resilience of vegetation to water deficit. Global Change Biology, 22(5), 1677– 1689. https://doi.org/10.1111/gcb.13177

Müller, L. M., & Bahn, M. (2022). Drought legacies and ecosystem responses to subsequent drought. *Global Change Biology*, *28*(17), 5086–5103. https://doi.org/10.1111/gcb.16270

Nepstad DC, De Carvalho CR, Davidson EA, Jipp PH, Lefebvre PA, Negreiros GH, Da Silva ED, Stone TA, Trumbore SE, Vieira S (1994) The role of deep roots in the hydrological and carbon cycles of Amazonian forests and pastures. Nature 372:666–669

Nepstad, D. C., Tohver, I. M., Ray, D., Moutinho, P., & Cardinot, G. (2007). Mortality of large trees and lianas following experimental drought in an amazon forest. Ecological Society of America, 88(9), 2259–2269. https://doi.org/10.1038/aps.2015.36

Niinemets Ü (2010) Responses of forest trees to single and multiple environmental stresses from seedlings to mature plants: past stress history, stress interactions, tolerance and acclimation. For Ecol Manag 260:1623–1639

O'Brien, M. J., Leuzinger, S., Philipson, C. D., Tay, J., & Hector, A. (2014). Drought survival of tropical tree seedlings enhanced by non-structural carbohydrate levels. Nature Climate Change, 4(8), 710-714.

Oliveira, R. S., Christoffersen, B. O., de V. Barros, F., Teodoro, G. S., Bittencourt, P., Brum-Jr, M. M., & Viani, R. A. G. (2014). Changing precipitation regimes and the water and carbon economies of trees. In *Theoretical and Experimental Plant Physiology* (Vol. 26, Issue 1, pp. 65–82). https://doi.org/10.1007/s40626-014-0007-1

Oliveira, R. S., Costa, F. R. C., van Baalen, E., de Jonge, A., Bittencourt, P. R., Almanza, Y., Barros, F. de V., Cordoba, E. C., Fagundes, M. V., Garcia, S., Guimaraes, Z. T. M., Hertel, M., Schietti, J., Rodrigues-Souza, J., & Poorter, L. (2019). Embolism resistance drives the distribution of Amazonian rainforest tree species along hydro-topographic gradients. New Phytologist, 221(3), 1457–1465. https://doi.org/10.1111/NPH.15463

Oliveira, R. S., Eller, C. B., Barros, F. de V., Hirota, M., Brum, M., & Bittencourt, P. (2021). Linking plant hydraulics and the fast-slow continuum to understand resilience to drought in tropical ecosystems. The New Phytologist, 230(3), 904–923. https://doi.org/10.1111/NPH.17266

Parsons, L. (2020). Implications of CMIP6 projected drying trends for 21st century Amazonian drought risk. Earth’s Futur. 8, e2020EF001608.

Sala, A., Woodruff, D. R., & Meinzer, F. C. (2012). Carbon dynamics in trees: feast or famine? Tree Physiology, 32(6), 764-775.

Sala, A., Piper, F., & Hoch, G. (2010). Physiological mechanisms of drought-induced tree mortality are far from being resolved. New Phytologist, 186(2), 274-281.

Scheiter, S., Langan, L., & Higgins, S. I. (2013). Next-generation dynamic global vegetation models: learning from community ecology. In The New phytologist (Vol. 198, Issue 3, pp. 957–969). https://doi.org/10.1111/nph.12210

Pavlick, R., Drewry, D. T., Bohn, K., Reu, B., & Kleidon, A. (2013). The Jena Diversity-Dynamic Global Vegetation Model (JeDi-DGVM): a diverse approach to representing terrestrial biogeography and biogeochemistry based on plant functional trade-offs. Biogeosciences, 10(6), 4137–4177. https://doi.org/10.5194/bg-10-4137-2013

Phillips OL, Malhi Y, Higuchi N, Laurance WF, Nunez PV, et al. (1998) Changes in the carbon balance of tropical forests: evidence from long-term plots. Science 282: 439–442.

Phillips, O. L., Aragão, L. E. O. C., Lewis, S. L., Fisher, J. B., Lloyd, J., López-González, G., Malhi, Y., Monteagudo, A., Peacock, J., Quesada, C. A., Van Der Heijden, G., Almeida, S., Amaral, I., Arroyo, L., Aymard, G., Baker, T. R., Bánki, O., Blanc, L., Bonal, D., … Torres-Lezama, A. (2009). Drought sensitivity of the amazon rainforest. *Science*, *323*(5919), 1344–1347. https://doi.org/10.1126/SCIENCE.1164033

Poorter, L., van der Sande, M. T., Thompson, J., Arets, E. J. M. M., Alarcón, A., Álvarez-Sánchez, J., Ascarrunz, N., Balvanera, P., Barajas-Guzmán, G., Boit, A., Bongers, F., Carvalho, F. A., Casanoves, F., Cornejo-Tenorio, G., Costa, F. R. C., de Castilho, C. V., Duivenvoorden, J. F., Dutrieux, L. P., Enquist, B. J., … Peña-Claros, M. (2015). Diversity enhances carbon storage in tropical forests. *Global Ecology and Biogeography*, *24*(11), 1314–1328. https://doi.org/10.1111/geb.12364

Poorter, L., Bongers, F., Aide, T. M., Almeyda Zambrano, A. M., Balvanera, P., Becknell, J. M., Boukili, V., Brancalion, P. H. S., Broadbent, E. N., Chazdon, R. L., Craven, D., de Almeida-Cortez, J. S., Cabral, G. A. L., de Jong, B. H. J., Denslow, J. S., Dent, D. H., DeWalt, S. J., Dupuy, J. M., Durán, S. M., … Rozendaal, D. M. A. (2016). Biomass resilience of Neotropical secondary forests. *Nature*, *530*(7589), 211–214. https://doi.org/10.1038/nature16512

Poulter, B., Hattermann, F., Hawkins, E., Zaehle, S., Sitch, S., Restrepo-Coupe, N., Heyder, U., & Cramer, W. (2010). Robust dynamics of Amazon dieback to climate change with perturbed ecosystem model parameters. *Global Change Biology*, *16*(9), 2476–2495. https://doi.org/10.1111/j.1365-2486.2009.02157.x

Rammig, A., Jupp, T., Thonicke, K., Tietjen, B., Heinke, J., Ostberg, S., Lucht, W., Cramer, W., & Cox, P. (2010). Estimating the risk of Amazonian forest dieback. *New Phytologist*, *187*(3), 694–706. https://doi.org/10.1111/j.1469-8137.2010.03318.x

Ratajczak, Z., Carpenter, S. R., Ives, A. R., Kucharik, C. J., Ramiadantsoa, T., Stegner, M. A., Williams, J. W., Zhang, J., & Turner, M. G. (2018). Abrupt change in ecological systems: Inference and diagnosis. Trends in Ecology and Evolution, 33, 513–526. https://doi.org/10.1016/j.tree.2018.04.013

Reich, P. B. (2014). The world-wide “fast-slow” plant economics spectrum: A traits manifesto. *Journal of Ecology*, *102*(2), 275–301. https://doi.org/10.1111/1365-2745.12211

Reiss, J., Bridle, J. R., Montoya, J. M., & Woodward, G. (2009). Emerging horizons in biodiversity and ecosystem functioning research. *Trends in Ecology and Evolution*, *24*(9), 505–514. https://doi.org/10.1016/j.tree.2009.03.018

Reu, B., Proulx, R., Bohn, K., Dyke, J. G., Kleidon, A., Pavlick, R., & Schmidtlein, S. (2011). The role of climate and plant functional trade-offs in shaping global biome and biodiversity patterns. Global Ecology and Biogeography, 20(4), 570–581. https://doi.org/10.1111/j.1466-8238.2010.00621.x

Rius, B. F., Filho, J. P. D., Fleischer, K., Hofhansl, F., Blanco, C. C., Rammig, A., Domingues, T. F., & Lapola, D. M. (2023). Higher functional diversity improves modeling of Amazon forest carbon storage. Ecological Modelling, 481(March 2022), 110323. https://doi.org/10.1016/j.ecolmodel.2023.110323

Ruiz-Vásquez, M. et al. (2020) Effects of Amazon basin deforestation on regional atmospheric circulation and water vapor transport towards tropical South America. Clim. Dyn., v. 54, p. 4169–4189.

Rowland, L., da Costa, A. C. L., Galbraith, D. R., Oliveira, R. S., Binks, O. J., Oliveira, A. A. R., Pullen, A. M., Doughty, C. E., Metcalfe, D. B., Vasconcelos, S. S., Ferreira, L. V., Malhi, Y., Grace, J., Mencuccini, M., & Meir, P. (2015). Death from drought in tropical forests is triggered by hydraulics not carbon starvation. *Nature*, 1–13. https://doi.org/10.1038/nature15539

Ryan, M. G. (1991a). A simple method for estimating gross carbon budgets for vegetation in forest ecosystems. Tree Physiology, 9(1_2), 255–266. https://doi.org/10.1093/treephys/9.1-2.255

Ryan, M. G. (1991b). Effects of Climate Change on Plant Respiration, 1(2), 157–167.

Saatchi, S., Asefi-Najafabady, S., Malhi, Y., Aragão, L. E. O. C., Anderson, L. O., Myneni, R. B., & Nemani, R. (2013). Persistent effects of a severe drought on Amazonian forest canopy. *Proceedings of the National Academy of Sciences of the United States of America*, *110*(2), 565–570. https://doi.org/10.1073/PNAS.1204651110/SUPPL_FILE/PNAS.201204651SI.PDF

Saatchi, S., Longo, M., Xu, L., Yang, Y., Abe, H., André, M., Aukema, J. E., Carvalhais, N., Cadillo-Quiroz, H., Cerbu, G. A., Chernela, J. M., Covey, K., Sánchez-Clavijo, L. M., Cubillos, I. V., Davies, S. J., De Sy, V., De Vleeschouwer, F., Duque, A., Sybille Durieux, A. M., … Elmore, A. C. (2021). Detecting vulnerability of humid tropical forests to multiple stressors. *One Earth*, *4*(7), 988–1003. https://doi.org/10.1016/j.oneear.2021.06.002

Sakschewski, B., von Bloh, W., Boit, A., Rammig, A., Kattge, J., Poorter, L., Pe??uelas, J., & Thonicke, K. (2015). Leaf and stem economics spectra drive diversity of functional plant traits in a dynamic global vegetation model. Global Change Biology, 2711–2725. https://doi.org/10.1111/gcb.12870

Sakschewski, B., von Bloh, W., Boit, A., Poorter, L., Peña-Claros, M., Heinke, J., Joshi, J., & Thonicke, K. (2016). Resilience of Amazon forests emerges from plant trait diversity. *Nature Climate Change*, *1*(August). https://doi.org/10.1038/nclimate3109

Saleska SR, Didan K, Huete AR, da Rocha HR (2007) Amazon forests green-up during 2005 drought. Science (80) 318 612

Samanta A, Ganguly S, Hashimoto H, Devadiga S, Vermote E, Knyazikhin Y, Nemani RR, Myneni RB (2010) Amazon forests did not green-up during the 2005 drought. Geophys Res Lett 37: L05401. doi:10.1029/2009GL042154

Scheiter, S., Kumar, D., Pfeiffer, M., & Langan, L. (2024). Modeling drought mortality and resilience of savannas and forests in tropical Asia. *Ecological Modelling*, *494*(May), 110783. https://doi.org/10.1016/j.ecolmodel.2024.110783

Scheiter, S., Langan, L., & Higgins, S. I. (2013). Next-generation dynamic global vegetation models: learning from community ecology. In *The New phytologist* (Vol. 198, Issue 3, pp. 957–969). https://doi.org/10.1111/nph.12210

Schmitt, S., Maréchaux, I., Chave, J., Fischer, F., Piponiot, C., Traissac, S., & Hérault, B. (2019). Functional diversity improves tropical forest resilience: insights from a long-term virtual experiment. In *Journal of Ecology*. https://doi.org/10.1111/1365-2745.13320

Scheffer M. 2009. Critical Transitions in Nature and Society. Princeton, NJ: Princeton Univ. Press

Scheffer, M., Carpenter, S. R., Dakos, V., & Van Nes, E. H. (2015). Generic Indicators of Ecological Resilience: Inferring the Chance of a Critical Transition. Https://Doi.Org/10.1146/Annurev-Ecolsys-112414-054242, 46, 145–167. https://doi.org/10.1146/ANNUREV-ECOLSYS-112414-054242

Schmitt, S., Maréchaux, I., Chave, J., Fischer, F. J., Piponiot, C., Traissac, S., & Hérault, B. (2020). Functional diversity improves tropical forest resilience: Insights from a long-term virtual experiment. Journal of Ecology, 108(3), 831–843. https://doi.org/10.1111/1365-2745.13320

Seddon, A. W. R., Macias-Fauria, M., Long, P. R., Benz, D., & Willis, K. J. (2016). Sensitivity of global terrestrial ecosystems to climate variability. *Nature*, 1–15. https://doi.org/10.1038/nature16986

Seidl, R., Rammer, W., & Spies, T. A. (2014). Disturbance legacies increase the resilience of forest ecosystem structure, composition, and functioning. Ecological Applications, 24, 2063–2077. https://doi.org/10.1890/14-0255.1

Silva, C. E., Kellner, J. R., Clark, D. B., & Clark, D. A. (2013). Response of an old- growth tropical rainforest to transient high temperature and drought. Global Change Biology, 19(11), 3423– 3434. https://doi. org/10.1111/gcb.12312

Sitch, S., Huntingford, C., Gedney, N., Levy, P. E., Lomas, M., Piao, S. L., Betts, R., Ciais, P., Cox, P., Friedlingstein, P., Jones, C. D., Prentice, I. C., & Woodward, F. I. (2008). Evaluation of the terrestrial carbon cycle, future plant geography and climate-carbon cycle feedbacks using five Dynamic Global Vegetation Models (DGVMs). *Global Change Biology*, *14*(9), 2015–2039. https://doi.org/10.1111/j.1365-2486.2008.01626.x

Sitch, S., Smith, B., Prentice, I. C., Arneth, A., Bondeau, A., Cramer, W., Kaplan, J. O., Levis, S., Lucht, W., Sykes, M. T., Thonicke, K., & Venevsky, S. (2003). Evaluation of ecosystem dynamics, plant geography and terrestrial carbon cycling in the LPJ dynamic global vegetation model. In *Global Change Biology* (Vol. 9, Issue 2, pp. 161–185). https://doi.org/10.1046/j.1365-2486.2003.00569.x

Staal, A., Tuinenburg, O. A., Bosmans, J. H. C., Holmgren, M., Van Nes, E. H., Scheffer, M., Zemp, D. C., & Dekker, S. C. (2018). Forest-rainfall cascades buffer against drought across the Amazon. *Nature Climate Change 2018 8:6*, *8*(6), 539–543. https://doi.org/10.1038/s41558-018-0177-y

Stahl C, Burban B, Wagner F, Goret JY, Bompy F, Bonal D (2013) Influence of seasonal variations in soil water availability on gas exchange of tropical canopy trees. Biotropica 45:155–164

Swann, A. L. et al. (2015). Future deforestation in the Amazon and consequences for South American climate. Agric. For. Meteorol., v. 214, p. 12–24.

Townsend AR, Asner GP, Cleveland CC (2008) The biogeochemical heterogeneity of tropical forests. Trends in Ecology & Evolution, 23, 424–431

Umaña, M. N., Salgado-Negret, B., Norden, N., Salinas, V., Garzón, F., Medina, S. P., Rodríguez-M, G. M., López-Camacho, R., Castaño-Naranjo, A., Cuadros, H., Franke-Ante, R., Avella, A., Idárraga-Piedrahita, Á., Jurado, R., Nieto, J., Pizano, C., Torres, A. M., García, H., & González-M, R. (2023). Upscaling the effect of traits in response to drought: The relative importance of safety–efficiency and acquisitive–conservation functional axes. *Ecology Letters*, *September*, 2098–2109. https://doi.org/10.1111/ele.14328

van Bodegom, P. M., Douma, J. C., & Verheijen, L. M. (2014). A fully traits-based approach to modeling global vegetation distribution. *Proceedings of the National Academy of Sciences*, *111*(38), 13733–13738. https://doi.org/10.1073/pnas.1304551110

Van Bodegom, P. M., Douma, J. C., Witte, J. P. M., Ordoñez, J. C., Bartholomeus, R. P., & Aerts, R. (2012). Going beyond limitations of plant functional types when predicting global ecosystem-atmosphere fluxes: Exploring the merits of traits-based approaches. *Global Ecology and Biogeography*, *21*, 625–636. https://doi.org/10.1111/j.1466-8238.2011.00717.x

Van der Molen, M. K., Dolman, a. J., Ciais, P., Eglin, T., Gobron, N., Law, B. E., Meir, P., Peters, W., Phillips, O. L., Reichstein, M., Chen, T., Dekker, S. C., Doubková, M., Friedl, M. a., Jung, M., van den Hurk, B. J. J. M., de Jeu, R. a M., Kruijt, B., Ohta, T., … Wang, G. (2011). Drought and ecosystem carbon cycling. *Agricultural and Forest Meteorology*, *151*(7), 765–773. https://doi.org/10.1016/j.agrformet.2011.01.018

Van Passel, J., de Keersmaecker, W., Bernardino, P. N., Jing, X., Umlauf, N., Van Meerbeek, K., & Somers, B. (2022). Climatic legacy effects on the drought response of the Amazon rainforest. *Global Change Biology*, *July*, 5808–5819. https://doi.org/10.1111/gcb.16336

Van Passel, J., Bernardino, P. N., Lhermitte, S., Rius, B. F., Hirota, M., Conradi, T., de Keersmaecker, W., Van Meerbeek, K., & Somers, B. (2024). Critical slowing down of the Amazon forest after increased drought occurrence. *Proceedings of the National Academy of Sciences*, *121*(22), 2017. https://doi.org/10.1073/pnas.2316924121

Verbesselt, J., Hyndman, R., Newnham, G., & Culvenor, D. (2010a). Detecting trend and seasonal changes in satellite image time series. *Remote Sensing of Environment*, *114*(1), 106–115. https://doi.org/10.1016/j.rse.2009.08.014

Verbesselt J, Hyndman R, Zeileis A, Culvenor D (2010a). “Phenological Change Detection while Accounting for Abrupt and Gradual Trends in Satellite Image Time Series.” Remote Sensing of Environment, 114(12), 2970–2980. doi:10.1016/j.rse.2010.08.003.

Verheijen, L. M., Brovkin, V., Aerts, R., Bönisch, G., Cornelissen, J. H. C., Kattge, J., Reich, P. B., Wright, I. J., & Van Bodegom, P. M. (2013). Impacts of trait variation through observed trait-climate relationships on performance of an Earth system model: A conceptual analysis. *Biogeosciences*, *10*(8), 5497–5515. https://doi.org/10.5194/bg-10-5497-2013

Violle, C., Navas, M., Vile, D., Kazakou, E., Fortunel, C., Hummel, I., & Garnier, E. (2007). Let the concept of trait be functional! *Oikos*, *116*(5), 882–892. https://doi.org/10.1111/j.2007.0030-1299.15559.x

Weedon, Graham P.; Balsamo, Gianpaolo; Bellouin, Nicolas; Gomes, Sandra; Best, Martin J.; Viterbo, Pedro. The WFDEI meteorological forcing data set: WATCH Forcing Data methodology applied to ERA-Interim reanalysis data. Water Resources Research, [S. l.], v. 50, n. 9, p. 7505–7514, 2014. http://doi.wiley.com/10.1002/2014WR015638.

Wright, I. J., Reich, P. B., Westoby, M., Ackerly, D. D., Baruch, Z., Bongers, F., Cavender-bares, J., Chapin, T., Cornelissen, J. H. C., Diemer, M., Flexas, J., Garnier, E., Groom, P. K., & Gulias, J. (2004). The worldwide leaf economics spectrum. *Nature*, *428*, 821–827.

Wunderling, N., Staal, A., Sakschewski, B., Hirota, M., Tuinenburg, O. A., Donges, J. F., Barbosa, H. M. J., & Winkelmann, R. (2022). Recurrent droughts increase risk of cascading tipping events by outpacing adaptive capacities in the Amazon rainforest. *Proceedings of the National Academy of Sciences of the United States of America*, *119*(32), e2120777119. https://doi.org/10.1073/pnas.2120777119

Wu, D., Vargas G., G., Powers, J. S., McDowell, N. G., Becknell, J. M., Pérez-Aviles, D., Medvigy, D., Liu, Y., Katul, G. G., Calvo-Alvarado, J. C., Calvo-Obando, A., Sanchez-Azofeifa, A., & Xu, X. (2022). Reduced ecosystem resilience quantifies fine-scale heterogeneity in tropical forest mortality responses to drought. *Global Change Biology*, *28*(6), 2081–2094. https://doi.org/10.1111/gcb.16046

Wullschleger, S. D., Epstein, H. E., Box, E. O., Euskirchen, E. S., Goswami, S., Iversen, C. M., Kattge, J., Norby, R. J., Van Bodegom, P. M., & Xu, X. (2014). Plant functional types in Earth system models: Past experiences and future directions for application of dynamic vegetation models in high-latitude ecosystems. *Annals of Botany*, *114*(1), 1–16. https://doi.org/10.1093/aob/mcu077

Xu, C., Mcdowell, N. G., Sevanto, S., & Fisher, R. A. (2013). Our limited ability to predict vegetation dynamics under water stress. *New Phytologist*, *200*(2), 298–300. https://doi.org/10.1111/nph.12450

Yang, J., Tian, H., Pan, S., Chen, G., Zhang, B., & Dangal, S. (2018). Amazon drought and forest response: Largely reduced forest photosynthesis but slightly increased canopy greenness during the extreme drought of 2015/2016. Global Change Biology, 24(5), 1919–1934. https://doi.org/10.1111/gcb.14056

Yang, Q., Huang, Z., Wu, L., Guo, B., Liu, M., Xue, X., Li, X., & Liu, X. (2024). Resilience changes of carbon stocks to quantify the long-term effects of ecological engineering projects in subtropical forests of China based on satellite-derived net ecosystem production time series and inventory data. *Land Degradation & Development*, *35*(7), 2329–2344. https://doi.org/10.1002/ldr.5063

Zhang, R. Q., Xiong, Q., Wu, L., Wang, P., Kong, J. Y., Shi, X., & Sun, Z. Y. (2024). Water supply following drought: Effects on drougt legacy and resilience in a tropical forest - A case study in Xishuangbanna, China. Ecological Informatics, 79(October 2023), 102422. https://doi.org/10.1016/j.ecoinf.2023.102422

Adler, P.B., Salguero-Gómez, R., Compagnoni, A., Hsu, J.S., Ray-Mukherjee, J., Mbeau-Ache, C., Franco, M., 2014. Functional traits explain variation in plant lifehistory strategies. *Proc. Natl. Acad. Sci. U. S. A.*, 111, 740–745. https://doi.org/10.1073/pnas.1315179111

Allen, C.D., Macalady, A.K., Chenchouni, H., Bachelet, D., McDowell, N., … Cobb, N., 2010. A global overview of drought and heat-induced tree mortality reveals emerging climate change risks for forests. *For. Ecol. Manage.* 259, 660–684. https://doi.org/10.1016/j.foreco.2009.09.001

Aguirre-Gutiérrez, J., Oliveras, I., Rifai, S., Fauset, S., Adu-Bredu, S., Affum-Baffoe, K., ... Malhi, Y.S., 2019. Drier tropical forests are susceptible to functional changes in response to a long- term drought. *Ecology Letters*. 855–865. https://doi.org/10.1111/ele.13243

Aguirre-Gutiérrez, J., Malhi, Y., Lewis, S.L., Fauset, S., Adu-Bredu, S., ... Oliveras, I., 2020. Long-term droughts may drive drier tropical forests towards increased functional, taxonomic and phylogenetic homogeneity. *Nat. Commun.* 11, 1–10. https://doi.org/10.1038/s41467-020-16973-4

Anderegg, W.R.L., Klein, T., Bartlett, M., Sack, L., Pellegrini, A.F.A., Choat, B., Jansen, S., 2016. Meta-analysis reveals that hydraulic traits explain cross-species patterns of drought-induced tree mortality across the globe. *Proc. Natl. Acad. Sci. U. S. A.* 113, 5024–5029.

https://doi.org/10.1073/pnas.1525678113

Avitabile, V., Herold, M., Heuvelink, G.B.M., Lewis, S.L., Phillips, O.L., Asner, G.P., … Willcock, S., 2016. An integrated pan-tropical biomass map using multiple reference datasets. *Glob. Chang. Biol.* 22, 1406–1420. https://doi.org/10.1111/gcb.13139

Baccini, A., Goetz, S. J., Walker, W. S., Laporte, N. T., Sun, M., Sulla-Menashe, D., … Houghton, R. A., 2012. Estimated carbon dioxide emissions from tropical deforestation improved by carbon-density maps. *Nature Clim. Change*, *2*(3), 182–185. https://doi.org/10.1038/nclimate1354

Barros, C., Thuiller, W., Georges, D., Boulangeat, I., & Münkemüller, T., 2016. N-dimensional hypervolumes to study stability of complex ecosystems. *Ecology Letters*, *19*(7), 729–742. https://doi.org/10.1111/ele.12617

Berzaghi, F., Wright, I.J., Kramer, K., Oddou-Muratorio, S., Bohn, … Hartig, F., 2020. Towards a New Generation of Trait-Flexible Vegetation Models. *Trends Ecol. Evol.*, 35, 191–205. https://doi.org/10.1016/j.tree.2019.11.006

Betts, R.A., Cox, P.M., Collins, M., Harris, P.P., Huntingford, C., Jones, C.D., 2004. The role of ecosystem-atmosphere interactions in simulated Amazonian precipitation decrease and forest dieback under global climate warming. *Theor. Appl. Climatol.* 78, 157–175. https://doi.org/10.1007/S00704-004-0050-Y/METRICS

Blonder, B., 2017. Hypervolume concepts in niche- and trait-based ecology. *Ecography*, (August), 1–13. https://doi.org/10.1111/ecog.03187

Blonder, B., Lamanna, C., Violle, C., & Enquist, B. J., 2014. The n-dimensional hypervolume. *Global Ecology and Biogeography*, *23*(5), 595–609. https://doi.org/10.1111/geb.12146

Boersma, K. S., Dee, L. E., Miller, S. J., Bogan, M. T., Lytle, D. A., & Gitelman, A. I., 2016. Linking multidimensional functional diversity to quantitative methods: A graphical hypothesis-evaluation framework. *Ecology*, *97*(3), 583–593. https://doi.org/10.1890/15-0688

Bongers, F., Poorter, L., Hawthorne, W.D., Sheil, D., 2009. The intermediate disturbance hypothesis applies to tropical forests, but disturbance contributes little to tree diversity. *Ecol. Lett.* 12, 798–805. https://doi.org/10.1111/j.1461-0248.2009.01329.x

Cadotte, M. W., Carscadden, K., & Mirotchnick, N., 2011. Beyond species: Functional diversity and the maintenance of ecological processes and services. *Journal of Applied Ecology*, *48*(5), 1079–1087. https://doi.org/10.1111/j.1365-2664.2011.02048.x

Cadotte, M. W., 2017. Functional traits explain ecosystem function through opposing mechanisms. *Ecology Letters*, *20*(8), 989–996. https://doi.org/10.1111/ele.12796

Cannell, M. G. R., & Dewar, R. C., 1994. *Carbon Allocation in Trees - a Review of Concepts for Modeling*. *Advances in Ecological Research* (Vol. 25. https://doi.org/10.1016/s0065-2504(08)60213-5

Carmona, C. P., de Bello, F., Mason, N. W. H., & Lepš, J., 2016. Traits Without Borders: Integrating Functional Diversity Across Scales. *Trends in Ecology and Evolution*, *31*(5), 382–394. https://doi.org/10.1016/j.tree.2016.02.003

Carmona, C. P., de Bello, F., Mason, N. W. H., & Lepš, J., 2019. Trait probability density (TPD): measuring functional diversity across scales based on TPD with R. *Ecology*, *100*(12), 1–8. https://doi.org/10.1002/ecy.2876

Chave, J., Coomes, D., Jansen, S., Lewis, S. L., Swenson, N. G., & Zanne, A. E., 2009. Towards a worldwide wood economics spectrum. *Ecology Letters*, *12*(4), 351–366. https://doi.org/10.1111/j.1461-0248.2009.01285.x

Chiang, J.M., Spasojevic, M.J., Muller-Landau, H.C., Sun, I.F., Lin, Y., Su, S.H., Chen, Z.S., Chen, C.T., Swenson, N.G., McEwan, R.W., 2016. Functional composition drives ecosystem function through multiple mechanisms in a broadleaved subtropical forest. *Oecologia,* 182, 829–840. https://doi.org/10.1007/s00442-016-3717-z

Cornwell, W. K., Schwilk, D. W., & Ackerly, D. D., 2006. A Trait-Based Test for Habitat Filtering: Convex Hull Volume. *Ecology*, *87*(6), 1465–1471. http://www.jstor.org/stable/20069097

Cox, P M, Betts, R. a, Jones, C. D., Spall, S. a, & Totterdell, I. J., 2000. Acceleration of global warming due to carbon-cycle feedbacks in a coupled climate model. *Nature*, *408*(6809), 184–187. https://doi.org/10.1038/35041539

Cox, Peter M., Betts, R. a., Collins, M., Harris, P. P., Huntingford, C., & Jones, C. D., 2004. Amazonian forest dieback under climate-carbon cycle projections for the 21st century. *Theoretical and Applied Climatology*, *78*(1–3), 137–156. https://doi.org/10.1007/s00704-004-0049-4

Da Costa, A. C. L., Galbraith, D., Almeida, S., Portela, B. T. T., da Costa, M., de Athaydes Silva Junior, J., … Meir, P., 2010. Effect of 7 yr of experimental drought on vegetation dynamics and biomass storage of an eastern Amazonian rainforest. *New Phytologist*, *187*(3), 579–591. https://doi.org/10.1111/j.1469-8137.2010.03309.x

De Bello, F., Lavorel, S., Hallett, L. M., Valencia, E., Garnier, E., Roscher, C., … Lepš, J., 2021. Functional trait effects on ecosystem stability: assembling the jigsaw puzzle. *Trends in Ecology and Evolution*, *36*(9), 822–836. https://doi.org/10.1016/j.tree.2021.05.001

De Kauwe, M. G., Medlyn, B. E., Zaehle, S., Walker, A. P., Dietze, M. C., Wang, Y. P., … Norby, R. J., 2014. Where does the carbon go? A model-data intercomparison of vegetation carbon allocation and turnover processes at two temperate forest free-air CO2 enrichment sites. *New Phytologist*, *203*(3), 883–899. https://doi.org/10.1111/nph.12847

De La Riva, E. G., Lloret, F., Pérez-Ramos, I. M., Marañón, T., Saura-Mas, S., Díaz-Delgado, R., & Villar, R., 2017. The importance of functional diversity in the stability of Mediterranean shrubland communities after the impact of extreme climatic events. *Journal of Plant Ecology*, *10*(2), 281–293. https://doi.org/10.1093/jpe/rtw027

Díaz, S., & Cabido, M., 2001. Vive la difference: plant functional diversity matters to ecosystem processes. *Proceedings. Biological Sciences / The Royal Society*, *16*(4), 646–655. https://doi.org/10.1098/rspb.2010.1923

Díaz, S., Lavorel, S., de Bello, F., Quétier, F., Grigulis, K., Robson, T.M., 2007. Incorporating plant functional diversity effects in ecosystem service assessments. *Proc. Natl. Acad. Sci. U. S. A.*, 104, 20684–20689. https://doi.org/10.1073/pnas.0704716104

Doughty, C. E., Malhi, Y., Araujo-Murakami, A., Metcalfe, D. B., Silva-Espejo, J. E., Arroyo, L., … Ledezma, R., 2014. Allocation trade-offs dominate the response of tropical forest growth to seasonal and interannual drought. *Ecology*, *95*(8), 2192–2201. https://doi.org/10.1890/13-1507.1

Eller, C. B., Barros, F. de V., Bittencourt, P. R. L., Rowland, L., Mencuccini, M., & Oliveira, R. S., 2018. Xylem hydraulic safety and construction costs determine tropical tree growth. *Plant Cell and Environment*, *41*(3), 548–562. https://doi.org/10.1111/pce.13106

Enquist, B. J., & Enquist, C. A. F., 2011. Long-term change within a Neotropical forest: Assessing differential functional and floristic responses to disturbance and drought. *Global Change Biology*, *17*(3), 1408–1424. https://doi.org/10.1111/j.1365-2486.2010.02326.x

Enquist, B. J., Bentley, L. P., Shenkin, A., Maitner, B., Savage, V., Michaletz, S., … Malhi, Y., 2017. Assessing trait-based scaling theory in tropical forests spanning a broad temperature gradient. *Global Ecology and Biogeography*, *26*(12), 1357–1373. https://doi.org/10.1111/geb.12645

Esquivel-Muelbert, A., Galbraith, D., Dexter, K. G., Baker, T. R., Lewis, S. L., Meir, P., … Phillips, O. L., 2017. Biogeographic distributions of neotropical trees reflect their directly measured drought tolerances. *Scientific Reports*, *7*(1), 1–11. https://doi.org/10.1038/s41598-017-08105-8

Esquivel-Muelbert, A., Baker, T. R., Dexter, K. G., Lewis, S. L., Brienen, R. J. W., Feldpausch, T. R., … Phillips, O. L., 2018. Compositional response of Amazon forests to climate change. *Global Change Biology*, (June 2018), 39–56. https://doi.org/10.1111/gcb.14413

Fauset, S., Baker, T. R., Lewis, S. L., Feldpausch, T. R., Affum-Baffoe, K., Foli, E. G., … Etienne, R., 2012. Drought-induced shifts in the floristic and functional composition of tropical forests in Ghana. *Ecology Letters*. https://doi.org/10.1111/j.1461-0248.2012.01834.x

Fauset, S., Johnson, M. O., Gloor, M., Baker, T. R., Monteagudo M., A., Brienen, R. J. W., … Phillips, O. L., 2015. Hyperdominance in Amazonian forest carbon cycling. *Nature Communications*, *6*, 6857. https://doi.org/10.1038/ncomms7857

Finegan, B., Peña-Claros, M., de Oliveira, A., Ascarrunz, N., Bret-Harte, M.S., Carreño-Rocabado, G., ... Poorter, L., 2015. Does functional trait diversity predict above-ground biomass and productivity of tropical forests? Testing three alternative hypotheses. *J. Ecol.*, 103, 191–201. https://doi.org/10.1111/1365-2745.12346

Fisher, R.A., Koven, C.D., Anderegg, W.R.L., Christoffersen, B.O., Dietze, M.C., … T., Moorcroft, P.R., 2018. Vegetation demographics in Earth System Models: A review of progress and priorities. *Glob. Chang. Biol.*, 24, 35–54. https://doi.org/10.1111/gcb.13910

Fleischer, K., Rammig, A., De Kauwe, M. G., Walker, A. P., Domingues, T. F., Fuchslueger, L., … Lapola, D. M., 2019. Amazon forest response to CO2 fertilization dependent on plant phosphorus acquisition. *Nature Geoscience*, *12*(9), 736–741. https://doi.org/10.1038/s41561-019-0404-9

Funk, J. L., Larson, J. E., Ames, G. M., Butterfield, B. J., Cavender-Bares, J., Firn, J., … Wright, J., 2017. Revisiting the Holy Grail: using plant functional traits to understand ecological processes. *Biological Reviews*, *92*(2), 1156–1173. https://doi.org/10.1111/brv.12275

Fyllas, N. M., Gloor, E., Mercado, L. M., Sitch, S., Quesada, C. a., Domingues, T. F., … Lloyd, J., 2014. Analysing Amazonian forest productivity using a new individual and trait-based model (TFS v.1. *Geoscientific Model Development*, *7*, 1251–1269. https://doi.org/10.5194/gmd-7-1251-2014

Galbraith, D., Levy, P. E., Sitch, S., Huntingford, C., Cox, P., Williams, M., & Meir, P., 2010. Multiple mechanisms of Amazonian forest biomass losses in three dynamic global vegetation models under climate change. *The New Phytologist*, *187*, 647–665. https://doi.org/10.1111/j.1469-8137.2010.03350.x

Gonzalez, A., & Loreau, M., 2009. The Causes and Consequences of Compensatory Dynamics in Ecological Communities. *Annu.Rev.Ecol.Syst.*, *40*, 393–414. https://doi.org/10.1146/annurev.ecolsys.39.110707.173349

Grime, J. P., 1998. Benefits of plant diversity to ecosystems: Immediate, filter and founder effects. *Journal of Ecology*, *86*(6), 902–910. https://doi.org/10.1046/j.1365-2745.1998.00306.x

Haghtalab, N., Moore, N., Heerspink, B.P., Hyndman, D.W., 2020. Evaluating spatial patterns in precipitation trends across the Amazon basin driven by land cover and global scale forcings. *Theor. Appl. Climatol*. 140, 411–427. https://doi.org/10.1007/s00704-019-03085-3

Herben, T., Klimešová, J., Chytrý, M., 2018. Effects of disturbance frequency and severity on plant traits: An assessment across a temperate flora. *Funct. Ecol.*, 32, 799–808. https://doi.org/10.1111/1365-2435.13011

Hillebrand, H., Bennett, D. M., & Cadotte, M. W., 2008. Consequences of Dominance: a Review of Evenness Effects on Local and Regional Ecosystem Processes. *Ecology*, *89*(6), 1510–1520. https://doi.org/10.1890/07-1053.1

Hofhansl, F., Chacón-Madrigal, E., Brännström, Å., Dieckmann, U., & Franklin, O., 2021. Mechanisms driving plant functional trait variation in a tropical forest. *Ecology and Evolution*. https://doi.org/10.1097/bot.0000000000002145

Holzwarth, F., Rüger, N., Wirth, C., 2015. Taking a closer look: Disentangling effects of functional diversity on ecosystem functions with a trait-based model across hierarchy and time. *R. Soc. Open Sci.*, 2. https://doi.org/10.1098/rsos.140541

Hooper, D.U., Chapin, F.S., Ewel, J.J., Hector, A., Inchausti, P., Lavorel, S., … Wardle, D.A., 2005. Effects of biodiversity on ecosystem functioning: A consensus of current knowledge.

Ecol. Monogr., 75, 3–35. https://doi.org/10.1890/04-0922

Houghton, R. a, Lawrence, K. T., Hackler, J. L., & Brown, S., 2001. The spatial distribution of forest biomass in the Brazilian Amazon: a comparison of estimates. *Global Change Biology*, *7*(7), 731–746. https://doi.org/DOI 10.1046/j.1365-2486.2001.00426.x

Hubau, W., Lewis, S. L., Phillips, O. L., Affum-Baffoe, K., Beeckman, H., Cuní-Sanchez, A., … Zemagho, L., 2020. Asynchronous carbon sink saturation in African and Amazonian tropical forests. *Nature*, *579*(7797), 80–87. https://doi.org/10.1038/s41586-020-2035-0

Huntingford, C., Zelazowski, P., Galbraith, D., Mercado, L. M., Sitch, S., Fisher, R., … Cox, P. M., 2013. Simulated resilience of tropical rainforests to CO2-induced climate change. *Nature Geoscience*, *6*(4), 268–273. https://doi.org/10.1038/ngeo1741

Hutyra, L. R., Munger, J. W., Nobre, C. A., Saleska, S. R., Vieira, S. A., & Wofsy, S. C., 2005. Climatic variability and vegetation vulnerability in Amazŏnia. *Geophysical Research Letters*, *32*(24), 1–4. https://doi.org/10.1029/2005GL024981

Joshi, J., Stocker, B. D., Hofhansl, F., Zhou, S., Dieckmann, U., & Prentice, I. C., 2020. Towards a unified theory of plant photosynthesis and hydraulics. *BioRxiv*. https://doi.org/10.1101/2020.12.17.423132

Joshi, J., Stocker, B.D., Hofhansl, F., Zhou, S., Dieckmann, U., & Prentice, I. C., 2022. Towards a unified theory of plant photosynthesis and hydraulics. *Nat. Plants*, 8, 1304–1316. https://doi.org/10.1038/s41477-022-01244-5

Kannenberg, S. A., Novick, K. A., Alexander, M. R., Maxwell, J. T., Moore, D. J. P., Phillips, R. P., & Anderegg, W. R. L., 2019. Linking drought legacy effects across scales: From leaves to tree rings to ecosystems. *Global Change Biology*, *25*(9), 2978–2992. https://doi.org/10.1111/gcb.14710

Keddy, P. A., 1992. Assembly and response rules: two goals for predictive community ecology. *Journal of Vegetation Science*, *3*(2), 157–164. https://doi.org/10.2307/3235676

Kleidon, A., Adams, J., Pavlick, R., & Reu, B., 2009. Simulated geographic variations of plant species richness, evenness and abundance using climatic constraints on plant functional diversity. *Environmental Research Letters*, *4*(1), 014007. https://doi.org/10.1088/1748-9326/4/1/014007

Koch, A., Hubau, W., & Lewis, S. L., 2021. Earth System Models Are Not Capturing Present-Day Tropical Forest Carbon Dynamics. *Earth's Future*, *9*(5), 1–19. https://doi.org/10.1029/2020EF001874

Lapola, D. M., Oyama, M. D., & Nobre, C. A., 2009. Exploring the range of climate biome projections for tropical South America: The role of CO2 fertilization and seasonality. *Global Biogeochemical Cycles*, *23*(3), 1–22. https://doi.org/10.1029/2008GB003357

Lapola, D.M., Pinho, P., Quesada, C.A., Strassburg, B.B.N., Rammig, A., ... Nobre, C.A., 2018. Limiting the high impacts of Amazon forest dieback with no-regrets science and policy action. *Proc. Natl. Acad. Sci. U. S. A.* 115, 11671–11679. https://doi.org/10.1073/pnas.1721770115

Law R., 1979. Ecological determinants in the evolution of life histories. In *Population dynamics* (eds R.M. Anderson, B.D. Turner & L.R. Taylor) pp. 267-292. Blackwell Scientific Publications, Oxford, UK.

Laughlin, D.C., Laughlin, D.E., 2013. Advances in modeling trait-based plant community assembly. *Trends Plant Sci.* ,18, 584–593. https://doi.org/10.1016/j.tplants.2013.04.012

Lavorel, S., & Garnier, E., 2002. Predicting changes in community composition and ecosystem functioning from plant traits: revisiting the Holy Grail. *Functional Ecology*, *16*(Essay Review), 545–556. https://doi.org/Doi 10.1046/J.1365-2435.2002.00664.X

Lee, J.-Y., Marotzke, J., Bala G., Cao, L., Corti, S., Dunne, J. P., … Zhou, T., 2021. Future Global Climate: Scenario-Based Projections and Near-Term Information. in: Masson-Delmotte, V., P. Zhai, A. Pirani, S.L. Connors, C. Péan, S. Berger, N. Caud, Y. Chen, L. Goldfarb, M.I. Gomis, M. Huang, K. Leitzell, E. Lonnoy, J.B.R. Matthews, T.K. Maycock, T. Waterfield, O. Yelekçi, R. Yu, and B. Zhou (Eds.), Climate Change 2021: The Physical Science Basis. Contribution of Working Group I to the Sixth Assessment Report of the Intergovernmental Panel on Climate Change Cambridge University Press. In Press.

Le Bagousse-Pinguet, Y., Gross, N., Maestre, F.T., Maire, V., de Bello, F., Fonseca, C.R., Kattge, J., Valencia, E., Leps, J., Liancourt, P., 2017. Testing the environmental filtering concept in global drylands. *J. Ecol.* ,105, 1058–1069. https://doi.org/10.1111/1365-2745.12735

Levine, N. M., Zhang, K., Longo, M., Baccini, A., Phillips, O. L., Lewis, S. L., … Moorcroft, P. R., 2016. Ecosystem heterogeneity determines the ecological resilience of the Amazon to climate change. *Proceedings of the National Academy of Sciences*, *113*(3), 793–797. https://doi.org/10.1073/pnas.1511344112

Lohbeck, M., Bongers, F., Martinez-Ramos, M., & Poorter, L., 2016. The importance of biodiversity and dominance for multiple ecosystem functions in a human- modified tropical landscape. *Ecology*, *97*(10), 2772–2779. http://onlinelibrary.wiley.com/journal/10.1002/(ISSN)1939-9170/issues

Longo, M., Knox, R.G., Levine, N.M., Alves, L.F., Bonal, D., Camargo, P.B... Moorcroft, P.R., 2018. Ecosystem heterogeneity and diversity mitigate Amazon forest resilience to frequent extreme droughts. *New Phytol.*, 219, 914–931. https://doi.org/10.1111/nph.15185

Lovejoy, T.E., Nobre, C., 2018. Amazon tipping point. *Sci. Adv.*, 4, 1–2. https://doi.org/10.1126/sciadv.aat2340

Malhi, Y., Aragao, L.E.O.C., Galbraith, D., Huntingford, C., Fisher, R., Zelazowski, P., Sitch, S., McSweeney, C., Meir, P., 2009. Exploring the likelihood and mechanism of a climate-change-induced dieback of the Amazon rainforest. *Proc. Natl. Acad. Sci.* 106, 20610–20615. https://doi.org/10.1073/pnas.0804619106

Malhi, Y., Rowland, L., Aragão, L.E.O.C., Fisher, R.A., 2018. New insights into the variability of the tropical land carbon cycle from the El Niño of 2015/2016. *Philos. Trans. R. Soc. B Biol. Sci*. 373. https://doi.org/10.1098/rstb.2017.0298

Marengo, J.A., Nobre, C.A., Tomasella, J., Oyama, M.D., de Oliveira, ... Brown, I.F., 2008. The drought of Amazonia in 2005. J. Clim. 21, 495–516. https://doi.org/10.1175/2007JCLI1600.1

Mason, N. W. H., Mouillot, D., Lee, W. G., & Wilson, J. B., 2005. Functional richness, functional evenness and functional divergence: The primary components of functional diversity. *Oikos*, *111*(1), 112–118. https://doi.org/10.1111/j.0030-1299.2005.13886.x

Metcalfe, D. B., Meir, P., Aragão, L. E. O. C., Lobo-do-Vale, R., Galbraith, D., Fisher, R. A., … Williams, M., 2010. Shifts in plant respiration and carbon use efficiency at a large-scale drought experiment in the eastern Amazon. *New Phytologist*, *187*(3), 608–621. https://doi.org/10.1111/j.1469-8137.2010.03319.x

Mitchard, E.T., Saatchi, S.S., Baccini, A., Asner, G.P., Goetz, S.J., Harris, N.L., Brown, S., 2013. Uncertainty in the spatial distribution of tropical forest biomass: a comparison of pan-tropical maps. *Carbon Balance Manag.*, 8, 10. https://doi.org/10.1186/1750-0680-8-10

Mori, A. S., Furukawa, T., & Sasaki, T., 2013. Response diversity determines the resilience of ecosystems to environmental change. *Biological Reviews*, *88*(2), 349–364. https://doi.org/10.1111/brv.12004

Morton, D.C., Le Page, Y., DeFries, R., Collatz, G.J., Hurtt, G.C., 2013. Understorey fire frequency and the fate of burned forests in southern Amazonia. Philos. Trans. R. Soc. B Biol. Sci. 368, 20120163. https://doi.org/10.1098/rstb.2012.0163

Mouillot, D., Graham, N. A. J., Villéger, S., Mason, N. W. H., & Bellwood, D. R., 2013a. A functional approach reveals community responses to disturbances. *Trends in Ecology and Evolution*, *28*(3), 167–177. https://doi.org/10.1016/j.tree.2012.10.004

Mouillot, D., Bellwood, D. R., Baraloto, C., Chave, J., Galzin, R., Harmelin-Vivien, M., … Thuiller, W., 2013b. Rare Species Support Vulnerable Functions in High-Diversity Ecosystems. *PLoS Biology*, *11*(5). https://doi.org/10.1371/journal.pbio.1001569

Mouillot, D., Villéger, S., Scherer-Lorenzen, M., & Mason, N. W. H., 2011. Functional structure of biological communities predicts ecosystem multifunctionality. *PLoS ONE*, *6*(3). https://doi.org/10.1371/journal.pone.0017476

Nobre, C.A., Sampaio, G., Borma, L.S., Castilla-Rubio, J.C., Silva, J.S., Cardoso, M., 2016. Land-use and climate change risks in the amazon and the need of a novel sustainable development paradigm. *Proc. Natl. Acad. Sci.* U. S. A. 113, 10759–10768. https://doi.org/10.1073/PNAS.1605516113/-/DCSUPPLEMENTAL

Oliveira, R.S., Eller, C.B., Barros, F. de V., Hirota, M., Brum, M., Bittencourt, P., 2021. Linking plant hydraulics and the fast-slow continuum to understand resilience to drought in tropical ecosystems. *New Phytol*. 230, 904–923. https://doi.org/10.1111/NPH.17266

Papastefanou, P., Zang, C. S., Pugh, T. A. M., Liu, D., Grams, T. E. E., Hickler, T., & Rammig, A., 2020. A Dynamic Model for Strategies and Dynamics of Plant Water-Potential Regulation Under Drought Conditions. *Frontiers in Plant Science*, *11*(April), 1–13.

https://doi.org/10.3389/fpls.2020.00373

Pappas, C., Fatichi, S., Rimkus, S., Burlando, P., Huber, M., 2015. The role of local scale heterogeneities in terrestrial ecosystem modeling. *J. Geophys. Res. Biogeosciences*, 120, 341–360. https://doi.org/10.1002/2014JG002735

Pavlick, R., Drewry, D. T., Bohn, K., Reu, B., & Kleidon, A., 2013. The Jena Diversity-Dynamic Global Vegetation Model (JeDi-DGVM): a diverse approach to representing terrestrial biogeography and biogeochemistry based on plant functional trade-offs. *Biogeosciences*, *10*(6), 4137–4177. https://doi.org/10.5194/bg-10-4137-2013

Perronne, R., & Gaba, S., 2017. How to design trait-based analyzes of community assembly mechanisms: Insights and guidelines from a literature review, *25*, 29–44. https://doi.org/10.1016/j.ppees.2017.01.004

Poorter, L., van der Sande, M. T., Thompson, J., Arets, E. J. M. M., Alarcón, A., Álvarez-Sánchez, J., … Peña-Claros, M., 2015. Diversity enhances carbon storage in tropical forests. *Global Ecology and Biogeography*, *24*(11), 1314–1328. https://doi.org/10.1111/geb.12364

Prentice, I. C., Bondeau, A., Cramer, W., Harrison, S. P., Hickler, T., Lucht, W., … Sykes, M. T., 2007. Dynamic Global Vegetation Modeling: Quantifying Terrestrial Ecosystem Responses to Large-Scale Environmental Change. *Terrestrial Ecosystems in a Changing World*, 175–192. https://doi.org/10.1007/978-3-540-32730-1_15

Quesada, C.A., Phillips, O.L., Schwarz, M., Czimczik, C.I., Baker, T.R., Patiño, S., … Lloyd, J., 2012. Basin-wide variations in Amazon forest structure and function are mediated by both soils and climate. *Biogeosciences*, 9, 2203–2246. https://doi.org/10.5194/bg-9-2203-2012

Rammig, A., Jupp, T., Thonicke, K., Tietjen, B., Heinke, J., Ostberg, S., … Shukla, J., 2010. Amazon deforestation and climate change. *Global Change Biology*, *4*(3), 957–988. https://doi.org/10.1111/j.1365-2486.2009.02157.x

Reich, A.P.B., Wright, I.J., Bares, J.C., Craine, J.M., Oleksyn, J., Westoby, M., Walters, M.B., 2003. The Evolution of Plant Functional Variation: Traits, Spectra, and Strategies. *Int. J. Plant Sci*. 164, S143–S164. https://doi.org/10.1086/374368

Reu, B., Proulx, R., Bohn, K., Dyke, J. G., Kleidon, A., Pavlick, R., & Schmidtlein, S., 2011. The role of climate and plant functional trade-offs in shaping global biome and biodiversity patterns. *Global Ecology and Biogeography*, *20*(4), 570–581. https://doi.org/10.1111/j.1466-8238.2010.00621.x

Reu, B., Zaehle, S., Bohn, K., Pavlick, R., Schmidtlein, S., Williams, J. W., & Kleidon, A., 2014. Future no-analogue vegetation produced by no-analogue combinations of temperature and insolation. *Global Ecology and Biogeography*, *23*(2), 156–167. https://doi.org/10.1111/geb.12110

Roscher, C., Schumacher, J., Gubsch, M., Lipowsky, A., Weigelt, A., Buchmann, N., Schmid, B., Schulze, E.D., 2012. Using plant functional traits to explain diversity-productivity relationships. *PLoS One*, 7. https://doi.org/10.1371/journal.pone.0036760

Rowland, L., da Costa, A. C. L., Galbraith, D. R., Oliveira, R. S., Binks, O. J., Oliveira, A. A. R., … Meir, P., 2015. Death from drought in tropical forests is triggered by hydraulics not carbon starvation. *Nature*, 1–13. https://doi.org/10.1038/nature15539

Rowland, Lucy, Hill, T. C., Stahl, C., Siebicke, L., Burban, B., Zaragoza-Castells, J., … Williams, M., 2014. Evidence for strong seasonality in the carbon storage and carbon use efficiency of an Amazonian forest. *Global Change Biology*, *20*(3), 979–991. https://doi.org/10.1111/gcb.12375

Ruiz-Jaen, M.C., Potvin, C., 2011. Can we predict carbon stocks in tropical ecosystems from tree diversity? Comparing species and functional diversity in a plantation and a natural forest. *New Phytol.*, 189, 978–987. https://doi.org/10.1111/j.1469-8137.2010.03501.x

Running, S., Zhao, M., 2021. *MODIS/Terra Net Primary Production Gap-Filled Yearly L4 Global 500m SIN Grid V061* [Data set]. NASA EOSDIS Land Processes DAAC. Accessed 2021-09-01 from https://doi.org/10.5067/MODIS/MOD17A3HGF.061

Saatchi, S., Houghton, R. A., Dos Santos Alval??, R. C., Soares, J. V., & Yu, Y., 2007. Distribution of aboveground live biomass in the Amazon basin. *Global Change Biology*, *13*(4), 816–837. https://doi.org/10.1111/j.1365-2486.2007.01323.x

Saatchi, S. S., Harris, N. L., Brown, S., Lefsky, M., Mitchard, E. T. A., Salas, W., … Morel, A., 2011. Benchmark map of forest carbon stocks in tropical regions across three continents. *Proceedings of the National Academy of Sciences*, *108*(24), 9899–9904. https://doi.org/10.1073/pnas.1019576108

Sakschewski, B., von Bloh, W., Boit, A., Poorter, L., Peña-Claros, M., Heinke, J., … Thonicke, K., 2016. Resilience of Amazon forests emerges from plant trait diversity. *Nature Climate Change*, *1*(August). https://doi.org/10.1038/nclimate3109

Sakschewski, B., von Bloh, W., Boit, A., Rammig, A., Kattge, J., Poorter, L., … Thonicke, K., 2015. Leaf and stem economics spectra drive diversity of functional plant traits in a dynamic global vegetation model. *Global Change Biology*, 2711–2725. https://doi.org/10.1111/gcb.12870

Salazar, L. F., Nobre, C. A., & Oyama, M. D., 2007. Climate change consequences on the biome distribution in tropical South America. *Geophysical Research Letters*, *34*(9), 2–7. https://doi.org/10.1029/2007GL029695

Scheiter, S., Langan, L., & Higgins, S. I., 2013. Next-generation dynamic global vegetation models: learning from community ecology. *The New Phytologist*. https://doi.org/10.1111/nph.12210

Schmitt, S., Maréchaux, I., Chave, J., Fischer, F. J., Piponiot, C., Traissac, S., & Hérault, B., 2019. Functional diversity improves tropical forest resilience: Insights from a long-term virtual experiment. *Journal of Ecology*, (October), 1–13. https://doi.org/10.1111/1365-2745.13320

Shen, Y., Yu, S., Lian, J., Shen, H., Cao, H., Lu, H., Ye, W., 2016. Tree aboveground carbon storage correlates with environmental gradients and functional diversity in a tropical forest. *Sci. Rep.*, 6. https://doi.org/10.1038/srep25304

Sitch, S., Smith, B., Prentice, I. C., Arneth, A., Bondeau, A., Cramer, W., … Venevsky, S. (2003). Evaluation of ecosystem dynamics, plant geography and terrestrial carbon cycling in the LPJ dynamic global vegetation model. *Global Change Biology*. https://doi.org/10.1046/j.1365-2486.2003.00569.x

Smith, E.A., Holden, E.M., Brown, C., Cahill, J.F., 2022. Disturbance has lasting effects on functional traits and diversity of grassland plant communities. *PeerJ.*, 10. https://doi.org/10.7717/peerj.13179

Sombroek, W., 2000. Amazon landforms and soils in relation to biological diversity. *Acta Amaz.*, 30, 81–81. https://doi.org/10.1590/1809-43922000301100

Song, Y., Wang, P., Li, G., & Zhou, D., 2014. Relationships between functional diversity and ecosystem functioning: A review. *Acta Ecologica Sinica*, *34*(2), 85–91. https://doi.org/10.1016/j.chnaes.2014.01.001

Ter Steege, H., Pitman, N.C.A., Phillips, O.L., Chave, J., Sabatier, D., Duque, A., … Vásquez, R., 2006. Continental-scale patterns of canopy tree composition and function across Amazonia. *Nature*, 443, 444–447. https://doi.org/10.1038/nature05134

Thomas, S. C., & Martin, A. R., 2012. Carbon content of tree tissues: A synthesis. *Forests*, *3*(2), 332–352. https://doi.org/10.3390/f3020332

Thornley, J. H. M., 1972. A balanced quantitative model for root: Shoot ratios in vegetative plants. *Annals of Botany*, *36*(2), 431–441. https://doi.org/10.1093/oxfordjournals.aob.a084602

Tilman, D., Isbell, F., Cowles, J.M., 2014. Biodiversity and Ecosystem Functioning. *Annu. Rev. Ecol. Evol. Syst.*, 45, 471–493. https://doi.org/10.1146/annurev-ecolsys-120213-091917

Tilman, D., Knops, J., Wedin, D., Reich, P., Ritchie, M., Siemann, E., 1997. The influence of functional diversity and composition on ecosystem processes. *Science*, 277, 1300–1302. https://doi.org/10.1126/science.277.5330.1300

Tilman, D., Reich, P.B., Knops, J.M.H., 2006. Biodiversity and ecosystem stability in a decade-long grassland experiment. *Nature*, 441, 629–632. https://doi.org/10.1038/nature04742

Verheijen, L. M., Brovkin, V., Aerts, R., Bönisch, G., Cornelissen, J. H. C., Kattge, J., … Van Bodegom, P. M., 2013. Impacts of trait variation through observed trait-climate relationships on performance of an Earth system model: A conceptual analysis. *Biogeosciences*, *10*(8), 5497–5515. https://doi.org/10.5194/bg-10-5497-2013

Verheijen, L. M., Aerts, R., Brovkin, V., Cavender-Bares, J., Cornelissen, J. H. C., Kattge, J., & van Bodegom, P. M., 2015. Inclusion of ecologically based trait variation in plant functional types reduces the projected land carbon sink in an earth system model. *Global Change Biology*, 3074–3086. https://doi.org/10.1111/gcb.12871

Villéger, S., Mason, N. W. H., & Mouillot, D., 2008. New Multidimensional Functional Diversity Indices for a Multifaceted Framework in Functional Ecology. *America*, *89*(8), 2290–2301. https://doi.org/10.1890/07-1206.1

Villéger, S., Miranda, J. R., Hernández, D. F., & Mouillot, D., 2010. Contrasting changes in taxonomie vs. functional diversity of tropical fish communities after habitat degradation. *Ecological Applications*, *20*(6), 1512–1522. https://doi.org/10.1890/09-1310.1

Violle, C., Navas, M., Vile, D., Kazakou, E., Fortunel, C., Hummel, I., & Garnier, E., 2007. Let the concept of trait be functional! *Oikos*, *116*(5), 882–892. https://doi.org/10.1111/j.2007.0030-1299.15559.x

Walker, B., Kinzig, A., & Langridge, J., 1999. Plant attribute diversity, resilience, and ecosystem function: The nature and significance of dominant and minor species. *Ecosystems*, *2*(2), 95–113. https://doi.org/10.1007/s100219900062

Webb, C. T., Hoeting, J. a., Ames, G. M., Pyne, M. I., & LeRoy Poff, N., 2010. A structured and dynamic framework to advance traits-based theory and prediction in ecology. *Ecology Letters*, *13*(3), 267–283. https://doi.org/10.1111/j.1461-0248.2010.01444.x

Wieczynski, D. J., Boyle, B., Buzzard, V., Duran, S. M., Henderson, A. N., Hulshof, C. M., … Savage, V. M., 2019. Climate shapes and shifts functional biodiversity in forests worldwide. *Proceedings of the National Academy of Sciences*, *116*(15), 7591–7591. https://doi.org/10.1073/pnas.1904390116

Wullschleger, S. D., Epstein, H. E., Box, E. O., Euskirchen, E. S., Goswami, S., Iversen, C. M., … Xu, X., 2014. Plant functional types in Earth system models: Past experiences and future directions for application of dynamic vegetation models in high-latitude ecosystems. *Annals of Botany*, *114*(1), 1–16. https://doi.org/10.1093/aob/mcu077

Yachi, S., & Loreau, M., 1999. Biodiversity and ecosystem productivity in a fluctuating environment: The insurance hypothesis. *Proceedings of the National Academy of Sciences of the United States of America*, *96*, 1463–1468. https://doi.org/10.1073/pnas.96.4.1463

Yang, X., Ricciuto, D.M., Thornton, P.E., Shi, X., Xu, M., …Norby, R.J., 2019. The Effects of Phosphorus Cycle Dynamics on Carbon Sources and Sinks in the Amazon Region: A Modeling Study Using ELM v1. *J. Geophys. Res. Biogeosciences*, 124, 3686–3698. https://doi.org/10.1029/2019JG005082

Zakharova, L., Meyer, K.M., Seifan, M., 2019. Trait-based modelling in ecology: lessons from two decades of research. *PeerJ Preprints*, 1–9. https://doi.org/.1037//0033-2909.I26.1.78

APPENDIX I

UNICAMP
COORDENADORIA DE PÓS-GRADUAÇÃO
INSTITUTO DE BIOLOGIA
Universidade Estadual de Campinas
Caixa Postal 6109. 13083-970, Campinas, SP, Brasil
Fone (19) 3521-6378. email: cpgib@unicamp.br
IB

DECLARAÇÃO

Em observância ao **§5º do artigo 1º da informação ccpg-unicamp/001/15**, referente a bioética e biossegurança, declaro que o conteúdo de minha Tese de Doutorado, intitulada "*Modeling functional diversity and resilience of the amazon forest to climate change beyond carbon stocks*", desenvolvida no programa de pós-graduação em Ecologia do instituto de biologia da unicamp, não versa sobre pesquisa envolvendo seres humanos, animais ou temas afetos a biossegurança.

Assinatura: Bianca Fazio Rius
Nome do(a) aluno(a): Bianca Fazio Rius

Assinatura: ______________________________
Nome do(a) orientador(a): David Montenegro Lapola

Data: 02 de agosto de 2024

APPENDIX II

Declaração

As cópias de artigos de minha autoria ou de minha co-autoria, já publicados ou submetidos para publicação em revistas científicas ou anais de congressos sujeitos a arbitragem, que constam da minha Dissertação/Tese de Mestrado/Doutorado, intitulada **Modeling functional diversity and resilience of the amazon forest to climate change beyond carbon stocks**, não infringem os dispositivos da Lei n.° 9.610/98, nem o direito autoral de qualquer editora.

Campinas, 06 de agosto de 2024

Assinatura : Bianca Fazio Rius
Nome do(a) autor(a): **Bianca Fazio Rius**
RG n.° 47.884.379-3

Assinatura : ______________________________
Nome do(a) orientador(a): **David Montenegro Lapola**
RG n.° 30.568.373-1